

Mechanisms of 4-aminobiphenyl-induced liver carcinogenesis in the mouse

by

Shuang Wang

A thesis submitted in conformity with the requirements
for the degree of Doctoral of Philosophy

Department of Pharmacology & Toxicology
University of Toronto

© Copyright by Shuang Wang 2014

Mechanisms of 4-aminobiphenyl-induced liver carcinogenesis in the mouse

Shuang Wang

Doctor of Philosophy

Pharmacology and Toxicology
University of Toronto

2014

Abstract

4-Aminobiphenyl (ABP) is a human carcinogen commonly found in cigarette smoke and hair dyes. In a tumor study carried out previously in our laboratory using ABP, female mice showed a dramatically lower incidence of liver tumors than male mice. This observation seems to parallel the prominent sex difference observed in human liver cancer, with women having a 3- to 5-fold lower incidence than men. Our overall goal is to elucidate the molecular mechanisms behind ABP-induced liver carcinogenesis in our mouse model, which we hope will improve our understanding of ABP as an important environmental carcinogen and also shed light on the molecular mechanism behind human liver cancer. According to a traditional model of ABP carcinogenesis, ABP *N*-hydroxylation by CYP1A2 initiates a cascade of bioactivation reactions that ultimately result in the formation of ABP-DNA adducts and the initiation of liver carcinogenesis. In the first part of my PhD studies, I generated evidence against this traditional model of ABP carcinogenesis by finding no sex differences in ABP-induced mutations in mouse liver. Re-examination of the ABP bioactivation pathway using both genetic and pharmacological tools revealed CYP2E1 as a novel major ABP *N*-hydroxylation enzyme in mouse liver. No sex differences were found in ABP *N*-hydroxylation activity. Since oxidative stress has been linked to ABP *in vitro* and represents a major etiological factor for human liver cancer, I investigated a potential role for oxidative stress in our ABP carcinogenesis model. Using a hepatoma cell line, I

found that the *N*-hydroxylation of ABP by CYP2E1 induced oxidative stress. Following *in vivo* exposure to ABP, I detected increased oxidative stress in male wild-type but not in male *Cyp2e1(-/-)* or female mice. On the other hand, a stronger antioxidant response was observed in females, which may protect them from ABP-induced oxidative stress and subsequent liver carcinogenesis.

Acknowledgments

I would like to thank my parents for supporting me through whichever career/life path I take, which I know is not always easy. I would like to thank Dr. Denis Grant, my boss and mentor, for all his training and inspiration. I would like to thank Dr. Kim Sugamori for her numerous intellectual inputs. I would like to thank my committee members Drs. Jane Mitchell and Peter McPherson for their wisdom and guidance. Finally, I would like to thank all the lab members that have contributed to my thesis work including Debbie Bott, Ivy Hsu, Adriana Calce, and Aveline Tung.

Table of Contents

Abstract	ii
Acknowledgments	iv
Table of Contents	v
List of Tables	viii
List of Figures	ix
List of Appendices	xii
Abbreviations	xiii
Chapter 1 GENERAL INTRODUCTION	1
1.1 Chemical carcinogenesis	2
1.1.1 Overview	2
1.1.2 The multi-stage model of chemical carcinogenesis	3
1.1.3 DNA modifications and tumor initiation	4
1.1.4 Tumor promotion and progression	10
1.1.5 Metabolic activation and detoxification of chemical carcinogens	11
1.2 Aromatic amines	19
1.2.1 Bladder cancer and occupational dye exposure	19
1.2.2 Aromatic amines as a major class of carcinogens	20
1.2.3 Diverse carcinogenic effects of aromatic amines	21
1.2.4 Metabolic activation and DNA adducts of aromatic amines	21
1.2.5 Aromatic amines and oxidative stress	24
1.3 Human liver cancer	26
1.3.1 Overview of liver physiology	26
1.3.2 Primary liver cancer	27
1.3.3 Risk factors for hepatocellular carcinoma (HCC)	28

1.3.4	Current treatments and future trends.....	33
1.4	ABP-induced liver carcinogenesis in mice	34
1.4.1	Mouse models for the study of liver carcinogenesis.....	34
1.4.2	4-Aminobiphenyl (ABP).....	36
1.4.3	A traditional model of ABP bioactivation and tumor initiation in the mouse liver	37
1.4.4	Evidence inconsistent with the traditional model of ABP bioactivation and tumor initiation in mouse liver.....	45
1.4.5	<i>In vitro</i> and <i>in vivo</i> evidence linking ABP to oxidative stress.....	47
1.5	Aims of the thesis.....	51
Chapter 2 MATERIALS AND METHODS		53
2.1	Chemicals and reagents.....	54
2.2	Animal treatment	54
2.3	Cell culture and cell transfection	55
2.4	Genotyping assays for NAT1/2, CYP2E1, and the Muta TM Mouse transgene.....	56
2.5	Liver genomic DNA isolation.....	57
2.6	λ phage packaging and <i>cII</i> mutation assay.....	57
2.7	<i>cII</i> mutant gene sequence analysis.....	58
2.8	Microsomal preparations from mouse liver and cell culture	58
2.9	<i>In vitro</i> and <i>in culture</i> ABP <i>N</i> -hydroxylation assays	59
2.10	<i>In vitro</i> and <i>in culture</i> pNP hydroxylation assays	59
2.11	Immunoblotting.....	60
2.12	DCF assay	61
2.13	Total and oxidized glutathione assays.....	61
2.14	RNA extraction and cDNA synthesis	62
2.15	Quantitative PCR	63
2.16	Statistical analyses	65

Chapter 3 RESULTS.....	66
3.1 ABP-induced mutations <i>in vivo</i>	67
3.1.1 ABP-induced <i>cII</i> mutation frequencies in neonatal mice	67
3.1.2 ABP-induced <i>cII</i> mutation frequencies in adult mice.....	69
3.1.3 ABP-induced <i>cII</i> mutation spectra in neonatal mice	70
3.1.4 ABP-induced <i>cII</i> mutation spectra in adult mice	72
3.2 ABP metabolic activation by cytochrome P450s.....	74
3.2.1 ABP <i>N</i> -hydroxylation by CYP1A2 in mouse liver microsomes	74
3.2.2 Identification of CYP2E1 as a major ABP <i>N</i> -hydroxylation enzyme in mouse liver microsomes.....	79
3.2.3 ABP <i>N</i> -hydroxylation by recombinantly expressed CYP1A2 or CYP2E1 in Hepa1c1c7 cells	88
3.3 ABP-induced oxidative stress in cell culture and <i>in vivo</i>	91
3.3.1 <i>N</i> -hydroxylation of ABP leads to oxidative stress in Hepa1c1c7 cells	92
3.3.2 Sex and strain differences in liver oxidative stress induced by tumorigenic doses of ABP in neonatal mice	103
3.3.3 Sex differences in liver antioxidant response induced by tumorigenic doses of ABP in neonatal mice	109
Chapter 4 GENERAL DISCUSSION.....	114
4.1 ABP-induced mutations <i>in vivo</i>	115
4.2 ABP metabolic activation by cytochrome P450s.....	121
4.3 ABP-induced oxidative stress in cell culture and <i>in vivo</i>	129
4.4 Overall conclusions and significance.....	139
References.....	141
List of Publications and Abstracts	163
Appendices.....	166
Copyright Acknowledgements.....	194

List of Tables

Table 1. Major classes of chemical carcinogens.....	2
Table 2. Phase II enzymes and their conjugation reactions	16
Table 3. Primer sequences for quantitative PCR.	63
Table 4. ABP-induced mutation spectra in neonatally exposed wild-type and <i>Nat1/2(-/-)</i> Muta TM Mouse.	71
Table 5. ABP-induced mutation spectra in adult wild-type and <i>Nat1/2(-/-)</i> Muta TM Mouse.	73
Table 6. Michaelis-Menten kinetic constants for ABP <i>N</i> -hydroxylation by liver microsomes from male and female wild-type and <i>Cyp1a2(-/-)</i> mice.....	77
Table 7. Michaelis-Menten kinetic constants for ABP <i>N</i> -hydroxylation by liver microsomes from male and female wild-type and <i>Cyp2e1(-/-)</i> mice.....	86

List of Figures

Figure 1. Phase I and phase II drug metabolism, using naphthalene as an example.	13
Figure 2. Sequential oxidation of catechol to quinone generates ROS.....	17
Figure 3. Degradation and activation of NRF2.....	19
Figure 4. Chemical structure of prototypical aromatic amines.....	20
Figure 5. NATs in the <i>N</i> -acetylation (detoxification) and <i>O</i> -acetylation (metabolic activation) of aromatic amines.	23
Figure 6. Proposed mechanism for decoupling of the mitochondrial electron transport chain by <i>N</i> -hydroxy-2-aminofluorene.	25
Figure 7. Metabolic activation and detoxification of ABP in mouse liver.	39
Figure 8. Traditional model of ABP-induced liver carcinogenesis in the mouse.	44
Figure 9. Proposed mechanism of HOABP-induced oxidative stress <i>in vitro</i>	48
Figure 10. Proposed mechanism linking ABP to the formation of methemoglobin and ABP-hemoglobin adducts.	50
Figure 11. Influence of sex and NATs on ABP-induced mutation frequencies in neonatally exposed wild-type and <i>Nat1/2(-/-)</i> Muta TM Mouse.....	68
Figure 12. Influence of sex and NATs on ABP-induced mutation frequencies in adult wild-type and <i>Nat1/2(-/-)</i> Muta TM Mouse.	69
Figure 13. ABP <i>N</i> -hydroxylation by mouse liver microsomes from male and female wild-type and <i>Cyp1a2(-/-)</i> mice.	75
Figure 14. Kinetics of ABP <i>N</i> -hydroxylation by liver microsomes from male and female wild-type and <i>Cyp1a2(-/-)</i> mice	76

Figure 15. Eadie-Hofstee analysis of ABP <i>N</i> -hydroxylation by male and female wild-type and <i>Cyp1a2</i> (-/-) mouse liver microsomes.....	78
Figure 16. Effect of ABT on ABP <i>N</i> -hydroxylation by <i>Cyp1a2</i> (-/-) mouse liver microsomes....	79
Figure 17. Effects of DMSO and acetonitrile on ABP <i>N</i> -hydroxylation by <i>Cyp1a2</i> (-/-) mouse liver microsomes.....	81
Figure 18. Mutual oxidation reaction inhibition between pNP and ABP.....	82
Figure 19. Effect of <i>in vivo</i> pyrazole administration on ABP <i>N</i> -hydroxylation by male and female <i>Cyp1a2</i> (-/-) mouse liver microsomes.....	83
Figure 20. ABP <i>N</i> -hydroxylation by liver microsomes from male and female wild-type and <i>Cyp2e1</i> (-/-) mice.....	84
Figure 21. Kinetics of ABP <i>N</i> -hydroxylation by liver microsomes from male and female wild-type and <i>Cyp2e1</i> (-/-) mice.....	85
Figure 22. Eadie-Hofstee analysis of ABP <i>N</i> -hydroxylation by male and female wild-type and <i>Cyp2e1</i> (-/-) mouse liver microsomes.....	87
Figure 23. In culture HOABP production by <i>Cyp1a2</i> -transfected Hepa1c1c7 cells.....	89
Figure 24. In culture HOABP production by <i>Cyp2e1</i> -transfected Hepa1c1c7 cells.....	90
Figure 25. ABP <i>N</i> -hydroxylation by microsomes isolated from <i>Cyp2e1</i> - or <i>Cyp1a2</i> -transfected Hepa1c1c7 cells, untransfected Hepa1c1c7 cells, and mouse liver.....	91
Figure 26. Effect of ABP on levels of oxidative DNA damage in Hepa1c1c7 cells.....	93
Figure 27. Effect of HOABP on levels of oxidative DNA damage in Hepa1c1c7 cells.....	94
Figure 28. Effect of NAC on HOABP-induced oxidative DNA damage in Hepa1c1c7 cells.....	95
Figure 29. Effects of ABP and HOABP on levels of reactive oxygen species in Hepa1c1c7 cells.....	96

Figure 30. Effect of ABP on levels of oxidative DNA damage and reactive oxygen species in <i>Cyp1a2</i> -, <i>Cyp2e1</i> -, or <i>Nat3</i> -transfected Hepa1c1c7 cells.....	97
Figure 31. Effect of CYP2E1 inhibitors and the antioxidant NAC on ABP-induced reactive oxygen species in <i>Cyp2e1</i> -transfected Hepa1c1c7 cells.....	100
Figure 32. Effect of ABP on levels of oxidative stress in Hepa1c1c7 cells transfected with mitochondria- vs. endoplasmic reticulum-targeting rat <i>Cyp2e1</i>	102
Figure 33. Oxidative DNA damage in male and female mouse livers exposed to tumorigenic doses of ABP.....	104
Figure 34. GSSG levels in male and female mouse livers exposed to tumorigenic doses of ABP.	105
Figure 35. Oxidative DNA damage in male and female <i>Cyp2e1</i> (+/+) and <i>Cyp2e1</i> (-/-) mouse livers exposed to tumorigenic doses of ABP.	107
Figure 36. Oxidative DNA damage in livers of male and female <i>Cyp1a2</i> (-/-) mice exposed to tumorigenic doses of ABP.	108
Figure 37. NRF2 protein expression in livers of male and female mice exposed to tumorigenic doses of ABP.....	110
Figure 38. Expression of oxidative stress-inducible antioxidant genes in livers of male and female mice exposed to tumorigenic doses of ABP.	112

List of Appendices

Appendix A. Transient transfection of <i>Cyp1a2</i> and <i>Cyp2e1</i> into Hepa1c1c7 cells.....	167
Appendix B. Expression and induction of the liver-specific enzyme CYP1A2 in various hepatocyte cultures.....	175
Appendix C. CYP2E1 transcript expression and activity in Hepa1c1c7 cells transfected with different rat <i>Cyp2e1</i> variants.....	183
Appendix D. Basal γ H2AX and NRF2 levels in neonatal male and female C57BL/6 mouse livers.	184
Appendix E. γ H2AX and NRF2 levels in day 8 male and female C57BL/6 mouse livers exposed to ABP.....	185
Appendix F. (Publication).....	186

Abbreviations

γ H2AX	Histone variant H2AX phosphorylated on serine 139
ABP	4-aminobiphenyl
ABT	1-aminobenzotriazole
AcN	acetonitrile
ATP	adenosine triphosphate
BAML cells	bipotent adult mouse liver cells
β NF	beta-naphthoflavone
bp	base pair
C/EBP α	CCAAT-enhancer-binding protein alpha
CYP1A2	cytochrome P450 isoform 1A2
CYP2E1	cytochrome P450 isoform 2E1
DBP	D site of albumin promoter (albumin D-box) binding protein
DCF	dichlorofluorescein
DMBA	1,2-dimethylbenz[<i>a</i>]anthracene
DMSO	dimethyl sulfoxide
DNA	deoxyribonucleic acid
dNTP	deoxyribonucleotide triphosphate
DTT	dithiothreitol
EDTA	ethylenediaminetetraacetic acid
EGFR	epidermal growth factor receptor
GAPDH	glyceraldehyde 3-phosphate dehydrogenase
G6P	glucose-6-phosphate
G6PD	glucose-6-phosphate dehydrogenase
GGT1	gamma-glutamyltransferase 1
GSSG	oxidized glutathione
GSH	glutathione
H ₂ O ₂	hydrogen peroxide
H3	histone 3
HBx	hepatitis B viral protein X
HBV	hepatitis B virus
HCC	hepatocellular carcinoma
HCV	hepatitis C virus
HMOX1	heme oxygenase 1
HOABP	<i>N</i> -hydroxy-4-aminobiphenyl
HPLC	high performance liquid chromatography
HPRT	hypoxanthine-guanine phosphoribosyltransferase
IARC	International Agency for Research on Cancer
IGF	insulin-like growth factors
IKK β	I κ B kinase β
JNK	c-Jun N-terminal kinase
kb	kilobase pairs
MAPK	mitogen-activated protein kinase
MEM	Minimum Essential Medium
mTOR	mammalian target of rapamycin
NAC	<i>N</i> -acetylcysteine

NaCl	sodium chloride
NADP+	nicotinamide adenine dinucleotide phosphate
NQO1	NADPH:quinone oxidoreductase 1
NAT	arylamine <i>N</i> -acetyltransferase
NIH	National Institutes of Health
NRF2	nuclear factor (erythroid-derived 2)-like 2
p38	p38 mitogen-activated protein kinase
PBS	phosphate buffered saline
PCR	polymerase chain reaction
PhD	Doctor of Philosophy
pNP	<i>p</i> -nitrophenol
rCYP2E1	rat CYP2E1
RNA	ribonucleic acid
ROS	reactive oxygen species
rRNA	ribosomal RNA
S.D.	standard deviation
SDS	sodium dodecyl sulfate
SDS-PAGE	sodium dodecyl sulfate-polyacrylamide gel electrophoresis
SULT	sulfotransferase
TCDD	2,3,7,8-tetrachlorodibenzo- <i>p</i> -dioxin
TPA	12- <i>O</i> -tetradecanoylphorbol-13-acetate
Tris	tris(hydroxymethyl)aminomethane
USA	United States of America
VEGFR	vascular endothelial growth factor receptor

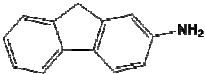
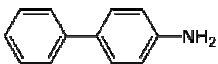
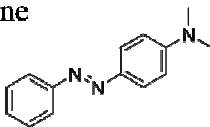
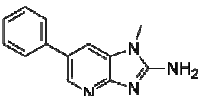
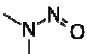
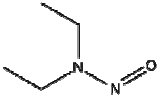
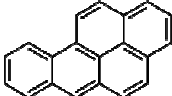
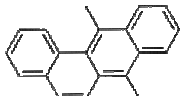
Chapter 1
GENERAL INTRODUCTION

1.1 Chemical carcinogenesis

1.1.1 Overview

As a consequence of the industrial revolution, a rapidly expanding number of synthetic chemicals are now produced and used to enhance every aspect of our modern lives. Such chemicals exist in cosmetics, cigarette smoke, car exhaust, and prepared foods, to name just a few. Unfortunately in many instances, conveniences brought by these chemicals have been more than offset by hidden health costs that they carry. Such grim realizations gave birth to a number of new fields in science, among which is the study of chemical carcinogenesis, or the study of how exposure to chemicals in our environment leads to cancer. Major classes of chemical carcinogens and well-studied examples within each class along with their chemical structures are shown in Table 1.

Table 1. Major classes of chemical carcinogens

Family	Example
aromatic amines	2-aminofluorene  4-aminobiphenyl 
azo dyes	<i>p</i> -dimethylaminoazobenzene 
heterocyclic aromatic amines	2-amino-1-methyl-6-phenylimidazo(4,5-b)pyridine 
<i>N</i> -nitroso compounds	<i>N</i> -nitrosodimethylamine  <i>N</i> -nitrosodiethylamine 
polycyclic aromatic hydrocarbons	Benzo[<i>a</i>]pyrene  7,12-dimethylbenz[<i>a</i>]anthracene 

The history of chemical carcinogenesis can be described as a closely intertwined series of epidemiological observations and animal experiments. In 1761, Hill reported a suspected increase in nasal polyps and cancer with the prolonged and excessive use of tobacco snuff, which was the first reported link between chemical exposure and subsequent cancer development (Redmond, 1970). This link was strengthened by Sir Percival Pott in 1775 when he noted an unusually high incidence of scrotal cancer among chimney sweeps that he suspected to result from exposure to soot (Potter, 1963). Pott's suspicions were confirmed more than a century later in 1917 when Yamagiwa and Ichikawa demonstrated for the first time that application of coal tar, a component of soot, to rabbit ears led to the reliable formation of carcinomas in ear that sometimes metastasized to lymph nodes (Yamagiwa and Ichikawa, 1918). However, coal tar, like most sources of environmental contaminants to which we are exposed, exists as a complex mixture of chemicals, making the attribution of disease to any specific chemical a daunting task. Eventually Cook, Hewett, and Hieger isolated polycyclic aromatic hydrocarbons, such as benzo[*a*]pyrene, from coal tar and demonstrated that application of benzo[*a*]pyrene to mouse skin led to cancer (Cook *et al.*, 1933). These discoveries gave birth to the first major class of human carcinogens known to man, the polycyclic aromatic hydrocarbons.

1.1.2 The multi-stage model of chemical carcinogenesis

In the initial studies by Yamagiwa and Ichikawa, tar was applied continuously to rabbit ear in order to produce carcinomas (Yamagiwa and Ichikawa, 1918). By altering this exposure paradigm, Rous revealed a fundamental principle in chemical carcinogenesis, namely, the "multi-stage" nature of this process. Rous found that a brief exposure to tar created "initiated" cells in rabbit ear, which otherwise looked normal but upon re-exposure to tar rapidly developed into highly malignant tumors (MacKenzie and Rous, 1941; Rous and Kidd, 1941). Intriguingly, a diverse array of irritants that are themselves non-carcinogenic, such as wounding, turpentine, and viral infection, was as effective as tar at triggering the conversion of initiated cells into highly malignant tumors. At around the same time, Berenblum made similar observations with regard to benzo[*a*]pyrene-induced skin carcinogenesis. A brief exposure to benzo[*a*]pyrene created initiated cells in the skin that are otherwise normal but can be readily "promoted" to form tumors in the presence of croton resin, a non-carcinogenic irritant (Berenblum, 1941). These observations led to the division of the process of chemical carcinogenesis into different temporal

stages. In the initiation stage, chemical carcinogens transform normal cells into initiated cells, which are primed for subsequent development into tumors. In the promotion stage, irritating agents that are themselves non-carcinogenic induce the proliferation of initiated cells to form benign tumors. Later events in the promotion stage can also be characterized as a distinct tumor "progression" stage, where further alteration of transformed cells leads to their metastasis and invasion into adjacent tissues in the process of transforming a benign tumor into a malignant tumor (Foulds, 1954). We now know that various stages of this model can occur more or less simultaneously given the complex nature of chemical mixtures that humans are constantly exposed to; however this relatively simple multi-stage representation of chemical carcinogenesis has served as a key conceptual framework for subsequent investigations into the mechanisms of chemical carcinogenesis. To aid in the description of the multi-stage model of chemical carcinogenesis, I will mainly draw examples from 7,12-dimethylbenz[*a*]anthracene (DMBA)-induced skin carcinogenesis in the mouse, which provided most of the experimental data that established the principles of this model.

1.1.3 DNA modifications and tumor initiation

How do chemical carcinogens transform normal cells into initiated cells? A seminal observation was made by Miller and Miller, who fed the azo dye *p*-dimethylaminoazobenzene to rats and observed its covalent binding in the liver, the known target tissue for subsequent tumor development (Miller and Miller, 1947). Furthermore, there was a significant correlation between level of dye binding and tumor outcome that held true across different species (Miller and Miller, 1947). Based on these observations, the Millers were the first to propose that binding of a chemical carcinogen within its target tissue may be important for carcinogenicity. But where in the target tissue does carcinogen binding occur and how does this initiate carcinogenesis? The discovery of DNA as the carrier of hereditary information from one generation of cells to the next immediately made DNA an ideal target for chemical carcinogens. In 1964, Brookes and Lawley measured the binding of polycyclic aromatic hydrocarbons to different cellular macromolecules *in vitro* and found a significant correlation between their carcinogenicity and their level of binding to DNA, but not to RNA or protein (Brookes and Lawley, 1964). This initiated a flurry of studies that reported positive correlations between carcinogenicity of chemical carcinogens *in vivo* and their ability to bind to DNA *in vitro*. Using a multi-stage

mouse skin carcinogenesis model, this correlation was further broken down to reveal a positive correlation between DNA binding and tumor initiating properties of chemical carcinogens. For example, tumor initiating agents with weak tumor promoting activity, such as DMBA, dose-dependently bound to DNA *in vitro*; on the other hand, tumor promoting agents with no tumor initiating activity, such as 12-*O*-tetradecanoylphorbol-13-acetate (TPA), failed to do so. In addition, agents that blocked tumor initiation by DMBA *in vivo*, such as 2,3,7,8-tetrachlorodibenzo-*p*-dioxin (TCDD), also blocked DNA binding by DMBA *in vitro* (Slaga *et al.*, 1982).

Aside from binding directly to DNA, chemical carcinogens can also damage DNA indirectly by producing oxidative stress, which is defined as an imbalance between the production of reactive oxygen species (ROS) and the ability to detoxify them. At least two families of chemical carcinogens have been suggested to produce oxidative DNA damage: estrogens and polycyclic aromatic hydrocarbons. The proposed redox mechanism for both of these chemical classes involves spontaneous one electron oxidations from their catechol forms, products of phase I metabolism (see Section 1.1.5), to quinone forms and in the process releasing ROS (Figure 2, (Lind *et al.*, 1982)). In turn, ROS can attack DNA directly leading to the formation of DNA oxidation products, such as 8-oxo-deoxyguanosine. Oxidation products of DNA, particularly 8-oxo-deoxyguanosine, have been routinely detected following exposure to polycyclic aromatic hydrocarbons and their metabolites (Park *et al.*, 2005; Park *et al.*, 2006; Park *et al.*, 2008; Penning *et al.*, 1996; Shen *et al.*, 2006). In addition, reactive oxygen species can attack lipids leading to the formation of reactive lipid peroxidation products that can also bind to DNA (Penning, 2011). Oxidative DNA modifications have been implicated in tumor initiation by chemical carcinogens. For example in the DMBA multi-stage mouse skin carcinogenesis model, application of antioxidants such as butylated hydroxytoluene (BHT), butylated hydroxyanisole (BHA), or vitamin E completely abolished the tumor initiating properties of DMBA (Slaga *et al.*, 1982). This being said, direct evidence that links oxidative DNA damage to tumor initiation by chemical carcinogens is lacking, since most studies have focused on the roles of oxidative DNA damage in tumor promotion and tumor progression.

At this point it should be noted that *in vitro* DNA modifications by most chemical carcinogens only occur in the presence of tissue homogenates and reduced nicotinamide adenine dinucleotide

phosphate (NADPH). As we shall see in Section 1.1.5, these additives provide functional metabolic enzymes that activate chemical carcinogens to their "ultimate" reactive forms.

The majority of DNA damage induced by chemical carcinogens, whether in the form of bulky DNA adducts or oxidative DNA lesions, are repaired by DNA repair enzymes. Bulky DNA adducts, such as those that arise from binding of polycyclic aromatic hydrocarbons and aromatic amines to DNA, are primarily repaired by the nucleotide excision repair pathway (Gillet and Scharer, 2006; Jackson and Bartek, 2009). On the other hand, oxidative DNA lesions, such as 8-oxo-deoxyguanosine and DNA single-strand breaks, are mostly repaired by the base excision repair pathway (David *et al.*, 2007; Jackson and Bartek, 2009). Some overlap in substrate specificity is found between these two DNA repair pathways. The efficiency and accuracy of both nucleotide and base excision repair are guided by many factors, such as type of lesion, sequence context, proliferative state of cell, and cellular localization (nuclear vs. mitochondrial). In instances where DNA damage is not repaired or is misrepaired, mutations arise.

1.1.3.1 Mutations

Long before the discovery of DNA, the somatic mutation theory of cancer had already suggested that something heritable must have been "mutated" in a tumor cell which provides a "tumor-like" phenotype (Bauer, 1928; Boveri, 1929; Boveri, 2008). When DNA's structure and role as the carrier of hereditary information were discovered in the 1950s, DNA was immediately proposed to be the carrier of mutations that gets passed from one generation of tumor cells to the next, with mutations representing permanent changes in the sequence of DNA (Watson and Crick, 1953). Compared to the unstable and transient nature of DNA lesions, one important feature of mutations is their irreversibility. It is the irreversibility of mutations that makes tumor initiation an irreversible and cumulative process; it is also the irreversibility of mutations that makes them ideal targets for quantification.

Various *in vitro* and *in vivo* assays based on both bacterial and mammalian systems have been used to measure the mutagenicity of chemicals. Perhaps the most widely used assay for the quantification of mutations is the Ames test (Roth and Ames, 1966). In this assay, a mutation is engineered into bacteria that prevents their growth on bacterial plates containing a particular growth medium. These bacteria are then exposed to a chemical of interest and tested for

reversion of the engineered mutation so as to allow them to grow into colonies. Counting the number of revertant colonies, in turn, provides a quantification of mutagenicity for the chemical of interest. Different types of mutations can be engineered into different strains of bacteria to provide information on the type(s) of mutation introduced by different chemicals. The sensitivity of the Ames test has been greatly improved with the introduction of repair-deficient bacterial strains; however, this also means that the Ames test does not take into account the effect of DNA repair on the eventual mutation profile. Overall, the Ames test represents a simple, sensitive, and economical test for the detection of chemical mutagenicity. One major drawback of the Ames test lies in the different metabolic capabilities of prokaryotes compared to mammalian cells, which led to the initial misclassification of several known chemical carcinogens as non-mutagens (Hollander, 1984). To circumvent this problem, post-mitochondrial tissue homogenates from rat liver (the 9000 x g supernatant, or "S9" fraction) were added to the Ames test as a source of mammalian metabolic enzymes. For example, the chemical carcinogen DMBA is non-mutagenic in the traditional Ames test and only becomes mutagenic in the presence of rat liver S9 fraction (Ames *et al.*, 1973). Another drawback of the Ames test is the tendency for generating false positives with extremely reactive chemicals, such as the ultimate carcinogens to be discussed in Section 1.1.5, since it is much easier for these compounds to act on the genome of bacterial cells that are in direct contact with the chemical solution than on the genome of target mammalian cells that are often separated from chemical exposure by other cells, extracellular matrix, blood, etc. Finally, the Ames test requires some foresight in choosing the appropriately engineered bacterial strain for detecting the expected type of mutation induced by a chemical of interest, which is not always available. Such issues for the Ames test also apply to most other bacteria-based and mammalian cell culture-based mutation detection systems, all of which can be circumvented in mutation assays that are based on *in vivo* mammalian systems.

In the last two decades, the increasing popularity of transgenic mice coupled with the decreasing cost of DNA sequencing have led to the development of transgenic mouse models for the detection of both mutation frequencies and spectra induced by chemicals of interest *in vivo*. The most popular of these transgenic mouse models are the MutaTMMouse and Big Blue rats and mice. The genomes of both MutaTMMouse and Big Blue contain a bacteriophage transgene that has no function in mammalian cells. Following *in vivo* exposure to a potential mutagen, this

transgene can be recovered from the tissue of interest and packaged into bacteriophage particles that are subsequently used to infect bacteria. Bacteria infected with a transgene that has been mutated so as to disrupt its function in bacteria form plaques under different growth conditions compared to bacteria infected with a non-mutated wild-type transgene. The ratio of the number of plaques that form under each growth condition represents the mutation frequency of the transgene induced by the potential mutagen *in vivo* in the tissue of interest. In addition, the transgenes in mutant plaques can be sequenced to determine the mutational spectrum induced by the potential mutagen *in vivo* in the tissue of interest. Compared to the Ames test, the most obvious advantage of the transgenic animal approach is its ability to incorporate effects of carcinogen metabolism and DNA repair on measured mutagenicity. This is not a trivial improvement given that most chemical carcinogens require metabolic activation to generate DNA lesions (as we shall see in Section 1.1.5), and that most DNA lesions are faithfully repaired by DNA repair machineries in our body. In addition, sequencing of the transgene allows a relatively unbiased survey of the *in vivo* mutation spectra. Despite marked improvements from bacteria-based assays, several shortcomings of *in vivo* mutation assays based on transgenic animals must still be kept in mind during the interpretation of results. DNA repair in the transgene, which is not transcribed in mammalian cells, may be different compared to that in actively transcribed regions in the genome. In addition, only mutations that disrupt the function of the transgene (i.e. non-silent mutations) are detected in mutation assays based on transgenic animals. Finally, species differences that may exist between rodents and humans with regard to metabolizing and repair enzymes would apply here as well.

In general a good correlation is found between mutagenicity and carcinogenicity of a given chemical (Rinkus and Legator, 1979). For example, members of the polycyclic aromatic hydrocarbon chemical family that are known to be carcinogenic (such as DMBA and dibenz[*a,h*]anthracene) are also mutagenic; on the other hand, polycyclic aromatic hydrocarbons that are known to be not carcinogenic (such as benzo[*e*]pyrene, and dibenz[*a,c*]anthracene) are also not mutagenic (Hollander, 1984). But how do mutations transform normal cells into initiated cells?

Most mutations induced by chemical carcinogens have no phenotypic effect - only when mutations affect functions of tumor suppressors and/or oncogenes do they contribute to the

transformation of a normal cell into an initiated one or a benign growth into a malignant tumor. Perhaps the best-studied example is mutations of the *Hras* oncogene in the multi-stage mouse skin carcinogenesis model. HRAS is a small GTPase protein that cycles between an active GTP-bound state and an inactive GDP-bound state. In turn, HRAS acts as a molecular switch that regulates cellular proliferation, differentiation, survival, and cell-cell interaction. Activating mutations in *Hras* lock HRAS in the active form, which provide cells with a growth advantage by increasing proliferation, promoting de-differentiation, inhibiting apoptosis, and stimulating cell motility (reviewed in (Penning, 2011)). *Hras* mutations have been observed in both papillomas and carcinomas in DMBA-induced mouse skin carcinogenesis, suggesting a potential role for HRAS in both initiation and promotion stages of this model (Balmain and Pragnell, 1983; Balmain *et al.*, 1984). As discussed previously, DMBA has been shown to bind to DNA and generate mutations in various *in vitro* and *in vivo* assays. Combining these observations, the ability for DMBA to generate mutations in *Hras* was established. Furthermore, DMBA induced a unique mutation spectrum in *Hras* with the most abundant mutation being an A to T transition in codon 61 (Brown *et al.*, 1990). Subsequently, several lines of evidence established *Hras* mutations, especially the A to T transition on codon 61, as initiating events that transformed normal skin cells into initiated cells. In one line of evidence, transgenic mice that over-express HRAS in skin developed tumors in the absence of an initiating agent such as DMBA (Bailleul *et al.*, 1990). In another line of evidence, mice deficient in HRAS were protected from DMBA-induced skin carcinogenesis (Ise *et al.*, 2000). Finally, mice deficient in STAT3, a downstream effector of HRAS, were also protected from DMBA-induced skin carcinogenesis (Kim *et al.*, 2009). In humans, *Hras* or its isoforms *Kras* and *Nras* are mutated in 15-20% of all cancers (Rajalingam *et al.*, 2007).

Aside from HRAS, mutations in a number of different oncogenes and tumor suppressors have been characterized and implicated in various chemically-induced cancers. In humans, *TP53* is the most frequently mutated tumor suppressor. P53 is a transcription factor that controls transcription of a number of genes involved in DNA repair, cell cycle arrest, and apoptosis (Meek, 2009; Sengupta and Harris, 2005). Inactivating mutations in *TP53* have been suggested to provide cells with a growth advantage by inhibiting apoptosis, interfering with proper DNA repair, and facilitating aberrant cell cycle re-entry. A well-established example that links *TP53*

mutations to chemical carcinogenesis in humans is illustrated with the liver carcinogen aflatoxin B1. Studies carried out *in vitro* and in cell culture have shown that aflatoxin B1 forms adducts with DNA and leads to a G to T mutation at codon 249 of *TP53* (Aguilar *et al.*, 1993; Foster *et al.*, 1983; Puisieux *et al.*, 1991). Subsequent epidemiological studies confirmed these laboratory findings with the frequent detection of G to T mutations at codon 249 of *TP53* in liver cancer patients exposed to aflatoxin B1 (Bressac *et al.*, 1991; Hsu *et al.*, 1991; Rajalingam *et al.*, 2007; Yeh *et al.*, 1998). It should be noted that oxidative DNA lesions, specifically 8-oxo-deoxyguanosine, introduced by cigarette smoke and other carcinogens can also lead to G to T mutations at codon 249 of *TP53* (Hussain *et al.*, 1994; Park *et al.*, 2008; Shen *et al.*, 2006). These studies established *TP53* as a mutagenic target for chemical carcinogens; however, the extent to which mutations in *TP53* contribute to the etiology of human cancer remains unclear. In general, the link between chemically-induced mutations in oncogenes/tumor suppressors and tumor initiation is mostly inferred from their known functions in providing cells with a growth advantage with the only exception being mutations in *Hras*, which were vigorously tested in the multi-stage skin carcinogenesis model as described previously. This link is further complicated by the fact that a chemical carcinogen can target multiple tumor suppressors/oncogenes simultaneously and that mutations in any one gene is often insufficient to drive tumor initiation. Nevertheless, it is now widely accepted that mutations in oncogenes and tumor suppressors confer a growth advantage to initiated cells, which are histologically indistinguishable from normal cells but can be triggered by a variety of tumor promoters to develop into a tumor.

1.1.4 Tumor promotion and progression

Unlike the process of tumor initiation, which has been characterized relatively well, less is known about molecular mechanisms behind tumor promotion and tumor progression. In the tumor promotion stage, initiated cells expand into a benign tumor. A number of tumor promoting agents have been characterized that do not modify DNA but can increase the expression and function of genes that promote cell growth and prevent cell death, often through the induction of inflammation and oxidative stress. For example, administration of TPA as a prototypical tumor promoting agent in the multi-stage mouse skin carcinogenesis model led to increases in both inflammation and oxidative stress that in turn stimulated a cascade of cell signaling pathways resulting in epidermal hyperproliferation (Boutwell, 1964; Perchellet *et al.*, 1987; Slaga *et al.*,

1976; Wei and Frenkel, 1993). In this model, deficiency in STAT3, a major cell mediator of inflammation, protected mice from skin papillomas (Chan *et al.*, 2004; Kim *et al.*, 2009). In the same model, administration of antioxidants or over-expression of antioxidant enzymes also protected mice from skin papillomas (Bilodeau and Mirault, 1999; Perchellet *et al.*, 1987; Zhao *et al.*, 2001). In the tumor progression stage, continued tumor growth and metastasis take place. It should be noted that considerable overlap exists between the promotion and progression stages of chemical carcinogenesis. Molecular mechanisms underlying tumor progression include chromosomal abnormalities, increased cell motility, and stromal invasion by tumor cells. In the multi-stage skin carcinogenesis mouse model, conversion from papillomas (benign) to squamous cell carcinomas (malignant) is associated with an increase in chromosomal abnormalities often culminating in aneuploidy after 30 to 40 weeks of continuous tumor promotion (Aldaz *et al.*, 1987; Conti *et al.*, 1986). Increased chromosomal abnormalities dramatically increase the rate of mutations in genes that control other processes necessary for tumor progression. Finally, decreased expression of E-cadherins and increased expression of matrix metalloproteinases lead to reactivation of epithelial-mesenchymal transition and stromal invasion by papilloma cells, resulting in metastasis (Kang and Massagué, 2004; Munshi and Stack, 2006).

1.1.5 Metabolic activation and detoxification of chemical carcinogens

In 1842, Keller detected and characterized hippuric acid in his own urine after ingesting large quantities of benzoic acid (Keller, 1842). This is the first study that suggested xenobiotics are metabolized in the mammalian body. A hundred years later in the 1940s, extensive work performed in laboratory of the Millers established many of the principles of chemical carcinogen metabolism that we know today. In one of their first studies, forty potential metabolites of the chemical carcinogen *p*-dimethylaminoazobenzene were fed to rats, and all except one (*p*-methylaminoazobenzene) were less carcinogenic than the parent compound (Miller and Miller, 1947). This study was the first to suggest that metabolism of a chemical carcinogen may alter its carcinogenicity. Subsequently, in a series of studies on the acetylated aromatic amine carcinogen 2-acetylaminofluorene, the Millers identified the novel urinary metabolite *N*-hydroxy-2-acetylaminofluorene, which upon injection into rats demonstrated markedly greater carcinogenicity than the parent compound (Cramer *et al.*, 1960). The importance of these studies is two-fold: firstly, this was the first demonstration of aromatic amine *N*-hydroxylation reactions

occurring *in vivo*, which has profound implications for my PhD project as we shall see in later chapters; and secondly, this suggested for the first time that *in vivo* metabolic activation may be key to the carcinogenicity of a chemical carcinogen.

We now know that most characterized chemical carcinogens are, in fact, relatively inert and require some form of metabolism to an active form in order to exert their carcinogenic effects. In addition, metabolism of chemical carcinogens can lead to metabolites that are either more carcinogenic or less carcinogenic than the parent compound. Since binding of chemical carcinogens to cellular macromolecules initiates chemical carcinogenesis, metabolic reactions that generate metabolites more reactive than their parent compounds are referred to as "metabolic activation" reactions, whereas metabolic reactions that generate metabolites less reactive than their parent compounds are referred to as "detoxification" reactions. A chemical carcinogen may undergo both metabolic activation and detoxification reactions. As a result, the carcinogenicity of a compound will depend on the net balance of competing metabolic activation and detoxification pathways, both of which are controlled by drug-metabolizing enzymes.

Historically, enzymes involved in the metabolism of xenobiotics are divided into two major classes: phase I and phase II enzymes. Phase I enzymes introduce polar groups mostly through oxidation and reduction reactions onto the parent compound, and phase II enzymes add larger, often polar side groups such as glucuronide, sulfate, or glutathione onto the newly formed group from phase I metabolism. A simple schematic representation of phase I and phase II metabolism using naphthalene as an example is shown in Figure 1 (Penning, 2011).

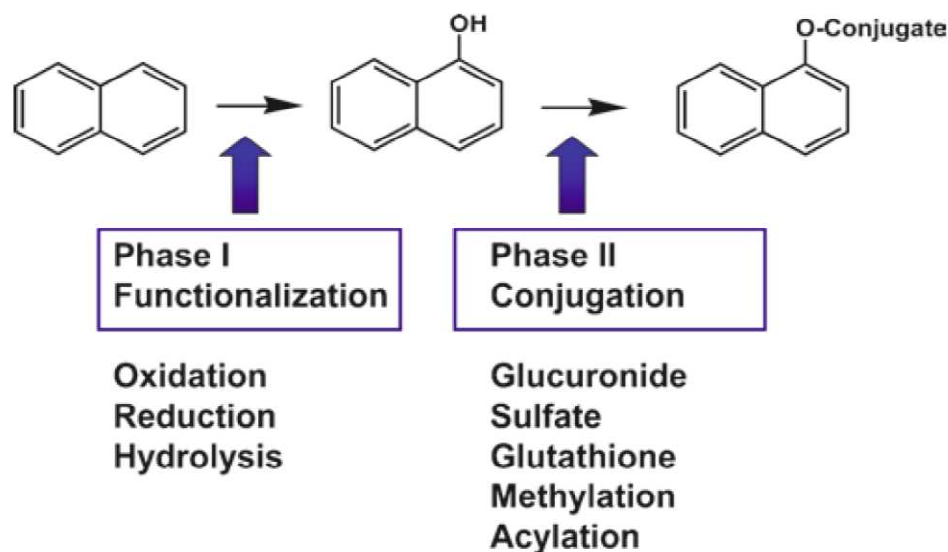


Figure 1. Phase I and phase II drug metabolism, using naphthalene as an example.

© Figure taken from Penning 2011 with permission from Springer.

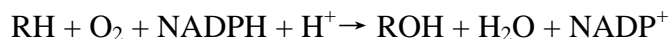
It should be noted that the metabolism of xenobiotics does not necessarily occur sequentially with phase I followed by phase II metabolism; for example, phase II enzymes can also directly modify the parent compound, as we shall see in Section 1.2.4.1 with arylamine *N*-acetyltransferases. Under normal circumstances, both phase I and phase II enzymes facilitate the inactivation and/or excretion of xenobiotics; however in the case of chemical carcinogens, metabolism can also convert an inert chemical (a procarcinogen) into an "ultimate" carcinogen.

1.1.5.1 Cytochromes P450

In 1948, Mueller and Miller first reported that addition of several cofactors dramatically increased the conversion of *p*-dimethylaminoazobenzene to its metabolites by liver homogenates *in vitro*. These cofactors include diphosphopyridine nucleotide (now commonly known as reduced nicotinamide adenine dinucleotide phosphate, NADPH), magnesium chloride, and an oxidizable substrate (such as hexose diphosphate). Requirement of physiological conditions and re-generating cofactors strongly supported the involvement of an enzyme in the metabolism of carcinogens (Mueller and Miller, 1948; Mueller and Miller, 1953). In addition, this enzyme was located to the microsomal fraction of liver homogenates (Mueller and Miller, 1949). The stage

was set for discovery of the largest family of phase I enzymes responsible for metabolism of chemical carcinogens, the cytochromes P450 (CYPs).

In 1962, Omura and Sato successfully characterized a novel hemoprotein from liver microsomes that they referred to as cytochrome “P-450” due to the distinct absorption peak of its reduced, carbon monoxide bound form at 450 nm (Omura and Sato, 1962). Early work in the field of steroid metabolism established this cytochrome “P-450” as the microsomal enzyme that carried out hydroxylation on C-21 of steroids (Estabrook, 2003). Subsequently it was found that aside from endogenous substrates, such as steroids, vitamins, and prostaglandins, CYPs can also metabolize xenobiotics including chemical carcinogens (Estabrook, 2003). Today, the cytochrome P450 superfamily of monooxygenases represents one of the largest known families of proteins, with 57 human and 102 mouse isoforms identified that are categorized into families and subfamilies based on sequence similarities (Nelson *et al.*, 2004). Out of 18 known families of CYPs, families 1 to 4 are most heavily associated with the metabolism of xenobiotics including chemical carcinogens, whereas families 5 to 18 are mostly concerned with the metabolism of endogenous compounds. The liver represents a major site for the expression of CYPs, although extrahepatic expression is also commonly found. Intracellularly, most CYPs are located in the endoplasmic reticulum, which partitions to the microsomal fraction of liver homogenates, but some cytochrome P450 isoforms are also found in the mitochondria (Guengerich, 1987). The most common oxidation reaction carried out by CYPs is as follows (“R” = substrate):



In most cases, transfer of electrons from NADPH to the heme iron of cytochrome P450 is carried out by NADPH-cytochrome P450 oxidoreductase, which is an essential auxiliary enzyme for cytochrome P450 activity. In addition to oxidation reactions, CYPs can also carry out a variety of other enzymatic reactions such as reduction and hydrolysis reactions, all of which are involved in the metabolic activation and/or detoxification of chemical carcinogens. In fact, such a broad spectrum of substrates represents a hallmark of the cytochrome P450 superfamily of enzymes, making it the most important class of enzymes in both metabolic activation and detoxification of chemical carcinogens.

A notable feature of CYPs that also played a major role in their discovery is their inducibility. This property of CYPs was first identified in the field of chemical carcinogenesis with studies on *p*-dimethylaminoazobenzene, where *in vivo* administration of the polycyclic aromatic hydrocarbon 3-methylcholanthrene protected rats against *p*-dimethylaminoazobenzene-induced liver tumors through increased demethylation and reduction of dimethylaminoazobenzene by microsomal enzymes (Conney *et al.*, 1956; Richardson and Cunningham, 1951). This was the first reported induction of CYPs, in this case enhancing the detoxification of *p*-dimethylaminoazobenzene. Today, the best characterized families of cytochrome P450 inducers include polycyclic aromatic hydrocarbons, such as 3-methylcholanthrene described above, and barbiturates, such as phenobarbital. Although some overlap and exceptions exist, polycyclic aromatic hydrocarbons mostly lead to the induction of family 1 members of CYPs, whereas barbiturates mostly lead to the induction of family 2 members of CYPs.

CYPs are not the only enzymes that carry out phase I metabolism of chemical carcinogens. Flavin monooxygenases, peroxidases, short-chain dehydrogenases/reductases, aldo-keto reductases, and epoxide hydrolases among other enzymes can also carry out phase I metabolism of chemical carcinogens, albeit to a lesser extent than CYPs.

1.1.5.2 Phase II enzymes

For some chemical compounds, metabolism by Phase I enzymes is followed by Phase II enzymes. A list of major phase II enzymes and the conjugation reactions they carry out are shown in Table 2.

Table 2. Phase II enzymes and their conjugation reactions

phase II enzyme	conjugation reaction
arylamine <i>N</i> -acetyltransferases	acetylation
glutathione <i>S</i> -transferases	glutathione conjugation
catechol- <i>O</i> -methyltransferases	methylation
sulfotransferases	sulfation
UDP-glucuronosyltransferases	glucuronidation

Phase II metabolism often increases the water solubility of chemical compounds and facilitates their excretion through bile, urine, or feces. For example, glucuronidation products have pKa around 4.0 which confers a negative charge to chemical compounds at physiological pH. The presence of a negative charge in turn makes chemical compounds highly soluble in the aqueous environment of our body and more easily excreted via anion transport systems in the bile duct and kidney. Notable exceptions to this paradigm of phase II metabolism are arylamine *N*-acetyltransferases and catechol-*O*-methyltransferases. Unlike other phase II enzymes listed in Table 2, metabolism by arylamine *N*-acetyltransferases and catechol-*O*-methyltransferases leads to the formation of less polar compounds, which are nonetheless considered detoxification pathways because they can terminate the pharmacological activity of drugs, or prevent the formation of more reactive compounds via alternative pathways. In addition, phase II enzymes may directly act on chemical compounds in the absence of phase I metabolism.

Unfortunately, the phase II conjugation of chemical carcinogens can also contribute to their metabolic activation. In initial studies with 2-acetylaminofluorene, its phase I metabolite *N*-hydroxy-2-acetylaminofluorene failed to react with DNA and form DNA adducts *in vitro* (Miller and Miller, 1966). This suggested that additional metabolism *in vivo* may be required to generate the ultimate carcinogen that readily binds to DNA. Through analysis of metabolites bound to DNA and experimentation with synthesized chemical precursors that would facilitate such binding, it was eventually revealed that formation of *O*-esters with sulfate or acetate converted

N-hydroxy-2-acetylaminofluorene into an ultimate carcinogen that readily bound to DNA *in vitro* (DeBaun *et al.*, 1968; Kerdar *et al.*, 1993; Miller *et al.*, 1966; Miller and Miller, 1981). The roles of *O*-sulfation and *O*-acetylation by sulfotransferases and arylamine *N*-acetyltransferases, respectively, in the metabolic activation of aromatic and heterocyclic amines are now well established. In cases where an enzyme can both metabolically activate and detoxify a chemical carcinogen, the eventual physiological consequence of metabolism will depend on the net balance of both pathways, as we shall see in the metabolism of aromatic amines by arylamine *N*-acetyltransferases as an example in Section 1.2.4.1.

1.1.5.3 Antioxidant enzymes

Antioxidant enzymes, which are enzymes that protect cells against oxidative stress, have been proposed to be involved in the detoxification of chemical carcinogens. A potentially key antioxidant enzyme that protects against chemical carcinogens is NAD(P)H:quinone oxidoreductase isoform 1 (NQO1). NQO1 carries out two-electron reduction reactions that prevent the formation of reactive quinones from catechols, a process that also generates ROS (Figure 2, (Gaikwad *et al.*, 2007; Lind *et al.*, 1982; Montano *et al.*, 2006)).

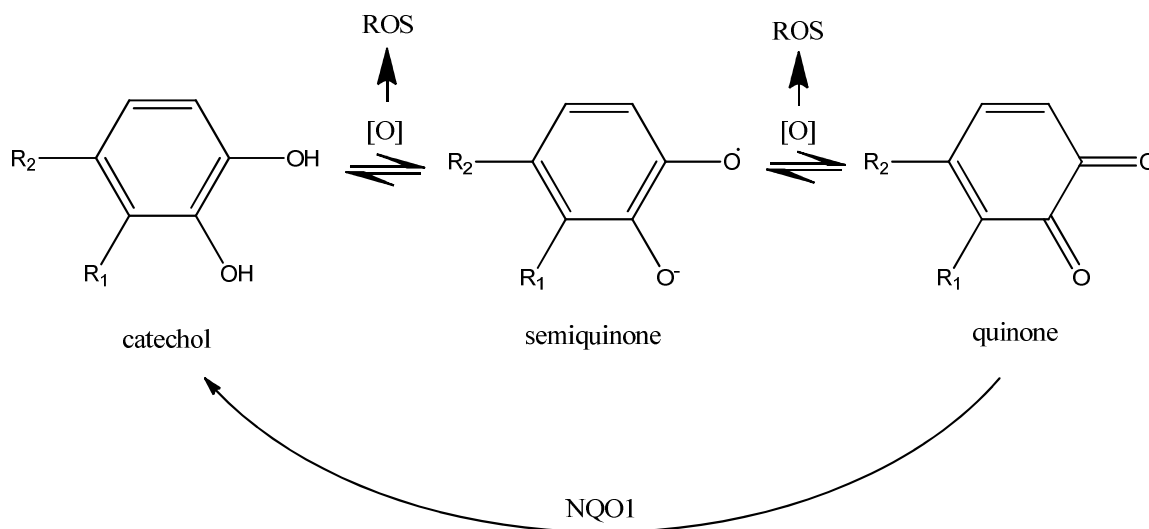


Figure 2. Sequential oxidation of catechol to quinone generates ROS.

"[O]" = oxidation reaction. "ROS" = reactive oxygen species. "R1" and "R2" = different functional groups of chemical carcinogens.

These catechols can be subsequently detoxified by catechol-*O*-methyltransferases (Penning, 2011). Several studies have supported the role of NQO1 in the detoxification of estrogens. *In vitro*, NQO1 directly reduced levels of quinone estrogen (Gaikwad *et al.*, 2007). In cell culture, down regulation of NQO1 led to an increase in quinone adducts of estrogen and cell transformation potential (Montano *et al.*, 2006). Finally, induction of NQO1 expression *in vivo* protected against estrogen-induced mammary tumors in rats (Montano *et al.*, 2006). It should be noted that evidence supporting a role of NQO1 in the detoxification of estrogen is still relatively circumstantial, and further studies are warranted (Chandrasena *et al.*, 2008).

Expression of NQO1 is regulated by the transcription factor nuclear factor (erythroid-derived 2)-like 2 (NRF2), which in recent years has been increasingly recognized as a major player in the cellular defense against oxidative stress (Kensler *et al.*, 2007; Slocum and Kensler, 2011). NRF2 is normally anchored in the cytoplasm by Kelch-like ECH-associated protein 1 (KEAP1), which binds to NRF2 and facilitates its ubiquitination and degradation. In the presence of oxidative or electrophilic stress, cysteine residues on KEAP1 become modified, leading to the release and nuclear translocation of NRF2 (Kensler *et al.*, 2007). Once inside the nucleus, NRF2 heterodimerizes with small MAF proteins, binds to antioxidant response elements in the genome, and activates transcription of antioxidant and phase II enzymes including NQO1, glutamate-cysteine ligase catalytic subunit (GCLC), heme oxygenase 1 (HMOX1), gamma-glutamyltransferase 1 (GGT1), glutathione *S*-transferases (GSTs), UDP-glucuronosyltransferases (UGT), and multidrug resistance-associated proteins (MRPs, Figure 3, (Kensler *et al.*, 2007)).

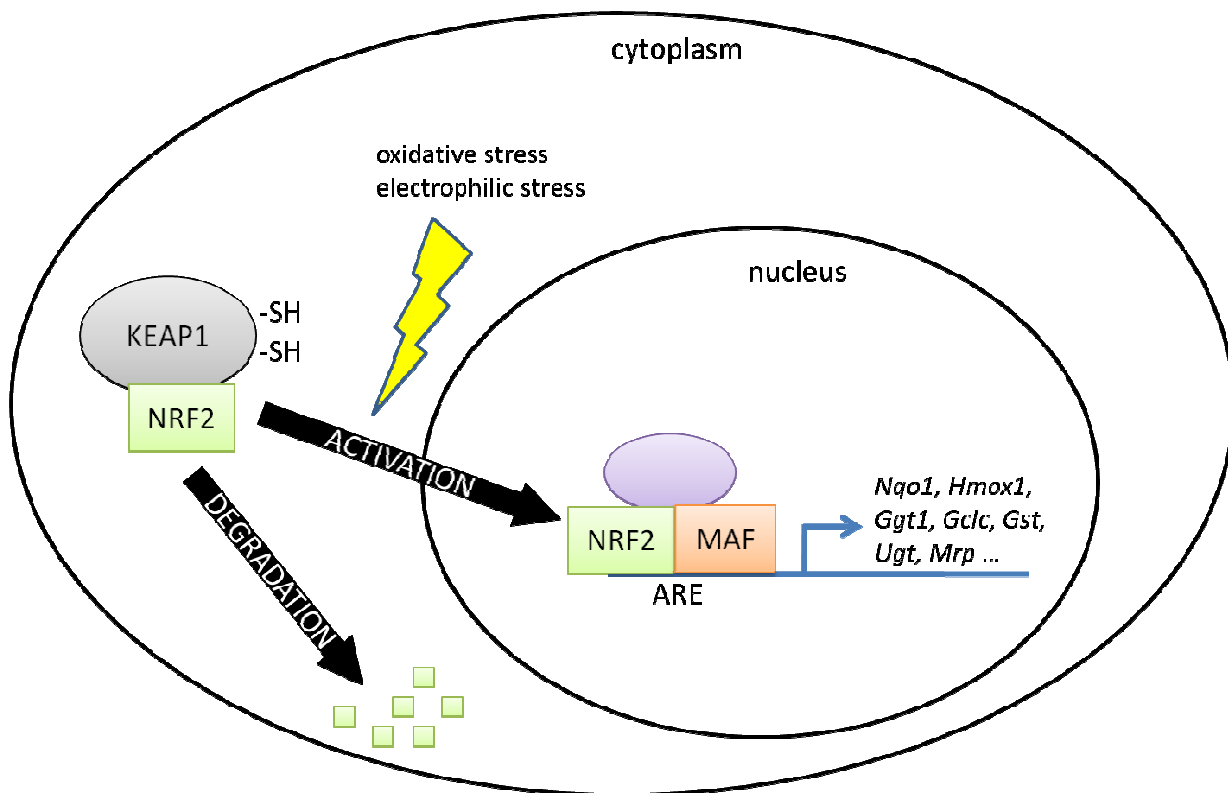


Figure 3. Degradation and activation of NRF2.

Regulation of such a diverse array of cytoprotective genes predicts a central role for NRF2 in cellular defense against chemical carcinogens. Indeed, NRF2 deficient mice demonstrate increased tumorigenicity, whereas mice treated with NRF2 inducers demonstrate decreased tumorigenicity, following exposure to chemical carcinogens such as benzo[*a*]pyrene, DMBA, aflatoxin B1, and hydroxybutyl-nitrosamine (Slocum and Kensler, 2011). In humans, administration of NRF2 inducers reduced the metabolic activation and thus the carcinogenicity of aflatoxin B1 (Wang *et al.*, 1999).

1.2 Aromatic amines

1.2.1 Bladder cancer and occupational dye exposure

Aromatic amines represent one of the largest and best characterized families of chemical carcinogens. As early as 1895, the German physician Rehn reported a suspected link between dye factory workers and bladder cancer based on his observation that two of his bladder cancer patients had worked in the same dye factory (Rehn, 1895). In 1912, Leuenberger reported a

stronger link between dye factory workers and bladder cancer when he analyzed all cases of bladder tumors in Basel and found that approximately half were dye factory workers (Leuenberger, 1912). Since the most common chemical used in dye factories at the time was aniline, Rehn and others had initially attributed bladder tumors to aniline exposure and referred to them as “aniline tumors” (Radomski, 1979). These epidemiological observations made in industrial settings were the first to bring attention to the potential carcinogenicity of aromatic amines.

1.2.2 Aromatic amines as a major class of carcinogens

Driven by initial observations of “aniline tumors” in dye factory workers, animal studies were carried out with aniline in attempts to reproduce bladder tumors with similar histological features. However, most animal studies with aniline failed to produce bladder tumors (Radomski, 1979). At the time it was already known that aniline belongs to a group of chemicals collectively called aromatic amines, which are amines attached to aromatic substituents (prototypical aromatic amines are shown in Figure 4).

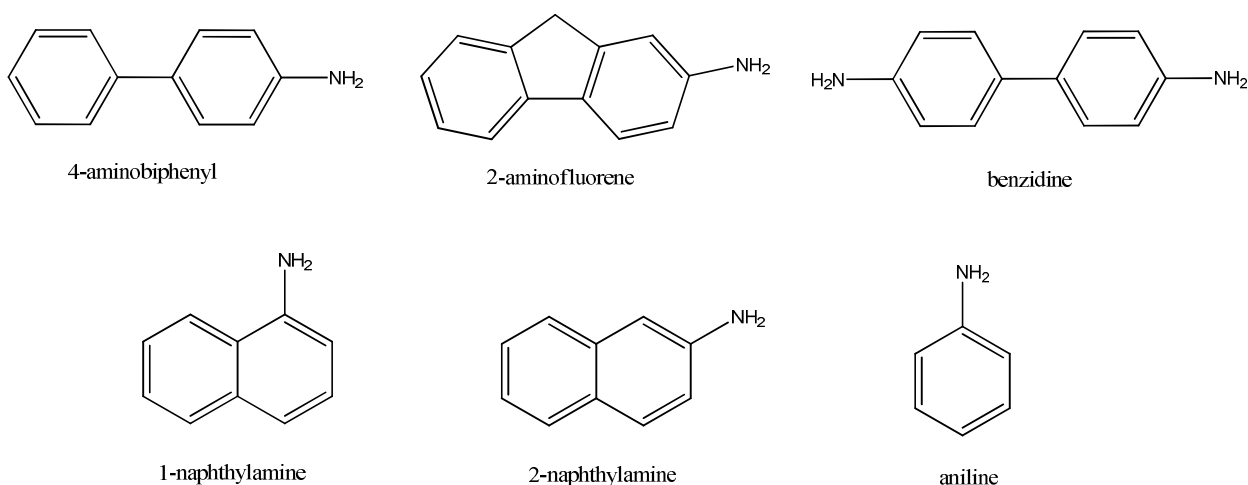


Figure 4. Chemical structure of prototypical aromatic amines.

After failing to reproduce the same “aniline tumors” in dogs using aniline, Hueper *et al.* decided to test other aromatic amines using the same tumor assay. Finally in a paper published in 1938, Hueper *et al.* reported the reliable reproduction of “aniline tumors” in bladders of dogs treated with 2-naphthylamine, an aromatic amine later shown to be a much more potent bladder carcinogen than aniline (Hueper *et al.*, 1937). Not only is 2-naphthylamine a potent bladder

carcinogen in dogs, it is also a potent bladder carcinogen in humans. When patients were treated with more than 100 grams of the chemotherapeutic agent chlornaphazine, a precursor of 2-naphthylamine, a large proportion of them went on to develop bladder cancer (Thiede and Christensen, 1969). We now know that approximately one in eight of all known human carcinogens is an aromatic amine or a chemical that can be converted into one, making aromatic amines a major class of human carcinogens (National Toxicology Program, 2011).

1.2.3 Diverse carcinogenic effects of aromatic amines

As previously illustrated with aniline and 2-naphthylamine, the carcinogenicity of different aromatic amines can vary dramatically. Even with aromatic amines that are highly similar in chemical structure, such as 1-naphthylamine and 2-naphthylamine, their carcinogenicity can be very different (Figure 4). 2-naphthylamine but not 1-naphthylamine leads to bladder tumors when administered to dogs, leading to the classification of 2-naphthylamine but not 1-naphthylamine as a human carcinogen by the International Agency of Research on Cancer (IARC, (Radomski, 1979)). In the laboratory, aromatic amine carcinogenicity is not only influenced by chemical structure but also by route of administration. The influence of route of administration on the carcinogenicity of aromatic amines is readily demonstrated with diacetylbenzidine-treated rats. Subcutaneous injection of diacetylbenzidine into rats leads to liver tumors, whereas intraperitoneal injection leads to ear duct, mammary, and skin tumors (Bremner and Tange, 1966). In addition, profound species differences exist with regard to aromatic amine carcinogenicity. For example, benzidine leads to the formation of bladder tumors in humans and dogs, mammary tumors in rats, and liver tumors in mice (Radomski, 1979). From a disease prevention point of view, such diverse carcinogenic effects of aromatic amines have made it very difficult to predict the carcinogenicity of aromatic amines from their chemical structures. On the other hand, from a mechanistic point of view they have provided chemically-induced carcinogenesis models for the study of a variety of malignancies that originate from different biological tissues.

1.2.4 Metabolic activation and DNA adducts of aromatic amines

The addition of a hydroxyl group to a primary aromatic amino nitrogen atom is a metabolic reaction unique to aromatic amines, and it represents the first step in the two-step metabolic

activation of these chemicals. As mentioned previously, the Millers were the first to observe the *N*-hydroxylated metabolite of the acetylated aromatic amine 2-acetylaminofluorene in biological systems (Cramer *et al.*, 1960). This reaction was later determined to be carried out by the cytochrome P450 isoform 1A2 (CYP1A2, (Butler *et al.*, 1989a)). In fact, CYPs carry out the *N*-hydroxylation reactions for most known aromatic amines (Butler *et al.*, 1989a; Hammons *et al.*, 1985; Hlavica *et al.*, 1997). Other enzymes that may play a minor part in the *N*-hydroxylation of aromatic amines or substituted aromatic amines, at least *in vitro*, include hemoglobins and peroxidases (Boyd *et al.*, 1983; Boyd and Eling, 1984; Huang and Dunford, 1991). The *N*-hydroxylated products of aromatic amines (arylhydroxylamines) are then subjected to further metabolic activation.

In the second step of the two-step metabolic activation of aromatic amines, a sulfuric, acetic, or glucuronic acid is conjugated to the newly formed *N*-hydroxyl group on aromatic amines by sulfotransferases, arylamine *N*-acetyltransferases, or UDP-glucuronosyltransferases, respectively, to generate a highly unstable ester linkage that spontaneously breaks down to release the ultimate carcinogen, the arylnitrenium ion (Miller and Miller, 1981). Arylnitrenium ions of aromatic amines can react non-enzymatically with various nucleophilic sites on macromolecules inside cells, with the most frequently characterized adduct found on C8 of the deoxyguanosine bases of DNA (Miller and Miller, 1981). These aromatic amine-DNA adducts, in turn, are suggested to give rise to mutations and initiate carcinogenesis as described in the multi-stage model of chemical carcinogenesis (Section 1.1.3).

1.2.4.1 Arylamine *N*-acetyltransferases

An important class of phase II enzymes that is critical to both the metabolic activation and detoxification of aromatic amines is the arylamine *N*-acetyltransferases (NATs). There are two expressed NAT isoforms in humans and three in mice. Due to the fact that different isoforms were discovered independently in humans and mice, naming conventions for NATs are somewhat confusing: human NAT1 is the orthologue of mouse NAT2, and human NAT2 is the orthologue of mouse NAT1. Human and mouse *Nat3* represent expressed but essentially non-functional pseudogenes that have no known substrates (Sugamori *et al.*, 2007). Functional homology between the mouse and human NAT isoforms is established from their shared

substrate profiles, especially with regard to the metabolism of aromatic amines (Estrada-Rodgers *et al.*, 1998; Fretland *et al.*, 1997). Furthermore, the expression of NATs demonstrates tissue specificity. Whereas mouse NAT1/human NAT2 is expressed primary in the liver, mouse NAT2/human NAT1 is expressed ubiquitously throughout the body.

Substrates of the NATs are restricted to homocyclic and heterocyclic primary aromatic amines and their *N*-hydroxylated metabolites, and primary aromatic hydrazines. In most cases, NATs conjugate acetate to the nitrogen atoms of these compounds, producing *N*-acetamide or *N*-acetylhydrazine metabolites. In the case of the *N*-hydroxylamine metabolites of aromatic amines, however, NATs can add acetate to the oxygen atom, generating *O*-acetylated hydroxylamines (acetoxy esters) with a highly unstable ester linkage that spontaneously degrades to arylnitrenium ions, as discussed previously (Miller and Miller, 1981). Figure 5 provides a schematic representation of NATs in both the metabolic activation and detoxification of aromatic amines.

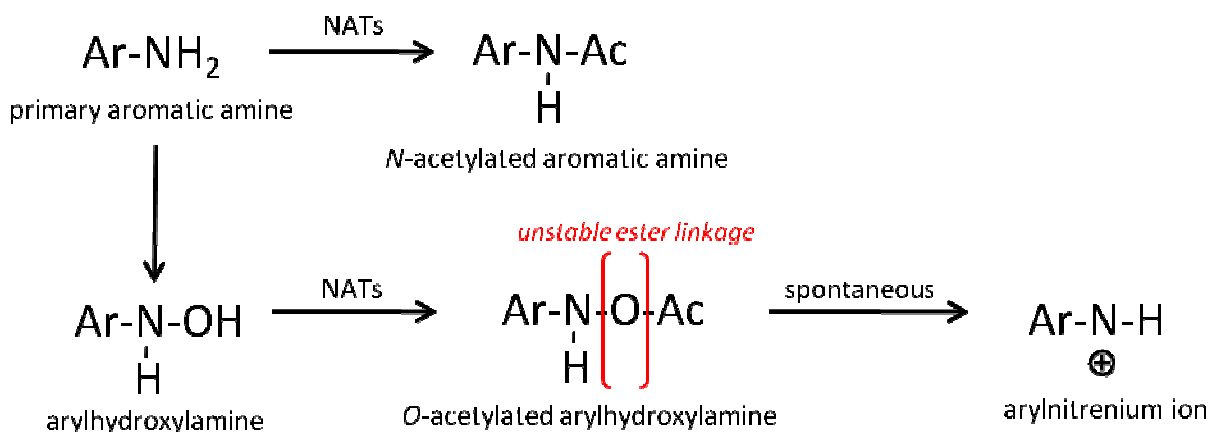


Figure 5. NATs in the *N*-acetylation (detoxification) and *O*-acetylation (metabolic activation) of aromatic amines.

"Ar" = aromatic substituent. "Ac" = acetyl group.

It should be noted that *N*-acetylation and *O*-acetylation are not necessarily mutually exclusive pathways and can sometimes act in concert. For example, an aromatic amine that is *N*-acetylated can still be *N*-hydroxylated and *O*-acetylated to form the unstable ester linkage depicted in Figure 5. In addition, both NAT1 and NAT2 can carry out *N*- and *O*-acetylation reactions (Hein *et al.*, 1993). Finally, the NAT enzymes can also catalyze an acetyl CoA-independent

intramolecular *N,O*-acyltransfer of the acetate group from the nitrogen to the oxygen atom of an *N*-acetylated, *N*-hydroxylated aromatic amine (an arylhydroxamic acid), again producing an unstable acetoxy ester (Hein, 1988).

The importance of NATs in aromatic amine carcinogenesis is supported by epidemiological studies linking NAT2 polymorphisms to human bladder cancer. Historically it was known that patients can be divided into rapid or slow acetylators of isoniazid (Bonicke and Reif, 1953). These phenotypic differences were subsequently attributed to the expression of different NAT2 allelic variants with rapid or slow NAT activity (Grant *et al.*, 1991). For example, the most common allelic variant in NAT2 is an isoleucine to threonine substitution at codon 114 that results in lower NAT2 enzyme activity (Grant *et al.*, 1997; Meyer and Zanger, 1997). In an epidemiology study, a significantly higher proportion of slow acetylators were found with bladder cancer patients occupationally exposed to the aromatic amine benzidine compared to control bladder cancer patients not exposed to benzidine (Cartwright *et al.*, 1982). Subsequent studies have mostly reproduced these results (Hanssen *et al.*, 1985; Ladero *et al.*, 1985). Together these epidemiological studies suggest that slow acetylators are at higher risk for aromatic amine-induced bladder cancer, presumably due to decreased *N*-acetylation and clearance of aromatic amines. These are rare studies in epidemiology where patients were exposed to such high doses of a single carcinogen (not part of a chemical mixture) and could be separated into different groups based on distinct metabolic capabilities that established NATs as key determinants in aromatic amine-induced human carcinogenesis.

1.2.5 Aromatic amines and oxidative stress

In addition to DNA adducts, aromatic amines can also generate oxidative stress. Initial studies linking aromatic amines to oxidative stress were carried out in the Neumann laboratory with the prototypical acetylated aromatic amine 2-acetylaminofluorene. Using isolated perfused rat livers, 2-acetylaminofluorene-treated rats demonstrated a 20% increase in oxygen consumption compared to untreated rats, which suggested the potential involvement of mitochondria and oxidative stress in 2-acetylaminofluorene-induced liver carcinogenesis (Neumann *et al.*, 1994). The fact that transformed hepatocytes first appeared in the oxygen-rich periportal area of 2-acetylaminofluorene-treated rat livers also suggested a role for oxidative stress in 2-

acetylaminofluorene-induced liver carcinogenesis (Neumann *et al.*, 1994). Using isolated mitochondria, major activated metabolites of 2-acetylaminofluorene, *N*-hydroxy-2-aminofluorene and nitrosofluorene, underwent redox cycling reactions in the presence of electrons donated by electron transport chain and generated ROS in the form of superoxide anions (Figure 6, (Klöhn *et al.*, 1995; Klöhn *et al.*, 1996; Klöhn and Neumann, 1997)).

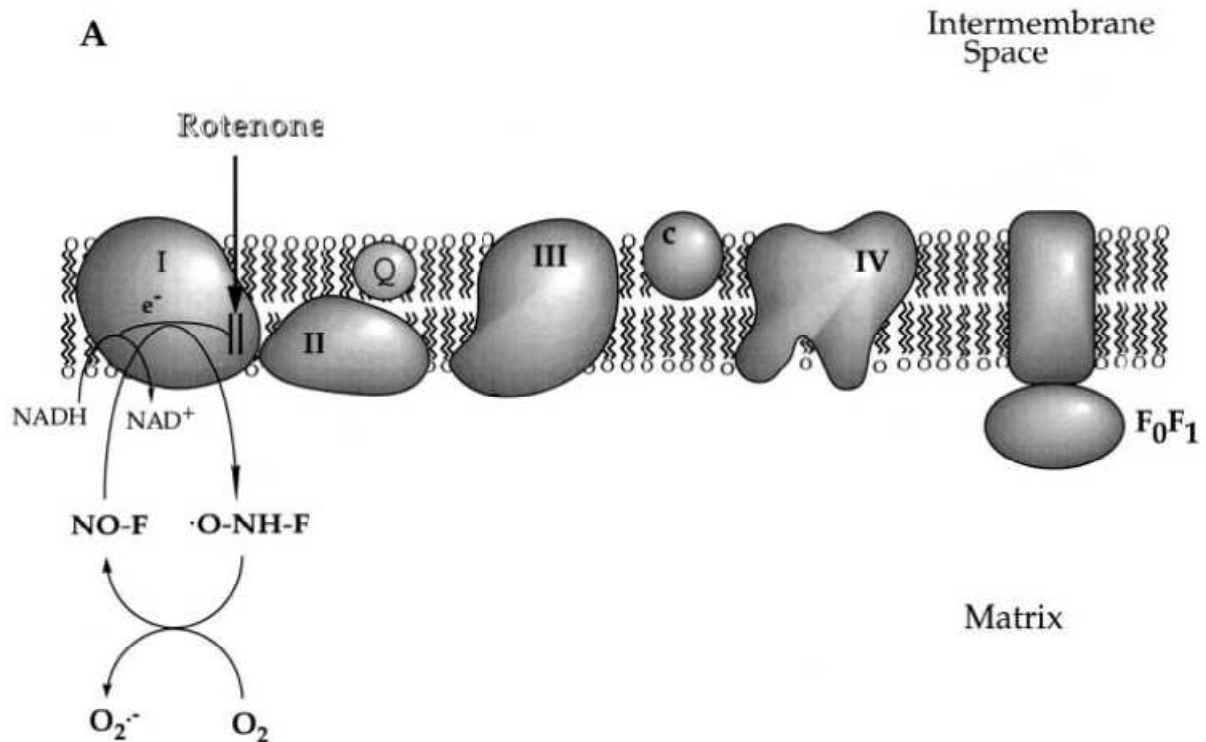


Figure 6. Proposed mechanism for decoupling of the mitochondrial electron transport chain by *N*-hydroxy-2-aminofluorene.

©Figure taken from Klöhn and Neumann 1997 with permission from Elsevier. "I-IV" = mitochondrial complexes I to IV. "Q" = co-enzyme Q. "C" = cytochrome c. F₀F₁ = ATP synthase.

Rotenone, an inhibitor of the electron transport chain at complex I, inhibited redox cycling of 2-acetylaminofluorene, which suggests that the site of action for 2-acetylaminofluorene is at complex I (Neumann *et al.*, 1997). Furthermore, 2-acetylaminofluorene and associated ROS altered permeability transition pores in isolated mitochondria and *in vivo* in rat liver; this in turn increased resistance to apoptosis and contributed to transformation of hepatocytes early in 2-acetylaminofluorene-induced rat liver carcinogenesis (Klöhn *et al.*, 1998; Klöhn *et al.*, 2003).

Following initial observations with 2-acetylaminofluorene, other aromatic amines, such as benzidine and 4-aminobiphenyl, have also been shown to generate oxidative stress *in vitro* through their *N*-hydroxy metabolites (Makena and Chung, 2007; Siraki *et al.*, 2002).

1.3 Human liver cancer

1.3.1 Overview of liver physiology

The liver is a vital organ in vertebrates. It represents 2-5% of total body weight in most species and is involved in a variety of physiological processes such as glycogen storage, protein synthesis, and nutrient metabolism. In addition, the liver is the most importance site for the metabolism of xenobiotics, including chemical carcinogens. This is mainly due to its strategic anatomical location downstream of the hepatic portal vasculature that carries xenobiotics absorbed through the gastrointestinal tract to the liver, where metabolism can occur before redistribution to other parts of the body, a phenomenon also known as the first-pass effect. The major cell type in liver is the highly differentiated and specialized hepatocyte, which makes up roughly 80% of total liver mass and carries out most biochemical functions of the liver (Arias, 2009). Minor cell types in the liver include Kupffer cells, stellate cells, and cholangiocytes that line the bile ducts, among others (Arias, 2009). Kupffer cells are the resident macrophages of the liver that have recently been implicated in the establishment and maintenance of an inflammatory environment that may promote liver carcinogenesis in mice (Arias, 2009; Roberts *et al.*, 2007). Stellate cells, on the other hand, are involved in fibrotic responses that may lead to liver fibrosis in rodent models (Czaja, 2014). The liver is normally considered as a slowly proliferating organ, with hepatocytes having an average turnover time of 400 days (Arias, 2009). Nevertheless, the liver possesses a remarkable potential to regenerate in the presence of massive cell death, most often inflicted by chemical or viral insults. In most cases, liver regeneration under pathophysiological conditions involves the rapid proliferation of existing hepatocytes (Zhang *et al.*, 2003). Based on evidence generated mostly in rodents, liver regeneration can also involve the rapid proliferation of adult liver stem cells, known as oval cells in rodents; however this only occurs when proliferation of hepatocytes is blocked by experimental means (Zhang *et al.*, 2003).

1.3.2 Primary liver cancer

Primary liver cancer (cancer originating from the liver) is a major form of human malignancy, representing the 3rd most common cause of death from cancer worldwide (Bosch *et al.*, 2004; Ferlay *et al.*, 2010). While liver cancer is more commonly found in under-developed areas of the world, such as Southeast Asia and sub-Saharan Africa, its incidence is on the rise in developed countries. Region-specific trends in liver cancer incidence have mainly reflected changes in exposure to various risk factors for liver cancer, as we shall see in later sections. Based on histopathology, liver cancer can be divided into different categories, with the major form being hepatocellular carcinoma (HCC), which originates from hepatocytes and makes up more than 80% of all liver cancer cases (Bosch *et al.*, 2004). Most studies on liver cancer have focused on HCC. Minor forms of primary human liver cancer include cholangiocarcinoma, which stems from cholangiocytes and makes up roughly 6% of all liver cancer cases, and hepatoblastoma, which is a rare form of human liver cancer that arises from immature hepatocytes in infants (White *et al.*, 2010). Even though our descriptions here have focused on primary liver cancer, specifically in the form of HCC, it should be noted that many cases of liver cancer are not primary in nature but represent metastasis from other parts of the body (also known as secondary liver cancer). Liver may represent a common site for metastasis due to its highly permeable nature, providing a convenient landing site for metastatic cancer cells travelling through blood. The five-year survival rate for patients diagnosed with HCC is only 7% (Bosch *et al.*, 2004). This extremely poor prognosis for HCC is attributed, at least in part, to an inadequate understanding of disease pathology.

The molecular pathogenesis of HCC is unclear and likely to be very heterogeneous. The concept of HCC being a highly heterogeneous disease is initially supported by large inter-individual variations in prognosis for patients with HCC, suggesting the presence of multiple subgroups with distinct pathogenic profiles (Thorgeirsson and Grisham, 2002). More recently, whole-genome sequencing of HCCs from different patients has revealed highly variable mutational profiles, again supporting the heterogeneous nature of this disease (Thorgeirsson and Grisham, 2002). It has been estimated that 5 to 6 genetic insults are needed to transform hepatocytes (Puisieux and Ozturk, 1997). Based on the sequencing of HCCs, multiple tumor suppressors and oncogenes from a number of signaling pathways have been implicated in the pathogenesis of

hepatocellular adenomas (benign tumors) and carcinomas (malignant tumors). Most commonly, mutations in genes encoding p53 (*TP53*) and beta-catenin have been found in 28 and 23% of all HCC cases, respectively (DeFrances, 2010). Other molecular signaling pathways often deregulated in HCC include epidermal growth factor receptor (EGFR), vascular endothelial growth factor receptor (VEGFR), RAS, mitogen-activated protein kinase (MAPK), mammalian target of rapamycin (MTOR), insulin-like growth factor (IGF), and histone modifications (DeFrances, 2010). Concurrently, epidemiological studies have revealed a number of risk factors for HCC that may have directly or indirectly resulted in the observed genetic aberrations in HCC.

1.3.3 Risk factors for hepatocellular carcinoma (HCC)

1.3.3.1 Viral infection

Hepatitis B (HBV) viral infection is the most frequent underlying cause for HCC, estimated to be responsible for 50-90% of HCC cases in high-risk regions (Chen *et al.*, 1997). HBV is highly contagious and transmits through bodily fluids such as blood, semen, and vaginal fluids (World Health Organization, 2001). Since the introduction of effective vaccine programs in the 1980s, incidences of HBV and HBV-associated HCC are on the decline. Unfortunately in areas of the world where the HBV vaccine is not readily available, such as sub-Saharan Africa, HBV remains the leading cause of HCC (White *et al.*, 2010). How HBV infection leads to HCC is not clearly understood despite decades of research. Several mechanisms have been proposed that may act in concert, including chronic infection-induced inflammation/necrosis, insertion of viral genes into the host genome and resultant DNA damage/mutagenesis, activation of oncogenes/inactivation of tumor suppressors by HBV protein X, and reactivation of telomerase through an unknown mechanism (Arbuthnot and Kew, 2001; Bonilla Guerrero and Roberts, 2005; Farazi *et al.*, 2003; Minami *et al.*, 2005). In addition to HBV, infection with hepatitis C virus (HCV) also represents a major risk factor for HCC. Unlike HBV, HCV is solely transmitted through blood, making it less contagious; however, no effective vaccine program yet exists for HCV and its global incidence is on the rise (Alter, 2007; White *et al.*, 2010). Due to high intrinsic mutability of this virus, *in vivo* detection and characterization of HCV have been challenging (Houghton and Abrignani, 2005). As a consequence, the mechanism that links HCV to HCC is less well understood than HBV and may involve chronic infection-induced inflammation/necrosis and

complex interactions between HCV proteins and molecular signaling pathways in host liver (McGivern and Lemon, 2009).

1.3.3.2 Chemical carcinogens

Aside from viral infections, chemical carcinogens are also established risk factors for HCC, with the best studied example being aflatoxin B1. Aflatoxin B1 is a mycotoxin produced by *Aspergillus flavus* and *Aspergillus parasiticus*, which are common fungi found as contaminants in agricultural commodities such as maize and peanuts. Exposure to aflatoxin B1 is the highest in tropical countries, which favor the growth of *aspergillus* fungi, but can also occur in non-tropical countries with the import of contaminated food (IARC Monographs Working Group, 2012). A strong association was observed between aflatoxin B1 exposure and HCC in several cohort studies that established aflatoxin B1 as a risk factor for HCC (Qian *et al.*, 1994; Ross *et al.*, 1992; Wang *et al.*, 1996). Mechanistically, aflatoxin B1 is metabolically activated in the liver to generate a reactive metabolite that binds to DNA. The most notable mutation that aflatoxin B1 forms with DNA is an inactivating G to T transversion at codon 249 of *TP53*, which has been subsequently observed in HCC patients from areas of aflatoxin B1 exposure, suggesting a causal role for this mutation in the etiology of HCC (as discussed in Section 1.1.3.1, (Puisieux *et al.*, 1991)).

HBV and aflatoxin B1 co-exposure has a striking synergistic effect on HCC. This synergistic effect was first observed in transgenic mice that over-express the HBV surface antigen but normally do not develop HCC. Exposure of these transgenic mice to aflatoxin B1, at a dose that also does not produce HCC on its own, led to the formation of both adenomas and carcinomas in mouse liver (Sell *et al.*, 1991). Spurred by these observations in mice, an epidemiological study detected relative risks for HCC of 4.8 with HBV alone, 1.9 with aflatoxin B1 alone, and 60 with HBV and aflatoxin B1 combined (Ross *et al.*, 1992). Subsequent studies to examine this interaction between HBV and aflatoxin B1 for HCC risk generated similar results (Lunn *et al.*, 1997; Qian *et al.*, 1994; Wang *et al.*, 1996). Several potential mechanisms have been proposed to explain this striking synergistic effect between HBV and aflatoxin B1. In one proposed mechanism, HBV infection and associated inflammation promote proliferation of aflatoxin B1 initiated cells, leading to increased HCC (Chisari *et al.*, 1989). In another proposed mechanism,

HBV infection increases metabolic activation and thus carcinogenicity of aflatoxin B1 (Chemin *et al.*, 1999). Finally, HBV infection may amplify the DNA damaging effects of aflatoxin B1 by interfering with nucleotide excision repair, leading to increased HCC (Jia *et al.*, 1999). It is unclear which, if any, of the proposed mechanisms contribute to the synergistic effect seen between HBV and aflatoxin B1.

Cigarette smoke is a recently established risk factor for HCC (Office of the Surgeon General, 2014). Over 5300 chemicals have been identified in cigarette smoke, of which 70 represent human carcinogens. These include the aromatic amine 4-aminobiphenyl (ABP), which is the focus of this thesis (IARC Monographs Working Group, 2009b). A vast number of epidemiological studies have examined a potential link between cigarette smoke and HCC, with mixed results. A recent meta-analysis combined data from a total of 31 studies and concluded that current smokers have a 70% increase in HCC risk compared to never smokers (Office of the Surgeon General, 2014). This relatively modest increase in HCC risk may explain why previous studies linking cigarette smoke to HCC have received mixed results. The most obvious biological explanation for why cigarette smoke leads to HCC would be through exposure to chemical carcinogens present in cigarette smoke, which can be metabolically activated in the liver and damage hepatocyte DNA. At least three classes of chemical carcinogens present in cigarette smoke can induce liver carcinogenesis in mice: aromatic amines, polycyclic aromatic hydrocarbons, and nitrosamines (IARC Monographs Working Group, 2009b). It is unclear which chemical in cigarette smoke, either alone or in combination with other chemicals, is responsible for increased HCC risk in humans.

Other risk factors for HCC include alcohol and obesity, although much less is known about molecular mechanisms that link them to HCC. It is possible that alcohol and obesity lead to HCC through the generation of liver cirrhosis. In fact, liver cirrhosis represents a major confounding factor associated with all known risk factors for HCC and may represent a risk factor for HCC on its own (Friedman, 2008). Liver cirrhosis, which precedes 80% of primary liver cancers (Severi *et al.*, 2010), is characterized by a gradual replacement of normal liver structure with fibrotic deposits as a result of chronic liver injury (i.e. from viral and chemical insults). How liver cirrhosis leads to HCC is unclear but may involve modifications to the tumor microenvironment by non-parenchymal cells, such as fibroblasts, Kupffer cells, leukocytes, hepatic stellate cells,

endothelial cells, neutrophils, and dendritic cells; through secretion of various growth factors and cytokines that lead to tissue fibrosis; by producing chronic inflammation; and by generating oxidative stress (Aravalli *et al.*, 2013).

1.3.3.3 Inflammation and HCC

Inflammation has always been an integral part of liver cirrhosis and is suspected to play a part in the pathogenesis of HCC by inhibiting apoptosis and promoting uncontrolled proliferation. Nevertheless, recent studies investigating sex differences in liver cancer incidence using genetically modified mouse models have brought inflammation back into the center of attention. Striking sex differences exist in HCC, such that men have a 3- to 5-fold higher risk compared to women even after correcting for exposure to known HCC risk factors (Altekruse *et al.*, 2009; Chen *et al.*, 1997). In a mouse model of liver carcinogenesis, a single exposure to diethylnitrosamine in neonates produced liver tumors in male but not female mice at one year, which seems to parallel sex differences found in human HCC (Maeda *et al.*, 2005; Naugler *et al.*, 2007). In studies carried out mostly by the Karin group, female mice showed lower levels of acute inflammation than male mice following exposure to the liver carcinogen diethylnitrosamine (Naugler *et al.*, 2007). Genetic manipulations that decreased liver inflammation, often through manipulation of the nuclear factor kappa-light-chain-enhancer of activated B cells (NF- κ B) signaling pathway, also decreased diethylnitrosamine-induced liver carcinogenesis in male mice (He *et al.*, 2010; Naugler *et al.*, 2007; Sakurai *et al.*, 2006; Sakurai *et al.*, 2008). In addition, the female sex hormone 17 β -estradiol seems to be a key mediator of the tumor-protective effects observed in female mice, perhaps through a dampening of inflammatory responses (Naugler *et al.*, 2007).

A key mediator of inflammatory responses is oxidative stress. Liver inflammatory cells release reactive oxygen and nitrogen species into neighboring hepatocytes (Hussain *et al.*, 2003). These highly reactive chemical species can directly attack DNA, leading to DNA modifications and mutations; they can also modulate cell signaling pathways, altering cell death and cell proliferation (Hussain *et al.*, 2003). Not only does oxidative stress contribute to the tumor-promoting effects of inflammation, oxidative stress may be considered as a risk factor for HCC in its own right.

1.3.3.4 Oxidative stress and HCC

Oxidative stress is involved in a wide range of human liver diseases. In hemochromatosis and Wilson's disease, excess levels of metal ions lead to altered cellular redox states that often result in liver disease and liver failure (Hussain *et al.*, 2000; Marrogi *et al.*, 2001). In transaldolase deficiency, an altered pentose phosphate pathway leads to the depletion of cellular NADPH molecules and antioxidants, which ultimately manifests as liver cirrhosis in patients (Hatting *et al.*, 2009). Moreover, all major etiological factors for HCC including viral hepatitis, chemical carcinogens, alcohol, and obesity described previously are associated with oxidative stress (Caldwell *et al.*, 2004; Hagen *et al.*, 1994; Jngst *et al.*, 2004; Loguercio and Federico, 2003; Shimoda *et al.*, 1994; Shiota *et al.*, 2002; Umarani *et al.*, 2008). Together these epidemiological studies suggest that the liver is highly susceptible to oxidative stress, but does oxidative stress play a causative role in liver cancer? In order to establish a causal relationship, researchers have turned to animal models of liver cancer.

Recent advances in animal models of liver cancer using transgenic animals, chemical carcinogens, or a combination of both have provided evidence for a causative role of oxidative stress in liver cancer. For example, mice that lack the key antioxidant enzymes superoxide dismutase or mut-T homologue 1 spontaneously develop HCC (Busuttil *et al.*, 2005; Elchuri *et al.*, 2004; Tsuzuki *et al.*, 2001). Mice that over-express the MYC oncogene spontaneously develop HCC through an oxidative stress-mediated mechanism, which can be suppressed by the antioxidants vitamin E or *N*-acetylcysteine (NAC, (Vafa *et al.*, 2002)). Mice deficient in transaldolase, which are designed to mimic human transaldolase deficiency, demonstrate high levels of oxidative stress and spontaneously develop HCC, and this HCC can be prevented with the lifelong administration of NAC (Hanczko *et al.*, 2009). Oxidative stress not only plays a causative role in spontaneous HCC of various genetically modified mouse models, but it has also been shown to be critical in diethylnitrosamine-induced liver carcinogenesis. For example, mice that are deficient in metallothionein, a cellular antioxidant enzyme, are significantly more susceptible to diethylnitrosamine-induced liver tumors than wild-type mice, and this increased susceptibility is associated with increased oxidative stress in mouse liver (Majumder *et al.*, 2010). Mice deficient in NADPH oxidase, the main source of ROS in cytoplasm, are protected from diethylnitrosamine-induced liver damage, which suggests that diethylnitrosamine exerts its

toxicity partially through the disruption of NADPH oxidase (Teufelhofer *et al.*, 2005). Furthermore, treatment with the antioxidant BHA eliminated initial liver damage induced by diethylnitrosamine, and the protective effect of BHA is most dramatic in diethylnitrosamine-treated I κ B kinase β (IKK β) or P38a deficient mice, which have increased susceptibility to diethylnitrosamine-induced liver damage and liver tumors. These studies suggest a potential involvement of the MAPK pathway in diethylnitrosamine-induced liver tumors following a neonatal dosing protocol (Kamata *et al.*, 2005; Sakurai *et al.*, 2008). In summary, oxidative stress is not only associated with liver cancer but may represent a causative factor for liver cancer as suggested by studies using various transgenic and diethylnitrosamine-induced mouse models for liver carcinogenesis.

1.3.4 Current treatments and future trends

Until recently the only treatment options for liver cancer were liver resection or transplantation surgeries (Carr, 2010). For the majority of HCC cases, surgery is no longer a viable option at the time of diagnosis as a result of extensive tissue damage (Aravalli *et al.*, 2013). Liver cancer has also proven to be resistant to conventional chemotherapy, which is attributed at least in part to the liver's extraordinary metabolic capabilities (Gillet *et al.*, 2009). Efforts toward elucidation of molecular mechanisms behind liver cancer through the combination of epidemiological and animal studies listed above, however, are beginning to reveal novel targets for the treatment of liver cancer (DeFrances, 2010). In November of 2007, sorafenib became the first and only US Food and Drug Administration approved drug for the treatment of HCC. Sorafenib was originally identified as an inhibitor of RAF kinases that are part of the MAPK pathway (Aravalli *et al.*, 2013). In subsequent studies sorafenib also demonstrated inhibitory activities toward receptor tyrosine kinases, such as EGFRs and VEGFRs (Aravalli *et al.*, 2013). Despite having a relatively modest therapeutic effect, on average extending HCC patient survival by only 3 months, sorafenib provides a proof of principle that understanding the molecular pathogenesis of HCC may one day translate into much needed treatments for this deadly disease (Zhang *et al.*, 2010).

1.4 ABP-induced liver carcinogenesis in mice

1.4.1 Mouse models for the study of liver carcinogenesis

Even though we rely heavily on various mouse models for the study of human cancer, it is important to keep in mind that "mice are not small people" (Rangarajan and Weinberg, 2003). Major species differences exist that may have profound implications in cancer biology. Mice have a much shorter lifespan than humans, yet both develop cancer at a similar lifetime risk, suggesting that mice are more prone to carcinogenesis (Anisimov *et al.*, 2005; Rangarajan and Weinberg, 2003). Experimental evidence suggests this may indeed be the case. In primary cell cultures, mutations in two genes (p53 and *Ras*) are enough to transform mouse cells, whereas mutations in 4 to 5 additional genes are needed to transform human cells (Rangarajan and Weinberg, 2003). Additional factors such as shorter telomeres and increased metabolism may also contribute to increased cancer susceptibility in mice (Rangarajan and Weinberg, 2003). On the other hand, spontaneous tumor regression is often found in mice but rarely found in humans (Anisimov *et al.*, 2005). Humans and mice also differ with respect to where cancer develops in the body. Some of the most common cancers in humans (prostate, lung, colon, and stomach) do not spontaneously develop in mice, highlighting species differences in carcinogenesis at a tissue level (Anisimov *et al.*, 2005).

Within mice, prominent strain differences exist that sometimes alter sensitivity towards different chemical carcinogens. For example, one of the most sensitive strains of mice used for the study of chemical carcinogenesis is C3H/HeJ; on the other hand, one of the most resistant strains of mice used is C57BL/6 (Drinkwater, 1994). Sensitive strains are more prone towards false positives and resistant strains are more prone towards false negatives. A strain of intermediate sensitivity, B6C3F₁, is derived from crossing C3H/HeJ to C57BL/6 and is routinely used for carcinogenicity testing by the National Toxicology Program (NTP) and the National Center of Toxicological Research (NCTR, (Flammang *et al.*, 1997)). Strain differences in sensitivity towards different carcinogens mainly act at the stage of tumor promotion, perhaps due to a longer duration and a larger number of biological factors involved compared to tumor initiation (Maronpot *et al.*, 2004).

Most mouse models used to study liver carcinogenesis can be divided into 3 categories: over-expression of hepatitis viral proteins, over-expression of oncogenes, and treatment with chemical carcinogens. In one study, Lee et al. compared gene expression profiles of HCCs from different mouse models to humans (Lee *et al.*, 2004). In this study, mouse HCCs were induced by diethylnitrosamine, ciprofibrate (a peroxisome proliferator), MYC over-expression, transcription factor E2F1 (E2F1) over-expression, MYC+E2F1 over-expression, MYC + transforming growth factor alpha (TGFA) over-expression, or peroxisomal acyl-coenzyme A oxidase 1 (ACOX1) deficiency. Overall, diethylnitrosamine- and MYC+TGFA-induced mouse HCCs demonstrated the most similar gene expression profiles to human HCCs, especially those with poor survival. On the other hand, ciprofibrate- and ACOX1 deficiency-induced mouse HCCs were least similar to human HCC (Lee *et al.*, 2004).

In the diethylnitrosamine-induced mouse liver carcinogenesis model discussed above, mice were exposed to a single dose of diethylnitrosamine on postnatal day 15 and assayed for tumors at one year. This type of tumor-inducing protocol in mice is referred to as the 1-year neonatal bioassay to distinguish it from the traditional chronic bioassay, where mice are dosed repeated with carcinogen over a span of several weeks and sometimes months, and assayed for tumors at 2 years of age. Compared to the chronic bioassay, the neonatal bioassay has obvious advantages of being cheaper and faster, requiring considerably less time, chemical, and manpower (Flammang *et al.*, 1997). In addition, reduced chemical administration often translates into less physical irritation that may influence carcinogen action. For certain classes of carcinogens, such as polycyclic aromatic hydrocarbons, aromatic amines, and nitrosamines, the neonatal bioassay has demonstrated increased sensitivity both in terms of shorter latency and increased tumor incidence, which can be attributed to increased tissue proliferation in developing mice (Flammang *et al.*, 1997). Moreover, a shorter latency in the neonatal bioassay translates into fewer spontaneous tumors, which develop at a rate proportional to age. Overall, a 76% concordance rate is found between the neonatal and chronic bioassays (Fujii, 1991). Disagreement between the neonatal and chronic bioassays may be attributed to age-dependent differences in metabolism or to any factor listed above. A two-stage protocol is sometimes used for the study of rodent liver carcinogenesis. In this two-stage protocol, brief exposure to a chemical carcinogen is used to initiate carcinogenesis, followed by hepatectomy and/or chronic

administration of a tumor promoter to promote carcinogenesis (Sleight, 1985). Compared to the neonatal bioassay, the two-stage protocol is more expensive and labor intensive, just like the chronic bioassay. In addition, the two-stage protocol introduces additional procedures and/or chemicals for tumor promotion that may confound carcinogenesis results for a given chemical carcinogen. Use of the innate proliferation potential of developing animals combined with the simplicity of this procedure make the neonatal bioassay an attractive system for the study of chemical carcinogenesis.

1.4.2 4-Aminobiphenyl (ABP)

My PhD studies focused on the aromatic amine chemical carcinogen ABP. ABP is classified as a group I carcinogen (“carcinogenic to humans”) by the IARC, and its structure is shown in Figure 4. Historically, the main route of ABP exposure was through its presence in rubber antioxidants and dye intermediates in the work place (IARC Monographs Working Group, 2009a). In light of epidemiological evidence linking aromatic amines to bladder cancer, ABP exposure in the workplace was greatly reduced. However, using recently established biomarkers ABP exposure can still be detected in the general population, which has been attributed to cigarette smoke in smokers and to yet unidentified sources in non-smokers (Grimmer *et al.*, 2000; Riedel *et al.*, 2006). Potential sources of ABP in non-smokers may include sidestream smoke, synthetic dyes, and cooking oil (Hammond *et al.*, 1995; Hoffmann *et al.*, 1997; Turesky *et al.*, 2003).

Like other aromatic amines, ABP is an established bladder carcinogen in humans. A link between ABP exposure and bladder cancer was first reported in male workers of a chemical plant engaged in the production of ABP. Out of 315 male workers exposed to ABP, 53 developed bladder tumors (Melick *et al.*, 1955; Melick *et al.*, 1971). ABP may also represent a liver carcinogen in humans. As described in Section 1.3.3, cigarette smoke is now an established risk factor for HCC (Office of the Surgeon General, 2014). The presence of ABP in cigarette smoke suggests a potential link between ABP exposure and HCC. This is supported by an epidemiological study that detected significantly higher levels of ABP-DNA adducts in the liver of HCC patients compared to non-HCC controls (Wang *et al.*, 1998).

ABP administration to mice leads mostly to the formation of liver tumors regardless of mouse strain, route of administration, and dosing paradigm (Clayson *et al.*, 1967; Kimura *et al.*, 1999;

Schieferstein *et al.*, 1985). In a chronic bioassay carried out by the NCTR, 4-week-old BALB/cStCrIfC3Hf/Nctr mice given ABP in drinking water for one week developed both liver and bladder tumors (Schieferstein *et al.*, 1985). This is the only study where ABP exposure led to bladder tumors in mice. In a different chronic bioassay, 12-week-old C57xIF F₁ mice given ABP 3 times a week for 50 weeks by gavage developed only liver tumors (Clayson *et al.*, 1967). Similarly, neonatal bioassays carried out with ABP lead to liver tumors regardless of mouse strain and route of administration. For example, a subcutaneous injection of ABP into newborn Swiss mice produced liver tumors at one year (Gorrod *et al.*, 1968). Intraperitoneal injections of ABP into neonatal B6C3F₁/nctr, B6C3F₁, CD1, B6/SVJ129, and C57BL/6 mice led predominantly to the formation of liver tumors (Dooley *et al.*, 1992; Kimura *et al.*, 1999; Parsons *et al.*, 2005; Sugamori *et al.*, 2012). Interestingly, in the three neonatal bioassays that used mice of both sexes, females demonstrated significantly lower tumor prevalence compared to males, reproducing the sex differences observed in human liver cancer (Altekruse *et al.*, 2009; Chen *et al.*, 1997; Gorrod *et al.*, 1968; Kimura *et al.*, 1999; Kimura *et al.*, 2003; Sugamori *et al.*, 2012).

1.4.3 A traditional model of ABP bioactivation and tumor initiation in the mouse liver

1.4.3.1 Role of CYP1A2 in the *N*-hydroxylation of ABP

Like other aromatic amines, ABP is believed to require metabolic activation in order to exert its deleterious effects. In the first step of ABP metabolic activation in mouse liver, ABP is *N*-hydroxylated to form *N*-hydroxy-ABP (HOABP). Several lines of evidence, mostly generated *in vitro* using human liver microsomes, have implicated the cytochrome P450 isoform CYP1A2 as the primary ABP *N*-hydroxylation enzyme in mouse liver. For example, phenacetin *O*-deethylation activity, which is used as a phenotyping reaction for CYP1A2, correlated with ABP *N*-hydroxylation activity across a panel of human liver microsomes (Butler *et al.*, 1989a). Furthermore, CYP1A2 antibodies and CYP1A2-selective chemical inhibitors inhibited ABP *N*-hydroxylation activity in human liver microsomes (Butler *et al.*, 1989a). In a separate study comparing across a panel of purified CYPs from rats, the highest ABP *N*-hydroxylation activity was detected with purified CYP1A2 (Butler *et al.*, 1989b). In addition, ABP *N*-hydroxylation activity significantly correlated with the amount of immunoreactive CYP1A2 in human liver microsomes, as detected using antibodies raised against rat CYP1A2 (Butler *et al.*, 1989b).

Finally, pre-treatment with inducers of the CYP1 family of enzymes, such as 3-methylcholanthrene, significantly increased ABP *N*-hydroxylation in rat primary hepatocytes (Orzechowski *et al.*, 1994).

A number of different species were used in these initial studies that established a link between CYP1A2 and ABP metabolism; this was made possible by a high degree of conservation in CYP1A2 cDNA sequences that translated into a high degree of conservation in CYP1A2 substrate profiles across different species including rodents and humans (Jaiswal *et al.*, 1987; Kimura *et al.*, 1984). For example, *in vitro* studies with human liver microsomes had established CYP1A2 as the first and rate-limiting enzyme in the metabolism of caffeine, results later confirmed *in vivo* using mice deficient in CYP1A2 (Buters *et al.*, 1996; Butler *et al.*, 1989a; Gu *et al.*, 1992). In addition, CYP1A2 is highly conserved across different strains of mice, as demonstrated by similar enzyme activities towards CYP1A2 probe substrates (Löfgren *et al.*, 2004).

1.4.3.2 O-conjugation of *N*-hydroxy ABP and the "ultimate" carcinogen

The *N*-hydroxy group introduced by CYP1A2 has been shown to be further *O*-conjugated with sulfuric acid or acetic acid, by sulfotransferases and NATs respectively, to generate a highly unstable ester form of ABP (Chou *et al.*, 1995; Minchin *et al.*, 1992). The highly unstable ester linkage spontaneously breaks down to give rise to a highly reactive ABP nitrenium ion, which is considered to be an "ultimate" carcinogen (Kerdar *et al.*, 1993; Novak *et al.*, 1993). A graphical representation of major ABP detoxification and metabolic activation pathways is shown in Figure 7.

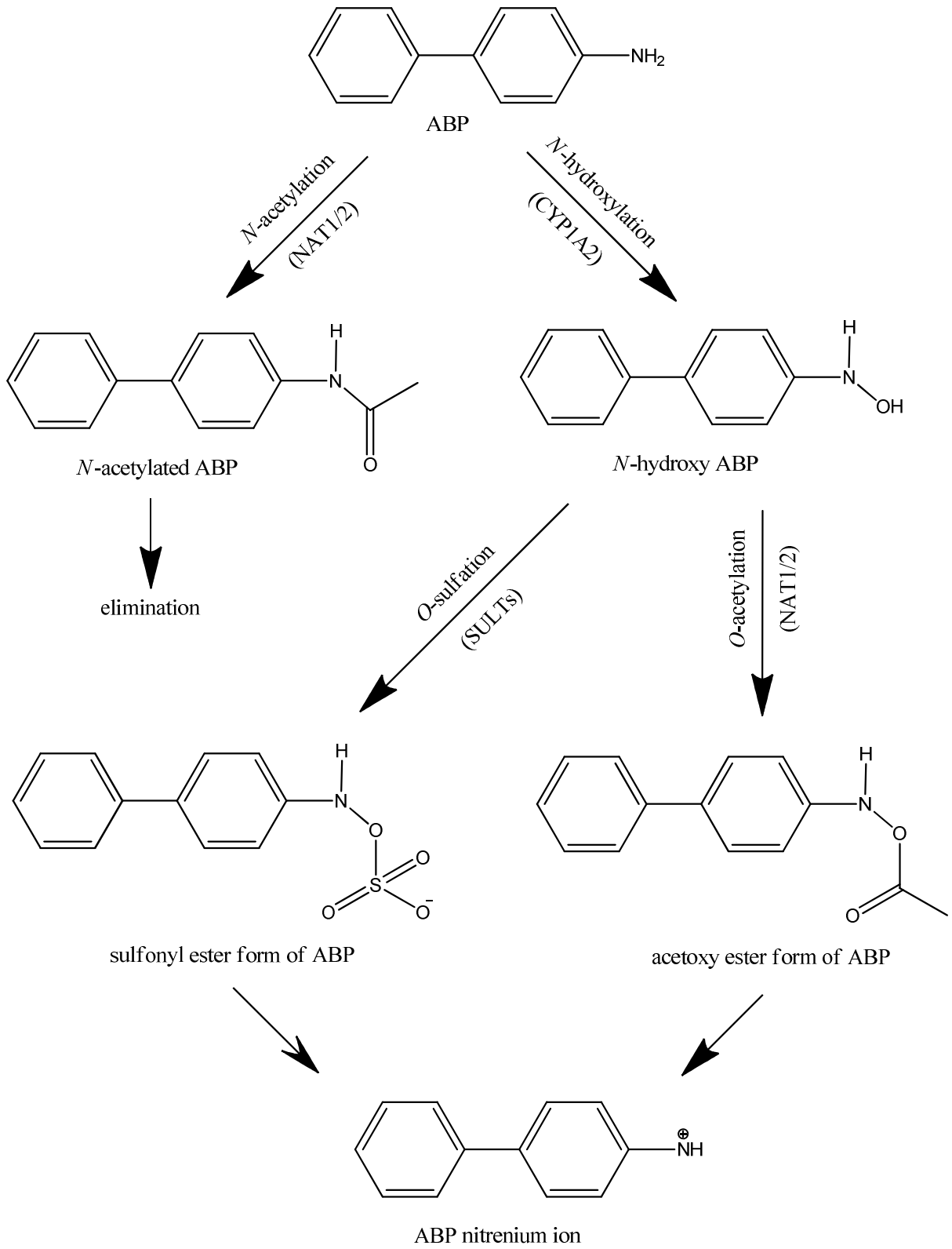


Figure 7. Metabolic activation and detoxification of ABP in mouse liver.

Like other aromatic amines, ABP can also undergo *N*-acetylation reactions catalyzed by NATs as described in Section 1.2.4.1. The *N*-acetylation of ABP has been shown to facilitate elimination of ABP from liver, thus acting as a major detoxification pathway (Hein *et al.*, 1993). Studies using primary rat hepatocytes have attributed 51% of total ABP metabolites to be the *N*-acetylation product (Orzechowski *et al.*, 1994). Other minor detoxification pathways not shown in Figure 7 include ring-hydroxylation and *N*-glucuronidation products of ABP, shown to represent 8% and 4% of total ABP metabolites, respectively (Orzechowski *et al.*, 1994).

1.4.3.3 C8-dG-ABP adducts, G to T transversions, and tumor initiation

The highly reactive ABP nitrenium ion, generated from the sequential metabolic activation of ABP by CYP1A2 and NATs/sulfotransferases, is considered the "ultimate" carcinogenic form of ABP (Miller and Miller, 1981). Due to its positive charge, the ABP nitrenium ion is highly electrophilic and attacks nucleophilic sites on cellular macromolecules such as DNA and protein. Direct incubation of ABP with DNA *in vitro*, under conditions that are favorable for generation of the ABP nitrenium ion, led to the formation of mostly *N*-(deoxyguanosin-8-yl)-ABP (C8-dG-ABP) adducts (80% of total yield), followed by *N*-(deoxyadenosin-8-yl)-ABP adducts (15% of total yield), and *N*-(deoxyguanosin-N2-yl)-ABP adducts (5% yield, (Beland and Kadlubar, 1985)). *In vivo*, C8-dG-ABP adducts represented ~80% of total ABP-DNA adducts formed in mouse liver following chronic exposure to ABP through drinking water using ³²P-postlabeling analysis (Flammang *et al.*, 1992). Compared to ABP-DNA adducts, ABP-protein adducts have received considerably less attention. Hemoglobin represents the only characterized protein target for ABP binding, and it is sometimes used as a biomarker for ABP exposure but has not been implicated in ABP carcinogenesis. In one proposed mechanism, 4-nitrosobiphenyl, an oxidation product of ABP (to be described in Section 1.4.5), covalently binds to thiol groups on cysteine residues in hemoglobin to produce ABP-hemoglobin adducts (Green *et al.*, 1984; Shertzer *et al.*, 2002).

ABP is a potent mutagen in both bacterial and mammalian cell culture systems. Using the Ames test, ABP was mutagenic in *Salmonella* strains TA98 and TA100 in the presence of liver "S9" fraction, which contains enzymes required for the metabolic activation of ABP (Chung *et al.*, 2000). Detection of mutations in both TA98 and TA100 strains of *Salmonella*, which are

sensitive to base substitutions and frameshifts respectively, suggests that ABP induced both base substitution and frameshift mutations (Chung *et al.*, 2000). The requirement for metabolic activation was confirmed in a separate study where ABP-induced mutations in the Ames test correlated with levels of host NAT activity, which is involved in the metabolic activation of ABP as described previously (Section 1.4.3.2, (Dang and McQueen, 1999)). In *E.coli*, ABP-treated single-stranded phage DNA led almost exclusively to base substitution mutations in the form of G to T transversions (Verghis *et al.*, 1997). G to T transversions were also detected in mammalian cell culture assays. For example, an activated metabolite of ABP produced predominantly G to T transversions in the *cII* and hypoxanthine-guanine phosphoribosyl-transferase (HPRT) reporter genes of mouse embryonic fibroblasts and human lymphoblastoid cells, respectively (Besaratina *et al.*, 2002; Zayas-Rivera *et al.*, 2001).

Interestingly, ABP also produced mutations in *Salmonella* strain TA102, which is sensitive to the presence of ROS, and produced chromosomal instability in human colon and bladder cancer cells (Makena and Chung, 2007). The implications of these observations will be discussed in Section 1.4.5.

Using transgenic mouse assays, ABP proved to be a potent mutagen *in vivo* as well as in culture. In one study using the MutaTMMouse transgenic mouse line, chronic feeding of ABP to adult mice led to significantly increased mutations in the *lacZ* transgene from the bladder, liver, and bone marrow (Fletcher *et al.*, 1998). Age strongly influences ABP-induced mutation response in mice. Again using the MutaTMMouse transgenic mouse line, the same dose of ABP (on a mg/kg basis) induced mutations in livers of neonatal but not adult mice on the *cII* transgene (Chen *et al.*, 2005). Authors of this study have attributed this age difference to increased tissue proliferation in developing mice that resulted in inadequate DNA repair and rapid expansion of mutated cells (Chen *et al.*, 2005). In the same study, sequencing of the *cII* transgene in ABP-treated neonatal mouse livers revealed the most common mutation to be G to T transversions, in line with results generated in bacterial and mammalian cell cultures (Chen *et al.*, 2005).

As described in the multi-stage model of chemical carcinogenesis, mutations in oncogenes and tumor suppressors, such as *Ras* and *TP53* in mouse, provide cells with a growth advantage in tumor initiation. In an earlier study with adult C57BL/10J mice, few mutations in codons 12, 13,

and 61 of *Hras*, *Kras*, and *Nras* (implicated in other mouse carcinogenesis models) were detected in either spontaneous or ABP-induced liver tumors, suggesting that the RAS oncogene did not contribute to liver carcinogenesis in this mouse model (Lord *et al.*, 1992). On the other hand, ABP-induced liver tumors from a neonatal bioassay using CD-1 and B6C3F₁ mice demonstrated significantly increased mutations in codon 61 of *Hras*, perhaps as a result of increased sensitivity of neonatal livers towards mutations or as a result of increased tumor sensitivity in these strains of mice (Manjanatha, 1996). Major strain differences were detected with mutations on codon 61 of *Hras*, with the most abundant being an A to T transversion for CD-1 mice (50% of all tumors) and a C to A transversion for B6C3F₁ mice (85% of all tumors, (Manjanatha, 1996)). Here, the prevalence of ABP-induced mutations on codon 61 of *Hras* appeared to correlate with the prevalence of ABP-induced liver tumors from different strains of mice (~50% in CD-1 and ~80% in B6C3F₁), supporting a strong tumor initiating role for HRAS in ABP-induced liver carcinogenesis of B6C3F₁ mice (Manjanatha, 1996). An extension of strain comparisons to C57BL/6 was carried out in a separate study, where the level of C to A transversions on codon 61 of *Hras* in C57BL/6 mice was roughly 16% of those found in B6C3F₁ mice following ABP treatment (Parsons *et al.*, 2005). The molecular mechanism leading to strain differences in ABP-induced *Hras* mutations is unclear.

No information is available with regard to potential mutagenic effects of ABP on *TP53* in mouse liver. *In vitro* incubation of metabolically activated ABP with *TP53* identified 9 binding "hotspots", with 2 out of 9 hotspots often mutated in human bladder cancer, suggesting a potential link between ABP exposure and human bladder cancer (Feng *et al.*, 2002). However, ABP-induced mutations are mostly in the form of G to T transversions, whereas G to A transitions predominate in human bladder cancer (Besaratina *et al.*, 2002).

Several lines of evidence support C8-dG-ABP adducts as the source of G to T transversions in mouse liver. Firstly, the highest levels of mutations are detected in the presence of metabolic activation, which also lead to the formation of ABP-DNA adducts. Secondly, guanosine bases in DNA represent the major target for both ABP-DNA adducts and ABP-induced mutations. Finally, a significant overlap was detected when both ABP-induced DNA adducts and mutations were mapped on the *cII* transgene of embryonic fibroblasts from Big Blue mice (Besaratina *et al.*, 2002).

Taken together, an ABP carcinogenesis model where sequential metabolic activation of ABP to form C8-dG-ABP adducts that result in G to T mutations in oncogenes and/or tumor suppressors leading to tumor initiation has gained wide acceptance. A graphical representation of the traditional ABP carcinogenesis model linking ABP nitrenium ions to liver tumors in mice is shown in Figure 8.

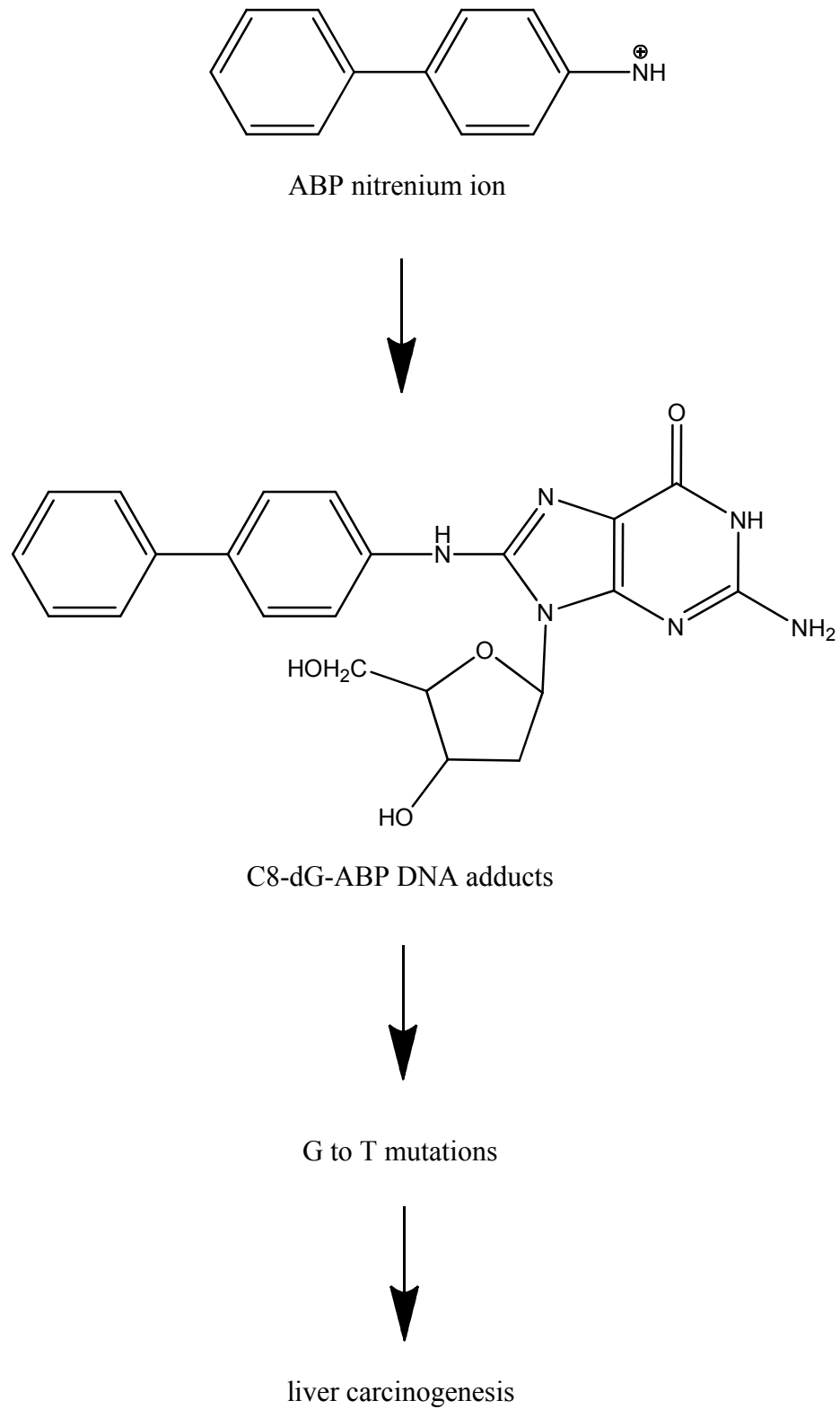


Figure 8. Traditional model of ABP-induced liver carcinogenesis in the mouse.

However, recent studies using genetically modified mice have generated evidence that is inconsistent with this traditional model of ABP carcinogenesis.

1.4.4 Evidence inconsistent with the traditional model of ABP bioactivation and tumor initiation in mouse liver

1.4.4.1 Studies with *Cyp1a2*(-/-) mice

According to the traditional ABP carcinogenesis model, *N*-hydroxylation by CYP1A2 represents the first step in two-step metabolic activation of ABP. Knocking out CYP1A2 is therefore expected to prevent ABP metabolic activation and carcinogenesis. Surprisingly, a single dose of ABP given to adult mice produced similar levels of C8-dG-ABP adducts in *Cyp1a2*(-/-) and wild-type males, and significantly higher levels of C8-dG-ABP adducts in *Cyp1a2*(-/-) compared to wild-type females (Tsuneoka *et al.*, 2003). In the same study, administration of the CYP1A2 inducer TCDD decreased, rather than increased, the level of C8-dG-ABP adducts (Tsuneoka *et al.*, 2003). In line with these observations, ABP produced similar levels of liver tumors in both *Cyp1a2*(-/-) and wild-type mice in a neonatal bioassay (Kimura *et al.*, 1999). Together these studies suggest that CYP1A2 has a greater role in the detoxification than in the metabolic activation of ABP *in vivo*, perhaps through ring hydroxylation. A net detoxification effect for CYP1A2 is also supported by observations from our own laboratory, where ABP clearance is significantly decreased in *Cyp1a2*(-/-) mice of both sexes (unpublished observations).

The fact that ABP produced similar levels of liver tumors in the presence and absence of CYP1A2 strongly suggests the existence of an alternative ABP *N*-hydroxylation enzyme in mouse liver. The existence of an alternative ABP *N*-hydroxylation enzyme is also supported by the detection of significant ABP *N*-hydroxylation activity in *Cyp1a2*(-/-) mouse liver microsomes (Kimura *et al.*, 1999). The only other enzyme shown to *N*-hydroxylate ABP is human CYP2A13 (Nakajima *et al.*, 2006). Compared to recombinantly expressed CYP1A2, recombinantly expressed CYP2A13 demonstrated a 4-fold higher k_m and 5-fold lower v_{max} for ABP *N*-hydroxylation, making it unlikely to play a major role in ABP-induced mouse liver carcinogenesis (Nakajima *et al.*, 2006).

A notable lack of correlation between ABP-induced DNA adducts and liver carcinogenesis surfaced in these *in vivo* studies using *Cyp1a2*(-/-) mice. Whereas a single dose of ABP produced

significantly more C8-dG-ABP adducts in females compared to males, males are much more susceptible to ABP-induced liver carcinogenesis (Kimura *et al.*, 1999; Tsuneoka *et al.*, 2003). This lack of correlation between C8-dG-ABP adducts and liver carcinogenesis suggests the presence of novel factors that can drive ABP carcinogenesis. Alternatively, minor ABP-DNA adducts not measured in these studies may play a critical role in ABP carcinogenesis. And finally, the lack of correlation between ABP-DNA adducts and liver carcinogenesis with *Cyp1a2(-/-)* mice may simply reflect differences in study design, such as different ABP doses, routes of administration, ages at exposure, and strains of mice.

1.4.4.2 Studies with *Nat1/2(-/-)* mice

NATs have been proposed to carry out the second step in the two-step metabolic activation of ABP according to the traditional ABP carcinogenesis model. In a neonatal bioassay carried out previously in our laboratory, we compared ABP-induced liver carcinogenesis between male and female mice that are wild-type or *Nat1/2(-/-)* (Sugamori *et al.*, 2012). In this study, mice were given a total of 600 nmol or 1200 nmol of ABP on postnatal days 8 and 15, and assessed at 1 year of age for liver tumor formation. The same metabolic activation pathway as depicted in the traditional ABP carcinogenesis model for adult mice is expected to operate in neonatal mice, since both mRNA and activity of CYP1A2 and NATs can be detected in mouse liver as early as 1-4 days after birth (Cui *et al.*, 2012; McQueen and Chau, 2003; Mitchell *et al.*, 1999). In this study, we observed similar sex differences as Kimura *et al.* (2009), with females being completely protected from liver tumors at 1 year. Sex differences in ABP-induced mouse liver carcinogenesis seem to parallel the sex differences found in human liver cancer and cannot be attributed to differences in ABP metabolism, since the expression of CYP1A2 and NATs show no major sex differences at any age in mice (Cui *et al.*, 2012; Kahl *et al.*, 1980; Sugamori *et al.*, 2012). Furthermore, within males, *Nat1/2(-/-)* mice had significantly lower tumor incidence and multiplicity than wild-type mice, which on the surface seemed to confirm the role of the NATs in the metabolic activation of ABP (Sugamori *et al.*, 2012). However, no sex differences were found in levels of C8-dG-ABP adducts (Sugamori *et al.*, 2012). Equally surprising was the observation that within each sex, *Nat1/2(-/-)* mice showed higher rather than lower levels of C8-dG-ABP adducts compared to wild-type mice (Sugamori *et al.*, 2012). Taken together, these results suggest that NATs, like CYP1A2, have a greater role in the detoxification rather than

metabolic activation of ABP, but may assume a novel tumor-promoting role in later stages of ABP carcinogenesis. Additional support for a novel tumor-promoting role for the NATs that is separate from their drug-metabolizing functions has been derived from cell culture studies, where over-expression of NAT1 promoted cellular proliferation and metastasis, while NAT1 inhibition produced decreased proliferation and invasiveness (Butcher and Minchin, 2012; Tiang *et al.*, 2011; Tiang *et al.*, 2010).

As with the *Cyp1a2(-/-)* studies, a complete lack of correlation was observed between ABP-induced C8-dG-ABP adducts and liver tumor incidence in *Nat1/2(-/-)* mice. However, unlike the *Cyp1a2(-/-)* studies, C8-dG-ABP adducts and liver tumors in *Nat1/2(-/-)* mice were measured under identical ABP exposure conditions, providing strong support for the existence of as yet uncharacterized factor(s) that drive ABP-induced mouse liver carcinogenesis and in turn produce the sex and strain differences observed in this tumor model. One such factor may be oxidative stress.

1.4.5 *In vitro* and *in vivo* evidence linking ABP to oxidative stress

Several lines of evidence originating from both *in vitro* and *in vivo* studies have supported a role for oxidative stress in ABP-induced mouse liver carcinogenesis. *In vitro*, HOABP produced hydrogen peroxide and oxidative DNA damage in the presence of copper, oxygen, and NADH (Makena and Chung, 2007; Murata *et al.*, 2001). The proposed mechanism linking HOABP to oxidative stress *in vitro* is shown in Figure 9.

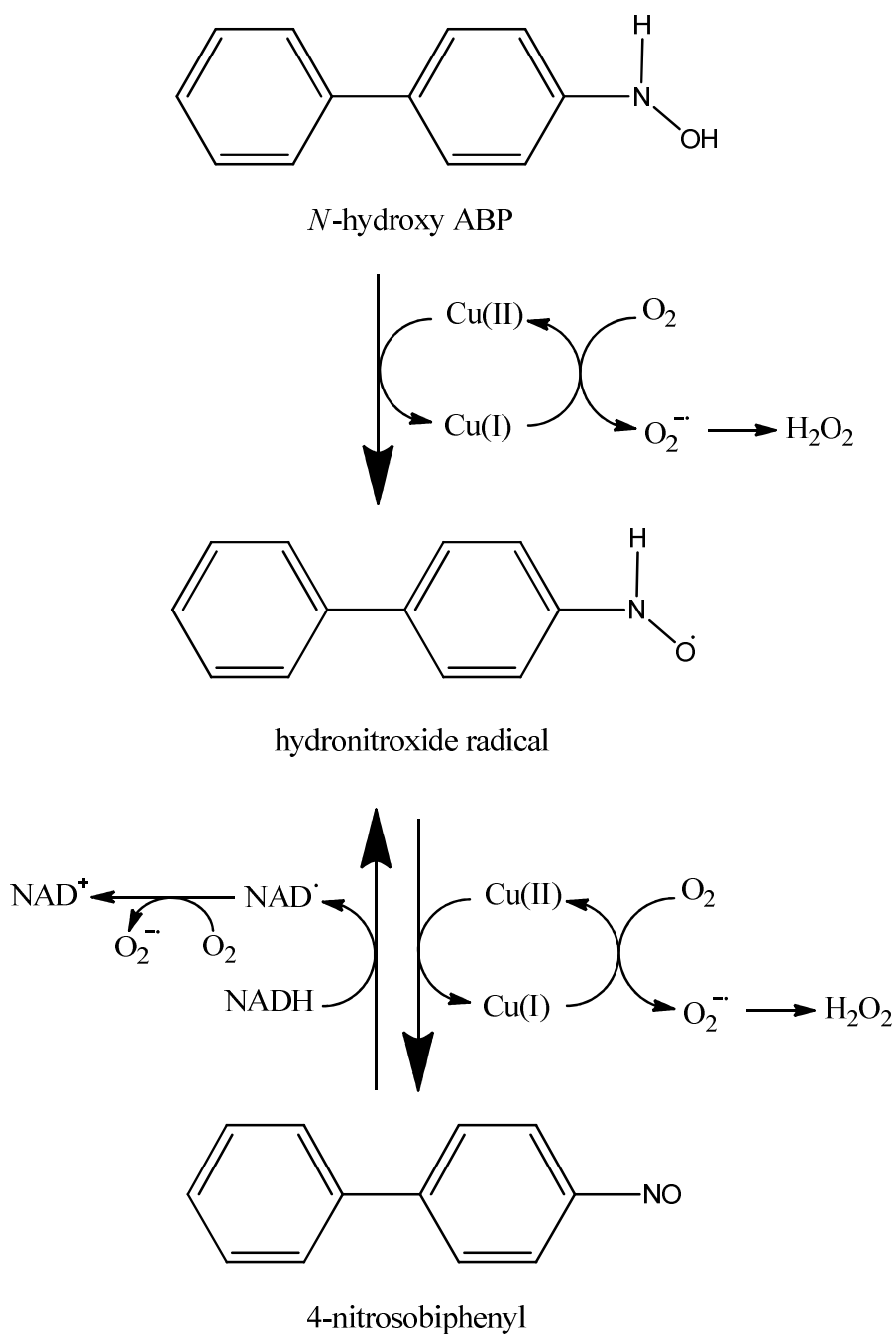


Figure 9. Proposed mechanism of HOABP-induced oxidative stress *in vitro*.

© Figure adapted from Murata *et al.* 2001 with permission from Elsevier.

The proposed mechanism involves a cycling reaction between the hydronitroxide and nitroso forms of ABP in the presence of NADH and oxygen, leading to continuous production of ROS. Dependence on NADH for redox cycling seems to be shared between ABP and 2-acetylaminofluorene (discussed in Section 1.2.5).

Using the Ames test, metabolically activated ABP induced mutations in *Salmonella* strain TA102, a strain with demonstrated sensitivity towards oxidative agents (Levin *et al.*, 1982; Makena and Chung, 2007). In addition, a number of antioxidants blocked the mutagenic effects of ABP in *Salmonella* strain TA102 (Makena and Chung, 2007). In the HepG2 human hepatoma cell line, ABP produced both ROS and oxidative DNA damage that can be blocked with antioxidants, although it should be noted that high concentrations of ABP and long incubation times were used in this study (Wang *et al.*, 2006). In cultured bladder and colorectal cancer cells, metabolically activated ABP produced chromosome instability, which often results from DNA strand breaks (Saletta *et al.*, 2007). DNA strand breaks, in turn, may arise from the attack of ROS on the DNA phosphate backbone (Geigl *et al.*, 2008). An ability for metabolically activated ABP to generate DNA strand breaks through oxidative stress may also explain initial observations of ABP-induced frameshift mutations in the Ames test, which have received relatively little attention compared to base-substitution mutations (Section 1.4.3.3(Ames *et al.*, 1972)).

In vivo, ABP leads to methemoglobinemia, which is characterized by a chocolate-brown appearance of blood and results from the oxidation of heme in hemoglobin, forming methemoglobin. According to one proposed mechanism, co-oxidation of HOABP with hemoglobin leads to the formation of nitrosobiphenyl and methemoglobin, respectively; nitrosobiphenyl can subsequently react with thiol groups on cysteine residues of hemoglobin to form ABP-hemoglobin adducts (Figure 10, (Green *et al.*, 1984; Shertzer *et al.*, 2002)).

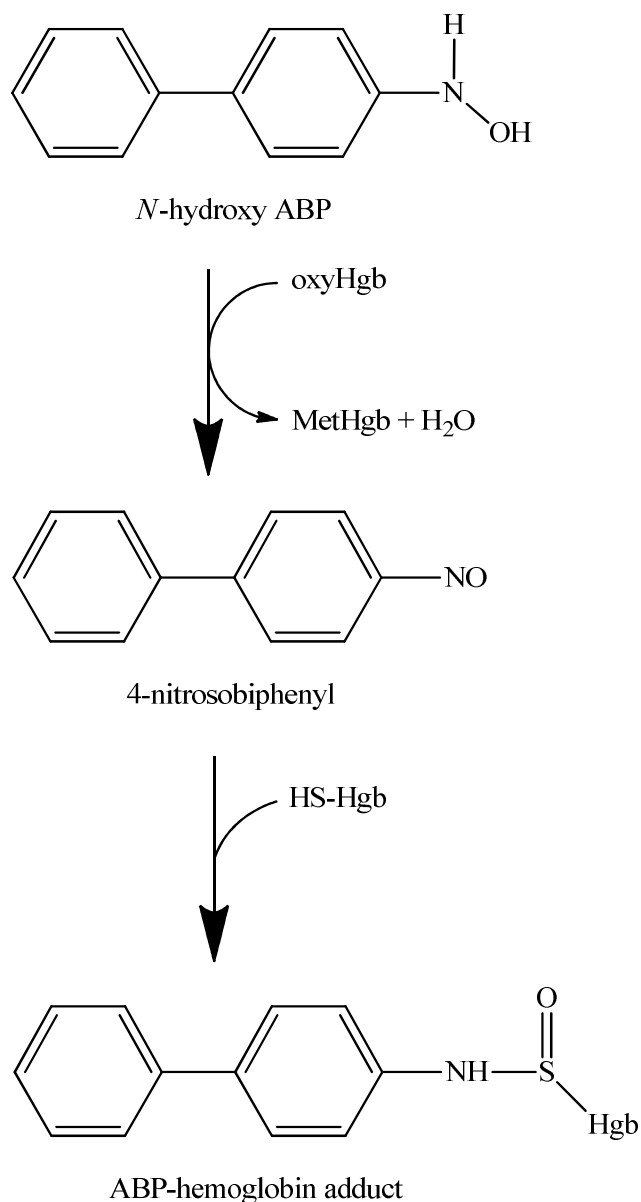


Figure 10. Proposed mechanism linking ABP to the formation of methemoglobin and ABP-hemoglobin adducts.

"oxyHgb" = hemoglobin. "MetHgb" = methemoglobin. "HS-Hgb" = thiol groups on hemoglobin.

It should be noted that, just like C8-dG-ABP adducts, ABP-induced methemoglobinemia increased in *Cyp1a2*(-/-) mice and decreased in TCDD-treated mice, supporting CYP1A2 as a detoxification rather than metabolic activation enzyme for ABP (Shertzer *et al.*, 2002). Finally, a single dose of ABP given to adult mice significantly depleted hepatic thiols, the major source of liver antioxidants, in males but not in females, suggesting that ABP produced oxidative stress in

adult mouse liver with a male preference (Shertzer *et al.*, 2002; Tsuneoka *et al.*, 2003). In addition, the protective effect seen in females seems to be mediated by CYP1A2, as *Cyp1a2*(-/-) females are not protected from ABP-induced oxidative stress under these conditions (Tsuneoka *et al.*, 2003).

1.5 Aims of the thesis

More than a century has passed since Rehn's initial discovery of aromatic amines as potent human carcinogens. As one of the first and largest classes of human carcinogens known to man, aromatic amines have been the focus of extensive research efforts, yet mechanisms that link the prototypical aromatic amine, ABP, to liver carcinogenesis in mice are still far from clear. Our overall goal is to gain a better understanding of the molecular mechanisms underlying ABP-induced mouse liver carcinogenesis. Specifically, we wish to unveil the biological factor(s) that drives pronounced sex and strain differences observed with ABP-induced liver tumors in our neonatal bioassay. Such factors may represent previously unidentified players in the carcinogenesis of aromatic amines, which may in turn lead to improved chemoprevention measures against this important class of human carcinogens. In addition, as human liver cancer demonstrates the same sex differences as observed in our ABP neonatal bioassay, our findings may reveal novel drug targets for the treatment of human liver cancer.

According to a widely-accepted model of chemical carcinogenesis, DNA damage that escapes repair prior to DNA replication can be fixed into the genome as mutations that can subsequently influence the extent and/or rate of tumor initiation and growth (Section 1.1.3). Both *in vitro* and *in vivo* studies have shown that ABP generates a high frequency of mutations, mostly in the form of G to T transversions, which are suggested to be critical in tumor initiation (Section 1.4.3.3). Furthermore, the ability for ABP to generate G to T transversions in mouse liver has been taken as evidence for the importance of C8-dG-ABP adducts, which produce mainly G to T transversions *in vitro*, in tumor initiation (Section 1.4.3.3). Given recent results from our laboratory that demonstrated a lack of correlation between C8-dG-ABP adducts and tumor incidence, in this thesis we measured ABP-induced *in vivo* mutation frequencies and spectra in male and female mice that are wild-type or *Nat1/2*(-/-), which were subsequently compared with liver tumor incidence observed in similarly treated mice (Section 3.1).

Since the proposal of CYP1A2 as the major enzyme responsible for aromatic amine *N*-hydroxylation in human liver microsomes, studies on aromatic amine carcinogenesis have often assumed an essential role for CYP1A2 in carrying out the initial metabolic activation of aromatic amines such as ABP (Section 1.4.3.1). Surprisingly, *Cyp1a2*(*-/-*) mice demonstrated a similar level of *in vitro* ABP *N*-hydroxylation activity and liver tumor incidence compared to wild-type mice in an ABP neonatal bioassay (Kimura *et al.*, 1999). In adults, a single dose of ABP produced similar levels of C8-dG-ABP adducts in wild-type mice, *Cyp1a2*(*-/-*) mice, and wild-type mice treated with TCDD (an inducer of CYP1A2, (Tsuneoka *et al.*, 2003)). These studies raise the possibility that CYP1A2 may not be the only or even the major ABP *N*-hydroxylation enzyme in mouse liver and that an alternative ABP *N*-hydroxylation enzyme(s) exists. Given the central importance of the ABP *N*-hydroxylation reaction to both ABP bioactivation and ABP-induced oxidative stress (Sections 1.4.3 and 1.4.5), we sought to identify the major ABP *N*-hydroxylation enzyme(s) in mouse liver microsomes (Section 3.2).

As described previously, a surprising lack of correlation was detected between levels of C8-dG-ABP adducts and liver tumor incidence in the ABP neonatal bioassay, which suggests that ABP-induced DNA damage may be necessary but neither sufficient nor rate-limiting for ABP-induced carcinogenesis in mouse liver (Section 1.4.4.2, (Sugamori *et al.*, 2012)). In turn, our data support the existence of a previously uncharacterized driver(s) of liver carcinogenesis that does not arise from DNA adducts induced by ABP and is responsible for the sex and/or strain differences observed in liver tumor incidence. In light of both *in vitro* and *in vivo* studies linking ABP to oxidative stress, which represents a major risk factor for liver cancer in both humans and mice, we investigated whether ABP produces oxidative stress in a cell culture setting and *in vivo* following our tumor-inducing neonatal exposure protocol, which is again correlated to liver tumor incidence observed in similarly treated mice. We also measured liver antioxidant response following tumorigenic doses of ABP, which represents a major determinant of oxidative stress in mouse liver (Section 3.3).

Chapter 2
MATERIALS AND METHODS

2.1 Chemicals and reagents

HOABP was purchased from Toronto Research Chemicals (Toronto, ON, Canada). MEM (-phenol red, cat. #51200038) was purchased from Life Technologies Inc. (Burlington, ON, Canada). HPLC grade methanol and acetonitrile were purchased from Caledon Laboratories Ltd. (Georgetown, ON, Canada). Protease and phosphatase inhibitors were purchased from Roche Diagnostics (Laval, QC, Canada). Anti- γ H2AX antibody was purchased from EMD Millipore Co. (Billerica, MA, USA). Anti-H3 antibody was purchased from Sigma-Aldrich Canada Ltd. (Oakville, ON, Canada). NRF2 antiserum was kindly provided by Ed Schmidt from the Department of Immunology and Infectious Diseases at the Montana State University, MT, USA. Anti-mouse and anti-rabbit secondary antibodies were purchased from Cell Signaling Technology Inc. (Danvers, MA, USA). Enhanced Chemiluminescence (ECL) Prime was purchased from GE Healthcare (Baied'Urfe, QC, Canada). All other chemicals were purchased from Sigma-Aldrich Canada Ltd. (Oakville, ON, Canada).

2.2 Animal treatment

All procedures involving animals were performed in accordance with the Canadian Council on Animal Care guidelines and approved by the University of Toronto Animal Care Committee. MutaTMMouse breeding stocks were kindly provided by Paul A. White and George R. Douglas at the Mechanistic Studies Division, Environmental and Radiation Health Sciences Directorate, Health Canada, Ottawa, Ontario, Canada (Gossen *et al.*, 1989). *Nat1/2(-/-)* MutaTMMouse animals were generated by other members of the laboratory by crossing MutaTMMouse with *Nat1/2(-/-)* mice, interbreeding the F1 hybrids, genotyping the F2 offspring for both the absence of the *Nat1/2* gene region and the presence of the MutaTMMouse λ gt10-*lacZ* transgene, and establishing appropriate breeding pairs for the generation of tester mice (Section 2.4, (Sugamori *et al.*, 2003)). Breeding stocks of *Cyp1a2(-/-)* mice (on a congenic C57BL/6 genetic background) were kindly provided by Daniel W. Nebert from the Department of Environmental Health, University of Cincinnati Medical Center, Cincinnati, OH, USA (Liang *et al.*, 1996). Breeding stocks of *Cyp2e1(-/-)* mice (on a congenic SVJ129 background) were kindly provided by Frank J. Gonzalez at the National Cancer Institute, Bethesda, MD, USA (Lee *et al.*, 1996). *Cyp2e1(-/-)* SVJ129 and C57BL/6 mixed-strain mice were generated by crossing *Cyp2e1(-/-)* SVJ129 with

C57BL/6 mice, interbreeding the F1 hybrids, and genotyping the F2 offspring for *Cyp2e1* status (*Cyp2e1*(+/+) or *Cyp2e1*(-/-)). C57BL/6 mice were purchased from Charles River Laboratories Inc. (Senneville, QC, Canada).

For the neonatal ABP exposure protocol, mice were injected intraperitoneally on postnatal days 8 and 15 with 1/3 and 2/3 of the total dose of ABP, respectively, at total doses of 600 nmol (~8.5 mg/kg per dose) or 1200 nmol (~17 mg/kg per dose), or with the corresponding volume of DMSO vehicle. For the adult subchronic exposure protocol, mice aged 8 weeks were injected intraperitoneally every second day for 28 days with ABP at 10 mg/kg per dose (total exposure ~20000 nmol) or 20 mg/kg per dose (total exposure ~40000 nmol), or with the corresponding volume of corn oil vehicle. Livers were collected 3 days after the final ABP treatment. For pyrazole treatment, day 15 *Cyp1a2*(-/-) mice were injected intraperitoneally with 50 mg/kg pyrazole daily for three consecutive days and sacrificed for liver collection one day following the last injection.

2.3 Cell culture and cell transfection

Hepal1c1c7 cells were cultured in Minimum Essential Medium (MEM, Life Technologies Inc., Burlington, ON, Canada) in the presence of 10% v/v fetal bovine serum (Sigma-Aldrich Canada Ltd., Oakville, ON, Canada), non-essential amino acids, penicillin-streptomycin, and 2 mM L-glutamine (Life Technologies Inc., Burlington, ON, Canada). PcDNA3.1(+) expression plasmid containing mouse *Cyp1a2* cDNA was kindly provided by Shigeyuki Uno at the Department of Biomedical Sciences, Nihon University, Itabashi-ku, Tokyo, Japan. PCMV6 expression plasmid containing mouse *Cyp2e1* cDNA was purchased from OriGene Technologies (Rockville, MD, USA). Rat CYP2E1 expression plasmids (wild-type and mutants) were kindly provided by Narayan Avadhani from the Department of Animal Biology at the University of Pennsylvania, PA, USA.

Transient transfection of Hepal1c1c7 cells was carried out using the lipid-based transfection reagent Lipofectamine[®] LTX (Life Technologies Inc., Burlington, ON, Canada) following the manufacturer's protocol. Briefly, cells were seeded at 5×10^5 cells per well onto 6-well plates, grown overnight, treated with transfection mix (6 μ L LTX : 2 μ g of DNA for CYP1A2 and 9 μ L LTX : 2 μ g of DNA for CYP2E1) for 6 hours in MEM only, and followed by a change back to

complete growth medium at 6 hours. Cells were used for in-culture drug metabolism assays at 24 hours following transfection. The transfection protocol for 96-well plates was the same as described for 6-well plates but scaled down proportionally (25-fold) to account for the decreased surface area of each well.

2.4 Genotyping assays for NAT1/2, CYP2E1, and the MutaTM Mouse transgene

For the isolation of genomic DNA from mouse tails, tail clips (~0.5 cm in length) were minced with scissors and digested with 0.5 mg/mL proteinase K in 500 μ L of proteinase K buffer (100 mM Tris pH 8.0, 5 mM EDTA, 200 mM NaCl, 0.4% w/v SDS) overnight at 55°C. Samples were centrifuged the next day to remove debris. The aqueous supernatant fraction was extracted twice with an equal volume of phenol:chloroform (1:1, v/v) and once with an equal volume of chloroform. Ethanol was then added to a final concentration of 70% v/v to precipitate genomic DNA from the aqueous phase. The genomic DNA pellet was washed once with 70% v/v ethanol and dissolved in 50 μ L of TE buffer (10 mM Tris-HCl, 1 mM EDTA, pH 8.0). Genomic DNA isolations for *in vivo* mutation studies were carried out by D. Bott.

The presence of the MutaTM Mouse transgene in genomic DNA was determined using polymerase chain reactions (PCR) by D. Bott, with the primers 5'-GGA CAG GAG CGT AAT GTG GCA-3' (sense) and 5'-AAT TGC AGC ATC CGG TTT CAC-3' (antisense), each at a final concentration of 0.4 μ M. The following PCR program was used for the MutaTM Mouse transgene primers: 3 minutes at 94°C; 35 cycles of 30 seconds at 95°C, 30 seconds at 56°C, 45 seconds at 72°C; and 5 minutes at 72°C.

PCR for the absence of *Nat1/2* was performed by D. Bott as described previously (Sugamori *et al.*, 2003). *Nat1/2*(-/-) mice that were either homozygous or hemizygous for the λ gt10-*lacZ* transgene were used in *in vivo* mutation detection studies.

Cyp2e1(-/-) genotyping protocols were adapted from those provided by the Gonzalez laboratory (Lee *et al.*, 1996). The wild-type allele was identified by the presence of a 125 bp PCR product using the primers 5'-AGT GTT CAC ACT GCA CCT GG-3' (sense) and 5'-CCT GGA ACA CAG GAA TGT CC-3' (antisense) each at a final concentration of 0.2 μ M. The *Cyp2e1*(-/-)

allele was identified by the presence of a 280 bp PCR product using the primers 5'-CTT GGG TGG AGA GGC TAT TC-3' (sense) and 5'-TAC CGG TGG ATG TGG AAT G-3' (antisense) each at a final concentration of 0.2 μ M. The following PCR program was used for both wild-type and *Cyp2e1*(-/-) primers: 10 minutes at 94°C; 40 cycles of 15 seconds at 95°C, 20 seconds at 60°C, 20 seconds at 72°C; and 7 minutes at 72°C.

2.5 Liver genomic DNA isolation

High molecular weight liver genomic DNA was isolated using a phenol-based extraction method. In brief, approximately 100 mg of frozen liver was thawed and manually homogenized in 5 mL of ice cold homogenization buffer (50 mM Tris-HCl pH 7.6, 5 mM MgCl₂, 50 mM NaCl, 1 mM EDTA, 5% v/v glycerol, and 0.1% w/v Triton X-100) using a Dounce homogenizer and Teflon pestle. The homogenate was centrifuged for 10 minutes at 1100 x g at 4°C, and the pellet of cell nuclei was resuspended in 3 mL of proteinase K buffer (100 mM Tris-HCl pH 8.0, 5 mM EDTA, 200 mM NaCl, 0.2% w/v SDS). RNase A (3 μ l of a 10 mg/ml stock) was added and the sample was incubated with gentle rocking for 60 minutes at 37°C. Proteinase K (10 μ l of a 20 mg/ml stock) was added, the mixture was incubated with gentle rocking for 90 minutes at 55°C, a second aliquot of enzyme was added, and the incubation was repeated. The mixture was then extracted using an equal volume of phenol, followed by phenol:chloroform:isoamyl alcohol (25:24:1, v/v/v) and chloroform:isoamyl alcohol (24:1, v/v) for 10 minutes each at room temperature with gentle rocking. Finally, an equal volume of ice-cold isopropanol was added to the extract and gently inverted until genomic DNA precipitated. DNA was spooled with a glass hook, briefly rinsed in 70% v/v ethanol, air-dried for 5 minutes, and redissolved in 50 μ L of 10 mM Tris-HCl, 1 mM EDTA, pH 7.6 at 37°C overnight. Only highly viscous DNA with concentrations greater than 1 μ g/ μ L and A260/280 ratios of >1.60 were used for subsequent *in vitro* packaging reactions.

2.6 λ phage packaging and *cII* mutation assay

The λ Select-*cII* Mutation Detection System and Transpack Packaging Extracts were purchased from Agilent Technologies (Mississauga, ON, Canada). λ phage packaging and *cII* mutation assays were performed according to the manufacturer's instructions, with the assessment of plaques on titering plates at 24 to 48 hours after plating and on screening plates at 48 to 72 hours

after plating. Re-plating experiments confirmed the *cII* mutation status of approximately 95% of initially detected screening plaques.

2.7 *cII* mutant gene sequence analysis

A total of 30-40 *cII* mutant plaques from among the animals in each treatment group were re-plated and sequenced using the manufacturer's protocol with the following modifications. PCR reactions were performed using the following program: 3 minutes at 95°C; 40 cycles of 30 seconds at 95°C, 1 minute at 54°C, 1 minute at 72°C; and 10 minutes at 72°C. PCR products were purified and sequenced at The Centre for Applied Genomics (located in the Hospital for Sick Children, Toronto, ON, Canada). DNA sequences of wild-type and mutant *cII* genes were compared using EMBOSS Needle software, available on the European Bioinformatics Institute website (<http://www.ebi.ac.uk/>). Mutational spectra were compared using the algorithm developed by Adams and Skopek (Adams and Skopek, 1987; Cariello *et al.*, 1994) with 6 pairwise comparisons made between treated and control animals, sexes, and strains.

2.8 Microsomal preparations from mouse liver and cell culture

Animals were sacrificed by cervical dislocation. Livers were collected, snap frozen in liquid nitrogen, and stored at -80°C until processing. Livers were homogenized in 4 volumes of homogenization buffer (155 mM KCl and 10 mM potassium phosphate, pH 7.4) at 15000 rpm for 20 seconds with a Polytron PT 1200E (Kinematicak Inc., Bohemia, NY, USA). To prepare microsomes from cell culture, two confluent 100 mm plates of transfected or untransfected Hepa1c1c7 cells were collected via scraping into 1 mL of homogenization buffer and homogenized as with liver tissue. Homogenates from both liver tissue and cell culture were centrifuged at 9000 x g for 20 minutes. The supernatant was further centrifuged at 105,000 x g for 1 hour to pellet the microsomal fraction. The microsomal pellet was washed by resuspending in an equal volume of homogenization buffer and centrifuging again at 105,000 x g for 1 hour to obtain the final microsomal pellet, which was resuspended in storage buffer (10 mM Tris, 1 mM EDTA, 20% w/w glycerol, pH 7.4) to a final volume of 1 ml per gram of original liver weight, aliquoted, snap frozen in liquid nitrogen, and stored at -80°C. Protein concentrations in microsomal preparations were determined using the Bio-Rad Protein Assay (Bio-Rad Laboratories Ltd., Mississauga, ON, Canada).

2.9 *In vitro* and *in culture* ABP *N*-hydroxylation assays

Each *in vitro* ABP *N*-hydroxylation reaction contained 20 μL of 0.5 M potassium phosphate buffer pH 7.4, 10 μL of 2 mM ABP in 10% v/v acetonitrile, 25 μL of 20 mM MgCl_2 , 5 μL of 10 mM NADP^+ , 10 μL of 50 mM glucose-6-phosphate, 1 μL of G6PD, and 29 μL of microsomal preparation (final concentration ~ 1 mg/mL) to a total volume of 100 μL . Reactions were incubated at 37°C for 10 minutes and terminated by addition of 50 μL of ice-cold acetonitrile containing 0.3 mM ascorbic acid. The samples were mixed and centrifuged at 13000 rpm for 5 minutes to precipitate proteins. 50 μL of the supernatant was then injected onto a reverse phase C18 Beckman Ultrasphere HPLC column at a flow rate of 2 mL/minute. The HPLC mobile phase contained 25% w/w acetonitrile and 75% w/w of 20 mM sodium perchlorate buffer at pH 2.5. UV absorbance was measured at 280 nm and 35°C. Under these conditions, ABP and HOABP had retention times of 3.0 and 6.6 minutes, respectively. For the 1-aminobenzotriazole (ABT) inhibition experiment, reaction mixtures (minus ABP) were pre-incubated with or without ABT for 30 minutes at 37°C prior to reaction initiation with the addition of ABP. For *in culture* ABP *N*-hydroxylation assays, ABP was added to cell culture medium to a final concentration of 100 μM . At 0.25, 1, and 4 hours following incubation, 50 μL of medium was withdrawn, mixed with 50 μL of ice-cold acetonitrile containing 0.3 M ascorbic acid, centrifuged at 13000 rpm for 5 minutes, and 50 μL of this supernatant was analyzed by HPLC using same conditions as described above for the *in vitro* assay.

2.10 *In vitro* and *in culture* pNP hydroxylation assays

Each *in vitro* pNP hydroxylation reaction contained 20 μL of 0.5 M potassium phosphate buffer pH 7.4, 10 μL of 2 mM pNP dissolved in H_2O , 25 μL of 20 mM MgCl_2 , 5 μL of 10 mM NADP^+ , 10 μL of 50 mM glucose-6-phosphate, 1 μL of G6PD, and 29 μL of microsomal preparation (final concentration ~ 1 mg/mL) to a total volume of 100 μL . Reactions were incubated at 37°C for 30 minutes and terminated by addition of 5 μL of 60% w/v HClO_4 . The samples were mixed and centrifuged at 13000 rpm for 5 minutes to precipitate proteins. 50 μL of the supernatant was then injected onto a reverse phase C18 Beckman Ultrasphere HPLC column at a flow rate of 1 mL/minute. The HPLC mobile phase contained 25% w/w acetonitrile and 75% w/w of 0.1% w/w acetic acid. UV absorbance was measured at 345 nm and 35°C. Using these

HPLC conditions, pNP and 4-nitrocatechol have retention times of 6.5 and 4.0 minutes, respectively. For the *in culture* pNP hydroxylation assay, pNP was added to cell culture medium to a final concentration of 200 μM and incubated with cells for 2 hours. Following incubation, 100 μL of medium was withdrawn, mixed with 5 μL of 60% w/v HClO_4 , spun at 13000 rpm for 5 minutes, and 50 μL of the supernatant was analyzed by HPLC using the same conditions as described above for the *in vitro* assay.

2.11 Immunoblotting

For the detection of γH2AX and H3 levels in cell culture, cells grown on 6-well plates were washed twice with PBS and collected via scraping into 500 μL of sonication buffer (150 mM NaCl, 150 mM Tris-HCl, pH 7.4, 1x protease inhibitors, and 1x phosphatase inhibitors). Samples were kept on ice at all times. Cells were lysed via sonication using a probe sonicator (Thermo Fisher Scientific Inc., Burlington, ON, Canada) at 25% amplitude with 4 x 5 second bursts on ice. Protein concentrations in cell lysates were determined using the Bio-Rad Protein Assay (Bio-Rad Laboratories Ltd., Mississauga, ON, Canada). 4x SDS-PAGE Laemmli buffer (250 mM Tris-HCl pH 6.8, 8% w/v SDS, 40% v/v glycerol, 20% v/v β -mercaptoethanol, and 0.1% w/v bromophenol blue) were added to lysates to make samples with $\sim 1 \mu\text{g}/\mu\text{L}$ protein in 1x SDS-PAGE Laemmli buffer. Samples were then boiled at 95°C for 10 minutes and loaded onto 2 x 12.5% SDS-PAGE gels. Both gels were run simultaneously until the loading dye was approximately 2 cm from the bottom of the separating gel. At this point, gels were taken out of the gel-running apparatus and transferred onto nitrocellulose blots at 100 V, 4°C , for 50 minutes. Subsequently, blots were blocked with 4% w/v powdered milk in TNT buffer (10 mM Tris-HCl, 150 mM NaCl, 0.05% v/v Tween 20, pH 8.0) for 2 hours at room temperature and incubated with primary antibodies (3:50000 dilution for γH2AX and 1:500000 dilution for H3) overnight. The next day, blots were washed for 3 x 5 minutes with TNT buffer, incubated with secondary antibodies (anti-mouse for γH2AX in TNT buffer and anti-rabbit for H3 in blocking solution, both at 1:10000 dilutions), washed for 3 x 10 minutes, incubated for 2 minutes with ECL prime, exposed against x-ray films, and developed in a film developer.

For the detection of γH2AX and H3 levels in liver tissue, animals were sacrificed by cervical dislocation, livers were perfused with PBS, collected, snap frozen in liquid nitrogen, and stored

at -80°C until processing. 50 mg of liver was homogenized in 2.5 mL of homogenization buffer (5 mM MgCl_2 , 50 mM Tris-HCl pH 7.6, 50 mM NaCl, 1 mM EDTA, 5% v/v glycerol, 0.1% w/w Triton X-100, and 1/1000 v/v β -mercaptoethanol added right before use) using a Dounce homogenizer and Teflon pestle. Contents were kept on ice at all times. Liver homogenate was centrifuged at $1100 \times g$ for 10 minutes to pellet nuclei, which were resuspended in 500 μL of sonication buffer for sonication. Subsequent steps were identical to those described above for cell culture with the addition of a brief centrifugation at $1000 \times g$ for 2 minutes at 4°C after sonication to remove tissue debris. For NRF2, a 10% SDS-PAGE gel, a 1 hour transfer period, and a 1:10 000 dilution of the antiserum were used.

2.12 DCF assay

Hepal1c7 cells were seeded at 3×10^4 cells per well into a 96-well plate (cat. #83.1835, SARSTEDT Inc., Montreal, QC, Canada) and grown overnight. The next day, cells were incubated with 50 μM of freshly prepared dichlorofluorescein (DCF) dye in complete cell culture medium for 1 hour, washed twice with 200 μL MEM (minus phenol red), treated with drugs of interest in 100 μL MEM (minus phenol red), and measured immediately on a fluorescence kinetic plate reader (37°C , excitation = 485 nm, emission = 528 nm, 1 read/minute for 30 minutes). Slopes of kinetic curves (rates of reactive oxygen species production) were recorded as the DCF signal. For transfected cells, cells were seeded at 2×10^4 cells per well onto a 96-well plate, grown overnight, transfected with the gene of interest on the second day, and tested in the DCF assay on the third day.

2.13 Total and oxidized glutathione assays

Animals were sacrificed by cervical dislocation. Livers were perfused with PBS, excised, snap frozen in liquid nitrogen, and stored at -80°C until processing. Levels of total and oxidized glutathione in liver tissue were quantified using the Glutathione Detection kit supplied by Enzo Life Sciences Inc. (Farmingdale, NY, USA) following the manufacturer's instructions. Briefly, 50 mg of frozen liver tissue was homogenized in 1 mL of 5% w/v meta-phosphoric acid, centrifuged at $14000 \times g$ for 15 minutes at 4°C , and the supernatant was snap frozen and stored at -80°C for future use in both total glutathione and oxidized glutathione assays. For the measurement of total glutathione, a 1:100 dilution of liver tissue homogenate with 1x Assay

Buffer was used. Reaction Buffer was prepared fresh with the addition of glutathione reductase. 150 μL of freshly prepared reaction buffer was added to 50 μL of diluted liver sample or glutathione standard and read immediately on an absorbance kinetic plate reader (37°C , absorbance = 410 nm, 1 read/11 seconds for 3 minutes). For the measurement of oxidized glutathione, a 1:2 dilution of liver tissue homogenate with 1x Assay Buffer was used. Diluted liver samples and glutathione standards were incubated with 40 mM of 4-vinylpyridine for 1 hour at room temperature to remove reduced glutathione in liver samples prior to the addition of Reaction Buffer. Subsequent steps were same as those described above for total glutathione. All buffers and reagents used in this assay were supplied by the manufacturer. Using glutathione standards, a standard curve (pmol glutathione vs. slope of kinetic curves) was generated that was then used to determine the concentration of glutathione present in liver samples using the slopes of their absorbance kinetic curves.

2.14 RNA extraction and cDNA synthesis

To extract RNA from liver, 10 mg of tissue was homogenized in 1 mL of Trizol[®] with a Polytron PT 1200E (Kinematicak Inc., Bohemia, NY, USA) at 15000 rpm for 20 seconds on ice and then incubated for 5 minutes at room temperature. 200 μL of chloroform was added to the mixture, vortexed for 15s, incubated for 5 minutes at room temperature, and centrifuged at 12000 x g for 15 minutes at 4°C . The top aqueous phase was precipitated with 0.5 mL isopropanol, vortexed, and centrifuged at 12000 x g for 10 minutes at 4°C . The resulting RNA pellet was washed with 1 mL of 75% v/v ethanol and centrifuged at 7500 x g for 5 minutes at 4°C . The supernatant was aspirated away and the RNA pellet was air-dried for 10 minutes at room temperature. Finally, the RNA pellet was resuspended in 50 μL of diethylpyrocarbonate (DEPC)-treated water and incubated for 10 minutes at 55°C to dissolve. The quality and concentration of RNA samples were determined using NanoDrop[®] (Thermo Fisher Scientific Inc., Burlington, ON, Canada). The integrity of RNA was verified by the presence of intact 28S (~5kb) and 18S (~2kb) rRNA bands on an agarose gel. RNA samples were stored at -80°C .

Prior to reverse transcription, RNA was first treated with DNase I (Thermo Fisher Scientific Inc., Burlington, ON, Canada) to remove potential DNA contamination. This was done by incubating RNA with DNase I in the appropriate buffer for 30 minutes at 37°C . The DNase I reaction was

terminated with the addition of EDTA followed by incubation for 10 minutes at 65°C. Reverse transcription was carried out using 1 µg of DNase I treated RNA in the presence of 0.5 mM dNTPs, 1x Random Hexamer primers (Life Technologies Inc., Burlington, ON, Canada), 0.01 M DTT, RiboLock RNase Inhibitor (Thermo Fisher Scientific Inc., Burlington, ON, Canada), and M-MLV Reverse Transcriptase (Life Technologies Inc., Burlington, ON, Canada). The PCR program for reverse transcription was as follows: 25°C for 10 minutes, 37°C for 50 minutes, and 70°C for 15 minutes. Final cDNA products were stored at -20°C.

2.15 Quantitative PCR

Quantitative PCR was conducted using SYBR[®] Green dye (Life Technologies Inc., Burlington, ON, Canada)-based PCR and Applied Biosystems 7500 Fast Real-Time PCR System (Life Technologies Inc., Burlington, ON, Canada). The *Gapdh* gene was used as the endogenous control. Each quantitative PCR reaction contained cDNA template, 0.4 µL each of forward and reverse primers (final concentrations indicated in Table 3), 7.5 µL of SYBR[®] Green, and made to a final volume of 15 µL with dH₂O. Cycling conditions for quantitative PCR were as follows: 50°C for 2 minutes; 95°C for 10 minutes; 40 cycles of 95°C for 15 seconds followed by 60°C for 1 minute.

Quantitative PCR primers were designed using the Primer-BLAST program provided by the National Center for Biotechnology Information website (National Library of Medicine, Bethesda, MD, USA. www.ncbi.nlm.nih.gov). The target PCR product length was set between 100 and 150 bp. Primers were designed to span exon-exon junctions whenever possible, and the specificity of primers was checked against all sequence databases available for a given species. All primers used in this thesis were synthesized by Integrated DNA Technologies Inc. (Coralville, IA, USA) and their sequences are shown in Table 3.

Table 3. Primer sequences for quantitative PCR.

Gene name		Forward primer	Reverse primer
Mouse	<i>Cyp1a2</i> (300) ^a	TGGAGCTGGCTTTGACACAGT	GCCATGTCACAAGTAGCAAAATG
	<i>Cyp2e1</i> (900)	AAAAGCCAAGGAACACCTTAAGTC	TTCTTGGCTGTGTTTTTCCTTCTC
	<i>Gclc</i> (300)	TCTGCCCAATTGTTATGGCTTT	ATCACTCCCCAGCGACAATC
	<i>Nqo1</i> (900)	TATTACGATCCTCCCTCAACATCTG	CCTTCATGGCGTAGTTGAATGA
	<i>Gapdh</i> (300)	CAGCCTCGTCCCGTAGACA	CGCCAATACGGCCAAA
Rat	<i>Cyp2e1</i> (300)	AAAAGCCAAGGAACACCTTCAGTC	TTCTTGGCTGTGTTTTTCCTTCTC
Human	<i>Nat2</i> (300)	TTGGAAGCAAGAGGATTGCAT	CAATGTCCATGATCCCTTTGG
	<i>Cyp1a2</i> (900)	ACATCTTTGGAGCAGGATTTGAC	TTCCTCTGTATCTCAGGCTTGGT
	<i>Dbp</i> (900)	AGGGAAACAGCAAGCCCAAAGAAC	AAAGGTCATTAGCACCTCCACGGT
	<i>C/ebpα</i> (900)	TCACTTGCAGTTCCAGATCGCACA	TCTTATCCACCGACTTCTTGGCCT
	<i>Gapdh</i> (900)	CTCTCTGCTCCTCCTGTTCTGA	AAATCCGTTGACTCCGACCTT

^aFinal concentration of primers (nanomolar).

All primers were tested experimentally for their primer annealing efficiency against endogenous control *Gapdh* to ensure similar efficiencies. Primer annealing efficiency graphs were generated by measuring Ct values over a range of cDNA concentrations (normally spanning two orders of magnitude) for both the gene of interest and *Gapdh*, and plotting differences in Ct values between these two genes on the y-axis against the log of [cDNA] on the x-axis. Primers for the gene of interest were considered to have similar annealing efficiencies as *Gapdh* primers when the primer annealing efficiency graph had a slope between -0.1 and 0.1. Only primers with similar annealing efficiencies as *Gapdh* were used for further experiments.

Data analyses were carried out using the comparative Ct method. For each cDNA sample, Ct values for the GAPDH endogenous control were subtracted from Ct values for the target gene within the same cDNA sample to generate delta Ct (Δ Ct), which was then subtracted from delta Ct of the reference cDNA sample (i.e. a vehicle-treated liver) to generate delta delta Ct ($\Delta\Delta$ Ct).

Relative expression of the target gene in a cDNA sample was then expressed as $2^{-\Delta\Delta C_t}$ fold of the reference cDNA sample.

2.16 Statistical analyses

For enzyme kinetic studies, apparent K_m and V_{max} for each group of mice were calculated using nonlinear regression analysis of the kinetic data based on the Michaelis-Menten model. Comparisons of enzyme kinetic values between different groups of mice were carried out using extra sum-of-squares F test ($\alpha = 0.05$, Prism 5, GraphPad Software Inc., La Jolla, CA, USA).

Chapter 3

RESULTS

3.1 ABP-induced mutations *in vivo*

To extend previous findings from our laboratory that had demonstrated a lack of correlation between the genotoxic effects of ABP and liver tumor incidence, in this section we compared the mutagenicity of ABP in male and female wild-type and *Nat1/2(-/-)* mice using both the neonatal tumor-inducing exposure protocol and an adult 28-day subchronic dosing protocol, which is used to improve the sensitivity of mutation detection in livers of the more mutation-resistant adult mice (Heddle *et al.*, 2003). We used the MutaTMMouse λ gt10-*lacZ* transgenic mouse line, which contains phenotypically selectable *cII* transgenes, for the quantification of both *in vivo* mutation frequency and spectra induced by ABP (Section 1.1.3.1).

3.1.1 ABP-induced *cII* mutation frequencies in neonatal mice

Following *in vivo* exposure to ABP, liver genomic DNA containing *cII* transgenes was packaged into lambda phage particles that were then used to infect E.coli leading to the formation of plaques on bacterial lawn. Based on a temperature selection, the number of plaques that contain mutant *cII* transgenes over the total number of plaques were calculated, which represents the mutation frequency of the *cII* transgene *in vivo*. Using this method, mutation frequencies were determined in male and female wild-type and *Nat1/2(-/-)* neonatal mice administered DMSO vehicle, 600 nmol, or 1200 nmol of ABP (Figure 11).

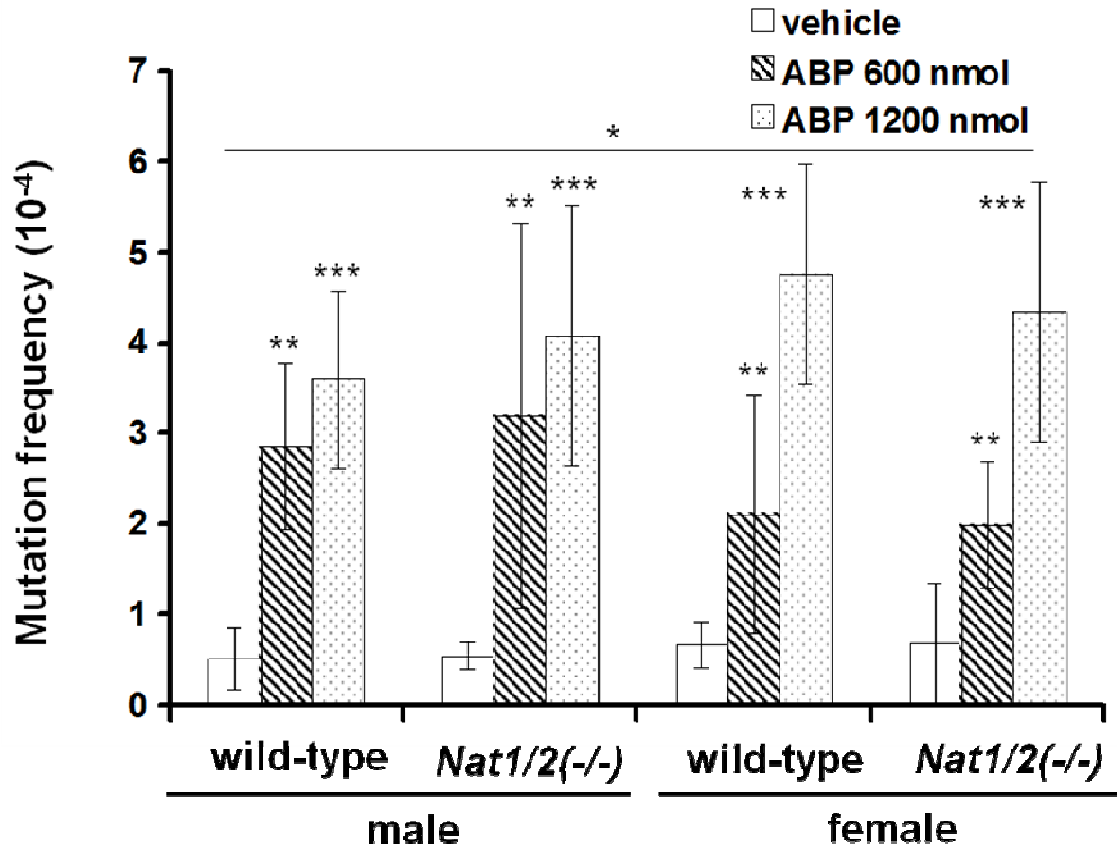


Figure 11. Influence of sex and NATs on ABP-induced mutation frequencies in neonatally exposed wild-type and *Nat1/2(-/-)* MutaTMMouse.

Mice (N=5 per group) were injected with vehicle, 600 nmol or 1200 nmol of ABP on postnatal days 8 and 15 and sacrificed 5 days after the final injection for liver mutation frequency determination using the MutaTMMouse assay. Error bars represent standard deviations of the mean. (* $P < 0.05$ for effect of ABP dose on mutation frequency across all groups. ** $P < 0.01$ relative to respective vehicle-dosed group. *** $P < 0.001$ relative to respective vehicle-dosed group).

Two-way and three-way ANOVA analyses of the neonatal mutation frequency data identified a significant dose-dependent increase in mean mutation frequencies with the administration of ABP ($P < 0.05$); however, no significant sex or strain differences were observed using either analysis ($P > 0.05$). Subsequent Bonferroni post-tests revealed significantly increased mutation frequencies with both low ($P < 0.01$) and high doses ($P < 0.001$) of ABP compared to vehicle controls for all groups of mice.

3.1.2 ABP-induced *cII* mutation frequencies in adult mice

To compare the ability of ABP to generate mutations between neonatal and adult mice, ABP-induced mutation frequencies were also determined in adult (8 week) male and female wild-type and *Nat1/2(-/-)* mice administered ABP at 10 mg/kg or 20 mg/kg every other day for 28 days, corresponding to total exposures of approximately 20,000 and 40,000 nmol per animal, respectively (Figure 12).

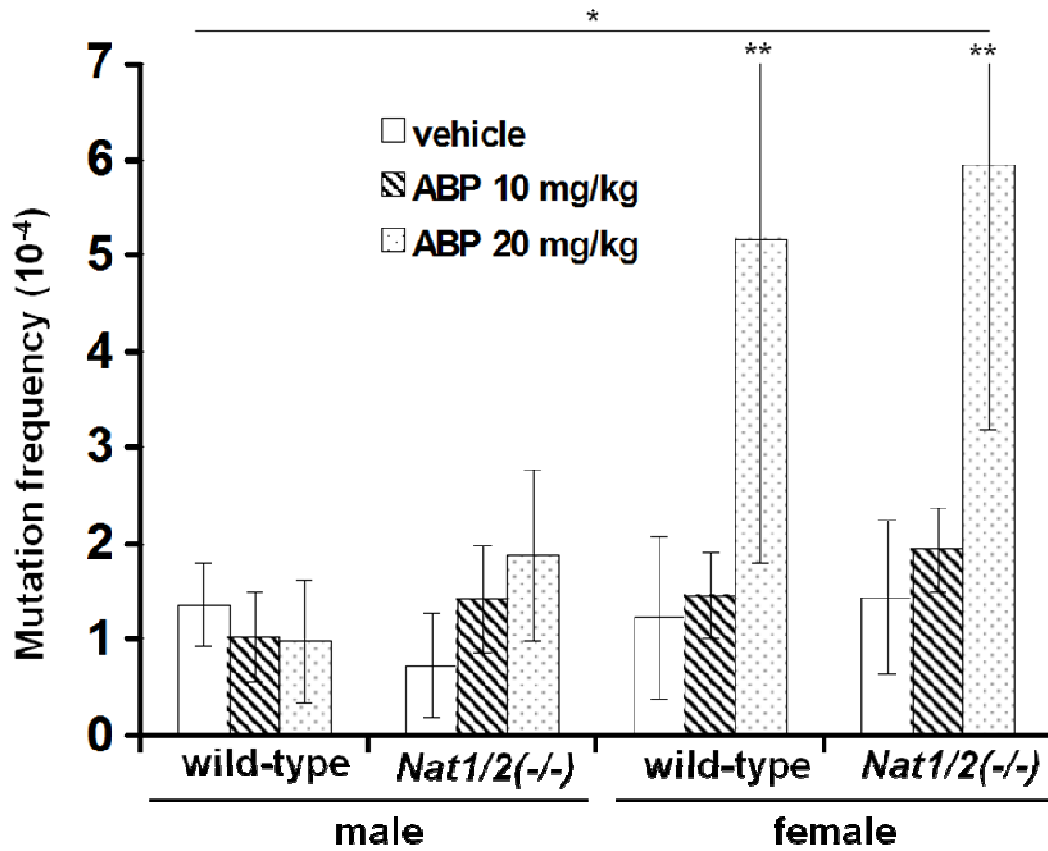


Figure 12. Influence of sex and NATs on ABP-induced mutation frequencies in adult wild-type and *Nat1/2(-/-)* MutaTMMouse.

Adult mice (N=5 per group) were injected with vehicle, 10 mg/kg or 20 mg/kg of ABP every second day for 28 days, and sacrificed 3 days after the last injection for liver mutation frequency determination using the MutaTMMouse assay. Error bars represent standard deviations of the mean. (**P* < 0.001 for effect of ABP dose on mutation frequency across all groups. ***P* < 0.001 relative to respective vehicle-dosed group).

Two-way ANOVA analyses of adult mutation frequency data identified a significant dose-dependent increase in mean mutation frequencies with the administration of ABP. However,

subsequent Bonferroni post-tests indicated that only females treated with the high dose of ABP (both wild-type and *Nat1/2(-/-)*) demonstrated significantly increased mutation frequencies compared to their respective vehicle controls. Accordingly, adult females displayed significantly higher mean mutation frequencies than males at the high dose of ABP ($P < 0.001$) but not at the low dose or in vehicle controls ($P > 0.05$). Furthermore, there was no significant difference between wild-type and *Nat1/2(-/-)* female mice ($P > 0.05$). A three-way ANOVA analysis confirmed a significant effect of ABP dose ($P < 0.001$) and sex ($P < 0.001$), as well as a sex \times dose interaction ($P < 0.001$).

To ensure that mutation frequencies were not unduly affected by jackpots of mutations from clonally expanded mutated cells, medians of mutation frequencies were also compared between groups of both neonatal and adult mice. The results were similar to those generated using mean values (data not shown, (Heddle *et al.*, 2003)), consistent with recent studies using the hepatocarcinogen diethylnitrosamine where correction for clonality had little influence on liver mutation frequency (Mirsalis *et al.*, 2005).

3.1.3 ABP-induced *c//* mutation spectra in neonatal mice

To determine the type(s) of DNA damage induced by ABP, we investigated ABP-induced mutation spectra for representative male and female wild-type and *Nat1/2(-/-)* mice exposed to either 1200 nmol ABP or vehicle control under the neonatal exposure protocol (Table 4). Using the Adams and Skopek algorithm we detected a significant change in mutation spectra with ABP treatment in all animals ($P < 0.01$) except *Nat1/2(-/-)* females ($P > 0.05$, (Adams and Skopek, 1987)). As expected, the largest changes observed were with the proportion of G to T transversions, which increased in all animals except *Nat1/2(-/-)* females, where a decrease was detected. Comparing across ABP-treated groups, we detected a significant change between ABP-induced mutation spectra of wild-type and *Nat1/2(-/-)* female mice ($P < 0.05$). The largest difference was found with the proportion of ABP-induced G to T transversions, where wild-type females showed an increase but *Nat1/2(-/-)* females showed a decrease compared to vehicle-treated controls.

Table 4. ABP-induced mutation spectra in neonatally exposed wild-type and *Nat1/2(-/-)* MutaTMMouse.

	Male			Female				
	Wild-type		<i>Nat1/2(-/-)</i>		Wild-type		<i>Nat1/2(-/-)</i>	
	Vehicle	ABP	Vehicle	ABP	Vehicle	ABP	Vehicle	ABP
G:C → A:T	11 (34%)	6 (15%)	12 (38%)	7 (17%)	11 (36%)	4 (12%)	6 (21%)	9 (28%)
G:C → T:A	7 (22%)	21 (54%) ^c	5 (16%)	21 (51%) ^b	5 (16%)	14 (42%) ^{bc}	7 (25%)	2 (6%) ^b
A:T → C:G	0	0	1 (3%)	0	0	2 (6%)	2 (7%)	4 (13%)
A:T → G:C	0	3 (8%)	2 (6%)	3 (7%)	0	1 (3%)	2 (7%)	3 (9%)
C:G → G:C	0	5 (13%)	0	3 (7%)	4 (13%)	4 (12%)	1 (4%)	4 (13%)
T:A → A:T	4 (13%)	3 (8%)	2 (6%)	2 (5%)	7 (23%)	2 (6%)	2 (7%)	2 (6%)
Others ^a	10 (31%)	1 (3%)	10 (31%)	5 (12%)	4 (13%)	6 (18%)	8 (29%)	8 (25%)
Total mutations	32 (100%)	39 (100%)	32 (100%)	41 (100%)	31 (100%)	33 (100%)	28 (100%)	32 (100%)

Mice were injected with vehicle (DMSO) or a total dose of 1200 nmoles of ABP on postnatal days 8-15 and sacrificed 5 days after the last injection for mutation spectra determination using the MutaTMMouse assay

^aThis category consists mostly of single base-pair insertions or deletions

^bABP treated mice are significantly different from the corresponding vehicle treated mice ($P < 0.05$, Chi-square test)

^cFemale ABP treated wild-type mice are significantly higher than the corresponding *Nat1/2(-/-)* mice ($P < 0.01$, Chi-square test)

3.1.4 ABP-induced *cII* mutation spectra in adult mice

To compare the nature of ABP-induced mutations between neonatal and adult mice, we also generated mutation spectra data for adult male and female wild-type and *Nat1/2(-/-)* mice exposed to either 20 mg/kg of ABP or vehicle control every other day for 28 days (total ABP ~ 40,000 nmol, Table 5). ABP did not induce a statistically significant change in mutation spectra of adult mice regardless of sex or NAT status using the Adams and Skopek algorithm. Comparing between ABP-treated animals, only *Nat1/2(-/-)* female mice had a significantly different mutation spectrum than wild-type females ($P < 0.05$). Closer examination revealed both a higher proportion of G to T transversions and a lower proportion of G to A transitions in *Nat1/2(-/-)* female mice.

Although we observed a modest degree of clustering with mutations on particular nucleotides of the *cII* gene in both neonatal and adult mice (data not shown), this is likely a consequence of the assay's selection for mutations that produce changes in the *cII* protein that markedly impair its function, rather than clonal expansion of jackpot mutations. In addition, the most common specific mutation detected among all *cII* gene sequences was a G insertion before G179, which represented up to 21% of all mutations in ABP-treated neonatal *Nat1/2(-/-)* females. This is probably due to its proximity to a six G repeat that makes this section of the *cII* gene particularly prone to both G insertions and G deletions. Although G to T transversions showed no clustering on any particular location within the *cII* transgene, this does not preclude the possibility that such hotspots could exist in relevant endogenous genes. Nonetheless, this finding along with the similar results that we obtained for mutation frequencies using mean and median values together suggest that the contribution of clonal jackpot mutations was minimal.

Table 5. ABP-induced mutation spectra in adult wild-type and *Nat1/2(-/-)* MutaTMMouse.

	Male				Female			
	Wild-type		<i>Nat1/2(-/-)</i>		Wild-type		<i>Nat1/2(-/-)</i>	
	Vehicle	ABP	Vehicle	ABP	Vehicle	ABP	Vehicle	ABP
G:C → A:T	18 (45%)	14 (50%)	10 (35%)	12 (43%)	5 (17%)	18 (45%)	14 (32%)	9 (22%)
G:C → T:A	6 (15%)	3 (11%)	6 (21%)	6 (21%)	12 (41%)	11 (28%)	17 (39%)	22 (54%) ^b
A:T → C:G	1 (3%)	2 (7%)	1 (3%)	2 (7%)	1 (3%)	1 (3%)	2 (5%)	0 (0%)
A:T → G:C	2 (5%)	3 (11%)	1 (3%)	1 (4%)	0 (0%)	1 (3%)	1 (2%)	2 (5%)
C:G → G:C	3 (8%)	1 (4%)	2 (7%)	1 (4%)	4 (14%)	6 (15%)	6 (14%)	4 (10%)
T:A → A:T	1 (3%)	0	1 (3%)	1 (4%)	4 (14%)	2 (5%)	1 (2%)	0 (0%)
Others ^a	9 (23%)	5 (18%)	8 (28%)	5 (18%)	3 (10%)	1 (3%)	3 (7%)	4 (10%)
Total mutations	40 (100%)	28 (100%)	29 (100%)	28 (100%)	29 (100%)	40 (100%)	44 (100%)	41 (100%)

^aAdult mice were injected with vehicle (corn oil) or 20mg/kg of ABP every other day for 28 days and sacrificed

3 days after the last injection for mutation spectra determination using the MutaTMMouse assay

^bThis category consists mostly of single base-pair insertions or deletions

^cABP treated female *Nat1/2(-/-)* mice are significantly higher than the corresponding wildtype mice ($P < 0.001$, Chi-square test)

3.2 ABP metabolic activation by cytochrome P450s

Given the central importance of the ABP *N*-hydroxylation reaction in mediating all known deleterious effects of ABP, the objective of studies in this section was to determine the identity(s) of the major ABP *N*-hydroxylation enzyme(s) in mouse liver that is responsible for the metabolic activation of ABP in our neonatal bioassay. Towards this goal, we first established *in vitro* and in culture assays for the quantification of ABP *N*-hydroxylation activity and subsequently used these assays to test the effects of genetic and/or pharmacological manipulations on ABP *N*-hydroxylation by mouse liver microsomes and mouse hepatoma cells.

3.2.1 ABP *N*-hydroxylation by CYP1A2 in mouse liver microsomes

With evidence that contradicts the largely assumed role of CYP1A2 as the ABP *N*-hydroxylation enzyme in mouse models of ABP carcinogenesis (Section 1.4.4.1), we first tested whether CYP1A2 can mediate the *N*-hydroxylation of ABP in developing mouse liver. This was achieved by comparing ABP *N*-hydroxylation activity between microsomes isolated from wild-type and *Cyp1a2*(*-/-*) mice on postnatal day 15, corresponding to the age of mice when the second of two ABP exposures occurred in our ABP neonatal bioassay (Figure 13).

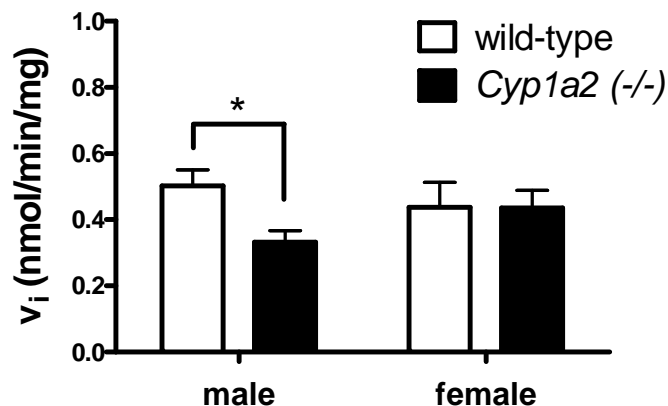


Figure 13. ABP *N*-hydroxylation by mouse liver microsomes from male and female wild-type and *Cyp1a2*(-/-) mice.

Liver microsomes were isolated from postnatal day 15 male and female wild-type and *Cyp1a2*(-/-) C57BL/6 mice (N=4). *In vitro* production of HOABP in the presence of liver microsomes and NADPH regenerating system at 200 μ M ABP was quantified by HPLC. Error bars represent standard deviations of the mean. (* $P < 0.05$).

We tested ABP *N*-hydroxylation activity at 200 μ M ABP since comparable concentrations of ABP were detected in mouse serum following exposure to ABP in our previous pharmacokinetic study (Sugamori *et al.*, 2006). Two-way ANOVA analysis followed by Bonferroni post-tests revealed a significant but modestly lower ABP *N*-hydroxylation activity (~34%) in *Cyp1a2*(-/-) males compared to wild-type controls ($P < 0.05$), and no significant difference between *Cyp1a2*(-/-) females and wild-type controls ($P > 0.05$, Figure 13). To better characterize the ABP *N*-hydroxylation reaction in wild-type and *Cyp1a2*(-/-) mice, we carried out full enzyme kinetic analyses using liver microsomes isolated from postnatal day 15 male and female wild-type and *Cyp1a2*(-/-) mice (Figure 14).

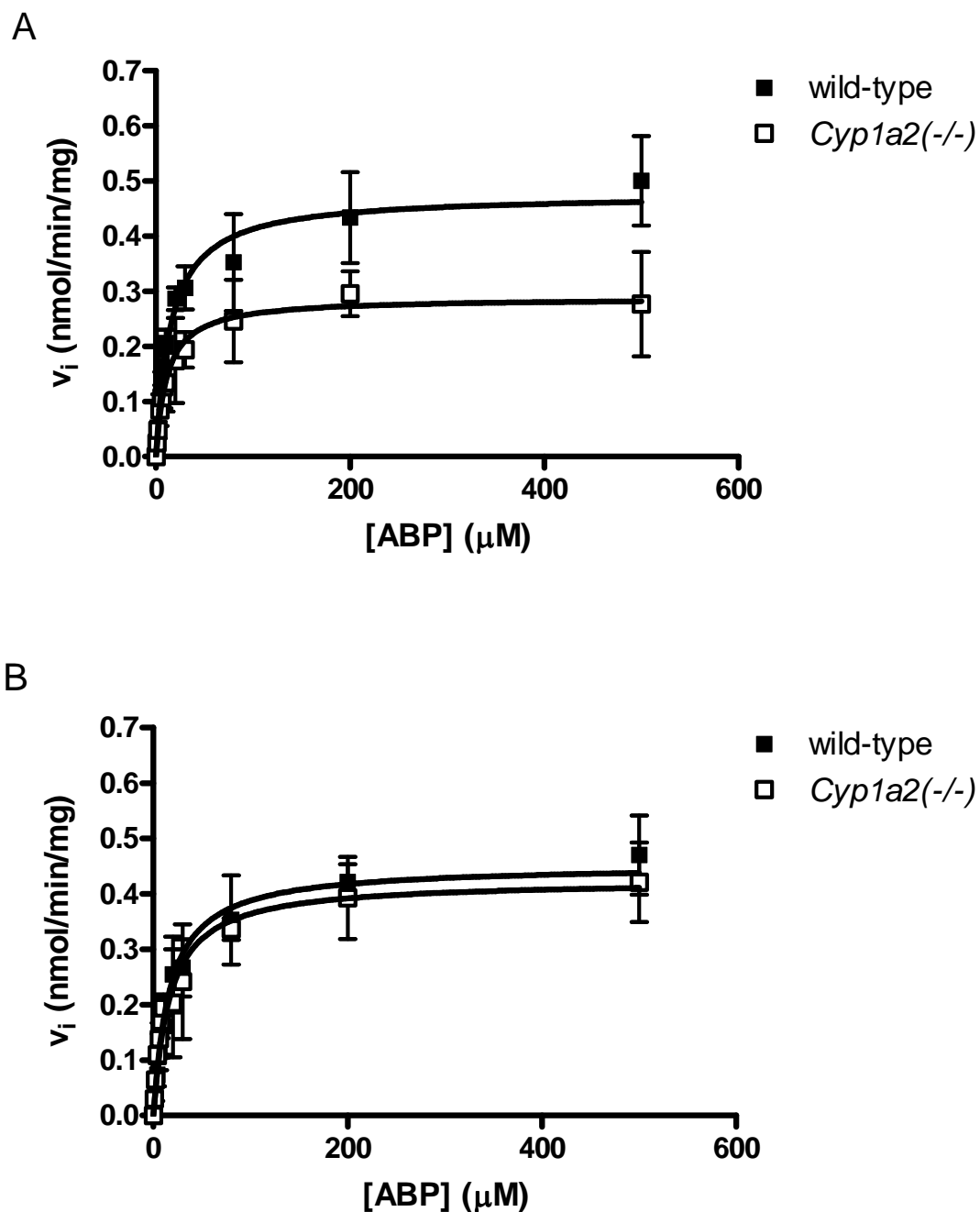


Figure 14. Kinetics of ABP N-hydroxylation by liver microsomes from male and female wild-type and *Cyp1a2*^{-/-} mice

Liver microsomes were isolated from postnatal day 15 male (A) and female (B) wild-type and *Cyp1a2*^{-/-} C57BL/6 mice (N=3). *In vitro* production of HOABP in the presence of liver microsomes and NADPH regenerating system at 0-500 μM ABP were quantified by HPLC. Error bars represent standard deviations of the mean.

We measured ABP *N*-hydroxylation activity over a range of ABP concentrations, fit the data to a Michaelis-Menten enzyme kinetic model and carried out non-linear regression analyses to generate Michaelis-Menten enzyme kinetic constants. Michaelis-Menten kinetic constants for male and female wild-type and *Cyp1a2*(-/-) mouse liver microsomes are shown in Table 6.

Table 6. Michaelis-Menten kinetic constants for ABP *N*-hydroxylation by liver microsomes from male and female wild-type and *Cyp1a2*(-/-) mice.

		$K_m \pm \text{S.D.} (\mu\text{M})$	$V_{\max} \pm \text{S.D.} (\text{nmol}/\text{min}/\text{mg})$
male	wild-type	15 ± 3.5	0.48 ± 0.031
	<i>Cyp1a2</i> (-/-)	11 ± 4.0	0.29 ± 0.029^a
female	wild-type	19 ± 4.5	0.47 ± 0.033
	<i>Cyp1a2</i> (-/-)	14 ± 4.2	0.41 ± 0.036

S.D. = standard deviation

^a $P < 0.05$ compared to corresponding wild-type group

Using the extra sum-of-squares F test, a significantly lower V_{\max} value was detected in male *Cyp1a2*(-/-) compared to wild-type mice ($P < 0.05$, Table 6, Figure 13), but not females, confirming our previous results using a single concentration of ABP. The presence of substantial remaining activity in *Cyp1a2*(-/-) mice suggests the existence of an alternative ABP *N*-hydroxylation enzyme(s) in developing mouse liver. In addition, similar K_m values between wild-type and *Cyp1a2*(-/-) mice for both males and females ($P > 0.05$) suggests that this alternative enzyme(s) has a similar affinity for ABP as CYP1A2 (Table 6). This is further supported by Eadie-Hofstee transformations of the enzyme kinetic data (Figure 15).

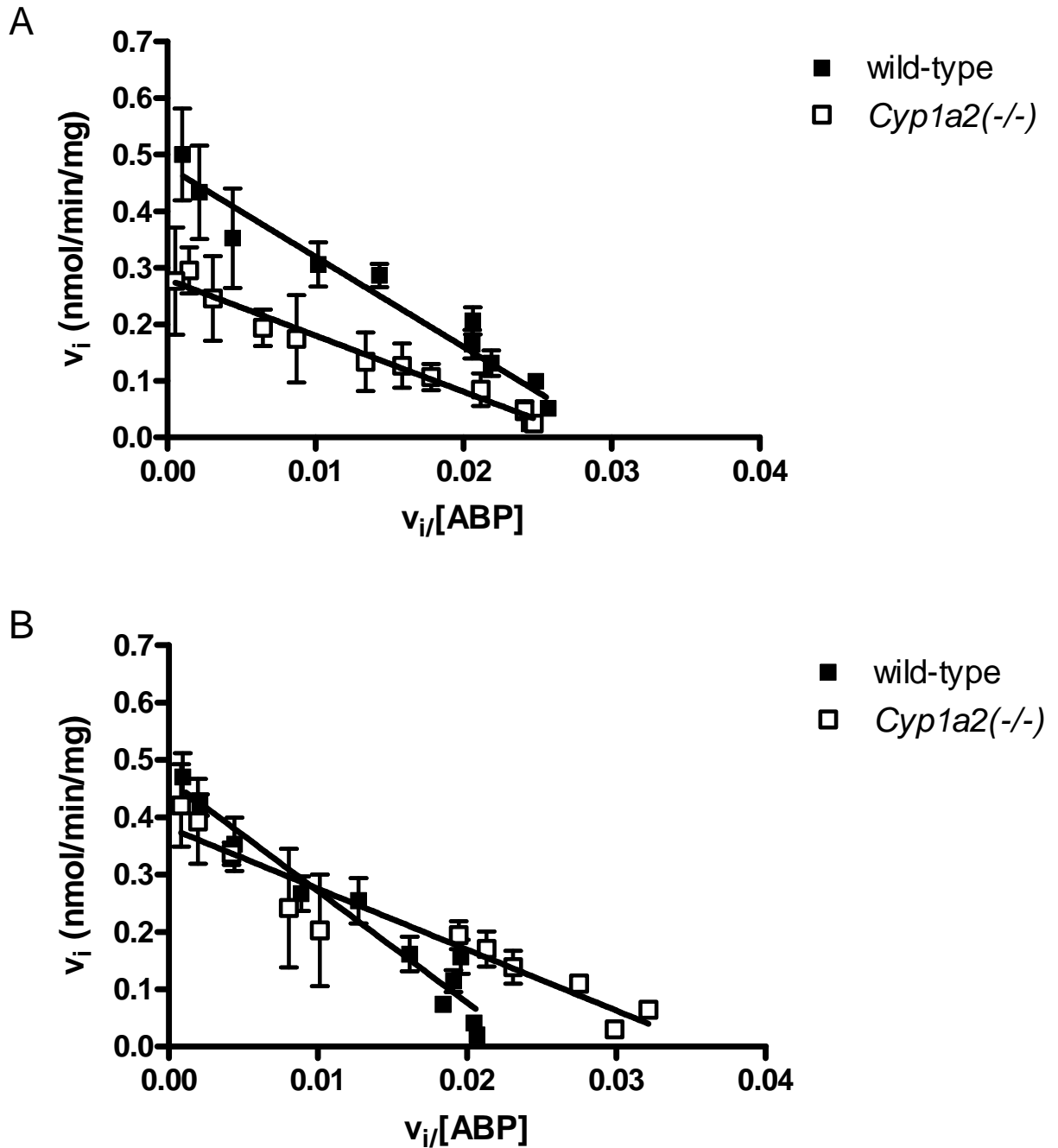


Figure 15. Eadie-Hofstee analysis of ABP *N*-hydroxylation by male and female wild-type and *Cyp1a2*^{-/-} mouse liver microsomes.

Eadie-Hofstee transformations of male (A) and female (B) data shown in Figure 14.

Linear Eadie-Hofstee plots for wild-type male and female mice indicate the presence of a single ABP *N*-hydroxylation enzyme, or of multiple ABP *N*-hydroxylation enzymes with similar affinities for ABP. Similar slopes on the Eadie-Hofstee plots between wild-type and *Cyp1a2*(-/-) microsomes again indicate similar affinities towards ABP *N*-hydroxylation in the presence and absence of CYP1A2. Overall, our results suggest the presence of an alternative ABP *N*-hydroxylation enzyme(s) in postnatal mouse liver that has similar affinity towards ABP as CYP1A2 and is responsible for the majority of ABP *N*-hydroxylation activity, especially in females.

3.2.2 Identification of CYP2E1 as a major ABP *N*-hydroxylation enzyme in mouse liver microsomes

To confirm that the alternative ABP *N*-hydroxylation enzyme represents a cytochrome P450, we tested the effect of the general cytochrome P450 inhibitor 1-aminobenzotriazole (ABT) on ABP *N*-hydroxylation by mouse liver microsomes (Figure 16).

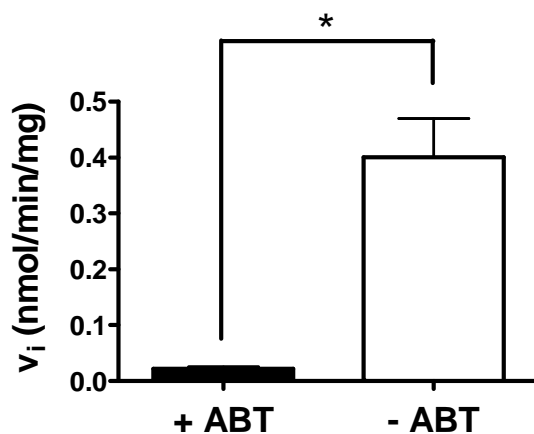


Figure 16. Effect of ABT on ABP *N*-hydroxylation by *Cyp1a2*(-/-) mouse liver microsomes.

Liver microsomes were isolated from day 15 male *Cyp1a2*(-/-) C57BL/6 mice (N=4). *In vitro* production of HOABP in the presence of liver microsomes and NADPH regenerating system at 200 μ M ABP with or without pre-treatment with 1 mM ABT were quantified by HPLC. Error bars represent standard deviations of the mean. (* $P < 0.01$).

We characterized the alternative ABP *N*-hydroxylation enzyme using liver microsomes from postnatal day 15 *Cyp1a2*(-/-) mice in order to exclude any contributions from CYP1A2. ABT inhibited most of the ABP *N*-hydroxylation activity in liver microsomes of neonatal male

Cyp1a2(-/-) mice (Student's t-test, $P < 0.01$, Figure 16). We also observed that dimethyl sulfoxide (DMSO) potently inhibited ABP *N*-hydroxylation when used as a chemical solvent vehicle (Figure 17A). Other commonly used solvents such as methanol and acetone also inhibited ABP *N*-hydroxylation by mouse liver microsomes (data not shown); however, a notable exception to the observed solvent effect was acetonitrile, which did not inhibit ABP *N*-hydroxylation (Figure 17B).

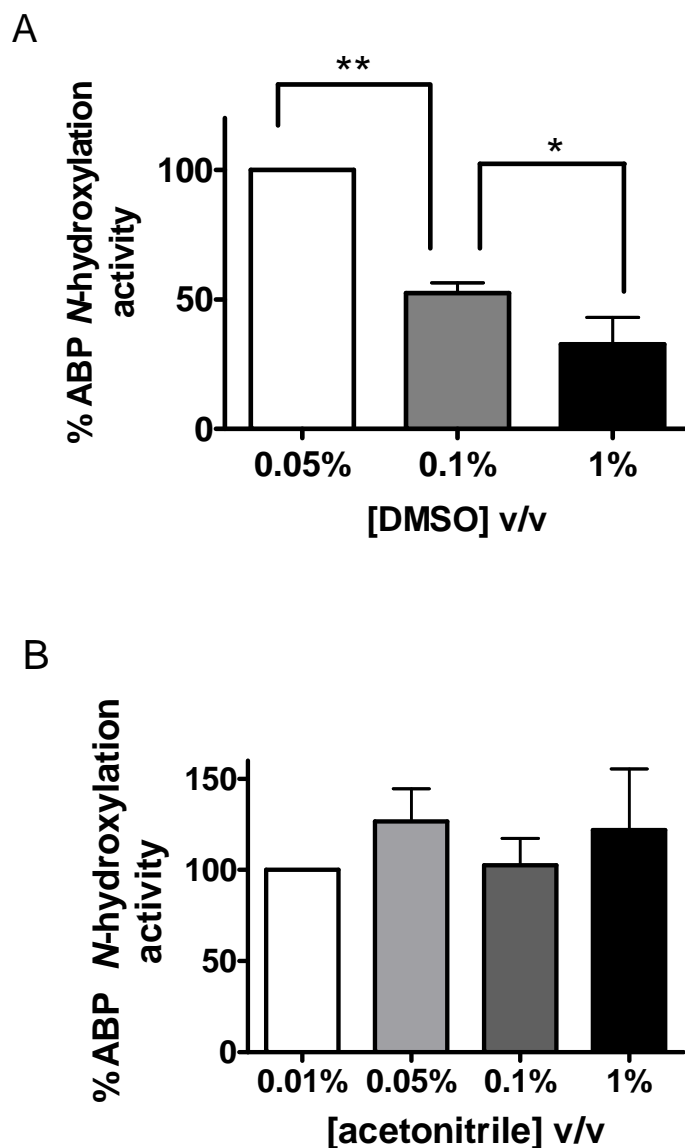


Figure 17. Effects of DMSO and acetonitrile on ABP N-hydroxylation by *Cyp1a2*(-/-) mouse liver microsomes.

Liver microsomes were isolated from day 15 male *Cyp1a2*(-/-) C57BL/6 mice (N=3). *In vitro* production of HOABP in the presence of liver microsomes and NADPH regenerating system at 200 μ M ABP co-incubated with various concentrations of DMSO (A) or acetonitrile (B) were quantified on the HPLC. Error bars represent standard deviations of the mean. (* $P < 0.05$ and ** $P < 0.001$).

Since the solvent inhibition profile for ABP N-hydroxylation matched those described for CYP2E1 (Hickman *et al.*, 1998), we tested the CYP2E1-selective substrate *p*-nitrophenol (pNP,

(Tassaneeyakul *et al.*, 1993)) as a potential inhibitor of ABP *N*-hydroxylation activity, again using liver microsomes from postnatal day 15 male *Cyp1a2*(*-/-*) mice (Figure 18).

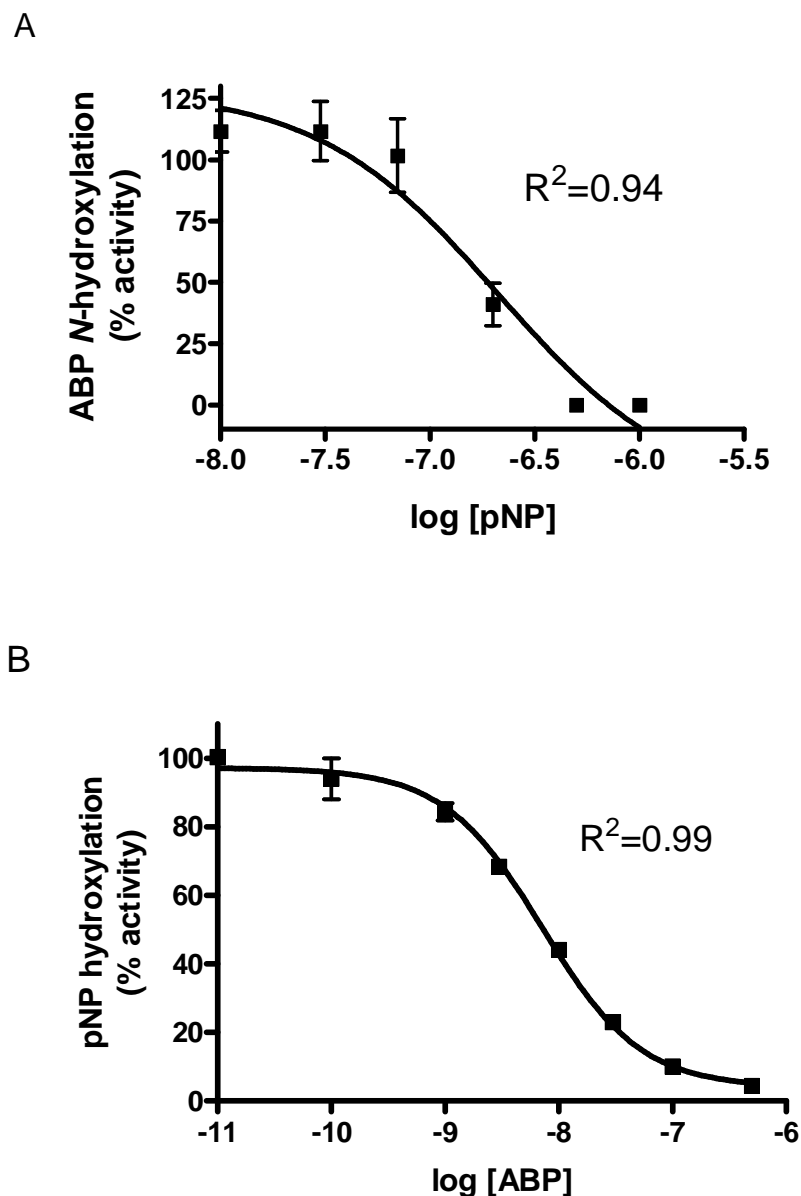


Figure 18. Mutual oxidation reaction inhibition between pNP and ABP.

Liver microsomes were isolated from day 15 male *Cyp1a2*(*-/-*) C57BL/6 mice (N=3). *In vitro* production of HOABP (A) or 4-nitrocatechol (B) in the presence of liver microsomes and NADPH regenerating system at 200 μ M substrate (ABP (A) or pNP (B)) co-incubated with various concentrations of inhibitor (pNP (A) or ABP (B)) were quantified by HPLC. Error bars represent standard deviations of the mean. R^2 values were calculated using non-linear regression analyses based on single-site competitive inhibition.

pNP dose-dependently inhibited ABP *N*-hydroxylation activity; non-linear regression analysis based on single-site competitive inhibition gave an R^2 value of 0.94 (Figure 18A). Conversely, ABP dose-dependently inhibited pNP hydroxylation; non-linear regression analysis based on single-site competitive inhibition gave an R^2 value of 0.99 (Figure 18B). These observations strongly support CYP2E1 as an alternative ABP *N*-hydroxylation enzyme in the developing mouse liver.

A further line of evidence supporting CYP2E1 as an ABP *N*-hydroxylation enzyme came from *in vivo* induction studies using pyrazole. Two-way ANOVA analysis followed by Bonferroni post-tests revealed a modest but significant increase in ABP *N*-hydroxylation activity of liver microsomes from male pyrazole-treated *Cyp1a2*(*-/-*) mice compared to vehicle-treated controls ($P < 0.05$); however, no significant effect of pyrazole was found in females ($P > 0.05$, Figure 19).

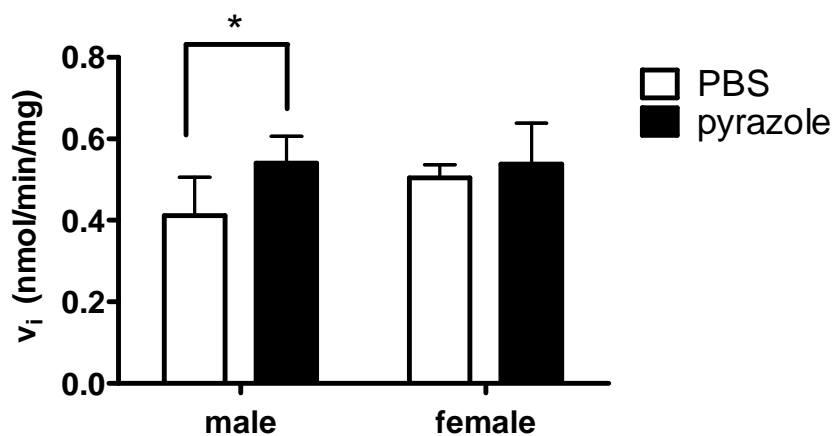


Figure 19. Effect of *in vivo* pyrazole administration on ABP *N*-hydroxylation by male and female *Cyp1a2*(*-/-*) mouse liver microsomes.

Liver microsomes were isolated from postnatal day 15 male and female *Cyp1a2*(*-/-*) C57BL/6 mice treated with 50 mg/kg pyrazole or PBS vehicle for 3 consecutive days (N=4). *In vitro* production of HOABP in the presence of liver microsomes and NADPH regenerating system at 200 μ M ABP was quantified by HPLC. Error bars represent standard deviations of the mean. (* $P < 0.05$).

We generated additional evidence supporting the role of CYP2E1 in the *N*-hydroxylation of ABP using *Cyp2e1*(*-/-*) mice. As with *Cyp1a2*(*-/-*) mice, we first compared *in vitro* ABP *N*-

hydroxylation activity between liver microsomes isolated from male and female postnatal day 15 wild-type and *Cyp2e1*(-/-) mice (Figure 20).

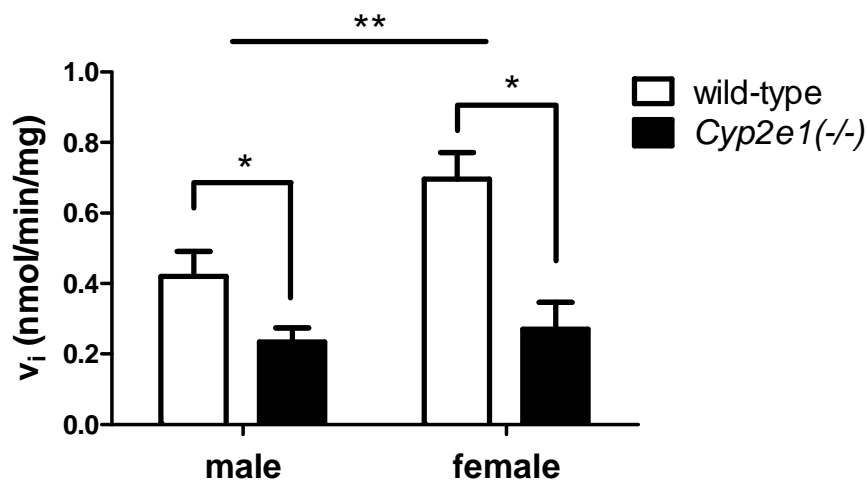


Figure 20. ABP *N*-hydroxylation by liver microsomes from male and female wild-type and *Cyp2e1*(-/-) mice.

Liver microsomes were isolated from postnatal day 15 male and female wild-type and *Cyp2e1*(-/-) SVJ129 and C57BL/6 mixed-strain mice (N=5). *In vitro* production of HOABP in the presence of liver microsomes and NADPH regenerating system at 200 μ M ABP were quantified by HPLC. Error bars represent standard deviations of the mean. (* $P < 0.001$ and ** $P < 0.0001$ for effects of sex and strain, respectively).

Two-way ANOVA analysis revealed significant effects of both sex and CYP2E1 status on ABP *N*-hydroxylation by mouse liver microsomes ($P < 0.0001$, Figure 20). Two-way ANOVA followed by Bonferroni post-tests revealed significantly decreased ABP *N*-hydroxylation activity in both male (44%, $P < 0.001$) and female (61%, $P < 0.001$) *Cyp2e1*(-/-) mice compared to wild-type controls (Figure 20). To better characterize the ABP *N*-hydroxylation reaction in wild-type and *Cyp2e1*(-/-) mouse liver microsomes, we carried out full enzyme kinetic analyses (Figure 21).

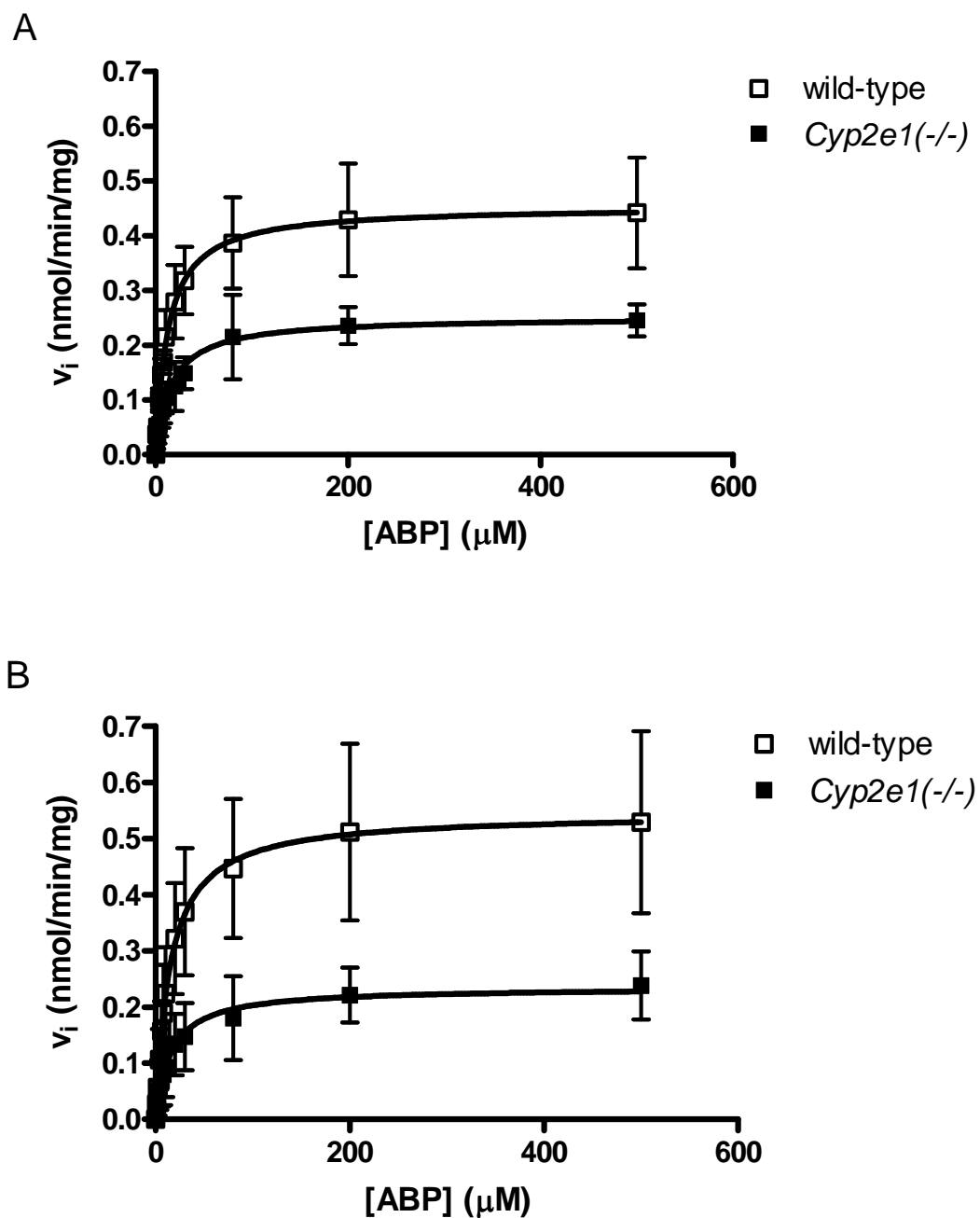


Figure 21. Kinetics of ABP N-hydroxylation by liver microsomes from male and female wild-type and *Cyp2e1*(-/-) mice.

Liver microsomes were isolated from postnatal day 15 male (A) and female (B) wild-type and *Cyp2e1*(-/-) SVJ129 and C57BL/6 mixed-strain mice (N=3). *In vitro* production of HOABP in the presence of liver microsomes and NADPH regenerating system at 0-500 μM ABP were quantified by HPLC. Error bars represent standard deviations of the mean.

As with *Cyp1a2*(-/-) microsomes, Michaelis-Menten kinetic constants were generated by measuring ABP *N*-hydroxylation activity over a range of ABP concentrations for male and female postnatal day 15 wild-type and *Cyp2e1*(-/-) mouse liver microsomes, and the derived kinetic constants are shown in Table 7.

Table 7. Michaelis-Menten kinetic constants for ABP *N*-hydroxylation by liver microsomes from male and female wild-type and *Cyp2e1*(-/-) mice.

		$K_m \pm \text{S.D.} (\mu\text{M})$	$V_{\text{max}} \pm \text{S.D.} (\text{nmol}/\text{min}/\text{mg})$
male	wild-type	13 ± 3.3	0.45 ± 0.035
	<i>Cyp2e1</i> (-/-)	16 ± 4.8	0.25 ± 0.020^a
female	wild-type	15 ± 4.7	0.55 ± 0.059
	<i>Cyp2e1</i> (-/-)	16 ± 6.9	0.23 ± 0.031^a

S.D. = standard deviation

^a $P < 0.0001$ compared to the corresponding wild-type group

Similar to the *Cyp1a2*(-/-) results, extra sum-of-squares F test revealed no significant change in K_m values between wild-type and *Cyp2e1*(-/-) mouse liver microsomes for both males and females ($P > 0.05$, Table 7). Unlike the *Cyp1a2*(-/-) results, however, extra sum-of-squares F test revealed significant reductions in V_{max} values of both male and female *Cyp2e1*(-/-) mice compared to wild-type controls ($P < 0.0001$, Table 7). These results confirmed our previous observations with *Cyp2e1*(-/-) mice using a single concentration of ABP shown in Figure 20, and together support CYP2E1 as a major ABP *N*-hydroxylation enzyme in both male and female neonatal mouse livers. The lack of change in K_m again suggests that the multiple ABP-hydroxylating enzymes in mouse liver have similar affinities towards ABP, which is further confirmed with Eadie-Hofstee transformations of *Cyp2e1*(-/-) enzyme kinetic data (Figure 22).

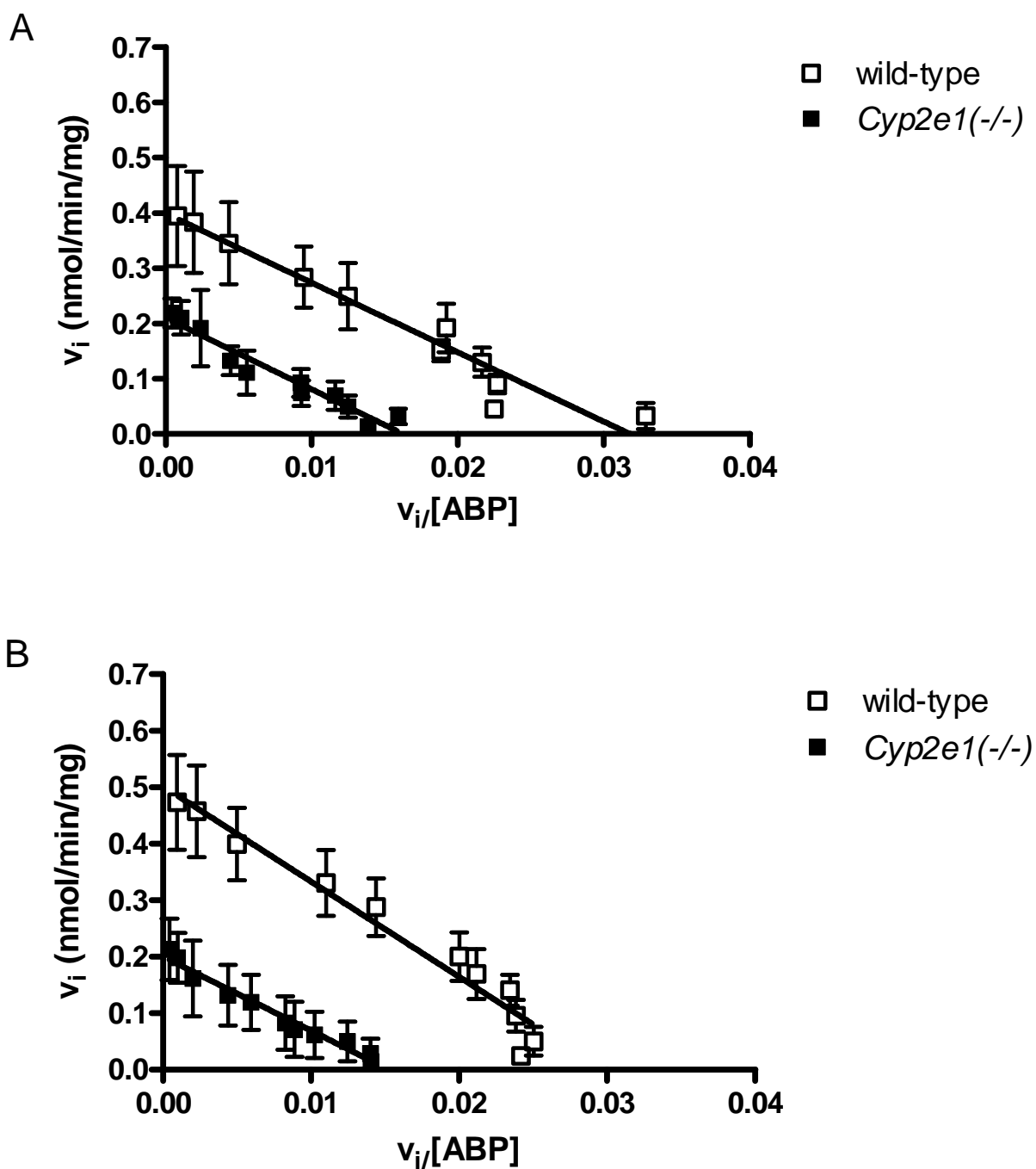


Figure 22. Eadie-Hofstee analysis of ABP *N*-hydroxylation by male and female wild-type and *Cyp2e1*(-/-) mouse liver microsomes.

Eadie-Hofstee transformations of male (A) and female (B) data shown in Figure 21.

As with our *Cyp1a2*(-/-) studies, linear Eadie-Hofstee plots for wild-type microsomes indicate the presence of a single enzyme or multiple enzymes with similar affinities for ABP *N*-hydroxylation in neonatal mouse livers. Overall our results support CYP2E1 as a major ABP *N*-hydroxylation enzyme that has similar affinity for ABP as CYP1A2 but accounts for an even greater proportion of ABP *N*-hydroxylation activity by neonatal mouse liver microsomes than CYP1A2, especially in females.

3.2.3 ABP *N*-hydroxylation by recombinantly expressed CYP1A2 or CYP2E1 in Hepa1c1c7 cells

To complement our *in vitro* studies using mouse liver microsomes, we recombinantly expressed mouse CYP1A2 or CYP2E1 in Hepa1c1c7 cells and tested for their ability to *N*-hydroxylate ABP using a live-cell assay for the measurement of ABP *N*-hydroxylation in cell culture. Following the manufacturer's protocols, we tested several different transfection ratios (transfection reagent:plasmid DNA) to arrive at optimized transfection conditions for the expression of CYP1A2 or CYP2E1, both in terms of mRNA level and enzyme activity, in Hepa1c1c7 cells (Appendix A). However, even with these optimized conditions, levels of enzyme activity in transfected cells were 8-fold and 32-fold lower than those in mouse liver microsomes for CYP1A2 and CYP2E1, respectively (Appendix figure 3). Nevertheless, ABP *N*-hydroxylation was detected in *Cyp1a2*-transfected but not in untransfected Hepa1c1c7 cells (Figure 23).

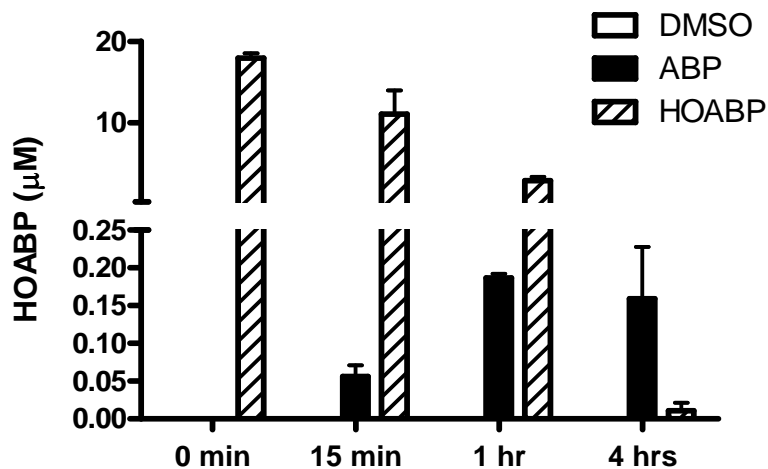


Figure 23. In culture HOABP production by *Cyp1a2*-transfected Hepa1c1c7 cells.

At 24 hours following transfection ABP was added to cell culture medium to a final concentration of 100 μM . Cells treated with 20 μM HOABP were used as a positive control. Aliquots of cell culture medium were withdrawn at 0-4 hours following drug incubation and analyzed by HPLC for the quantification of HOABP. Error bars represent standard deviations of the mean, which was calculated based on 3 replicates from a single experiment.

Interestingly, the level of HOABP in HOABP-treated positive control wells decreased to nearly undetectable levels by 4 hours following addition. This observation is consistent with our *in vitro* studies, where HOABP spontaneously degraded in solution at room temperature over a period of a few hours as measured by HPLC (data not shown), and support the unstable nature of this ABP metabolite.

In a separate experiment, we also detected ABP *N*-hydroxylation in *Cyp2e1*-transfected but not in untransfected Hepa1c1c7 cells (Figure 24).

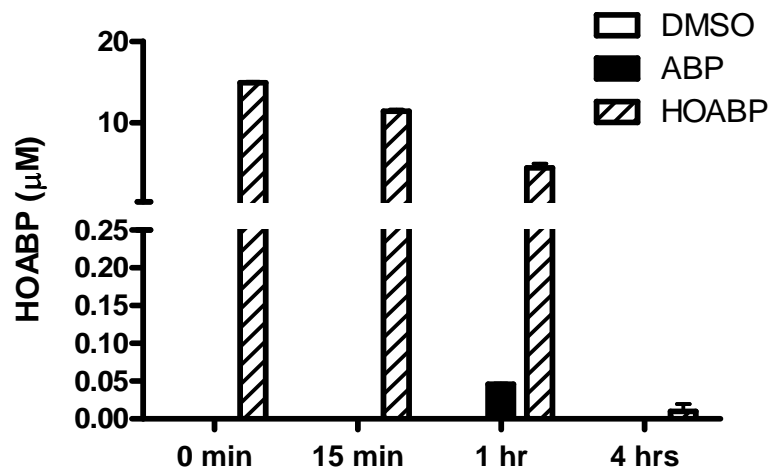


Figure 24. In culture HOABP production by *Cyp2e1*-transfected Hepa1c1c7 cells.

At 24 hours following transfection ABP was added to cell culture medium to a final concentration of 100 µM. Cells were treated with 20 µM HOABP as a positive control. Aliquots of cell culture medium were withdrawn at 0-4 hours following drug incubation and analyzed by HPLC for the quantification of HOABP. Error bars represent standard deviations of the mean, which was calculated based on 3 replicates from a single experiment.

To confirm these observations we also tested for ABP *N*-hydroxylation activity in microsomes isolated from *Cyp1a2*-transfected, *Cyp2e1*-transfected, and untransfected Hepa1c1c7 cells (Figure 25).

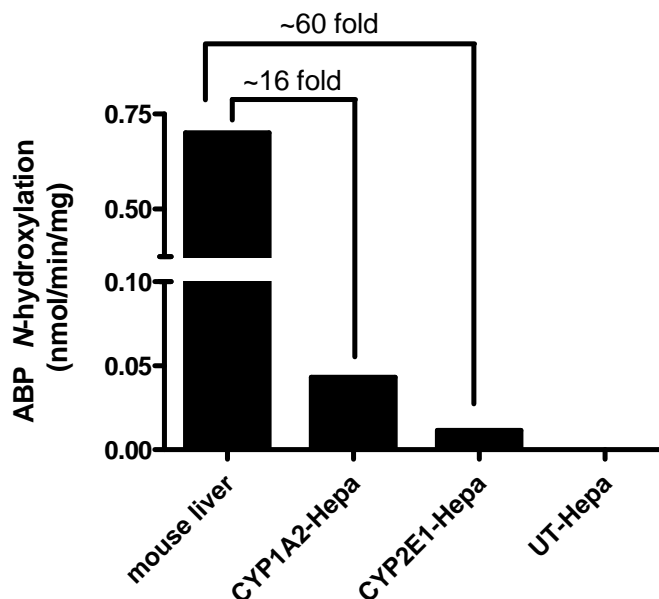


Figure 25. ABP N-hydroxylation by microsomes isolated from *Cyp2e1*- or *Cyp1a2*-transfected Hepa1c1c7 cells, untransfected Hepa1c1c7 cells, and mouse liver

Microsomes were isolated from a day 15 male C57BL/6 mouse liver and *Cyp1a2*-transfected, *Cyp2e1*-transfected, or untransfected Hepa1c1c7 cells. *In vitro* production of HOABP in the presence of microsomes and NADPH regenerating system at 200 μ M ABP was quantified by HPLC. "mouse liver" = C57BL/6 liver microsomes. "CYP1A2-Hepa" = microsomes isolated from Hepa1c1c7 cells transfected with *Cyp1a2*. "CYP2E1-Hepa" = microsomes isolated from Hepa1c1c7 cells transfected with *Cyp2e1*. "UT-Hepa" = untransfected Hepa1c1c7 cells.

Similar to the cell culture results, *in vitro* studies using microsomes isolated from transfected Hepa1c1c7 cells demonstrated significant ABP N-hydroxylation activity in both *Cyp1a2*- and *Cyp2e1*-transfected but not in untransfected Hepa1c1c7 cells (Figure 25). ABP N-hydroxylation activity in microsomes from transfected cells was much lower than in microsomes from mouse liver on a per mg microsomal protein basis, as expected from lower levels of CYP1A2 and CYP2E1 enzyme activities detected in transfected cells (Figure 25, Appendix figure 3).

3.3 ABP-induced oxidative stress in cell culture and *in vivo*

Oxidative stress represents a risk factor for human liver cancer that is capable of driving liver carcinogenesis in mice (Section 1.3.3.4). In light of both *in vitro* and *in vivo* studies linking ABP to oxidative stress (Section 1.4.5), the objective of studies in this section was to determine whether ABP produces oxidative stress in Hepa1c1c7 cells and *in vivo* following our tumor-

inducing neonatal exposure protocol. As the NRF2 antioxidant response represents a major determinant of oxidative stress in the mouse liver, we also measured changes in NRF2 and NRF2-regulated antioxidant genes following our tumor-inducing neonatal exposure protocol.

3.3.1 *N*-hydroxylation of ABP leads to oxidative stress in Hepa1c1c7 cells

Using immunoblotting, we measured levels of γ H2AX as a biomarker of oxidative DNA damage in cell culture. γ H2AX represents histone variant H2AX phosphorylated on serine 139. This phosphorylation event is triggered by DNA strand breaks, which represent one form of oxidative DNA damage, and is a rapid, initial event in DNA damage signaling pathways. In our first studies, we did not detect any changes in oxidative DNA damage, as measured by γ H2AX, using a variety of ABP concentrations and incubation times (results from a typical experiment are shown in Figure 26).

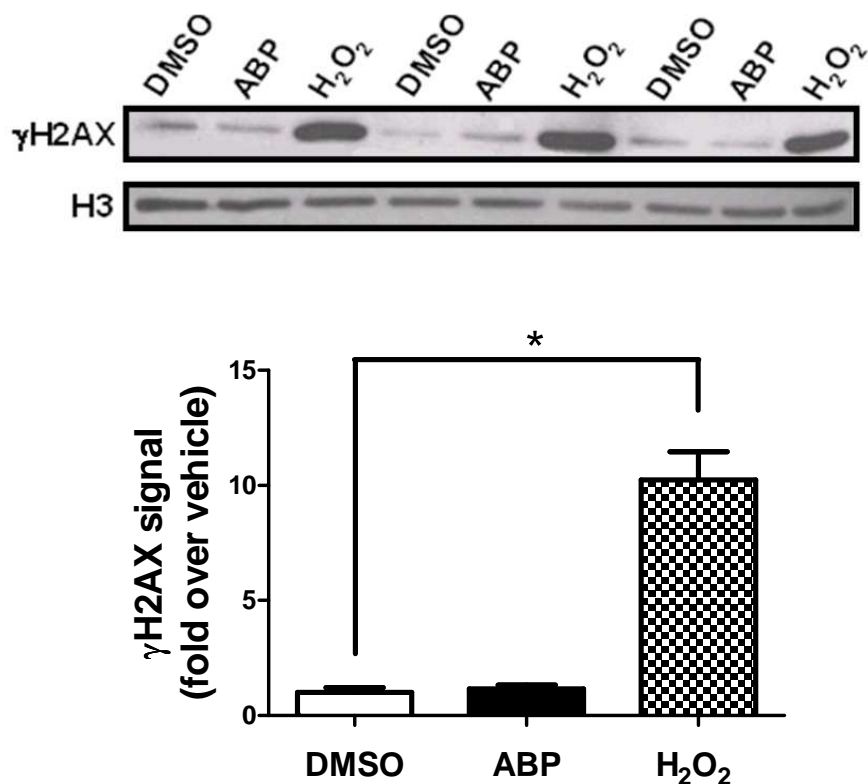


Figure 26. Effect of ABP on levels of oxidative DNA damage in Hepa1c1c7 cells.

Immunoblot from Hepa1c1c7 cells treated with DMSO vehicle (0.01%), 100 μ M ABP, or 100 μ M hydrogen peroxide (H₂O₂) for 4 hours (top), and quantification of blots using densitometry (bottom). Cell lysates were separated on a 12.5% SDS-PAGE gel and subjected to immunoblot analysis with anti- γ H2AX or H3 (loading control) antibodies, quantified using densitometry, and analyzed by Image J software (NIH). Error bars represent standard deviations of the mean, which was calculated based on 3 replicates from a single experiment. (* $P < 0.001$).

On the other hand, hydrogen peroxide (H₂O₂), used as a positive control, induced significantly increased γ H2AX in Hepa1c1c7 cells as revealed by one-way ANOVA followed by Bonferroni post-tests ($P < 0.001$, Figure 26). Previous studies from our own laboratory and others have shown that it is the HOABP metabolite that produces oxidative stress *in vitro* and that Hepa1c1c7 cells lack ABP *N*-hydroxylation activity ((Makena and Chung, 2007; Murata *et al.*, 2001); Figure 25). In the next experiment we directly tested HOABP for its ability to produce oxidative stress in Hepa1c1c7 cells (Figure 27).

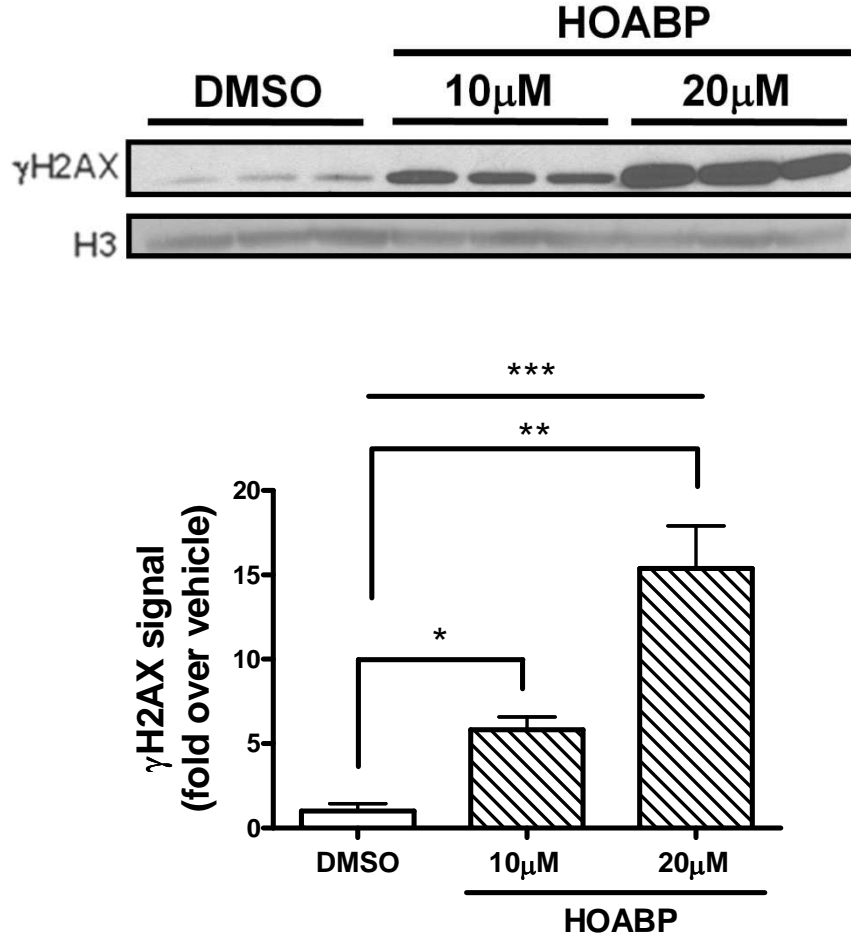


Figure 27. Effect of HOABP on levels of oxidative DNA damage in Hepa1c1c7 cells.

Immunoblot from Hepa1c1c7 cells treated with DMSO vehicle (0.01%), 10 μ M or 20 μ M HOABP for 4 hours (top) and quantification of blots using densitometry (bottom). Cell lysates were separated on a 12.5% SDS-PAGE gel and subjected to immunoblot analysis with anti- γ H2AX or H3 (loading control) antibodies, quantified using densitometry, and analyzed by Image J software (NIH). Error bars represent standard deviations of the mean, which was calculated based on 3 replicates from a single experiment. (* $P < 0.05$, ** $P < 0.001$, and *** $P < 0.0001$ for the effect of drug). Results have been reproduced in a separate experiment (data not shown).

One-way ANOVA analysis revealed a highly significant overall effect of HOABP treatment on γ H2AX levels in Hepa1c1c7 cells ($P < 0.0001$, Figure 27). 10 μ M and 20 μ M HOABP induced significantly higher γ H2AX compared to DMSO control, with $P < 0.05$ and $P < 0.001$, respectively, using one-way ANOVA analysis followed by Bonferroni post-tests (Figure 27). In addition, co-treatment with the antioxidant N-acetylcysteine (NAC) completely blocked the

HOABP-induced γ H2AX response, as shown by the complete reversion of the γ H2AX response in HOABP + NAC co-treated cells back to vehicle-treated levels (Figure 28).

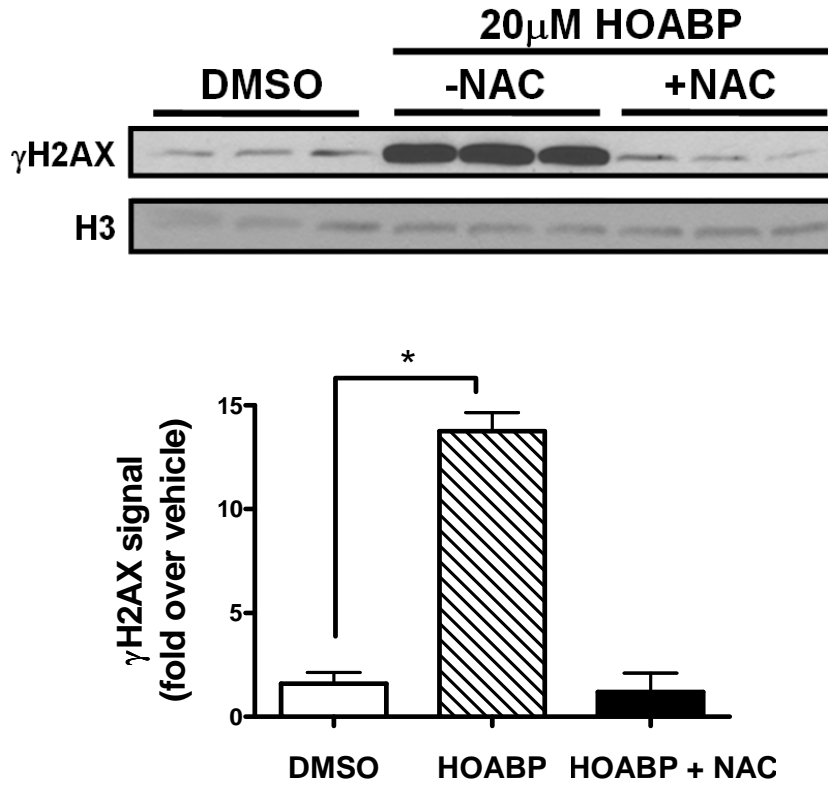


Figure 28. Effect of NAC on HOABP-induced oxidative DNA damage in Hepa1c1c7 cells

Immunoblot from Hepa1c1c7 cells treated with DMSO vehicle (0.01%), 20 μ M HOABP, or 20 μ M HOABP + 1 mM NAC for 4 hours (top) and quantification of blots using densitometry (bottom). Cell lysates were separated on a 12.5% SDS-PAGE gel and subjected to immunoblot analysis with anti- γ H2AX or H3 (loading control) antibodies, quantified using densitometry, and analyzed by Image J software (NIH). Error bars represent standard deviations of the mean, which was calculated based on 3 replicates from a single experiment. (* $P < 0.001$). Results have been reproduced in a separate experiment (data not shown).

To confirm the results generated using the γ H2AX assay, we measured levels of reactive oxygen species produced by ABP and HOABP in Hepa1c1c7 cells using the DCF assay. In the DCF assay, intracellular fluorescence of live cells is quantified in the presence of the dichlorofluorescein (DCF) dye, which fluoresces upon oxidation by reactive oxygen species.

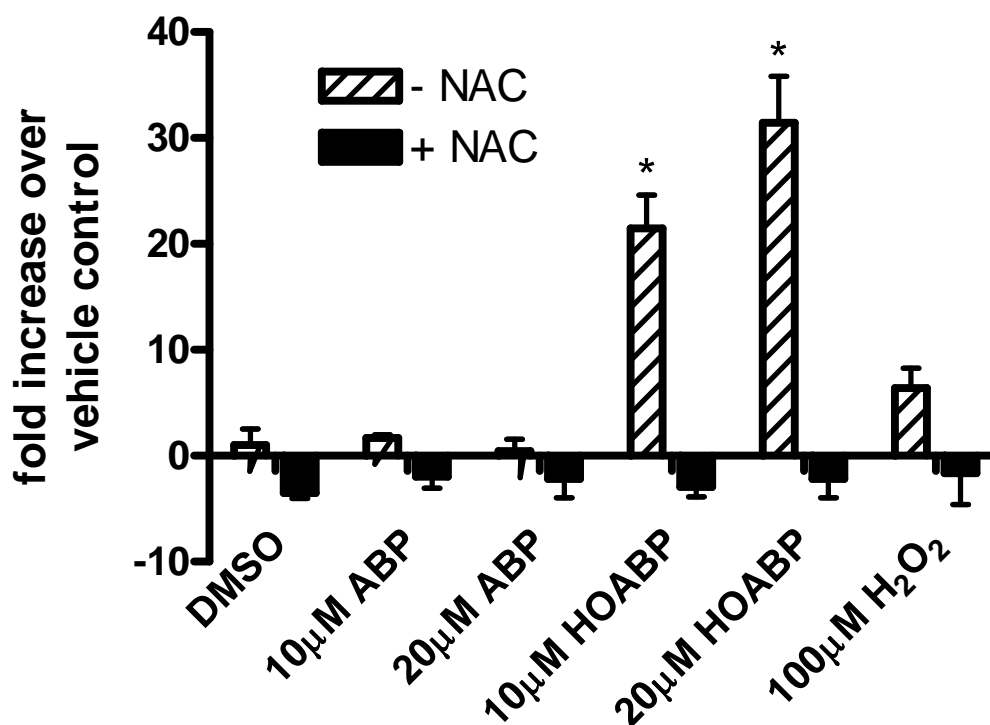


Figure 29. Effects of ABP and HOABP on levels of reactive oxygen species in Hepa1c1c7 cells.

Cells pre-incubated with dichlorofluorescein dye were exposed to DMSO vehicle (0.01%), 10 and 20 μM of ABP or HOABP, or 100 μM H₂O₂. Slopes of fluorescence kinetic curves at 528 nm were measured and compared to vehicle-treated control group. Error bars represent standard deviations of the mean, which was calculated based on 4 replicates from a single experiment. (* $P < 0.001$ compared to vehicle-treated control). Results have been reproduced in a separate experiment (data not shown).

Two-way ANOVA analysis followed by Bonferroni post-tests revealed significant increases in DCF signal with HOABP ($P < 0.0001$ for both 10 μM and 20 μM), but not with equimolar concentrations of ABP (Figure 29). In addition, NAC completely blocked the HOABP-induced DCF signal (Figure 29). Together our cell culture studies support previous *in vitro* findings from other laboratories that HOABP, but not the parent compound ABP, is a potent inducer of oxidative stress.

In Section 3.2 we established both CYP1A2 and CYP2E1 as ABP *N*-hydroxylation enzymes in mouse liver and detected ABP *N*-hydroxylation activity in Hepa1c1c7 cells transfected with *Cyp1a2* or *Cyp2e1*. In the next study we therefore tested whether the endogenous production of

HOABP, through the *N*-hydroxylation of ABP in CYP1A2- or CYP2E1-expressing Hepa1c1c7 cells, leads to oxidative stress. ABP produced significant increases in both oxidative DNA damage ($P < 0.05$, Student's t-test) and reactive oxygen species ($P < 0.01$ for the effect of ABP, one-way ANOVA) compared to vehicle-treated controls in *Cyp2e1*-transfected Hepa1c1c7 cells (Figure 30).

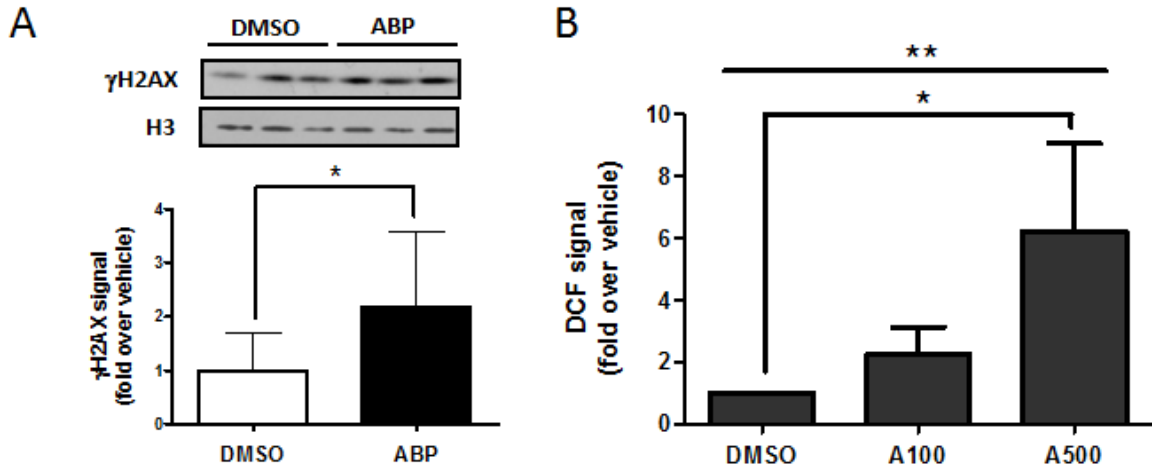


Figure 30. Effect of ABP on levels of oxidative DNA damage and reactive oxygen species in *Cyp2e1*-transfected Hepa1c1c7 cells.

Immunoblot showing Hepa1c1c7 cells transiently transfected with *Cyp2e1* and treated with 0.1% DMSO vehicle or 100 μ M ABP (A). Cell lysates were separated on a 12.5% SDS-PAGE gel, subjected to immunoblot analysis with anti- γ H2AX or H3 (loading control) antibodies, quantified using densitometry, and analyzed by Image J software (NIH). A typical experiment is shown. Error bars represent standard deviations of the mean, which was calculated from 9 replicates of 3 independent experiments. Fluorometric quantification of DCF signal in Hepa1c1c7 cells transiently transfected with *Cyp2e1* and treated with 0.3% DMSO vehicle, 100 μ M ABP (A100), or 500 μ M ABP (A500). Error bars represent standard deviations of the mean, which was calculated from 3 independent experiments. (* $P < 0.05$ and ** $P < 0.01$ for the effect of drug).

However, ABP failed to produce either oxidative DNA damage or reactive oxygen species in *Cyp1a2*- and *Nat3*-transfected (negative control) Hepa1c1c7 cells (Figure 31 and Figure 32).

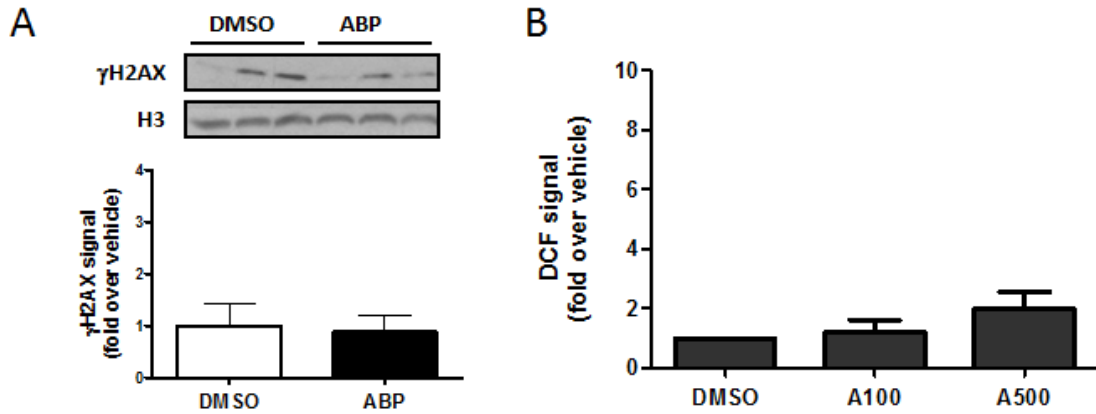


Figure 31. Effect of ABP on levels of oxidative DNA damage and reactive oxygen species in *Cyp1a2*-transfected Hepa1c1c7 cells.

Immunoblot showing Hepa1c1c7 cells transiently transfected with *Cyp1a2* and treated with 0.1% DMSO vehicle or 100 μ M ABP (A). Cell lysates were separated on a 12.5% SDS-PAGE gel, subjected to immunoblot analysis with anti- γ H2AX or H3 (loading control) antibodies, quantified using densitometry, and analyzed by Image J software (NIH). A typical experiment is shown. Error bars represent standard deviations of the mean, which was calculated from 9 replicates of 3 independent experiments. Fluorometric quantification of DCF signal in Hepa1c1c7 cells transiently transfected with *Cyp1a2* and treated with 0.3% DMSO vehicle, 100 μ M ABP (A100), or 500 μ M ABP (A500). Error bars represent standard deviations of the mean, which was calculated from 3 independent experiments.

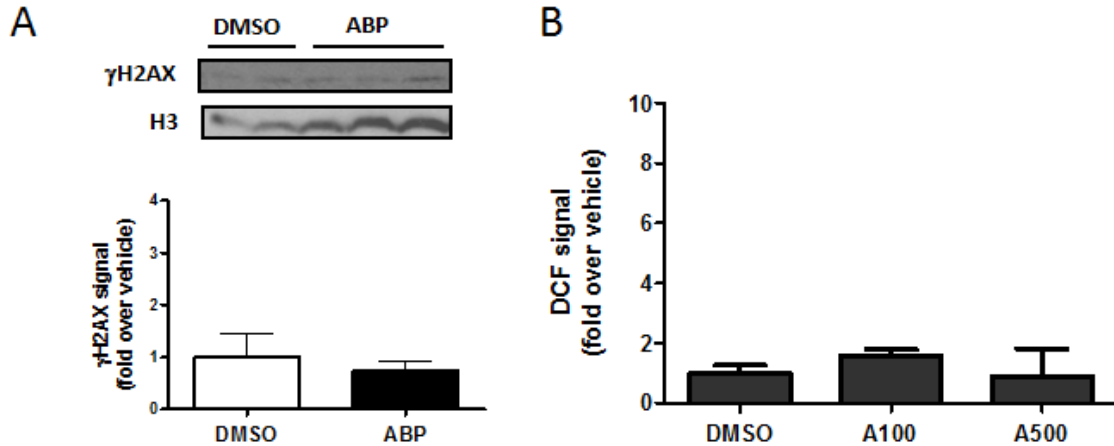


Figure 32. Effect of ABP on levels of oxidative DNA damage and reactive oxygen species in *Nat3*-transfected Hepa1c1c7 cells.

Immunoblot showing Hepa1c1c7 cells transiently transfected with *Nat3* and treated with 0.1% DMSO vehicle or 100 μ M ABP. Cell lysates were separated on a 12.5% SDS-PAGE gel, subjected to immunoblot analysis with anti- γ H2AX or H3 (loading control) antibodies, quantified using densitometry, and analyzed by Image J software (NIH). A typical experiment is shown. Error bars represent standard deviations of the mean, which was calculated from 9 replicates of 3 independent experiments. Fluorometric quantification of DCF signal in Hepa1c1c7 cells transiently transfected with *Nat3* and treated with 0.3% DMSO vehicle, 100 μ M ABP (A100), or 500 μ M ABP (A500). Error bars represent standard deviations of the mean, which was calculated from 3 independent experiments.

To test whether ABP-induced oxidative stress was mediated by CYP2E1 enzyme activity, we tested the effects of CYP2E1 substrates/inhibitors on ABP-induced reactive oxygen species using the DCF assay. ABP-induced reactive oxygen species in *Cyp2e1*-transfected Hepa1c1c7 cells could be blocked by the CYP2E1 substrates pNP and chlorzoxazone (CLX, $P < 0.01$), as demonstrated by one-way ANOVA analysis followed by Bonferroni post-tests (Figure 33).

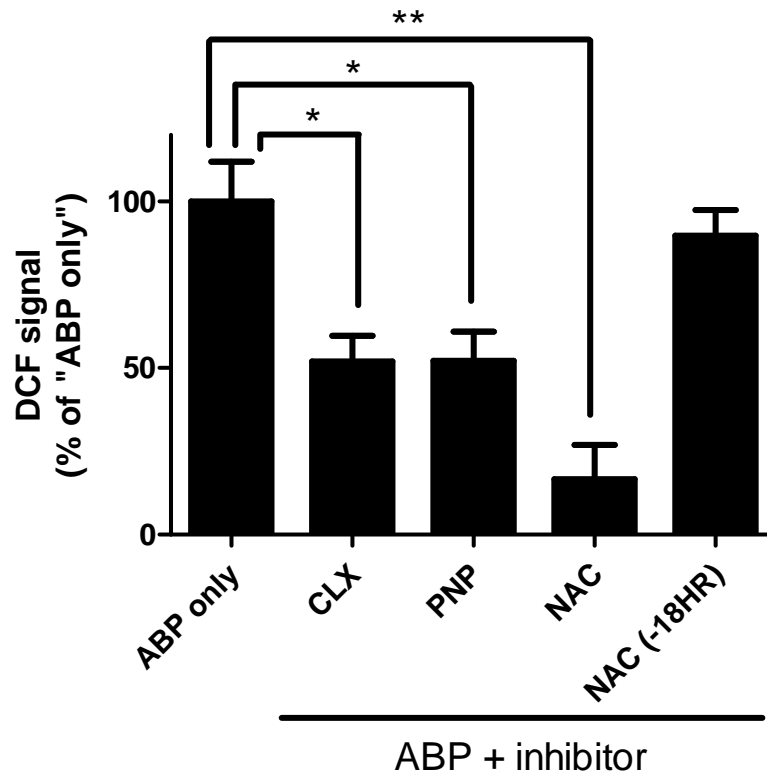


Figure 33. Effect of CYP2E1 inhibitors and the antioxidant NAC on ABP-induced reactive oxygen species in *Cyp2e1*-transfected Hepa1c1c7 cells.

Fluorometric quantification of DCF signal in Hepa1c1c7 cells transiently transfected with *Cyp2e1* and treated with 500 μ M ABP only or in combination with inhibitor. Concentration of CLX, pNP, and NAC used was 1 mM. "NAC" = co-treatment with NAC. "NAC (-18HR)" = pretreatment with NAC for 18 hours. Error bars represent standard deviations of the mean, which was calculated based on 4 replicates from a single experiment. (* $P < 0.01$ and ** $P < 0.001$). Results have been reproduced in a separate experiment (data not shown).

Co-treatment of ABP with the antioxidant NAC also blocked ABP-induced reactive oxygen species in *Cyp2e1*-transfected Hepa1c1c7 cells ($P < 0.001$); on the other hand, pre-treatment with NAC for 18 hours had no inhibitory effect (Figure 33).

The detection of ABP-induced oxidative stress in *Cyp2e1*- but not *Cyp1a2*- transfected cells is surprising given our previous observation of higher ABP *N*-hydroxylation activity in *Cyp1a2*-compared to *Cyp2e1*-transfected cells (Figure 25). Recently, both human and rat CYP2E1 were shown to be expressed in the mitochondria in addition to the endoplasmic reticulum (Bansal *et al.*, 2010; Bansal *et al.*, 2013). Since the mitochondrion represents a key organelle in the *in vivo*

production of reactive oxygen species by the aromatic amine 2-acetylaminofluorene (Klöhn *et al.*, 1998; Klöhn *et al.*, 2003), we carried out a pilot study to examine the potential involvement of mitochondrial CYP2E1 in ABP-induced oxidative stress. We tested the effect of ABP on Hepa1c1c7 cells transiently transfected with different rat *Cyp2e1* variants that express CYP2E1 protein at similar total levels in cells but target differentially between mitochondria and endoplasmic reticulum (Figure 34).

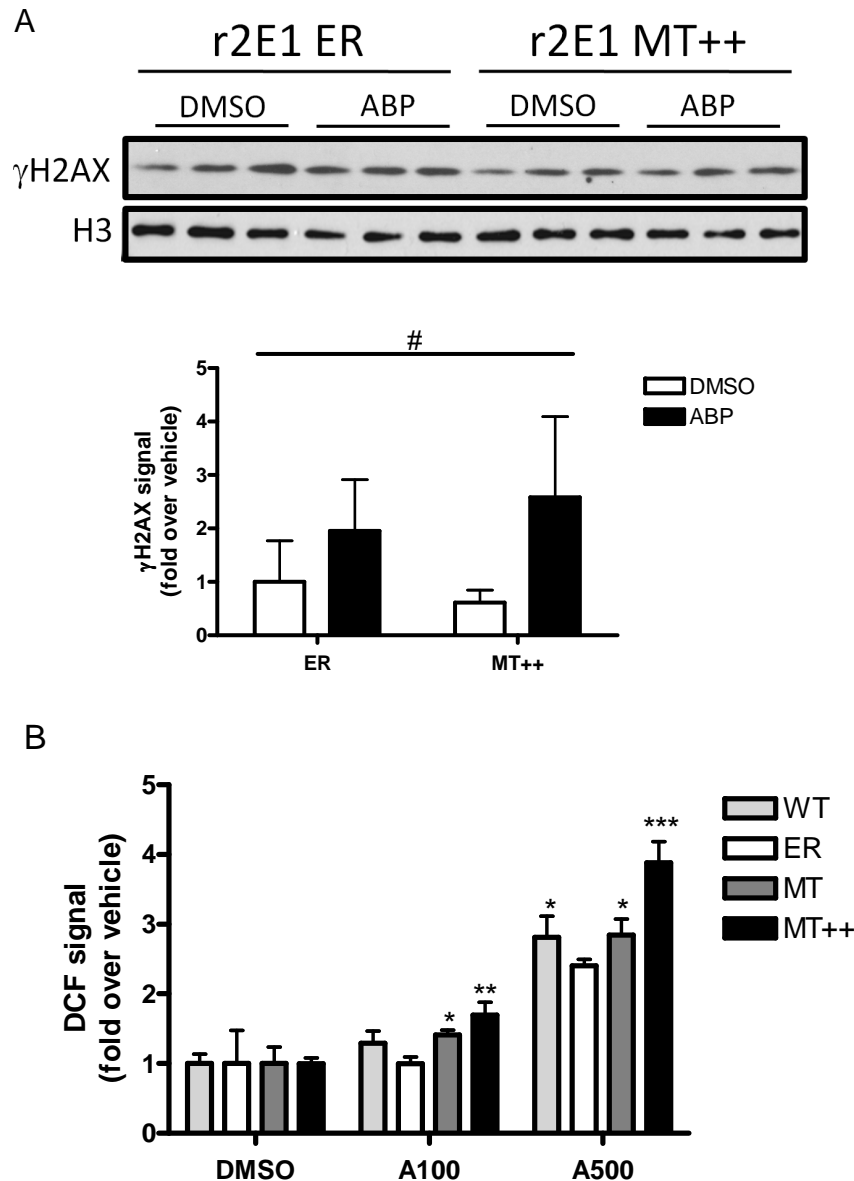


Figure 34. Effect of ABP on levels of oxidative stress in Hepa1c1c7 cells transfected with mitochondria- vs. endoplasmic reticulum-targeting rat *Cyp2e1*.

A) Immunoblot from Hepa1c1c7 cells transiently transfected with ER or MT++ variant of rat *Cyp2e1* (r2E1) treated with 0.1% DMSO vehicle or 100 μ M ABP. Cell lysates were separated on a 12.5% SDS-PAGE gel, subjected to immunoblot analysis with anti- γ H2AX or H3 antibodies, quantified using densitometry, and analyzed by Image J software (NIH). Error bars represent standard deviations of the mean, which was calculated from 3 replicates of a single experiment. B) Fluorometric quantification of DCF signal in Hepa1c1c7 cells transiently transfected with WT, ER, MT, or MT++ variant of rat *Cyp2e1* and treated with 0.3% DMSO vehicle, 100 μ M ABP (A100), or 500 μ M ABP (A500). Error bars represent standard deviations of the mean, which was calculated from 4 replicates of a single experiment. (# $P < 0.05$ for effect of ABP, * $P < 0.05$ compared to ER variant, ** $P < 0.001$ compared to ER variant, and *** $P < 0.001$ compared to all other variants).

Based on original publications from the Avadhani group, these rat *Cyp2e1* variants ranked from low to high expression in mitochondria in the following order: ER (20%) < WT (47%) < MT (58%) < MT++ (85%), where the percentage in parentheses represents the proportion of total CYP2E1 protein expressed in the mitochondria of COS-7 cells (Bansal *et al.*, 2010). In our studies, ABP produced slightly higher oxidative DNA damage in Hepa1c1c7 cells transfected with the MT++ compared to the ER rat *Cyp2e1* variant; however, the effect of ABP failed to reach significance in either the MT++- or ER-variant transfected cells ($P > 0.05$, two-way ANOVA followed by Bonferroni post-tests), despite being significant overall ($P < 0.05$ by two-way ANOVA, Figure 34A). In terms of reactive oxygen species, treatment with 100 μM ABP significantly induced levels of reactive oxygen species in MT ($P < 0.05$) and MT++ ($P < 0.001$) rat *Cyp2e1* variant-transfected cells but not ER or WT variant-transfected cells, as determined using two-way ANOVA followed by Bonferroni post-tests. Treatment with 500 μM ABP significantly increased levels of reactive oxygen species in WT ($P < 0.05$), MT ($P < 0.05$), and MT++ ($P < 0.001$) but still not in ER rat *Cyp2e1* variant-transfected Hepa1c1c7 cells, as shown by two-way ANOVA followed by Bonferroni post-tests (Figure 34B). Overall, ABP-induced reactive oxygen species in Hepa1c1c7 cells positively correlated with the extent of mitochondrial expression for each rat *Cyp2e1* variant, with $\text{MT++} > \text{MT} > \text{WT} \geq \text{ER}$. To rule out the possibility that differences in ABP-induced oxidative stress with different rat *Cyp2e1* transfected cells is due to different levels of total CYP2E1 expression, we measured levels of CYP2E1 transcript and activity in transfected cells. We found no difference in CYP2E1 transcript and activity between ER, WT, and MT rat *Cyp2e1* variant-transfected cells; on the other hand, MT++ variant-transfected cells demonstrated much reduced levels of CYP2E1 transcript (< 50% of other variants) and activity (< 10% of other variants) despite showing the highest level of ABP-induced reactive oxygen species (Appendix C, Figure 34B).

3.3.2 Sex and strain differences in liver oxidative stress induced by tumorigenic doses of ABP in neonatal mice

In this series of studies we tested whether ABP produced oxidative stress *in vivo* following the same postnatal exposure protocol used in our ABP neonatal bioassay. We adapted our in culture γH2AX detection method to measure γH2AX levels *in vivo* in male and female mouse livers at 7 and 24 hours following a postnatal day 15 dose of ABP (Figure 35).

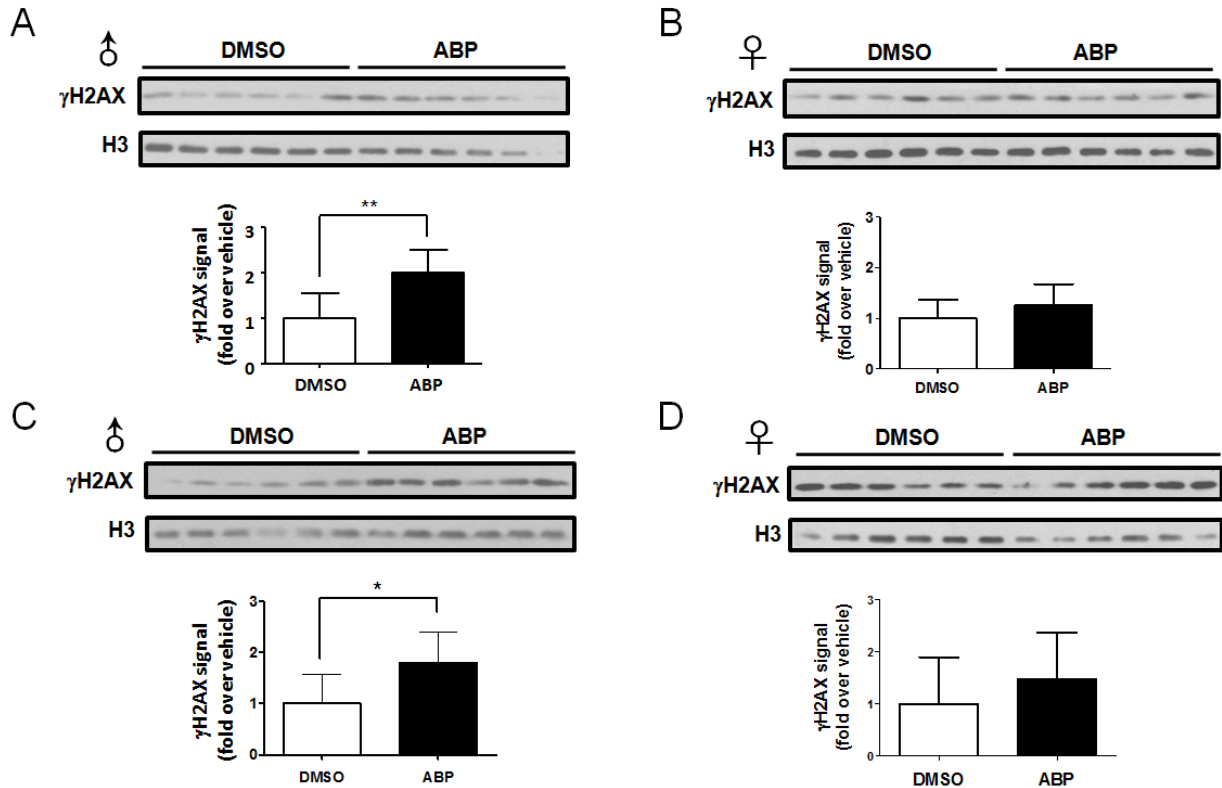


Figure 35. Oxidative DNA damage in male and female mouse livers exposed to tumorigenic doses of ABP.

Mice (N=6 per group) were injected with vehicle or 1200 nmol of ABP on postnatal days 8 and 15. Immunoblot of ABP-induced γ H2AX in male C57BL/6 mouse livers at 7 hours (A) and 24 hours (C) following postnatal day 15 dose of ABP or DMSO vehicle (N=6). Immunoblot of ABP-induced γ H2AX in female C57BL/6 mouse livers at 7 hours (B) and 24 hours (D) following postnatal day 15 dose of ABP or DMSO vehicle. For immunoblots, liver nuclei homogenates were separated on a 12.5% SDS-PAGE gel, subjected to immunoblot analysis with anti- γ H2AX or H3 antibodies, quantified using densitometry, and analyzed by Image J software (NIH). Error bars represent standard deviations of the mean, which was first normalized to H3 and then normalized to DMSO-treated controls. (* $P < 0.05$ and ** $P < 0.01$).

Compared to vehicle-treated controls, tumorigenic doses of ABP induced significantly higher oxidative DNA damage in male livers at both 7 ($P < 0.01$) and 24 hours ($P < 0.05$) as determined by Student's t-test (Figure 35). In contrast, tumorigenic doses of ABP failed to induce significant increases in oxidative DNA damage of female livers at any time-point tested ($P > 0.05$, Figure 35). Finally in a pilot study, a postnatal day 8 dose of ABP (1/3 of the total tumor-inducing dose) failed to produce significantly increased oxidative DNA damage in either male or female mouse livers at 24 hours ($P > 0.05$, Appendix figure 9).

Glutathione represents the main source of antioxidant molecules in mouse liver that provide the first line of defense against oxidative insults. Oxidation of glutathione by oxidants leads to the accumulation of oxidized glutathione (GSSG), which we quantified as an alternative measure of oxidative stress in mouse liver. We measured levels of GSSG in male and female mice at various acute time-points following tumorigenic doses of ABP or vehicle control (Figure 36).

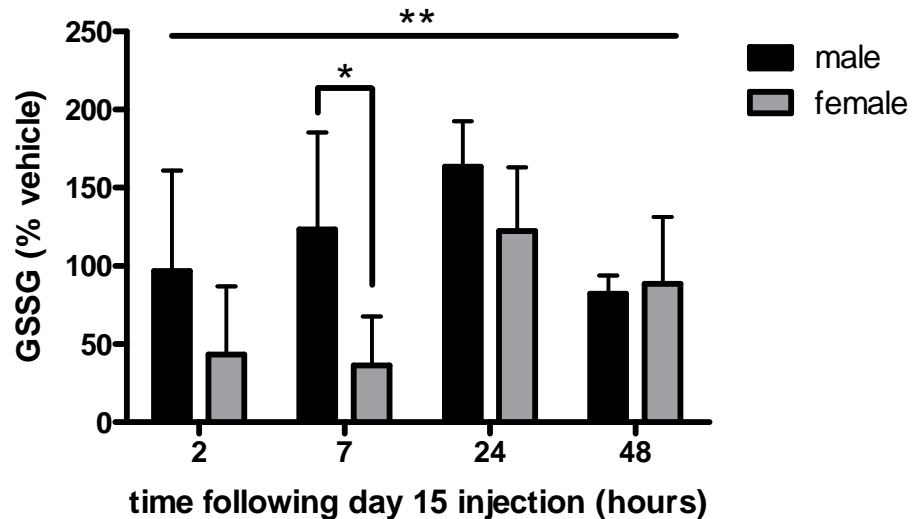


Figure 36. GSSG levels in male and female mouse livers exposed to tumorigenic doses of ABP.

Mice (N=4-5 per group) were injected with vehicle or 1200 nmol of ABP on postnatal days 8 and 15. Levels of GSSG in DMSO- or ABP-treated livers of male and female C57BL/6 mice were detected using the Glutathione Detection kit (Enzo Life Sciences Inc., Farmingdale, NY, USA) at 2, 7, 24, and 48 hours following postnatal day 15 dose of ABP. Levels of GSSG in ABP-treated samples were normalized to their corresponding vehicle controls in order to compare between different sexes. Error bars represent standard deviations of the mean. (* $P < 0.05$ and ** $P < 0.01$ for overall effects of sex and time).

At each time-point within each sex, the absolute change in GSSG with ABP-treated samples was not significant compared to vehicle-treated controls (data not shown). Nevertheless, a non-significant trend towards increased GSSG in males combined with a non-significant trend towards decreased GSSG in females, each normalized to their corresponding vehicle-treated controls, led to significant overall effects of both sex and time on relative GSSG levels (two-way ANOVA, $P < 0.01$, Figure 36). Subsequent Bonferroni post-tests revealed significantly higher GSSG levels in males compared to females at 7 hours following a postnatal day 15 dose of ABP ($P < 0.05$, Figure 36). On the other hand, no significant changes in levels of total glutathione

were detected in the same liver samples (data not shown). Together, our *in vivo* γ H2AX and GSSG results suggest higher levels of oxidative stress in livers of male mice following acute exposure to tumorigenic doses of ABP compared to female mice.

Using mice that are deficient in CYP1A2 or CYP2E1, we tested the potential roles of ABP *N*-hydroxylation enzymes in the generation of oxidative DNA damage following tumorigenic doses of ABP. Since *Cyp2e1*(*-/-*) mice are on a mixed-strain background, they were compared to their corresponding *Cyp2e1*(*+/+*) mixed-strain mice. At 7 hours following a tumorigenic dose of ABP, *Cyp2e1*(*+/+*) males demonstrated a significant increase in liver oxidative DNA damage (Student's t-test, $P < 0.001$, Figure 37) that was not found in the corresponding females as measured using γ H2AX (Student's t-test, $P > 0.05$, Figure 37), reproducing the sex differences observed in C57BL/6 mice shown in Figure 35. Interestingly, *Cyp2e1*(*-/-*) males were protected from liver oxidative DNA damage following tumorigenic doses of ABP (Student's t-test, $P > 0.05$, Figure 37). On the other hand, *Cyp1a2*(*-/-*) males were not protected from liver oxidative DNA damage following tumorigenic doses of ABP (Student's t-test, $P < 0.01$, Figure 38).

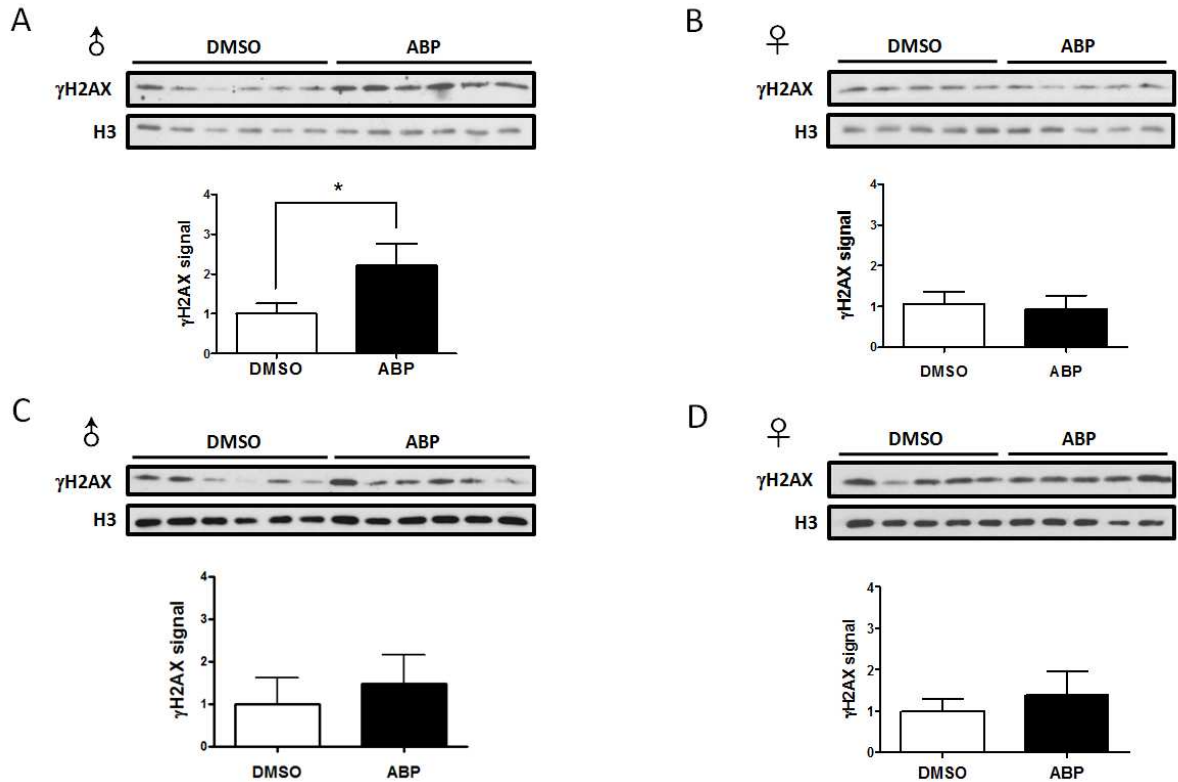


Figure 37. Oxidative DNA damage in male and female *Cyp2e1*(+/+) and *Cyp2e1*(-/-) mouse livers exposed to tumorigenic doses of ABP.

Mice (N=5-6 per group) were injected with vehicle or 1200 nmol of ABP on postnatal days 8 and 15. Immunoblot of ABP-induced γ H2AX in *Cyp2e1*(+/+) SVJ129 and C57BL/6 mixed-strain male (A) and female (B) mouse livers at 7 hours following day 15 dose of ABP or DMSO vehicle (N=5-6). Immunoblot of ABP-induced γ H2AX in *Cyp2e1*(-/-) SVJ129 and C57BL/6 mixed-strain male (C) and female (D) mouse livers at 7 hours following day 15 dose of ABP or DMSO vehicle (N=5-6). For immunoblots, liver nuclei homogenates were separated on a 12.5% SDS-PAGE gel, subjected to immunoblot analysis with anti- γ H2AX or H3 antibodies, quantified using densitometry, and analyzed by Image J software (NIH). Error bars represent standard deviations of the mean, which was first normalized to H3 and then normalized to DMSO-treated controls. (* $P < 0.001$).

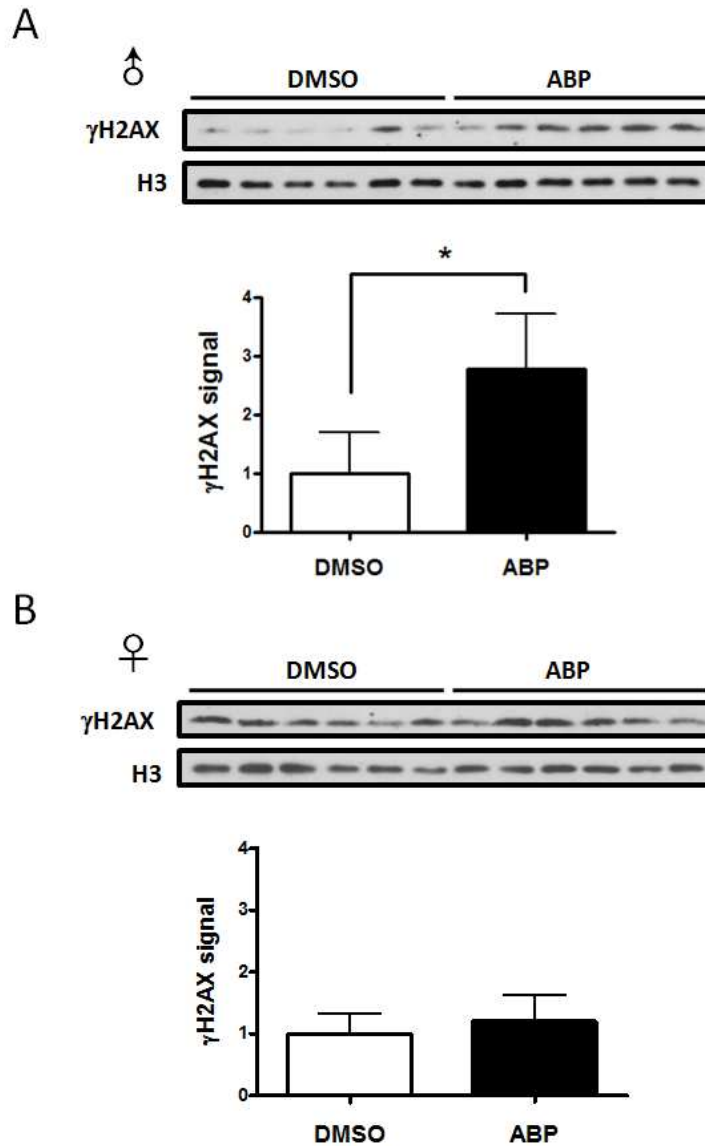


Figure 38. Oxidative DNA damage in livers of male and female *Cyp1a2*(*-/-*) mice exposed to tumorigenic doses of ABP.

Mice (N=6 per group) were injected with vehicle or 1200 nmol of ABP on postnatal days 8 and 15. Immunoblot of ABP-induced γ H2AX in *Cyp1a2*(*-/-*) C57BL/6 male (A) and female (B) mouse livers at 7 hours following day 15 dose of ABP or DMSO vehicle. For immunoblots, liver nuclei homogenates were separated on a 12.5% SDS-PAGE gel, subjected to immunoblot analysis with anti- γ H2AX or H3 antibodies, quantified using densitometry, and analyzed by Image J software (NIH). Error bars represent standard deviations of the mean, which was first normalized to H3 and then normalized to DMSO-treated controls. (* $P < 0.01$).

As with our cell culture results, *in vivo* studies using mice deficient in ABP *N*-hydroxylation enzymes support the involvement of CYP2E1, but not CYP1A2, in the production of oxidative

stress following ABP exposure. As was observed in wild-type mice (C57BL/6 and *Cyp2e1*(+/+)), ABP failed to induce γ H2AX in livers of both *Cyp2e1*(-/-) and *Cyp1a2*(-/-) females, highlighting sex differences in the oxidative stress response to ABP that are conserved across different strains of mice (Student's t-test, $P > 0.05$, Figure 37 and Figure 38).

3.3.3 Sex differences in liver antioxidant response induced by tumorigenic doses of ABP in neonatal mice

In attempt to explain the sex differences observed in ABP-induced oxidative stress *in vivo*, we examined antioxidant responses in mouse liver following tumorigenic doses of ABP. Specifically, we focused on the NRF2 transcription factor, which represents a master regulator of antioxidant response in mouse liver. At 24 hours following a postnatal day 15 dose of ABP, nuclear levels of NRF2 were significantly up-regulated in both male and female mouse livers (Figure 39).

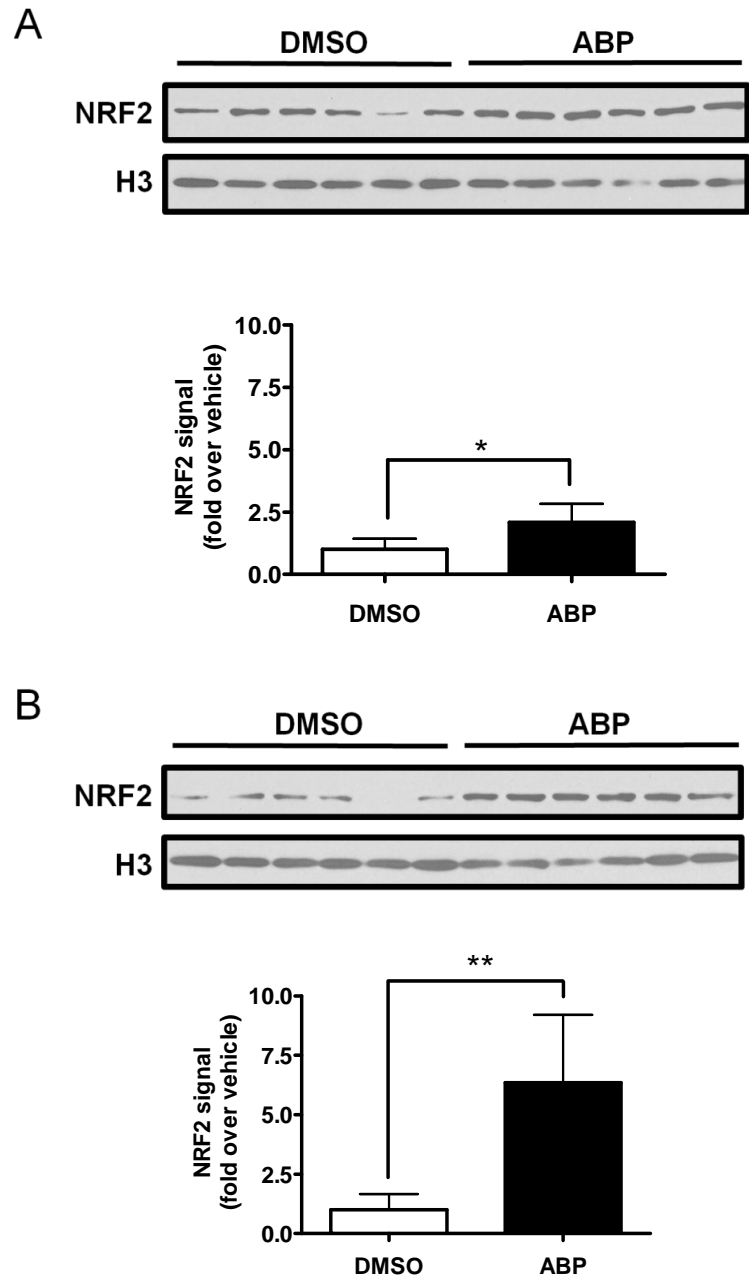


Figure 39. NRF2 protein expression in livers of male and female mice exposed to tumorigenic doses of ABP.

Mice (N=6 per group) were injected with vehicle or 1200 nmol of ABP on postnatal days 8 and 15. Immunoblot showing ABP-induced NRF2 in C57BL/6 male (A) and female (B) livers at 24 hours following the day 15 dose of ABP or DMSO vehicle (N=6). Liver nuclei homogenates were separated on a 12.5% SDS-PAGE gel, subjected to immunoblot analysis with anti-NRF2 or H3 (loading control) antibodies, quantified using densitometry, and analyzed by Image J software (NIH). Error bars represent standard deviations of the mean, which was first normalized to H3 and then normalized to DMSO-treated controls. (* $P < 0.01$ and ** $P < 0.001$).

Compared to vehicle-treated controls, ABP-treated females demonstrated greater NRF2 induction (~6.3 fold, Student's t-test, $P < 0.001$) compared to males (~2.1 fold, Student's t-test, $P < 0.01$), despite both sexes having similar basal expressions of NRF2 (Figure 39, Appendix figure 8). On the other hand in a pilot study, the postnatal day 8 dose of ABP (1/3 of the total tumor-inducing dose) failed to produce a significant increase in nuclear NRF2 compared to vehicle-treated controls at 24 hours (Appendix figure 9).

To extend our NRF2 findings, we measured the effect of tumorigenic doses of ABP on the expression of antioxidant genes (*Ggt1*, *Nqo1*, and *Hmox1*) that have been shown to be induced by oxidative stress and are at least in part regulated by NRF2 (Figure 40).

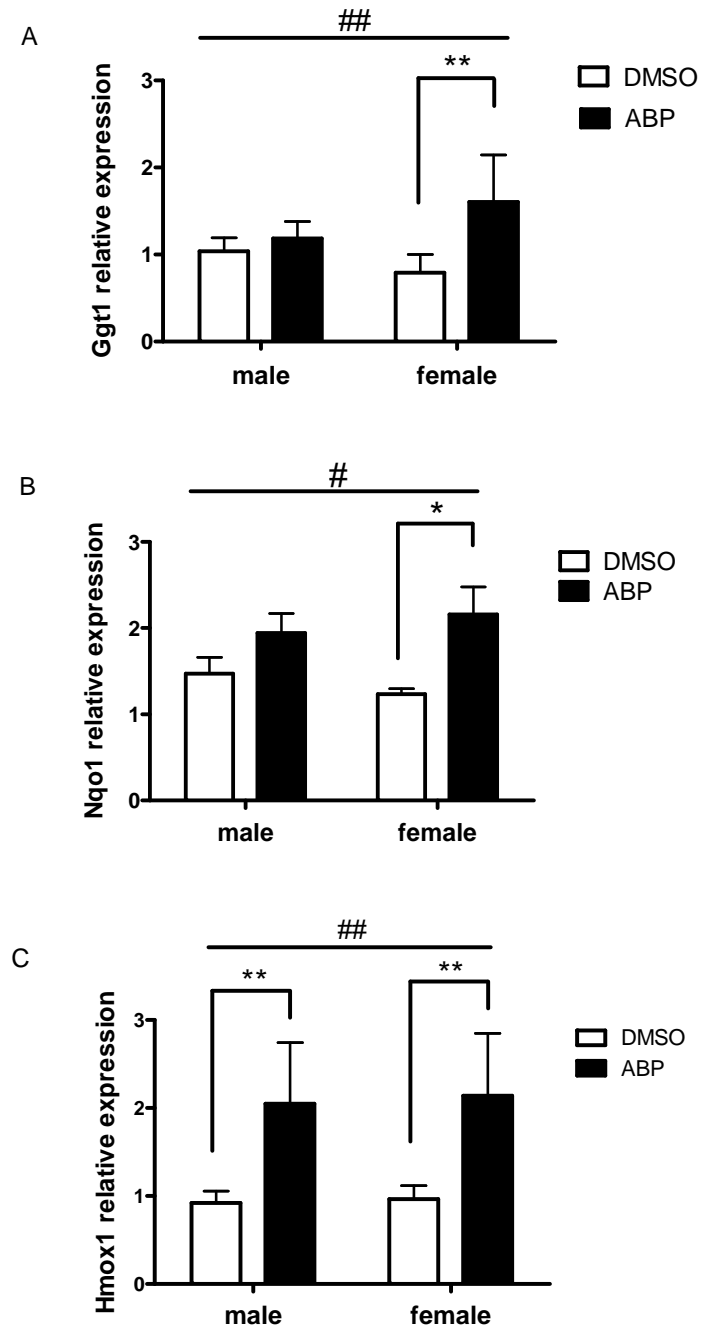


Figure 40. Expression of oxidative stress-inducible antioxidant genes in livers of male and female mice exposed to tumorigenic doses of ABP.

Mice (N=6 per group) were injected with vehicle or 1200 nmol of ABP on postnatal days 8 and 15. QPCR was used to quantify levels of *Ggt1* (A), *Nqo1* (B), and *Hmox1* (C) gene expressions in C57BL/6 male and female mouse livers at 24 hours following day 15 dose of ABP or DMSO vehicle. Error bars represent standard deviations of the mean, which was first normalized to *Gapdh* and then normalized to a single DMSO vehicle-treated control. (* $P < 0.05$ and ** $P < 0.001$. # $P < 0.01$ and ## $P < 0.001$ for the effect of ABP).

ABP induced significant increases in all three genes: *Ggt1* ($P < 0.001$), *Nqo1* ($P < 0.01$), and *Hmox1* ($P < 0.001$), as revealed by two-way ANOVA analyses (Figure 40). Interestingly, for two of the three genes, *Ggt1* and *Nqo1*, Bonferroni post-tests revealed a significant sex difference such that induction by ABP was only significant in females but not in males, demonstrating a female preference in the induction of antioxidant genes by tumorigenic doses of ABP (Figure 40).

Chapter 4
GENERAL DISCUSSION

4.1 ABP-induced mutations *in vivo*

ABP has been proposed to exert its carcinogenic effect in the liver through metabolic activation by CYP1A2 and NAT1/2 to generate C8-dG-ABP adducts, which translate into G to T transversions in the genome that can initiate tumor growth by altering the functions of key gene products that control cell survival and proliferation (Section 1.4.3). However, we and others have provided evidence against the involvement of CYP1A2 and NAT1/2 in ABP metabolic activation to form C8-dG-ABP adducts and have also observed no correlation between C8-dG-ABP adducts and liver tumor incidence (Kimura *et al.*, 1999; Sugamori *et al.*, 2012; Tsuneoka *et al.*, 2003). Aside from C8-dG-ABP adducts, ABP has also been shown to produce other types of DNA damage such as *N*-(deoxyadenosin-8-yl)-ABP adducts, *N*-(deoxyguanosin-N2-yl)-ABP adducts, and frameshift mutations among others (Beland and Kadlubar, 1985; Chung *et al.*, 2000). Only DNA damage left unrepaired prior to DNA replication becomes fixed into the genome as mutations, yet essentially nothing is known about the *in vivo* repair efficiency of different types of DNA damage induced by ABP. This leaves the possibility that minor ABP-DNA adducts other than C8-dG-ABP may account for a larger proportion of mutations that in turn lead to sex- and NAT1/2-related differences in liver tumor incidence found in our ABP neonatal bioassay. In studies carried out in this section, we wished to expand our knowledge regarding genotoxic properties of ABP that may contribute to carcinogenesis by investigating the roles of NAT1/2 enzyme function, sex, and age on ABP-induced mutation frequencies and spectra *in vivo* in mouse liver. We quantified *in vivo* mutation frequencies and spectra using a line of transgenic mice, the MutaTMMouse, that harbours multiple copies of a lambda phage gene in its genome that act as mutation “sensors”. We carried out our studies in both neonatal and adult mice in order to correlate to tumor incidence findings in our ABP neonatal bioassay and to compare with previous results generated using adult mice. Finally, we measured both ABP-induced mutation frequencies and mutation spectra in order to provide information regarding both overall mutational load and types of DNA lesions that may have led to these mutations.

ABP administration following the postnatal exposure protocol that we used to induce tumors in our previous neonatal bioassay led to a significant dose-dependent increase in mutation frequencies in neonatal mouse liver, confirming the ability for ABP to generate mutations using

this tumor-inducing protocol (Figure 11, (Sugamori *et al.*, 2012)). However, these mutation frequencies do not correlate with levels of C8-dG-ABP adducts that we measured using the same ABP exposure protocol, where *Nat1/2(-/-)* mice demonstrated significantly higher C8-dG-ABP adducts compared to wild-type mice (Sugamori *et al.*, 2012). This lack of correlation suggests that C8-dG-ABP adducts may not be the main DNA lesion induced by ABP in mouse liver that translates into mutations, and that other types of DNA lesions may account for a larger proportion of ABP-induced mutations *in vivo*. Our data add to accumulating evidence against a rate-determining role for C8-dG-ABP adducts in ABP carcinogenesis (Sugamori *et al.*, 2012). Moreover, the lack of any sex- or NAT-dependent differences in ABP-induced mutation frequencies in neonatally exposed mice suggest that differences in ABP-induced mutations may not be directly responsible for the observed sex and NAT-dependent differences in tumor incidence in our ABP neonatal bioassay.

Similar to neonates, ABP administration to adults also led to a dose-dependent increase in mutation frequencies (Figure 12). However, absolute mutation frequencies tended to be lower in adults than in neonates, especially at the lower ABP dose, despite much greater total ABP exposures (20,000–40,000 nmol vs. 600–1,200 nmol). This confirms previous findings that neonatally exposed mice are much more sensitive to the mutagenic effects of ABP, presumably because the increased rate of cell proliferation in developing liver enhances the likelihood of fixation of mutations before DNA repair can occur (Chen *et al.*, 2005). Unlike in neonates where no sex differences were observed, adult females demonstrated significantly higher levels of ABP-induced mutation frequencies than males. Increased mutation frequencies in females seems to correlate with our previous observation of higher C8-dG-ABP adducts in adult female mice and suggest that, unlike in neonates, C8-dG-ABP adducts may be responsible for ABP-induced mutations in adults (Sugamori *et al.*, 2012).

Previous studies to investigate the mutagenicity of ABP in mice had observed an increase in G to T transversions following ABP exposure that was attributed to the formation of C8-dG-ABP adducts (Chen *et al.*, 2005). In this section using the MutaTMMouse assay we have also measured ABP-induced mutation spectra in livers of both neonatal and adult mice. Following the postnatal ABP exposure protocol, we observed a significant increase in the proportion of G to T transversions in wild-type mice, similar to observations made by others (Table 4). However, no

sex differences were observed with wild-type mice, and in *Nat1/2(-/-)* mice males demonstrated a similar increase in the proportion of G to T transversions compared to wild-type mice, but females demonstrated a significant decrease. These observations are inconsistent with patterns observed in C8-dG-ABP adducts induced by ABP following a similar postnatal dosing protocol described previously, where *Nat1/2(-/-)* mice demonstrated significantly higher C8-dG-ABP adducts compared to wild-type mice for both sexes (Sugamori *et al.*, 2012). Although the reason behind this lack of correlation is unclear, our mutation spectra results are consistent with our mutation frequency results and suggest that ABP-induced G to T transversions in neonatal mouse liver result from sources of DNA damage other than C8-dG-ABP adducts. One alternative source of G to T transversions is the major oxidative DNA lesion, 8-oxo-deoxyguanosine (Shibutani *et al.*, 1991). Given suggested links between ABP and oxidative stress (Sections 1.4.5 and 3.3), the possibility that ABP induces G to T transversions in neonatal mouse liver via formation of 8-oxo-deoxyguanosine remains to be investigated. Another interesting observation from our neonatal mutation spectra study is the apparent decrease in G to T transversions following tumorigenic doses of ABP found only in female *Nat1/2(-/-)* mice, whereas significant increases in G to T transversions were found with all other groups of mice. These results suggest a potentially synergistic effect between the female sex and NAT1/2 deficiency, acting on a common molecular pathway in protecting against ABP-induced G to T transversions. In support of our mutation frequency results, overall levels of G to T transversions do not demonstrate the same sex and strain differences as those found with liver tumor incidence following tumorigenic doses of ABP used in our neonatal bioassay.

As with mutation frequencies, ABP-induced mutation spectra in adults were distinct from those in neonates, with the most prominent difference being a lack of increase in G to T transversions in all groups of adult mice (Table 5). In fact, no single type of mutation predominated in ABP-treated adult mouse livers, which suggests a broader spectrum of DNA lesions induced by ABP in adults than in neonates. Increased mutation frequencies in adult females, then, likely reflect a general increase in different types of DNA lesions in female compared to male adult livers following ABP exposure. This is supported by a non-significant trend towards higher liver C8-dG-ABP adducts in ABP-treated adult females compared to males (Sugamori *et al.*, 2012). In addition, despite a relatively small number of sequenced mutations (30-40 mutant plaques) per

strain, sex, and treatment group, our results are consistent with a previous study by another group, where ABP induced G to T mutations in neonatal but not adult mouse livers (Chen *et al.*, 2005).

Overall, our mutation data demonstrated different mutagenic responses to ABP between adults and neonates, where a single type of mutation (G to T transversions) predominated in neonates regardless of sex but multiple types of mutations appeared in adults that preferably target females. Striking age-related differences in the mutagenicity of ABP were unexpected, since enzymes involved in the metabolic activation and detoxification of ABP demonstrated no major developmental differences (Cui *et al.*, 2012), and suggested age-related differences in biological processes not involving drug metabolism as a source for age-related differences in mutations. One such biological process is DNA repair. As mentioned previously, essentially nothing is known regarding the repair of ABP-induced DNA lesions *in vivo*. Since DNA repair controls the extent to which DNA lesions convert into permanent mutations, age-related differences in DNA repair may translate into age-related differences in ABP-induced mutations observed in our studies. For example, another group has observed defective repair of 8-oxo-deoxyguanosine in neonatal mouse livers, which may explain the predominance of G to T transversions in neonatal but not adult mouse livers (Sejersted *et al.*, 2009). Alternatively, age-related differences in the mutagenicity of ABP observed in our studies may be due to the use of different dosing regimens between neonatal and adult mice, but it is unclear how prolonged ABP exposure in adults leads to a completely different mutation profile.

The finding that female mice were not protected from ABP-induced mutation frequencies and G to T transversions is in stark contrast to the tumor protective effects observed with females in our ABP neonatal bioassay (Sugamori *et al.*, 2012). Our mutation results are in line with the lack of correlation observed between C8-dG-ABP adducts and liver tumors, and suggest that sex differences in ABP-induced liver tumors do not stem from differences in ABP-DNA adduct and base-pair mutations induced by ABP. In turn, our results would support the existence of a novel factor in our ABP neonatal bioassay that is ultimately responsible for sex differences observed in tumor incidence. The importance of this finding is twofold. First of all, ABP is a prototypical member of the aromatic amine chemical family, which represents a major class of both human and rodent carcinogens that are believed to exert their carcinogenic effects solely through DNA-

adductation mechanisms; to the contrary, our results clearly indicate the involvement of a novel mechanism(s) in ABP carcinogenesis that may apply to other members of this important chemical family as well. Secondly, since human liver cancer demonstrates the same female protection as that observed in our ABP neonatal bioassay, our results suggest that the same novel mechanism(s) may also underlie sex differences in human liver cancer.

Even though our work supports the involvement of a novel mechanism(s) in ABP-induced liver carcinogenesis, the identity of this mechanism remains elusive. Given established links between ABP and oxidative stress, and a potential involvement of 8-oxo-deoxyguanosine in ABP-induced G to T transversions, oxidative stress represents one such novel mechanism that may influence ABP carcinogenesis in our neonatal bioassay. In a different model of chemically-induced liver carcinogenesis in mice, the structurally unrelated carcinogen diethylnitrosamine induced a similar sex difference in mouse liver carcinogenesis through the modulation of inflammatory pathways that may also be involved in ABP carcinogenesis (Naugler *et al.*, 2007). In the same diethylnitrosamine tumor model, transcription factors FOXA1 and FOXA2 were found to control sex differences in liver carcinogenesis through regulation of genes involved in cellular proliferation and drug metabolism, representing additional mechanisms that may influence ABP carcinogenesis (Li *et al.*, 2012). In subsequent sections we have investigated both the metabolism and oxidative properties of ABP in the neonatal mouse liver, through which we hope to provide evidence for or against the involvement of these mechanisms in our ABP neonatal bioassay.

The lack of protective effects observed with *Nat1/2(-/-)* mice from ABP-induced mutation frequencies and G to T transversions also failed to correlate with tumor-protective effect of NAT deficiency in our ABP neonatal bioassay (Sugamori *et al.*, 2012). However, our findings are again in line with the previously observed lack of correlation between C8-dG-ABP adducts and tumor incidence in *Nat1/2(-/-)* mice. Together our results suggest that the NAT proteins could play key roles in tumor development that are entirely independent of their ability to bioactivate or detoxify carcinogens, since *Nat1/2(-/-)* mice are significantly protected from liver tumor growth in the absence of any evidence so far for reduced DNA damage or mutations (Sugamori *et al.*, 2012). This would be consistent with a number of recent studies demonstrating that human NAT1 is over-expressed in tumors of the breast and other tissues, that increasing NAT1 expression in cultured transformed cells enhances their growth, survival, and resistance to

cytotoxic agents, and that inhibition of NAT1 expression leads to contact inhibition of cell growth and decreased tissue invasion potential (Butcher and Minchin, 2012). However, it is also possible that decreased NAT-mediated ABP metabolic activation in *Nat1/2(-/-)* mice is compensated for by other metabolic activation pathways, such as *O*-sulfation or *O*-glucuronidation, which can also lead to reactive nitrenium ion formation. The potential contributions of *O*-sulfation and *O*-glucuronidation to the metabolic activation of ABP in our neonatal bioassay remain to be investigated.

Another possibility that is not addressed in our studies is the potential involvement of mutation “hotspots” in our ABP neonatal bioassay. It remains possible that ABP produces mutations in key tumor suppressor and/or oncogene hotspots in mouse liver, without affecting overall mutation frequencies and spectra, that in turn lead to the sex and strain differences observed in our neonatal bioassay. The best-studied mutation hotspot in chemical carcinogenesis is codon 61 of *Hras*, which has proven to be a decisive player in the two-step DMBA skin carcinogenesis model described in Section 1.1.3.1 and represents a major target of ABP in B6C3F₁ and CD-1 mice. It is possible that ABP produces mutations in codon 61 of *Hras* that in turn drive liver carcinogenesis in our neonatal bioassay and that female and *Nat1/2(-/-)* mice are somehow protected from mutations at this hotspot, which in turn protects them from liver carcinogenesis. However, Parsons *et al.* detected much lower levels of mutations in codon 61 of *Hras* in ABP-treated C57BL/6 mice, which represents the genetic background of mice used in our neonatal bioassay, compared to B6C3F₁ mice, making mutations in *Hras* an unlikely driver of the sex- and NAT1/2-dependent differences in ABP carcinogenesis found in our tumor model (Parsons *et al.*, 2005). Nevertheless, it remains possible that ABP acts on other, yet uncharacterized mutation hotspots within oncogenes and/or tumor suppressors that in turn drive liver carcinogenesis, a possibility that cannot be addressed in our studies.

Strain differences in ABP-induced *Hras* mutations also highlight a potential shortcoming of our studies presented in this section, namely, the potential effect of strain differences on our mutation results. Our previous tumor study was performed in wild-type and *Nat1/2(-/-)* mice on an inbred C57BL/6 genetic background, while mice used in our mutation study consist of a mixed C57BL/6 x BALB/c x DBA/2 background (Sugamori *et al.*, 2012). Although strain differences in multiple factors that contribute to ABP mutagenicity are possible, we see comparable levels of

NAT enzyme activity between C57BL/6 mice and our wild-type MutaTMMouse strains, and no sex difference in activity (data not shown). In addition, as mentioned previously, strain differences are more likely to affect chronic processes such as tumor promotion and progression, which evoke a larger number of biological determinants, compared to acute events such as DNA damage and mutagenesis measured in our studies.

Finally, our mutation results are vulnerable to issues commonly associated with mutation assays based on the use of transgenic animals. For example, it is unclear whether the same repair efficiency of ABP-induced DNA damage applies to the *cII* transgene, which is not transcribed in mouse liver, compared to the rest of the genome. As described previously, DNA repair may affect both mutation frequencies and spectra measured in our studies. In future studies we could investigate the effect of DNA repair on ABP-induced DNA damage and mutations *in vivo*, which can be done through the use of genetically modified mice deficient in various DNA repair enzymes. Another potential drawback of the MutaTMMouse assay is that only mutations that affect the function of the *cII* transgene are detected, which may favour the detection of certain types of mutations over others. However, this is not supported by our results, where a variety of different mutations were detected that were distributed throughout the *cII* gene (data not shown).

Overall, the discrepancies that we observed between neonates and adults and between acute damage/mutation studies and tumor induction experiments seem to suggest the importance of age- and sex-related factors, but not NAT-related differences, in the genotoxic and mutagenic actions of ABP, while NAT differences clearly influence liver tumor incidence. In addition, they suggest that short-term and *in vitro* studies on ABP-induced DNA damage and mutation that have been carried out in either neonatal or adult mice must be interpreted and extrapolated with caution as predictors of tumor risk. And finally, our data support the notion that DNA damage is necessary but neither sufficient nor rate-determining for eventual tumor growth, and that a novel mechanism(s) is likely involved in ABP carcinogenesis that drives the sex and strain differences observed in our ABP neonatal bioassay.

4.2 ABP metabolic activation by cytochrome P450s

In a traditional model of ABP-induced liver carcinogenesis, the *N*-hydroxylation of ABP represents the first of a two-step metabolic activation process that leads to the formation of

reactive ABP nitrenium ions that bind to DNA, form ABP-DNA adducts, and initiate liver carcinogenesis (see Section 1.4.3 for details). The *N*-hydroxylation of ABP is also necessary for the production of oxidative stress, at least in an *in vitro* setting (Murata *et al.*, 2001). Previous studies using mainly human liver microsomes had suggested CYP1A2 as the key enzyme responsible for carrying out the *N*-hydroxylation of aromatic amines such as ABP (Butler *et al.*, 1989a; Butler *et al.*, 1989b). As a result, studies on aromatic amine carcinogenesis in rodents have often assumed a critical role for CYP1A2 in the metabolic activation and carcinogenicity of aromatic amines including ABP. Surprisingly, however, mice deficient in CYP1A2 demonstrated significant ABP *N*-hydroxylation activity *in vitro* and formed similar levels of ABP-DNA adducts and liver tumors as wild-type mice (Kimura *et al.*, 1999). These findings cast doubt on the involvement of CYP1A2 in the *N*-hydroxylation of ABP and suggest the presence of an alternative ABP *N*-hydroxylation enzyme(s) in mouse liver. Given the importance of the ABP *N*-hydroxylation reaction in mediating all known toxic effects of ABP, our goal in this section was to identify the major ABP *N*-hydroxylation enzyme(s) in postnatal day 15 mouse liver microsomes, which represents the age when most ABP exposure occurs in our neonatal bioassay.

We began our investigations by testing whether CYP1A2 is involved in the *N*-hydroxylation of ABP by neonatal mouse liver microsomes. We compared ABP *N*-hydroxylation activity between liver microsomes isolated from wild-type and *Cyp1a2*(*-/-*) mice. At a concentration of 200 μ M ABP, which represents the expected *in vivo* plasma ABP concentration following a tumorigenic dose of ABP based on our previous pharmacokinetic studies (Sugamori *et al.*, 2006), we detected significantly lower ABP *N*-hydroxylation activity in *Cyp1a2*(*-/-*) compared to wild-type males (~34%); however, no significant differences were observed between wild-type and *Cyp1a2*(*-/-*) females (Figure 13). Our results are comparable to those generated by Kimura *et al.* where they observed a 44% decrease in ABP *N*-hydroxylation activity with *Cyp1a2*(*-/-*) mice. However, a lack of information regarding the sex of the mice used in their study precludes further comparisons (Kimura *et al.*, 1999). To rule out the possibility that an alternative ABP *N*-hydroxylation enzyme with lower affinity for ABP compared to CYP1A2 contributes to ABP *N*-hydroxylation only in the absence of CYP1A2, we carried out detailed enzyme kinetic studies with both wild-type and *Cyp1a2*(*-/-*) mouse liver microsomes (Figure 14). Non-linear regression analyses combined with Eadie-Hofstee transformations of enzyme kinetics data revealed similar

affinities toward ABP between wild-type and *Cyp1a2(-/-)* mouse liver microsomes, indicating that the alternative ABP *N*-hydroxylation enzyme has a similar affinity for ABP as CYP1A2 (Table 6 and Figure 15). In addition, a significantly lower V_{\max} was detected with *Cyp1a2(-/-)* compared to wild-type mice in males but not in females, supporting our previous observations at 200 μ M ABP (Table 6). Overall our studies with *Cyp1a2(-/-)* mice strongly support the existence of a major ABP *N*-hydroxylation enzyme(s) in neonatal mouse liver, especially in females, that is not CYP1A2 but has similar affinity towards ABP as CYP1A2.

Subsequent studies aimed to uncover the identity of this alternative ABP *N*-hydroxylation enzyme in neonatal mouse liver. We carried out pilot studies using liver microsomes from *Cyp1a2(-/-)* mice in order to focus on non-CYP1A2 enzymes. Since cytochrome P450s are often implicated in the metabolism of xenobiotics such as aromatic amines and our *in vitro* ABP *N*-hydroxylation assay is designed to detect cytochrome P450 activity, we began with the assumption that the alternative ABP *N*-hydroxylation enzyme belongs to the cytochrome P450 enzyme superfamily. This assumption was validated by the observation that a general inhibitor of cytochrome P450s, ABT, completely inhibited ABP *N*-hydroxylation activity in *Cyp1a2(-/-)* mouse liver microsomes (Figure 16). Even though ABT is often used as a non-selective mechanism-based inhibitor of cytochrome P450, and is used in our studies as such, its inhibitory activity has been shown to vary between different cytochrome P450s. For example, under similar conditions as those used in our study, ABT inhibited human CYP2A6 and CYP3A4 activities by >98% but only inhibited human CYP2C9 activity by 42% in human liver microsomes (Linder *et al.*, 2009). On the one hand these studies instilled caution in the interpretation of our ABT results; on the other hand they provided information with regard to the identity of the alternative ABP *N*-hydroxylation enzyme in neonatal mouse liver microsomes (i.e. not likely to be a mouse orthologue of CYP2C9).

One of the first hints that CYP2E1 may be involved in the *N*-hydroxylation of ABP came from the observed inhibitory effects of solvents on ABP *N*-hydroxylation activity by *Cyp1a2(-/-)* mouse liver microsomes. We found that several solvents including DMSO were potent inhibitors of ABP *N*-hydroxylation activity, whereas acetonitrile was a clear exception with no inhibitory effect at concentrations as high as 1% v/v (Figure 17). Since a number of small solvent molecules are known inhibitors of CYP2E1 with the notable exception being acetonitrile

(Hickman *et al.*, 1998), these results suggested the potential involvement of CYP2E1 in the *N*-hydroxylation of ABP. In the next experiment we tested the effect of the CYP2E1-selective substrate pNP on ABP *N*-hydroxylation activity by *Cyp1a2*(*-/-*) mouse liver microsomes. Human microsomal CYP2E1 has an apparent K_m for pNP of 30 μ M (Tassaneeyakul *et al.*, 1993). In one study, pNP competitively inhibited CYP2E1 enzyme activity measured by the hydroxylation of chlorzoxazone, another CYP2E1-selective substrate (Tassaneeyakul *et al.*, 1993). In our studies, pNP dose-dependently inhibited ABP *N*-hydroxylation activity, achieving almost complete inhibition at high pNP concentrations (Figure 18A). We then established the pNP hydroxylation assay that is often used as a reaction phenotyping assay for CYP2E1 enzyme activity, and found that ABP dose-dependently inhibited pNP hydroxylation, similarly reaching almost complete inhibition at high ABP concentrations (Figure 18B). Mutual inhibition between pNP and ABP on their respective oxidation reactions, like those observed between pNP and chlorzoxazone, strongly implicates the presence of an enzyme that acts on both substrates, and this enzyme is likely to be CYP2E1 based on its well-documented selectivity for pNP.

We also carried out an *in vivo* induction study using the CYP2E1 inducer pyrazole. In this study, we treated both male and female postnatal day 15 *Cyp1a2*(*-/-*) mice *in vivo* with pyrazole using a dosing regimen shown to induce CYP2E1 activity in mouse liver, and tested for an increase in ABP *N*-hydroxylation activity compared to vehicle-treated controls. We observed a significant but modest increase (~24%) in ABP *N*-hydroxylation by male but not female mouse liver microsomes (Figure 19). It is unclear why sex differences exist in the effect of pyrazole on ABP *N*-hydroxylation activity, but the selective use of male rodents in previous studies by others suggest perhaps increased inducibility of CYP2E1 in male mice (Gong *et al.*, 2003; Lu and Cederbaum, 2006). Overall a modest induction of ABP *N*-hydroxylation was generated with pyrazole treatment in our study, whereas a similar treatment in adult male mice led to a twofold induction of CYP2E1 enzyme activity in a previous study (Lu and Cederbaum, 2006). Observed differences in the effect of pyrazole between our study and others may be attributed to age-related differences in the inducibility of CYP2E1. Alternatively, pyrazole may have induced ABP *N*-hydroxylation through mechanisms not related to CYP2E1. In fact, the lack of specificity is a common issue with the use of pharmacological tools, where a single chemical entity may

affect the activity of several different enzymes simultaneously. As an example, pyrazole can induce CYP2A5 in addition to CYP2E1 (Lu and Cederbaum, 2006).

To overcome this lack of specificity with pharmacological tools and to provide conclusive evidence in support of CYP2E1 as a major ABP *N*-hydroxylation enzyme in mouse liver, we turned to the use of *Cyp2e1(-/-)* mice.

We first compared the level of ABP *N*-hydroxylation activity between wild-type and *Cyp2e1(-/-)* mice at a single concentration of 200 μ M ABP. Unlike in our studies using *Cyp1a2(-/-)* mice where a modest but significant decrease in ABP *N*-hydroxylation activity was only observed in males, we found significantly decreased ABP *N*-hydroxylation activity in both male and female *Cyp2e1(-/-)* mice compared to wild-type controls (44 and 61% respectively, Figure 20). Subsequent enzyme kinetic studies revealed significantly decreased V_{\max} values in both male and female *Cyp2e1(-/-)* mice compared to wild-type mice, confirming our observations at 200 μ M ABP (Table 7). On the other hand, similar K_m values between wild-type and *Cyp2e1(-/-)* mice and linear Eadie-Hofstee plots are complementary to the results generated using *Cyp1a2(-/-)* mice, which together support the involvement of CYP2E1 as an alternative ABP *N*-hydroxylation enzyme in mouse liver with a similar affinity for ABP as CYP1A2 (Table 7 and Figure 22).

Together our studies with *Cyp1a2(-/-)* and *Cyp2e1(-/-)* mice support the involvement of CYP2E1 in the *N*-hydroxylation of ABP by both male and female neonatal mouse liver microsomes but the involvement of CYP1A2 only in males. At the predicted concentration of ABP achieved following tumorigenic doses of ABP in our neonatal bioassay, CYP1A2 and CYP2E1 together account for ~78% of total ABP *N*-hydroxylation activity in male neonatal mouse liver microsomes and CYP2E1 alone accounts for 61% of total ABP *N*-hydroxylation activity in female neonatal mouse liver microsomes. Even though the majority of ABP *N*-hydroxylation activity has been accounted for with CYP2E1 and CYP1A2, significant ABP *N*-hydroxylation activity remains in the neonatal mouse liver that may be attributed to yet other cytochrome P450s. One cytochrome P450 that may represent a minor ABP *N*-hydroxylation enzyme in mouse liver is CYP2A5. Mouse CYP2A5 is a liver homologue of human CYP2A13, which is expressed in human bladder. In a recent study, recombinant human CYP2A13 demonstrated

significant ABP *N*-hydroxylation activity *in vitro* (Nakajima *et al.*, 2006). In a pilot study, we found that selective substrates of CYP2A5, nicotine and cotinine, failed to inhibit ABP *N*-hydroxylation activity by *Cyp1a2*(-/-) mouse liver microsomes (data not shown). Even though our preliminary results do not support CYP2A5 as a major ABP *N*-hydroxylation enzyme in neonatal mouse liver microsomes, our study may have lacked sensitivity for the detection of minor ABP *N*-hydroxylation enzymes. With our identification of CYP2E1 as a major ABP *N*-hydroxylation enzyme in mouse liver, future chemical inhibition studies in search of minor ABP *N*-hydroxylation enzymes can be carried out using liver microsomes isolated from mice deficient in both CYP2E1 and CYP1A2 for improved sensitivity. In addition, ABP *N*-hydroxylation activity attributed to CYP1A2 and CYP2E1 may be even higher as other enzymes may have partially compensated for CYP1A2/CYP2E1 activity in knockout mice, which would suggest even less activity attributable to minor ABP *N*-hydroxylation enzymes.

Our evidence for CYP2E1 as a major ABP *N*-hydroxylation enzyme in mouse liver described thus far arose mainly from the inhibition of ABP *N*-hydroxylation activity *in vitro* using a combination of pharmacological and genetic tools. In subsequent studies, we performed "gain-of-function" experiments using transiently transfected mouse hepatoma cells to test whether the recombinant expression of CYP1A2 or CYP2E1 leads to the *N*-hydroxylation of ABP in a physiological cell culture system. Using a live-cell assay, we detected HOABP production (indicative of ABP *N*-hydroxylation activity) by ABP-treated Hepa1c1c7 cells transfected with either *Cyp1a2* or *Cyp2e1* but not from untransfected cells (Figure 23 and Figure 24). The lack of ABP *N*-hydroxylation activity in untransfected Hepa1c1c7 cells is consistent with the well-known loss of phase I enzymes, such as cytochrome P450s, in liver cells cultured *ex vivo* (for detailed discussion see Appendix B). In accordance with this phenomenon, CYP1A2 and CYP2E1 enzyme activities, measured in culture using phenacetin *O*-deethylation and pNP hydroxylation live-cell assays, respectively, were undetectable in Hepa1c1c7 cells (Appendix A). A rough comparison between levels of ABP *N*-hydroxylation activity in transfected cells to those found in mouse liver using isolated microsomes revealed ~16- and ~60-fold lower ABP *N*-hydroxylation activities in *Cyp1a2*- and *Cyp2e1*-transfected Hepa1c1c7 cells, respectively, compared to mouse liver (Figure 25). This is in line with dramatically lower levels of CYP1A2- and CYP2E1 enzyme activities in microsomes isolated from transfected cells compared to mouse

liver (Appendix figure 3). Overall, our results with Hepa1c1c7 cells demonstrated that despite dramatically reduced enzyme activities compared to mouse liver, both recombinantly-expressed CYP1A2 and CYP2E1 can *N*-hydroxylate ABP in live cells.

To our knowledge, these results are the first to propose CYP2E1 as a major ABP *N*-hydroxylation enzyme in mouse liver. In fact, very few enzymes other than CYP1A2 have been implicated in the metabolism of aromatic amines in general. Since a significant body of work from both our laboratory and others investigating the metabolism of aromatic amines such as ABP have been carried out using adult mice, in future studies we would like to extend our findings and test whether CYP2E1 also represents a major ABP *N*-hydroxylation enzyme in adult mouse liver (Sugamori *et al.*, 2012; Tsuneoka *et al.*, 2003). This can be done by comparing *in vitro* ABP *N*-hydroxylation activity between liver microsomes isolated from adult wild-type or *Cyp2e1(-/-)* mice, as we have done in this section using neonatal mice. In addition, we would like to carry out pharmacokinetic studies using adult wild-type and *Cyp2e1(-/-)* mice to investigate a potential involvement of CYP2E1 in the metabolism and clearance of ABP *in vivo*. If CYP2E1 also represents a major ABP *N*-hydroxylation enzyme in adult mouse liver, then the obvious question one would ask next is whether CYP2E1 is involved in the metabolism of ABP in humans. From a chemistry point of view, a high level of sequence homology between human and mouse CYP2E1 (79.4% DNA and 78.1% protein sequence identity) and a strong overlap in substrate profile support the possibility that CYP2E1 is an ABP *N*-hydroxylation enzyme in humans as well as mice. However, given well-established large inter-individual variations in CYP1A2 expression in humans as a result of varying environmental exposure to CYP1A inducers, the involvement of CYP2E1 in ABP *N*-hydroxylation may be highly variable. Support for this is provided by a pilot study carried out in our laboratory, where liver microsomes from adult mice treated with the CYP1A2 inducer beta-naphthoflavone had greater than 10-fold higher ABP *N*-hydroxylation activity than untreated mice, making contributions from other enzymes irrelevant in inducer-treated mice (data not shown).

Previously in our ABP neonatal bioassay we observed striking sex differences in ABP-induced liver tumors with complete protection observed in females (Sugamori *et al.*, 2012). However, no sex differences were observed in ABP *N*-hydroxylation activity between male and female neonatal mouse liver microsomes (Figure 13). This observation rules out sex differences in

overall ABP *N*-hydroxylation activity as the basis for sex differences observed in our ABP neonatal bioassay, and it is consistent with the lack of sex differences in levels of C8-dG-ABP adducts following tumorigenic doses of ABP, which is presumably a consequence of ABP metabolic activation (Sugamori *et al.*, 2012). On the other hand, sex differences clearly exist in the activities of enzymes that *N*-hydroxylate ABP in neonatal mouse liver microsomes, such that both CYP1A2 and CYP2E1 were involved in the metabolism of ABP in male mice but only CYP2E1 was involved in female mice. It is unclear how the involvement of different cytochrome P450s in the *N*-hydroxylation of ABP may contribute to differences in tumor outcome but some plausible mechanisms will be described in Section 4.3.

A potential shortcoming of our studies is the use of mice from different genetic backgrounds for our ABP metabolism studies. Specifically, the *Cyp1a2*(*-/-*) mice were on a C57BL/6 background whereas the *Cyp2e1*(*-/-*) mice were on a SVJ129 and C57BL/6 mixed-strain background. Using established phenotyping reactions for CYP1A2 and CYP2E1 (phenacetin *O*-deethylation and pNP hydroxylation respectively), Löfgren *et al.* directly compared levels of enzyme activity between C57BL/6 and SVJ129 adult mice. No major strain differences were found in CYP1A2 and CYP2E1 enzyme activities in their study, as SVJ129 mice demonstrated 86% and 142% of CYP1A2 and CYP2E1 enzyme activities, respectively, compared to C57BL/6 mice (Löfgren *et al.*, 2004). Since our mixed-strain mice used for *Cyp2e1*(*-/-*) studies represented F₂ mice from a cross between SVJ129 and C57BL/6, we would expect even smaller differences in CYP1A2 and CYP2E1 enzyme activities between our mixed-strain and C57BL/6 mice. In addition, the similar levels of ABP *N*-hydroxylation activity we detected between our mixed-strain and C57BL/6 mice would also support similar ABP metabolism between these mice. How strain differences may affect minor ABP *N*-hydroxylation enzymes in mouse liver is not known but is not likely to influence the interpretation of our results due to their limited contributions to overall ABP *N*-hydroxylation activity. This being said, we are currently backcrossing *Cyp2e1*(*-/-*) mice onto a C57BL/6 background in order to completely eliminate strain differences as a potential confounding factor in our future studies using *Cyp2e1*(*-/-*) mice. The use of congenic mice will be especially important for an ABP neonatal bioassay with *Cyp2e1*(*-/-*) mice, as many more factors are involved in the process of carcinogenesis and each may be susceptible to strain differences.

The role of CYP1A2 in the *N*-hydroxylation of aromatic amines has been an important and unique feature in the prevailing model of aromatic amine bioactivation and carcinogenesis described in Section 1.2.4, where it constitutes the first of a two-step metabolic activation paradigm that leads to the formation of ultimate carcinogens. However, the link between metabolic activation of aromatic amines by CYP1A2 and carcinogenesis *in vivo* has been largely assumed, since most supporting evidence was generated *in vitro* using microsomal preparations or recombinantly expressed enzymes. In a seminal paper by Kimura *et al.*, *Cyp1a2(-/-)* mice demonstrated significant ABP *N*-hydroxylation activity and no protection from ABP-induced liver tumors in a neonatal bioassay, questioning the primary role of CYP1A2 in metabolic activation and carcinogenesis of ABP *in vivo*. In this section, we have confirmed the results from the Kimura study by demonstrating that the majority of ABP *N*-hydroxylation activity remained in *Cyp1a2(-/-)* neonatal mouse liver microsomes. In addition, we have shown that CYP2E1 represents a major ABP *N*-hydroxylation enzyme in neonatal mouse liver. Given our current findings, future studies should investigate the influence of CYP2E1 on ABP carcinogenesis through the use of *Cyp2e1(-/-)* mice in a similar ABP neonatal bioassay as was used for *Cyp1a2(-/-)* mice (Kimura *et al.*, 1999). The availability of the *Cyp2e1(-/-)* mouse model and our work in this section establishing CYP2E1 as a major metabolic activation enzyme for ABP provide an opportunity to generate evidence for or against the role of metabolic activation in aromatic amine carcinogenesis in an *in vivo* setting. A tumor protective effect observed in *Cyp2e1(-/-)* mice would establish CYP2E1 and the ABP *N*-hydroxylation reaction as rate-determining steps in ABP-induced carcinogenesis *in vivo*. Similar studies can be conducted using mice that are deficient in both CYP1A2 and CYP2E1 (i.e. by crossing *Cyp1a2(-/-)* mice with *Cyp2e1(-/-)* mice), which may lead to even more dramatic tumor protective effects.

4.3 ABP-induced oxidative stress in cell culture and *in vivo*

Previous studies from both our laboratory and others using male and female mice deficient in key ABP metabolic activation enzymes had revealed a surprising lack of correlation between the DNA-damaging effects and the liver tumorigenicity of ABP in a neonatal bioassay (Kimura *et al.*, 1999; Sugamori *et al.*, 2012; Wang *et al.*, 2012). From these studies we concluded that despite the well-established genotoxic effects of ABP, a previously unrecognized novel factor(s) must play a critical role in ABP carcinogenesis. Given the close association of oxidative stress

with human liver cancer, its ability to drive mouse liver carcinogenesis, and recent evidence linking oxidative stress to ABP, we investigated the potential involvement of oxidative stress as a novel driver of ABP carcinogenesis in our ABP neonatal bioassay.

In the first part of our studies, we investigated whether ABP produced oxidative stress in a cell culture system. Using a mouse hepatoma cell line, Hep1c1c7, we found that ABP failed to produce oxidative stress both in forms of oxidative DNA damage and reactive oxygen species under a variety of different experimental conditions (Figure 26 and Figure 29). On the other hand, the major *in vivo* metabolite of ABP, HOABP, was a potent inducer of oxidative stress, producing 5- to 10-fold increases over vehicle-treated controls in both oxidative DNA damage and reactive oxygen species at concentrations as low as 10 μM , which could be completely blocked with antioxidants (Figure 27, Figure 28, and Figure 29). Our results are consistent with previous *in vitro* studies carried out by other laboratories, and together they support HOABP but not ABP as a potent inducer of oxidative stress (Makena and Chung, 2007; Murata *et al.*, 2001). In addition, the lack of oxidative stress detected with ABP in Hep1c1c7 cells supports our previous observation from Section 3.2.3 that these cells lack key metabolic enzymes for the *N*-hydroxylation of ABP. However, our results are in contrast to results generated by another group, where ABP produced significant oxidative DNA damage in a human hepatoma cell line, HepG2 (Wang *et al.*, 2006). This discrepancy may be attributed to the use of different cell lines and/or cell culture conditions. Previously we observed that HepG2 cells possess slightly higher drug metabolizing capabilities, both in terms of basal and inducible CYP1A2 enzyme activities, than Hep1c1c7 cells (Appendix B). Increased ABP metabolism in the presence of high ABP concentrations (up to 500 μM) and long incubation times (up to 24 hours) used in their study together may have led to greater production of HOABP that in turn induced a modest increase in oxidative DNA damage (Wang *et al.*, 2006). In addition, exposing cells to high concentrations of ABP for extended periods of time may have led to significant cell death and associated DNA damage that is unrelated to the oxidative effects of ABP, a phenomenon that has been observed in our laboratory (unpublished observations).

Our cell culture results thus far suggest that the exposure of Hep1c1c7 cells to an exogenous source of HOABP leads to oxidative stress. To confirm that the same is true for endogenously produced HOABP, we tested ABP's ability to generate oxidative stress in Hep1c1c7 cells

transiently transfected with CYP1A2 or CYP2E1, which are the ABP *N*-hydroxylation enzymes that we identified in Section 3.2. Since a higher level of ABP *N*-hydroxylation activity was detected in CYP1A2- compared to CYP2E1-expressing Hepa1c1c7 cells, we initially expected ABP to produce a higher level of oxidative stress in CYP1A2-expressing cells. To our surprise, ABP produced oxidative stress only in CYP2E1- but not in CYP1A2-expressing Hepa1c1c7 cells (Figure 30). To rule out potentially confounding variables associated with our transfection system, additional experiments showed that oxidative stress produced by ABP in CYP2E1-expressing Hepa1c1c7 cells could be inhibited with CYP2E1 substrates and is thus dependent on CYP2E1 enzyme activity (Figure 33). Again, co-treatment with NAC completely blocked ABP-induced reactive oxygen species in CYP2E1-expressing Hepa1c1c7 cells (Figure 33). On the other hand, pretreatment with NAC failed to block ABP-induced reactive oxygen species in CYP2E1-expressing cells (Figure 33). This result supports the direct involvement of NAC as an antioxidant in our cell culture system, rather than an indirect effect via increasing the synthesis of glutathione. Together our results suggest that while the *N*-hydroxylation of ABP by both CYP1A2 and CYP2E1 leads to HOABP production, only the *N*-hydroxylation of ABP by CYP2E1 leads to oxidative stress in a cell culture setting.

One possible explanation for detecting ABP-induced oxidative stress with CYP2E1- but not CYP1A2-expressing cells lies within the recent discovery of mitochondria as a major localization site for CYP2E1, accounting for 10~40% of total CYP2E1 expression (Bansal *et al.*, 2010; Bansal *et al.*, 2013). As described in Section 1.2.5, the *N*-hydroxy metabolite of the aromatic amine 2-acetylaminofluorene (*N*-hydroxyfluorene) produces reactive oxygen species *in vivo* with help from complex I of the electron transport chain located on the inner mitochondrial membrane, which provides a source of NADH and O₂ that serve as cofactors in redox cycling reactions of *N*-hydroxyfluorene *in vitro* (Klöhn *et al.*, 1998; Klöhn and Neumann, 1997; Klöhn *et al.*, 2003). Given shared *in vitro* redox cycling mechanisms between HOABP and *N*-hydroxyfluorene, the *N*-hydroxylation of ABP by mitochondrial CYP2E1 may have resulted in HOABP production in the vicinity of the electron transport chain, leading to heightened reactive oxygen species production and oxidative stress. We briefly tested this possibility by comparing the ability of ABP to produce oxidative stress in Hepa1c1c7 cells transfected with different rat CYP2E1 variants that target differentially between mitochondria and endoplasmic reticulum. We

found that the level of reactive oxygen species produced by ABP was directly proportional to the extent of mitochondrial localization by rat CYP2E1 (Figure 34). For example, ABP produced the highest level of reactive oxygen species in Hepa1c1c7 cells transfected with the most mitochondrial targeting rat CYP2E1 construct (MT⁺⁺), despite this construct showing the lowest level of rat CYP2E1 expression and activity following transfection (Figure 34, Appendix figure 7). A similar trend was observed with ABP-induced oxidative DNA damage in Hepa1c1c7 cells expressing different rat CYP2E1 variants, but the differences failed to reach statistical significance (Figure 34). Overall, however, our observations are consistent with the involvement of mitochondrial CYP2E1 in the production of oxidative stress by ABP, and they warrant further experimentation using mouse CYP2E1 constructs that target differentially between the endoplasmic reticulum and mitochondria in Hepa1c1c7 cells.

Thus far our cell culture results support HOABP, a major *in vivo* metabolite of ABP, as a potent inducer of oxidative stress. Next, we tested whether tumorigenic doses of ABP, i.e. those given in our ABP neonatal bioassay, induce significant oxidative stress *in vivo* in neonatal mouse livers, and whether sex differences exist. We focused on sex differences in order to correlate to our tumor results and draw relevance to human liver cancer, which demonstrates a similar sex difference in incidence. Since essentially nothing is known regarding ABP's ability to produce oxidative stress in neonatal mouse livers, we first carried out a time-course study and measured levels of oxidative DNA damage as a biomarker of oxidative stress in male and female neonatal livers at various acute time-points following tumorigenic doses of ABP. In this experiment, we found significantly increased oxidative DNA damage in males at 7 and 24 hours following tumorigenic doses of ABP. On the other hand, no significant increase was detected in females at any of the time points tested (Figure 35). Using GSSG as an alternative measure of oxidative stress, we detected a non-significant increase in males and a non-significant initial decrease in females following tumorigenic doses of ABP (Figure 36). When compared together, significant overall sex differences were detected such that ABP-treated males demonstrated significantly higher levels of GSSG compared to females at 7 hours following tumorigenic doses of ABP (Figure 36). In contrast to GSSG, levels of total GSH did not change with ABP treatment, which might be due to a much higher basal level of GSH in the neonatal mouse liver, making relative changes in total GSH a less sensitive measure of oxidative stress. Taken together, our results

point to higher levels of liver oxidative stress in neonatal males compared to females following tumorigenic doses of ABP, sex differences that seem to correlate with those observed in our neonatal bioassay, where tumorigenic doses of ABP produced liver tumors in males but not females at one year (Sugamori *et al.*, 2012).

As described in Section 1.4.5, studies from the Nebert laboratory were the first to quantify the oxidative effects of ABP in mouse liver. In their studies, a 10 mg/kg dose of ABP dissolved in acetone applied to the dorsal skin of C57BL/6 adult mice led to significantly depleted hepatic thiols, in the forms of GSH and cysteine, in male but not female livers at 2 hours following exposure, which indicate a similar sex difference as those observed in our studies. However, ABP's ability to deplete levels of GSH shown in their studies was not observed in our studies. Several factors such as differences in age of animal and route of administration may explain the observed discrepancies. In our studies we observed a greater resistance against acute ABP toxicity in neonates compared to adults, which may be attributed to increased levels of endogenous protective factors (such as hepatic thiols), increased clearance of ABP, or decreased metabolic activation of ABP in neonates. A higher basal level or faster regeneration of hepatic thiols in neonates compared to adults may result in lower levels of oxidative stress and GSH depletion in neonates. This is also supported by increased tolerance of neonatal mice to a number of other chemicals with known oxidative properties, such as acetaminophen and carbon tetrachloride, compared to adults (D. Hanna, unpublished observations). Age differences in ABP metabolism may also contribute to the protective effects observed in neonates, but this is not supported by our observation of similar ABP *N*-hydroxylation activity between neonates and adults (data not shown). Compared to differences in age at exposure, it is less clear how differences in route of ABP administration may have led to observed differences in oxidative stress. However, different routes of ABP administration may have resulted in slightly different time-courses for measured levels of oxidative stress, as peak differences occurred at 2 hours following ABP exposure in the Nebert study but at 7 hours in our study (not measured in the Nebert studies).

The failure to detect significant changes in some measures of oxidative stress (i.e. total GSH) may result from the relatively low levels of oxidative stress detected in neonatal mouse livers (maximum ~twofold) in our ABP studies. This led to our use of γ H2AX as a sensitive biomarker

of oxidative DNA damage. In mammalian cells, the histone variant H2AX becomes phosphorylated in the vicinity of DNA strand breaks, which may result from the attack by reactive oxygen species on the DNA phosphate backbone, to form γ H2AX and initiates a cascade of DNA damage signaling responses. The sensitivity of this assay is derived from the fact that a number of H2AX molecules become phosphorylated for each break in DNA, effectively amplifying the DNA damage signal. However, DNA strand breaks may also arise from non-oxidative stress related events, which represent one potential drawback of the γ H2AX assay. For example, the collapse of the DNA replication fork when it encounters bulky DNA adducts (such as C8-dG-ABP) during DNA replication may also lead to the formation of DNA strand breaks and γ H2AX. We believe this is not likely to be the case in our studies because our γ H2AX data do not correlate with levels of C8-dG-ABP adducts or with mutations. Additionally, we have detected significant γ H2AX at time-points as short as 30 minutes in Hepa1c1c7 cells (data not shown) and 7 hours in mouse liver following ABP exposure, which we believe is not enough time for DNA replication fork to travel through a significant section of the genome within a significant number of actively replicating cells .

The detection of oxidative stress in our tumor model provides some indirect support for 8-oxo-deoxyguanosine as a source of G to T transversions detected in Section 3.1.3. However, the lack of oxidative stress in females is inconsistent with patterns of G to T transversions in similarly treated animals. In future studies we can measure levels of 8-oxo-deoxyguanosine in neonatal mouse livers treated with tumorigenic doses of ABP in order to provide direct evidence for or against 8-oxo-deoxyguanosine as the source of G to T transversions in our tumor model. The protective effect observed in female *Nat1/2(-/-)* mice from G to T transversions suggests the presence of a common underlying mechanism behind the sex and strain differences observed in our ABP neonatal bioassay. Although it is unclear how NAT1/2 deficiency may affect levels of oxidative stress in mouse liver, it will be very tempting to test oxidative stress as a unifying mechanism that leads to both sex and strain differences observed in our ABP neonatal bioassay.

To test for the potential influence of ABP *N*-hydroxylation enzymes on ABP-induced oxidative stress *in vivo*, we have measured levels of γ H2AX in livers of *Cyp2e1(-/-)* and *Cyp1a2(-/-)* mice (Figure 37). Compared to the corresponding *Cyp2e1(+/+)* mice, where a significant increase in

γ H2AX is found in males but not females, *Cyp2e1*(-/-) mice demonstrated no significant increase in γ H2AX (Figure 37). On the other hand, *Cyp1a2*(-/-) males demonstrated a similar increase in γ H2AX as the corresponding wild-type C57BL/6 males (Figure 38). These results are consistent with our cell culture findings and together support the involvement of CYP2E1, but not CYP1A2, in the production of oxidative stress following tumorigenic doses of ABP. In all strains of mice tested, females were protected from ABP-induced γ H2AX, suggesting that sex differences observed with C57BL/6 mice are conserved across different strains of mice. This observation also provides justification for our use of mice from different genetic backgrounds to study the acute toxic effects of ABP.

Since the antioxidant response represents a major determinant of oxidative stress, in parallel studies we investigated the potential effect of ABP on the NRF2 response in male and female neonatal mouse livers, following the same neonatal exposure protocol used in our tumor assay. We focused our investigations on the transcription factor NRF2 because it represents a master regulator of cellular antioxidant defense as described in Section 1.1.5.3. Tumorigenic doses of ABP significantly induced nuclear levels of the NRF2 protein in both male and female neonatal livers compared to vehicle-treated controls (Figure 39). Interestingly, a higher NRF2 induction was found in females compared to males (Figure 39). In addition to nuclear levels of NRF2, we also measured the expression of three antioxidant genes (*Ggt1*, *Nqo1*, and *Hmox1*) that are regulated at least in part by NRF2, and we found significant induction of all three genes in neonatal livers following tumorigenic doses of ABP (Figure 40). A detailed analysis revealed significant induction in female but not male livers for *Ggt1* and *Nqo1*, and no sex differences for *Hmox1* (Figure 40). Since a female preference was observed for both NRF2 and NRF2-regulated genes, our studies suggest that increased NRF2 activation led to greater upregulation of certain NRF2-regulated genes in female than in male livers. However, given the lack of sex difference found with *Hmox1* induction, it is likely that other transcription factors also contribute to the induction of genes measured in our studies. For example, the transcription factor Activator Protein-1 (AP-1) is often up-regulated under conditions of oxidative stress and has also been suggested to regulate *Hmox1* (Dalton *et al.*, 1999). Overall, our results suggest a stronger antioxidant response in females than in males, as measured using NRF2 and NRF2-regulated antioxidant genes, that may protect female neonates against liver oxidative stress induced by

ABP. Furthermore, this protective effect observed in females against oxidative stress induced by ABP seems to correlate with their subsequent protection against liver carcinogenesis in our neonatal bioassay (Sugamori *et al.*, 2012).

There are at least two mechanisms by which ABP may activate NRF2. In one mechanism, ABP may indirectly activate NRF2 by producing oxidative stress. Under conditions of oxidative stress, thiol groups on key cysteine residues of KEAP1 become oxidized, which leads to conformational changes in KEAP1 and the release of NRF2. As described in Section 1.1.5.3, the release from KEAP1 prevents NRF2 degradation and results in NRF2 translocation to the nucleus and transcriptional activation. In a second mechanism, ABP or its reactive metabolites may directly activate NRF2 through covalent modification of key cysteine residues on KEAP1, again leading to the release and activation of NRF2. A direct interaction between ABP (or its more reactive metabolites) and KEAP1 represents an intriguing possibility that to our knowledge has not been investigated for any aromatic amine. In our studies, a strong NRF2 response in female neonatal livers in the absence of detectable oxidative stress seems to provide some support for the second mechanism, although alternative explanations clearly cannot be ruled out. To uncover the mechanism behind the ABP-induced NRF2 response, in future experiments we can test the effect of antioxidant co-administration on ABP-induced NRF2 signaling in female neonatal livers. If antioxidants prevent NRF2 induction, then ABP likely induces NRF2 through oxidative stress; on the other hand, if antioxidants do not prevent NRF2 induction, this would support a previously uncharacterized, direct interaction between ABP and NRF2 that leads to NRF2 activation. Chemical inducers of NRF2 that have been shown to bind to KEAP1 and may have profound implications for our studies are the major *in vivo* metabolites of estrogen, 2- and 4-hydroxyestradiol (Wang *et al.*, 2010). A higher level of estrogen metabolites in female livers may disrupt binding between NRF2 and KEAP1 that in turn leads to a higher level of activated NRF2 in females in our ABP neonatal bioassay. This can be easily tested in Hepa1c1c7 cells, where NRF2 is both expressed and inducible (Nguyen *et al.*, 2010). If estrogen potentiates NRF2 activation, then co-administration of ABP with estrogen metabolites should lead to higher NRF2 activation than ABP alone.

The sex differences in oxidative stress and antioxidant response shown in this section represent the first time that toxic and protective cellular responses induced by tumorigenic doses of ABP

demonstrated the same sex differences as those observed in our ABP neonatal bioassay. Based on our results, we propose that tumorigenic doses of ABP produce oxidative stress in male neonatal mouse livers that in turn drive liver carcinogenesis, while in females a stronger antioxidant response centered on NRF2 induction by ABP protects them from liver oxidative stress and subsequent carcinogenesis. However, correlation does not equate to causation, and additional experiments are needed in order to more directly establish oxidative stress as a causal factor in ABP carcinogenesis. This can be done through the administration of antioxidants, such as NAC or vitamin E, to neonatal mice exposed to tumorigenic doses of ABP to see whether this protects males from ABP-induced liver carcinogenesis. Similarly, the administration of established NRF2 inducers, such as oltipraz or sulforaphane, prior to ABP exposure and the use of *Keap1*(-/-) mice would be expected to block ABP-induced liver carcinogenesis in males based on our proposed mechanisms. In another line of studies, we can repeat our ABP neonatal bioassay with NRF2 deficient mice to see whether females become susceptible to ABP-induced liver carcinogenesis.

The establishment of oxidative stress as a driving force behind the sex differences in ABP-induced liver carcinogenesis could have profound clinical implications, since the same mechanism may underlie human liver cancer, which exhibits a similar sexual dimorphism in incidence. Exploration of downstream signaling pathways affected by oxidative stress in male mice in our mouse model may reveal novel drug targets for the prevention and/or treatment of human liver cancer. For example, one signaling pathway affected by oxidative stress is the MAPK pathway, which is frequently mutated in human liver cancer (Section 1.3.2). Oxidation of critical cysteine residues within the active site of MAPK phosphatase by reactive oxygen species has been shown to inhibit MAPK phosphatase activity, which leads to a hyper-activation of MAPK signaling that may result in inhibition of cell death, excessive cell proliferation, and liver carcinogenesis (Kamata *et al.*, 2005). It is possible that ABP induces an oxidative environment in males that leads to hyper-activation of the MAPK pathway, which in turn drives liver tumor formation selectively in male mouse livers. If this is true, then our tumor model may serve as a simple animal model for screening MAPK inhibitors for their ability to prevent or treat liver cancer. Furthermore, the detection of significantly induced γ H2AX in our ABP tumor model opens up interesting research avenues since γ H2AX represents an upstream signaling molecule

that leads to the activation of p53, the most commonly mutated tumor suppressor in human liver cancer. As described previously, p53 regulates multiple genes involved in different cellular pathways such as DNA repair, cell cycle arrest and apoptosis, all of which may impact liver carcinogenesis in our tumor model. An understanding of how p53 may be involved in our ABP neonatal bioassay may in turn contribute to our understanding of p53's involvement in human liver cancer. In addition, if higher NRF2 inducibility in females compared to males indeed confers protection against ABP-induced carcinogenesis, additional experiments could test whether this may represent a generalized phenomenon that is shared across different chemical carcinogens and animal species. If so, this may lead to the design of chemoprevention trials to test the effect of established NRF2 inducers in prevention against liver cancer in high risk populations, such as males with high levels of exposure to chemical carcinogens (i.e. aflatoxin B1, cigarette smoke, and alcohol). Similarly, an understanding of the mechanisms behind sex differences in NRF2 inducibility may also lead to the discovery of novel chemopreventive agents.

Our current results support oxidative stress as a novel factor that may contribute to ABP carcinogenesis in mouse liver, ultimately leading to the sex differences that are observed in liver tumor incidence in this species. Even though previous studies from other laboratories have reported oxidative properties of ABP both *in vitro* and *in vivo*, we believe our results provide the strongest evidence to date that links redox effects of ABP to its carcinogenicity. Thus far, two of the best-studied aromatic amines, 2-acetylaminofluorene and ABP, are both found to exert non-DNA adduct-related effects in rodent liver through the production of oxidative stress. Furthermore, mitochondria have been implicated in the production of oxidative stress by both 2-acetylaminofluorene and ABP (Klöhn *et al.*, 1998; Klöhn *et al.*, 1995; Klöhn *et al.*, 1996). It will be very interesting to test whether CYP2E1 can also metabolically activate 2-acetylaminofluorene *in vitro* and whether metabolic activation of 2-acetylaminofluorene by mitochondrial CYP2E1 leads to oxidative stress in our cell culture system. Ultimately, we may wish to test whether the metabolic activation of both ABP and 2-acetylaminofluorene by mitochondrial CYP2E1 leads to oxidative stress *in vivo*, and the extent to which this mechanism contributes to liver carcinogenesis. To test this, we can generate transgenic mouse lines with targeted mutations in the localization sequence of *Cyp2e1* that result in different levels of

CYP2E1 expression in mitochondria versus endoplasmic reticulum, as was done in culture with the rat *Cyp2e1* expression plasmids, and compare levels of oxidative stress and carcinogenicity between these mouse lines following exposure to ABP and 2-acetylaminofluorene. A positive correlation between levels of mitochondrial CYP2E1 expression, oxidative stress, and carcinogenicity in these mice would support central roles for metabolic activation by mitochondrial CYP2E1 and oxidative stress in ABP and 2-acetylaminofluorene carcinogenesis. Since 2-acetylaminofluorene and ABP represent two of the best-studied aromatic amines, it is possible that mitochondrion-based metabolic activation and associated oxidative stress represent a novel, unifying feature of aromatic amines in general that contributes to their carcinogenicity in humans.

4.4 Overall conclusions and significance

The overall goal of my PhD project was to gain a better understanding of the tumorigenic mechanisms behind ABP-induced liver carcinogenesis in mice. In a neonatal bioassay carried out previously in our laboratory using ABP, female mice and male *Nat1/2(-/-)* mice demonstrated significant protection against ABP-induced liver tumors. In the first part of our investigations, we measured ABP-induced mutations in mouse liver and correlated them to liver tumor incidence observed in our neonatal bioassay. A lack of correlation between ABP-induced mutations and liver tumor incidence is consistent with previous observations from our laboratory where the major ABP-DNA adduct, C8-dG-ABP, also failed to correlate with liver tumor incidence. Together these results support the presence of a novel factor that is capable of influencing ABP carcinogenicity in mouse liver. Our mutation study is now published (Wang *et al.*, 2012). In subsequent studies using mouse liver microsomes we have established CYP2E1 as a novel enzyme that is involved in the metabolic activation of ABP alongside CYP1A2. In addition, we found that the *N*-hydroxylation of ABP by CYP2E1, but not CYP1A2, leads to the production of oxidative stress both in cell culture and *in vivo*. Finally, we detected a higher level of liver oxidative stress in males and a stronger antioxidant response mediated by NRF2 in females in response to tumorigenic doses of ABP. These findings represent the first time that measures of toxicity correlate with liver tumor incidence in our tumor model and together support oxidative stress as a novel contributor to ABP carcinogenesis. Since a similar sex difference is found in human liver cancer, our results suggest that oxidative stress-related

mechanisms may also underlie the male susceptibility/female protection found in this human disease. In addition, our results expand our current knowledge of non-genotoxic mechanisms involved in chemical carcinogenesis, which have received relatively little attention compared to well-established genotoxic mechanisms and may represent a "missing link" between chemical exposure and "spontaneous" cases of human cancer.

References

- Adams WT and Skopek TR. 1987. Statistical test for the comparison of samples from mutational spectra. *Journal of Molecular Biology* 194(3):391-6.
- Aguilar F, Hussain SP, Cerutti P. 1993. Aflatoxin B1 induces the transversion of G-->T in codon 249 of the p53 tumor suppressor gene in human hepatocytes. *Proceedings of the National Academy of Sciences* 90(18):8586-90.
- Aldaz CM, Conti CJ, Klein-Szanto AJ, Slaga TJ. 1987. Progressive dysplasia and aneuploidy are hallmarks of mouse skin papillomas: Relevance to malignancy. *Proceedings of the National Academy of Sciences* 84(7):2029-32.
- Altekruse SF, McGlynn KA, Reichman ME. 2009. Hepatocellular carcinoma incidence, mortality, and survival trends in the united states from 1975 to 2005. *Journal of Clinical Oncology* 27(9):1485-91.
- Alter MJ. 2007. Epidemiology of hepatitis C virus infection. *World Journal of Gastroenterology* 13(17):2436-41.
- Ames BN, Durston WE, Yamasaki E, Lee FD. 1973. Carcinogens are mutagens: A simple test system combining liver homogenates for activation and bacteria for detection. *Proceedings of the National Academy of Sciences* 70(8):2281-5.
- Ames BN, Gurney EG, Miller JA, Bartsch H. 1972. Carcinogens as frameshift mutagens: Metabolites and derivatives of 2-acetylaminofluorene and other aromatic amine carcinogens. *Proceedings of the National Academy of Sciences* 69(11):3128-32.
- Anisimov VN, Ukraintseva SV, Yashin AI. 2005. Cancer in rodents: Does it tell us about cancer in humans? *Nature Reviews Cancer* 5(10):807-19.
- Aravalli R, Cressman EK, Steer C. 2013. Cellular and molecular mechanisms of hepatocellular carcinoma: An update. *Archives of Toxicology* 87(2):227-47.
- Arbuthnot P and Kew M. 2001. Hepatitis B virus and hepatocellular carcinoma. *International Journal of Experimental Pathology* 82(2):77-100.
- Arias IM. 2009. *The liver: Biology and pathobiology*. 5th ed. Hoboken, NJ: John Wiley & Sons.
- Bailleul B, Surani MA, White S, Barton SC, Brown K, Blessing M, Jorcano J, Balmain A. 1990. Skin hyperkeratosis and papilloma formation in transgenic mice expressing a ras oncogene from a suprabasal keratin promoter. *Cell* 62(4):697-708.
- Balmain A and Pragnell IB. 1983. Mouse skin carcinomas induced in vivo by chemical carcinogens have a transforming harvey-ras oncogene. *Nature* 303(5912):72-4.
- Balmain A, Ramsden M, Bowden GT, Smith J. 1984. Activation of the mouse cellular harvey-ras gene in chemically induced benign skin papillomas. *Nature* 307(5952):658-60.

- Bansal S, Anandatheerthavarada HK, Prabu GK, Milne GL, Martin MV, Guengerich FP, Avadhani NG. 2013. Human cytochrome P450 2E1 mutations that alter mitochondrial targeting efficiency and susceptibility to ethanol-induced toxicity in cellular models. *Journal of Biological Chemistry* 288(18):12627-44.
- Bansal S, Liu C, Sepuri NBV, Anandatheerthavarada HK, Selvaraj V, Hoek J, Milne GL, Guengerich FP, Avadhani NG. 2010. Mitochondria-targeted cytochrome P450 2E1 induces oxidative damage and augments alcohol-mediated oxidative stress. *Journal of Biological Chemistry* 285(32):24609-19.
- Bauer KH. 1928. *Mutations theorie der geschwulst-entstehung: Übergang von körperzellen in geschwulstzellen durch gen-änderung*. J. Springer.
- Beland FA and Kadlubar FF. 1985. Formation and persistence of arylamine DNA adducts in vivo. *Environmental Health Perspectives* 62:19-30.
- Berenblum I. 1941. The mechanism of carcinogenesis. A study of the significance of cocarcinogenic action and related phenomena. *Cancer Research* 1(10):807-14.
- Besaratinia A, Bates SE, Pfeifer GP. 2002. Mutational signature of the proximate bladder carcinogen N-hydroxy-4-acetylamino-biphenyl. *Cancer Research* 62(15):4331-8.
- Bilodeau J and Mirault M. 1999. Increased resistance of GPx-1 transgenic mice to tumor promoter-induced loss of glutathione peroxidase activity in skin. *International Journal of Cancer* 80(6):863-7.
- Bonicke R and Reif W. 1953. Enzymatic inactivation of isonicotinic acid hydrazide in human and animal organism. *Naunyn-Schmiedebergs Archiv Fur Experimentelle Pathologie Und Pharmakologie* 220(4):321-3.
- Bonilla Guerrero R and Roberts LR. 2005. The role of hepatitis B virus integrations in the pathogenesis of human hepatocellular carcinoma. *Journal of Hepatology* 42(5):760-77.
- Bosch FX, Ribes J, Díaz M, Cléries R. 2004. Primary liver cancer: Worldwide incidence and trends. *Gastroenterology* 127(5, Supplement 1):S5-S16.
- Boutwell RK. 1964. Some biological aspects of skin carcinogenesis. *Progress in Experimental Tumor Research* 4:207-50.
- Boveri T. 1929. *The origin of malignant tumors*. Baltimore: Waverly Press.
- Boveri T. 2008. *Concerning the origin of malignant tumours by theodor boveri*. translated and annotated by henry harris. *Journal of Cell Science* 121(Supplement 1):1-84.
- Boyd JA and Eling TE. 1984. Evidence for a one-electron mechanism of 2-aminofluorene oxidation by prostaglandin H synthase and horseradish peroxidase. *Journal of Biological Chemistry* 259(22):13885-96.

- Boyd JA, Harvan DJ, Eling TE. 1983. The oxidation of 2-aminofluorene by prostaglandin endoperoxide synthetase. comparison with other peroxidases. *Journal of Biological Chemistry* 258(13):8246-54.
- Bremner DA and Tange JD. 1966. Renal and neoplastic lesions after injection of N-n1-diacetylbenzidine. *Archives of Pathology* 81(2):146-51.
- Bressac B, Kew M, Wands J, Ozturk M. 1991. Selective G to T mutations of p53 gene in hepatocellular carcinoma from southern africa. *Nature* 350(6317):429-31.
- Brookes P and Lawley PD. 1964. Evidence for the binding of polynuclear aromatic hydrocarbons to the nucleic acids of mouse skin : Relation between carcinogenic power of hydrocarbons and their binding to deoxyribonucleic acid. *Nature* 202(4934):781-4.
- Brown K, Buchmann A, Balmain A. 1990. Carcinogen-induced mutations in the mouse c-ha-ras gene provide evidence of multiple pathways for tumor progression. *Proceedings of the National Academy of Sciences* 87(2):538-42.
- Busuttill RA, Garcia AM, Cabrera C, Rodriguez A, Suh Y, Kim WH, Huang T, Vijg J. 2005. Organ-specific increase in mutation accumulation and apoptosis rate in CuZn-superoxide dismutase deficient mice. *Cancer Research* 65(24):11271-5.
- Butcher NJ and Minchin RF. 2012. Arylamine N-acetyltransferase 1: A novel drug target in cancer development. *Pharmacological Reviews* 64(1):147-65.
- Buters JTM, Tang BK, Pineau T, Gelboin HV, Kimura S, Gonzalez FJ. 1996. Role of CYP1A2 in caffeine pharmacokinetics and metabolism: Studies using mice deficient in CYP1A2. *Pharmacogenetics* 6(4):291-6.
- Butler MA, Iwasaki M, Guengerich FP, Kadlubar FF. 1989a. Human cytochrome P-450PA (P-450IA2), the phenacetin O-deethylase, is primarily responsible for the hepatic 3-demethylation of caffeine and N-oxidation of carcinogenic arylamines. *Proceedings of the National Academy of Sciences* 86(20):7696-700.
- Butler MA, Guengerich FP, Kadlubar FF. 1989b. Metabolic oxidation of the carcinogens 4-aminobiphenyl and 4,4'-methylenebis(2-chloroaniline) by human hepatic microsomes and by purified rat hepatic cytochrome P-450 monooxygenases. *Cancer Research* 49(1):25-31.
- Caldwell SH, Crespo DM, Kang HS, Al-Osaimi AMS. 2004. Obesity and hepatocellular carcinoma. *Gastroenterology* 127:S97-S103.
- Cariello NF, Piegorsch WW, Adams WT, Skopek TR. 1994. Computer program for the analysis of mutational spectra: Application to p53 mutations. *Carcinogenesis* 15(10):2281-5.
- Carr BI. 2010. *Hepatocellular carcinoma: Diagnosis and treatment*. 2nd ed. Totowa, N.J.: Humana.

- Cartwright RA, Glashan RW, Rogers HJ, Ahmad RA, Barham-Hall D, Higgins E, Kahn MA. 1982. Role of N-acetyltransferase phenotypes in bladder carcinogenesis: A pharmacogenetic epidemiological approach to bladder cancer. *Lancet* 2(8303):842-5.
- Chan KS, Sano S, Kiguchi K, Anders J, Komazawa N, Takeda J, DiGiovanni J. 2004. Disruption of Stat3 reveals a critical role in both the initiation and the promotion stages of epithelial carcinogenesis. *The Journal of Clinical Investigation* 114(5):720-8.
- Chandrasena RE, Edirisinghe PD, Bolton JL, Thatcher GRJ. 2008. Problematic detoxification of estrogen quinones by NAD(P)H-dependent quinone oxidoreductase and glutathione-S-transferase. *Chemical Research in Toxicology* 21(7):1324-9.
- Chemin I, Ohgaki H, Chisari FV, Wild CP. 1999. Altered expression of hepatic carcinogen metabolizing enzymes with liver injury in HBV transgenic mouse lineages expressing various amounts of hepatitis B surface antigen. *Liver* 19(2):81-7.
- Chen CJ, Yu MW, Liaw YF. 1997. Epidemiological characteristics and risk factors of hepatocellular carcinoma. *Journal of Gastroenterology and Hepatology* 12(9-10):S294-308.
- Chen T, Mittelstaedt RA, Beland FA, Heflich RH, Moore MM, Parsons BL. 2005. 4-aminobiphenyl induces liver DNA adducts in both neonatal and adult mice but induces liver mutations only in neonatal mice. *International Journal of Cancer* 117(2):182-7.
- Chisari FV, Klopchin K, Moriyama T, Pasquinelli C, Dunsford HA, Sell S, Pinkert CA, Brinster RL, Palmiter RD. 1989. Molecular pathogenesis of hepatocellular carcinoma in hepatitis B virus transgenic mice. *Cell* 59(6):1145-56.
- Chou HC, Lang NP, Kadlubar FF. 1995. Metabolic activation of the N-hydroxy derivative of the carcinogen 4-aminobiphenyl by human tissue sulfotransferases. *Carcinogenesis* 16(2):413-7.
- Chung K, Chen S, Wong TY, Li Y, Wei C, Chou MW. 2000. Mutagenicity studies of benzidine and its analogs: Structure-activity relationships. *Toxicological Sciences* 56(2):351-6.
- Clayson D, Lawson T, Pringle J. 1967. The carcinogenic action of 2-aminodiphenylene oxide and 4-aminodiphenyl on the bladder and liver of the C57 X IF mouse. *British Journal of Cancer* 21:755-762.
- Conney AH, Miller EC, Miller JA. 1956. The metabolism of methylated aminoazo dyes: V. evidence for induction of enzyme synthesis in the rat by 3-methylcholanthrene. *Cancer Research* 16(5):450-9.
- Conti CJ, Aldaz CM, O'Connell J, Klein-Szanto AJP, Slaga TJ. 1986. Aneuploidy, an early event in mouse skin tumor development. *Carcinogenesis* 7(11):1845-8.
- Cook JW, Hewett CL, Hieger I. 1933. The isolation of a cancer-producing hydrocarbon from coal tar. parts I, II, and III. *Journal of the Chemical Society (Resumed)* (0):395-405.

- Cramer JW, Miller JA, Miller EC. 1960. N-hydroxylation: A new metabolic reaction observed in the rat with the carcinogen 2-acetylaminofluorene. *Journal of Biological Chemistry* 235(3):885-8.
- Cui JY, Renaud HJ, Klaassen CD. 2012. Ontogeny of novel cytochrome P450 gene isoforms during postnatal liver maturation in mice. *Drug Metabolism and Disposition* 40(6):1226-37.
- Czaja AJ. 2014. Hepatic inflammation and progressive liver fibrosis in chronic liver disease. *World Journal of Gastroenterology* 20(10):2515.
- Dalton TP, Shertzer HG, Puga A. 1999. Regulation of gene expression by reactive oxygen. *Annual Review of Pharmacology and Toxicology* 39(1):67-101.
- Dang LN and McQueen CA. 1999. Mutagenicity of 4-aminobiphenyl and 4-acetylaminobiphenyl in salmonella typhimurium strains expressing different levels of N-acetyltransferase. *Toxicology and Applied Pharmacology* 159(2):77-82.
- David SS, O'Shea VL, Kundu S. 2007. Base-excision repair of oxidative DNA damage. *Nature* 447(7147):941-50.
- DeBaun JR, Rowley JY, Miller EC, Miller JA. 1968. Sulfotransferase activation of N-hydroxy-2-acetylaminofluorene in rodent livers susceptible and resistant to this carcinogen. *Experimental Biology and Medicine* 129(1):268-73.
- DeFrances M. 2010. Molecular mechanisms of hepatocellular carcinoma: Insights to therapy. Carr BI, editor. Humana Press. 130 p.
- Dooley KL, Von Tungeln LS, Bucci T, Fu PP, Kadlubar FF. 1992. Comparative carcinogenicity of 4-aminobiphenyl and the food pyrolysates, glu-P-1, IQ, PhIP, and MeIQx in the neonatal B6C3F1 male mouse. *Cancer Letters* 62(3):205-9.
- Drinkwater NR. 1994. Genetic control of hepatocarcinogenesis in C3H mice. *Drug Metabolism Reviews* 26(1-2):201-8.
- Elchuri S, Oberley TD, Qi W, Eisenstein RS, Jackson Roberts L, Van Remmen H, Epstein CJ, Huang T. 2004. CuZnSOD deficiency leads to persistent and widespread oxidative damage and hepatocarcinogenesis later in life. *Oncogene* 24(3):367-80.
- Estabrook RW. 2003. A passion for P450s (remembrance of the early history of research on cytochrome P450). *Drug Metabolism and Disposition* 31(12):1461-73.
- Estrada-Rodgers L, Levy GN, Weber WW. 1998. Substrate selectivity of mouse N-acetyltransferases 1, 2, and 3 expressed in COS-1 cells. *Drug Metabolism and Disposition* 26(5):502-5.

- Farazi PA, Glickman J, Jiang S, Yu A, Rudolph KL, DePinho RA. 2003. Differential impact of telomere dysfunction on initiation and progression of hepatocellular carcinoma. *Cancer Research* 63(16):5021-7.
- Feng Z, Hu W, Rom WN, Beland FA, Tang M. 2002. N-hydroxy-4-aminobiphenyl-DNA binding in human p53 gene: Sequence preference and the effect of C5 cytosine methylation. *Biochemistry* 41(20):6414-21.
- Ferlay J, Shin H, Bray F, Forman D, Mathers C, Parkin DM. 2010. Estimates of worldwide burden of cancer in 2008: GLOBOCAN 2008. *International Journal of Cancer* 127(12):2893-917.
- Flammang TJ, Tungeln LSV, Kadlubar FF, Fu PP. 1997. Neonatal mouse assay for tumorigenicity: Alternative to the chronic rodent bioassay. *Regulatory Toxicology and Pharmacology* 26(2):230-40.
- Flammang TJ, Couch LH, Levy GN, Weber WW, Wise CK. 1992. DNA adduct levels in congenic rapid and slow acetylator mouse strains following chronic administration of 4-aminobiphenyl. *Carcinogenesis* 13(10):1887-992.
- Fletcher K, Tinwell H, Ashby J. 1998. Mutagenicity of the human bladder carcinogen 4-aminobiphenyl to the bladder of mutaTMMouse transgenic mice. *Mutation Research/Fundamental and Molecular Mechanisms of Mutagenesis* 400(1-2):245-50.
- Foster PL, Eisenstadt E, Miller JH. 1983. Base substitution mutations induced by metabolically activated aflatoxin B1. *Proceedings of the National Academy of Sciences* 80(9):2695-8.
- Foulds L. 1954. The experimental study of tumor progression: A review. *Cancer Research* 14(5):327-39.
- Fretland AJ, Doll MA, Gray K, Feng Y, Hein DW. 1997. Cloning, sequencing, and recombinant expression of NAT1, NAT2, and NAT3 derived from the C3H/HeJ (rapid) and A/HeJ (slow) acetylator inbred mouse: Functional characterization of the activation and deactivation of aromatic amine carcinogens. *Toxicology and Applied Pharmacology* 142(2):360-6.
- Friedman SL. 2008. Mechanisms of hepatic fibrogenesis. *Gastroenterology* 134(6):1655-69.
- Fujii K. 1991. Evaluation of the newborn mouse model for chemical tumorigenesis. *Carcinogenesis* 12(8):1409-15.
- Gaikwad NW, Rogan EG, Cavalieri EL. 2007. Evidence from ESI-MS for NQO1-catalyzed reduction of estrogen ortho-quinones. *Free Radical Biology and Medicine* 43(9):1289-98.
- Geigl JB, Obenauf AC, Schwarzbraun T, Speicher MR. 2008. Defining 'chromosomal instability'. *Trends in Genetics* 24(2):64-9.

- Gillet J, Gottesman MM, Okabe M. 2009. The hepatocyte and the cancer cell: Dr Jekyll and Mr Hyde. John Wiley & Sons, Ltd. 1090 p.
- Gillet LCJ and Scharer OD. 2006. Molecular mechanisms of mammalian global genome nucleotide excision repair. *Chemical Reviews* 106(2):253-76.
- Gong P, Cederbaum AI, Nieto N. 2003. Increased expression of cytochrome P450 2E1 induces heme oxygenase-1 through ERK MAPK pathway. *Journal of Biological Chemistry* 278(32):29693-700.
- Gorrod JW, Carter RL, Roe FJ. 1968. Induction of hepatomas by 4-aminobiphenyl and three of its hydroxylated derivatives administered to newborn mice. *Journal of the National Cancer Institute* 41(2):403-10.
- Gossen JA, de Leeuw WJ, Tan CH, Zwarthoff EC, Berends F, Lohman PH, Knook DL, Vijg J. 1989. Efficient rescue of integrated shuttle vectors from transgenic mice: A model for studying mutations in vivo. *Proceedings of the National Academy of Sciences* 86(20):7971-5.
- Grant DM, Blum M, Beer M, Meyer UA. 1991. Monomorphic and polymorphic human arylamine N-acetyltransferases: A comparison of liver isozymes and expressed products of two cloned genes. *Molecular Pharmacology* 39(2):184-91.
- Grant DM, Hughes NC, Janezic SA, Goodfellow GH, Chen HJ, Gaedigk A, Yu VL, Grewal R. 1997. Human acetyltransferase polymorphisms. *Mutation Research* 376(1-2):61-70.
- Green LC, Skipper PL, Turesky RJ, Bryant MS, Tannenbaum SR. 1984. In vivo dosimetry of 4-aminobiphenyl in rats via a cysteine adduct in hemoglobin. *Cancer Research* 44(10):4254-9.
- Grimmer G, Dettbarn G, Seidel A, Jacob J. 2000. Detection of carcinogenic aromatic amines in the urine of non-smokers. *Science of the Total Environment* 247(1):81-90.
- Gu L, Gonzalez FJ, Kalow W, Tang BK. 1992. Biotransformation of caffeine, paraxanthine, theobromine and theophylline by cDNA-expressed human CYP1A2 and CYP2E1. *Pharmacogenetics* 2(2):73-7.
- Guengerich FP. 1987. Mammalian cytochromes P-450. Boca Raton, FL: CRC Press.
- Hagen TM, Huang S, Curnutte J, Fowler P, Martinez V, Wehr CM, Ames BN, Chisari FV. 1994. Extensive oxidative DNA damage in hepatocytes of transgenic mice with chronic active hepatitis destined to develop hepatocellular carcinoma. *Proceedings of the National Academy of Sciences* 91(26):12808-12.
- Hammond S, Sorensen G, Youngstrom R, Ockene JK. 1995. Occupational exposure to environmental tobacco smoke. *The Journal of the American Medical Association* 274(12):956-60.

- Hammons GJ, Guengerich FP, Weis CC, Beland FA, Kadlubar FF. 1985. Metabolic oxidation of carcinogenic arylamines by rat, dog, and human hepatic microsomes and by purified flavin-containing and cytochrome P-450 monooxygenases. *Cancer Research* 45(8):3578-85.
- Hanczko R, Fernandez D, Doherty E, Qian Y, Vas G, Niland B, Telarico T, Garba A, Banerjee S, Middleton F, et al. 2009. Prevention of hepatocarcinogenesis and increased susceptibility to acetaminophen-induced liver failure in transaldolase-deficient mice by N-acetylcysteine. *The Journal of Clinical Investigation* 119(6):1546-57.
- Hanssen HP, Agarwal DP, Goedde HW, Bucher H, Huland H, Brachmann W, Ovenbeck R. 1985. Association of N-acetyltransferase polymorphism and environmental factors with bladder carcinogenesis. study in a north german population. *European Urology* 11(4):263-6.
- Hatting M, Trautwein C, Cubero F. 2009. TAL deficiency, all roads lead to oxidative stress? *Hepatology* 50(3):979-81.
- He G, Yu G, Temkin V, Ogata H, Kuntzen C, Sakurai T, Sieghart W, Peck-Radosavljevic M, Leffert HL, Karin M. 2010. Hepatocyte IKK β /NF- κ B inhibits tumor promotion and progression by preventing oxidative stress-driven STAT3 activation. *Cancer Cell* 17(3):286-97.
- Heddle JA, Martus H, Douglas GR. 2003. Treatment and sampling protocols for transgenic mutation assays. *Environmental and Molecular Mutagenesis* 41(1):1-6.
- Hein DW. 1988. Acetylator genotype and arylamine-induced carcinogenesis. *BBA - Reviews on Cancer* 948(1):37-66.
- Hein DW, Doll MA, Rustan TD, Gray K, Feng Y, Ferguson RJ, Grant DM. 1993. Metabolic activation and deactivation of arylamine carcinogens by recombinant human NAT1 and polymorphic NAT2 acetyltransferases. *Carcinogenesis* 14(8):1633-8.
- Hickman D, Wang J, Wang Y, Unadkat JD. 1998. Evaluation of the selectivity of in vitro probes and suitability of organic solvents for the measurement of human cytochrome P450 monooxygenase activities. *Drug Metabolism and Disposition* 26(3):207-15.
- Hlavica P, Golly I, Lehnerer M, Schulze J. 1997. Primary aromatic amines: Their N-oxidative bioactivation. *Human and Experimental Toxicology* 16(8):441-8.
- Hoffmann D, Djordjevic MV, Hoffmann I. 1997. The changing cigarette. *Preventive Medicine* 26(4):427-34.
- Hollander A. 1984. *Chemical mutagens: Principles and methods for their detection*. Plenum Press.
- Houghton M and Abrignani S. 2005. Prospects for a vaccine against the hepatitis C virus. *Nature* 436(7053):961-6.

- Hsu IC, Metcalf RA, Sun T, Welsh JA, Wang NJ, Harris CC. 1991. Mutational hot spot in the p53 gene in human hepatocellular carcinomas. *Nature* 350(6317):427-8.
- Huang J and Dunford HB. 1991. One-electron oxidative activation of 2-aminofluorene by horseradish peroxidase compounds I and II: Spectral and kinetic studies. *Archives of Biochemistry and Biophysics* 287(2):257-62.
- Hueper WC, Leming MF, Wolfe HD. 1937. Experimental production of bladder tumors in dogs by administration of beta-naphthylamine. *Journal of Industrial Hygiene*: 46.
- Hussain SP, Hofseth LJ, Harris CC. 2003. Radical causes of cancer. *Nature Reviews Cancer* 3(4):276-85.
- Hussain SP, Aguilar F, Amstad P, Cerutti P. 1994. Oxy-radical induced mutagenesis of hotspot codons 248 and 249 of the human p53 gene. *Oncogene* 9(8):2277-81.
- Hussain SP, Raja K, Amstad PA, Sawyer M, Trudel LJ, Wogan GN, Hofseth LJ, Shields PG, Billiar TR, Trautwein C, et al. 2000. Increased p53 mutation load in nontumorous human liver of wilson disease and hemochromatosis: Oxyradical overload diseases. *Proceedings of the National Academy of Sciences* 97(23):12770-5.
- IARC Monographs Working Group. 2012. Aflatoxins. IARC Monographs.
- IARC Monographs Working Group. 2009a. 4-aminobiphenyl. IARC Monographs.
- IARC Monographs Working Group. 2009b. Tobacco smoking. IARC Monographs.
- Ise K, Nakamura K, Nakao K, Shimizu S, Harada H, Ichise T, Miyoshi J, Gondo Y, Ishikawa T, Aiba A, et al. 2000. Targeted deletion of the H-ras gene decreases tumor formation in mouse skin carcinogenesis. *Oncogene* 19(26):2951-6.
- Jackson SP and Bartek J. 2009. The DNA-damage response in human biology and disease. *Nature* 461(7267):1071-8.
- Jaiswal AK, Nebert DW, McBride OW, Gonzalez FJ. 1987. Human P(3)450: CDNA and complete protein sequence, repetitive alu sequences in the 3' nontranslated region, and localization of gene to chromosome 15. *Journal of Experimental Pathology* 3(1):1-17.
- Jia L, Wei Wang X, Harris CC. 1999. Hepatitis B virus X protein inhibits nucleotide excision repair. *International Journal of Cancer* 80(6):875-9.
- Jungst C, Cheng B, Gehrke R, Schmitz V, Nischalke H, Ramakers J, Schramel P, Schirmacher P, Sauerbruch T, Caselmann W. 2004. Oxidative damage is increased in human liver tissue adjacent to hepatocellular carcinoma. *Hepatology* 39(6):1663-72.
- Kahl GF, Friederici DE, Bigelow SW, Okey AB, Nebert DW. 1980. Ontogenetic expression of regulatory and structural gene products associated with the ah locus. comparison of rat,

- mouse, rabbit and sigmodon hispedis. *Developmental Pharmacology and Therapeutics* 1(2-3):137-62.
- Kamata H, Honda S, Maeda S, Chang L, Hirata H, Karin M. 2005. Reactive oxygen species promote TNF alpha-induced death and sustained JNK activation by inhibiting MAP kinase phosphatases. *Cell* 120(5):649-61.
- Kang Y and Massagué J. 2004. Epithelial-mesenchymal transitions: Twist in development and metastasis. *Cell* 118(3):277-9.
- Keller W. 1842. On the conversion of benzoic acid into hippuric acid. *Provincial Medical Journal and Retrospect of the Medical Sciences* 4(13):256-7.
- Kensler TW, Wakabayashi N, Biswal S. 2007. Cell survival responses to environmental stresses via the Keap1-Nrf2-ARE pathway. *Annual Review of Pharmacology and Toxicology* 47(1):89-116.
- Kerdar RS, Dehner D, Wild D. 1993. Reactivity and genotoxicity of arylnitrenium ions in bacterial and mammalian cells. *Toxicology Letters* 67(1-3):73-85.
- Kim DJ, Kataoka K, Rao D, Kiguchi K, Cotsarelis G, DiGiovanni J. 2009. Targeted disruption of Stat3 reveals a major role for follicular stem cells in skin tumor initiation. *Cancer Research* 69(19):7587-94.
- Kimura S, Gonzalez FJ, Nebert DW. 1984. Mouse cytochrome P3-450: Complete cDNA and amino acid sequence. *Nucleic Acids Research* 12(6):2917-28.
- Kimura S, Kawabe M, Ward JM, Morishima H, Kadlubar FF, Hammons GJ, Fernandez-Salguero P, Gonzalez FJ. 1999. CYP1A2 is not the primary enzyme responsible for 4-aminobiphenyl-induced hepatocarcinogenesis in mice. *Carcinogenesis* 20(9):1825-30.
- Kimura S, Kawabe M, Yu A, Morishima H, Fernandez-Salguero P, Hammons GJ, Ward JM, Kadlubar FF, Gonzalez FJ. 2003. Carcinogenesis of the food mutagen PhIP in mice is independent of CYP1A2. *Carcinogenesis* 24(3):583-7.
- Klöhn PC, Bitsch A, Neumann HG. 1998. Mitochondrial permeability transition is altered in early stages of carcinogenesis of 2-acetylaminofluorene. *Carcinogenesis* 19(7):1185-90.
- Klöhn PC, Massalha H, Neumann HG. 1995. A metabolite of carcinogenic 2-acetylaminofluorene, 2-nitrosofluorene, induces redox cycling in mitochondria. *Biochimica Et Biophysica Acta* 1229(3):363-72.
- Klöhn P and Neumann H. 1997. Impairment of respiration and oxidative phosphorylation by redox cyclers 2-nitrosofluorene and menadione. *Chemico-Biological Interactions* 106(1):15-28.

- Klöhn P, Brandt U, Neumann H. 1996. 2-nitrosofluorene and N-hydroxy-2-aminofluorene react with the ubiquinone-reduction center (center N) of the mitochondrial cytochrome bc₁ complex. *FEBS Letters* 389(3):233-7.
- Klöhn P, Soriano ME, Irwin W, Penzo D, Scorrano L, Bitsch A, Neumann H, Bernardi P. 2003. Early resistance to cell death and to onset of the mitochondrial permeability transition during hepatocarcinogenesis with 2-acetylaminofluorene. *Proceedings of the National Academy of Sciences* 100(17):10014-9.
- Ladero JM, Kwok CK, Jara C, Fernandez L, Silmi AM, Tapia D, Uson AC. 1985. Hepatic acetylator phenotype in bladder cancer patients. *Annals of Clinical Research* 17(3):96-9.
- Lee J, Chu I, Mikaelyan A, Calvisi DF, Heo J, Reddy JK, Thorgeirsson SS. 2004. Application of comparative functional genomics to identify best-fit mouse models to study human cancer. *Nature Genetics* 36(12):1306-11.
- Lee SST, Buters JTM, Pineau T, Fernandez-Salguero P, Gonzalez FJ. 1996. Role of CYP2E1 in the hepatotoxicity of acetaminophen. *Journal of Biological Chemistry* 271(20):12063-7.
- Leuenberger SG. 1912. Die unter dem einfluss der synthetischen farbenindustrie beobachtete geschwulstentwicklung. *Beitr z Klin Chir* 5(11):1029.
- Levin DE, Hollstein M, Christman MF, Schwiers EA, Ames BN. 1982. A new salmonella tester strain (TA102) with A X T base pairs at the site of mutation detects oxidative mutagens. *Proceedings of the National Academy of Sciences* 79(23):7445-9.
- Li Z, Tuteja G, Schug J, Kaestner K. 2012. Foxa1 and Foxa2 are essential for sexual dimorphism in liver cancer. *Cell* 148(1):72-83.
- Liang HC, Li H, McKinnon RA, Duffy JJ, Potter SS, Puga A, Nebert DW. 1996. Cyp1a2(-/-) null mutant mice develop normally but show deficient drug metabolism. *Proceedings of the National Academy of Sciences* 93(4):1671-6.
- Lind C, Hochstein P, Ernster L. 1982. DT-diaphorase as a quinone reductase: A cellular control device against semiquinone and superoxide radical formation. *Archives of Biochemistry and Biophysics* 216(1):178-85.
- Linder CD, Renaud NA, Hutzler JM. 2009. Is 1-aminobenzotriazole an appropriate in vitro tool as a nonspecific cytochrome P450 inactivator? *Drug Metabolism and Disposition* 37(1):10-3.
- Löfgren S, Hagbjörk A-, Ekman S, Fransson-Steen R, Terelius Y. 2004. Metabolism of human cytochrome P450 marker substrates in mouse: A strain and gender comparison. *Xenobiotica* 34(9):811-34.
- Loguercio C and Federico A. 2003. Oxidative stress in viral and alcoholic hepatitis. *Free Radical Biology Medicine* 34(1):1-10.

- Lord PG, Hardaker KJ, Loughlin JM, Marsden AM, Orton TC. 1992. Point mutation analysis of ras genes in spontaneous and chemically induced C57Bl/10J mouse liver tumours. *Carcinogenesis* 13(8):1383-7.
- Lu Y and Cederbaum AI. 2006. Enhancement by pyrazole of lipopolysaccharide-induced liver injury in mice: Role of cytochrome P450 2E1 and 2A5. *Hepatology* 44(1):263-74.
- Lunn RM, Zhang Y, Wang L, Chen C, Lee P, Lee C, Tsai W, Santella RM. 1997. p53 mutations, chronic hepatitis B virus infection, and aflatoxin exposure in hepatocellular carcinoma in taiwan. *Cancer Research* 57(16):3471-7.
- MacKenzie I and Rous P. 1941. The experimental disclosure of latent neoplastic changes in tarred skin. *The Journal of Experimental Medicine* 73(3):391-416.
- Maeda S, Kamata H, Luo JL, Leffert H, Karin M. 2005. IKK β couples hepatocyte death to cytokine-driven compensatory proliferation that promotes chemical hepatocarcinogenesis. *Cell* 121(7):977-90.
- Majumder S, Roy S, Kaffenberger T, Wang B, Costinean S, Frankel W, Bratasz A, Kuppusamy P, Hai T, Ghoshal K, et al. 2010. Loss of metallothionein predisposes mice to diethylnitrosamine-induced hepatocarcinogenesis by activating NF-kappaB target genes. *Cancer Research* 70(24):10265-76.
- Makena PS and Chung K. 2007. Evidence that 4-aminobiphenyl, benzidine, and benzidine congeners produce genotoxicity through reactive oxygen species. *Environmental and Molecular Mutagenesis* 48(5):404-13.
- Manjanatha MG. 1996. H- and K-ras mutational profiles in chemically induced liver tumors from B6C3F1 and CD-1 mice. *Journal of Toxicology and Environmental Health* 47(2):195-208.
- Maronpot RR, Flake G, Huff AJ. 2004. Relevance of animal carcinogenesis findings to human cancer predictions and prevention. *Toxicologic Pathology* 32(1 suppl):40-8.
- Marrogi AJ, Khan MA, van Gijssel HE, Welsh JA, Rahim H, Demetris AJ, Kowdley KV, Hussain SP, Nair J, Bartsch H, et al. 2001. Oxidative stress and p53 mutations in the carcinogenesis of iron overload-associated hepatocellular carcinoma. *Journal of the National Cancer Institute* 93(21):1652-5.
- McGivern DR and Lemon SM. 2009. Tumor suppressors, chromosomal instability, and hepatitis C Virus-Associated liver cancer. *Annual Review of Pathological Mechanical Disease* 4:399-415.
- McQueen CA and Chau B. 2003. Neonatal ontogeny of murine arylamine N-acetyltransferases: Implications for arylamine genotoxicity. *Toxicological Sciences* 73(2):279-86.
- Meek DW. 2009. Tumour suppression by p53: A role for the DNA damage response? *Nature Reviews Cancer* 9(10):714-23.

- Melick WF, Naryka JJ, Kelly RE. 1971. Bladder cancer due to exposure to para-aminobiphenyl: A 17-year followup. *The Journal of Urology* 106(2):220-6.
- Melick WF, Escue HM, Naryka JJ, Mezera RA, Wheeler EP. 1955. The first reported cases of human bladder tumors due to a new carcinogen-xenylamine. *The Journal of Urology* 74(6):760-6.
- Meyer UA and Zanger UM. 1997. Molecular mechanisms of genetic polymorphisms of drug metabolism. *Annual Review of Pharmacology and Toxicology* 37(1):269-96.
- Miller EC and Miller JA. 1981. Searches for ultimate chemical carcinogens and their reactions with cellular macromolecules. *Cancer* 47(10):2327-45.
- Miller EC and Miller JA. 1966. Mechanisms of chemical carcinogenesis: Nature of proximate carcinogens and interactions with macromolecules. *Pharmacological Reviews* 18(1):805-38.
- Miller EC and Miller JA. 1947. The presence and significance of bound aminoazo dyes in the livers of rats fed p-dimethylaminoazobenzene. *Cancer Research* 7(7):468-80.
- Miller EC, Juhl U, Miller JA. 1966. Nucleic acid guanine: Reaction with the carcinogen N-acetoxy-2-acetylaminofluorene. *Science* 153(3740):1125-7.
- Minami M, Daimon Y, Mori K, Takashima H, Nakajima T, Itoh Y, Okanoue T. 2005. Hepatitis B virus-related insertional mutagenesis in chronic hepatitis B patients as an early drastic genetic change leading to hepatocarcinogenesis. *Oncogene* 24(27):4340-8.
- Minchin RF, Reeves PT, Teitel CH, McManus ME, Mojarrabi B, Ilett KF, Kadlubar FF. 1992. N- and O-acetylation of aromatic and heterocyclic amine carcinogens by human monomorphic and polymorphic acetyltransferases expressed in COS-1 cells. *Biochemical and Biophysical Research Communications* 185(3):839-44.
- Mirsalis JC, Shimon JA, Johnson A, Fairchild D, Kanazawa N, Nguyen T, de Boer J, Glickman B, Winegar RA. 2005. Evaluation of mutant frequencies of chemically induced tumors and normal tissues in λ /cII transgenic mice. *Environmental and Molecular Mutagenesis* 45(1):17-35.
- Mitchell MK, Futscher BW, McQueen CA. 1999. Developmental expression of N-acetyltransferases in C57BI/6 mice. *Drug Metabolism and Disposition* 27(2):261-4.
- Montano MM, Chaplin LJ, Deng H, Mesia-Vela S, Gaikwad N, Zahid M, Rogan E. 2006. Protective roles of quinone reductase and tamoxifen against estrogen-induced mammary tumorigenesis. *Oncogene* 26(24):3587-90.
- Mueller GC and Miller JA. 1948. The metabolism of 4-dimethylaminoazobenzene by rat liver homogenates. *Journal of Biological Chemistry* 176(2):535-44.

- Mueller GC and Miller JA. 1953. The metabolism of methylated aminoazo dyes: II. oxidative demethylation by rat liver homogenates. *Journal of Biological Chemistry* 202(2):579-87.
- Mueller GC and Miller JA. 1949. The reductive cleavage of 4-dimethylaminoazobenzene by rat liver: The intracellular distribution of the enzyme system and its requirement for triphosphopyridine nucleotide. *Journal of Biological Chemistry* 180(3):1125-36.
- Munshi HG and Stack MS. 2006. Reciprocal interactions between adhesion receptor signaling and MMP regulation. *Cancer and Metastasis Reviews* 25(1):45-56.
- Murata M, Tamura A, Tada M, Kawanishi S. 2001. Mechanism of oxidative DNA damage induced by carcinogenic 4-aminobiphenyl. *Free Radical Biology and Medicine* 30(7):765-73.
- Nakajima M, Itoh M, Sakai H, Fukami T, Katoh M, Yamazaki H, Kadlubar FF, Imaoka S, Funae Y, Yokoi T. 2006. CYP2A13 expressed in human bladder metabolically activates 4-aminobiphenyl. *International Journal of Cancer* 119(11):2520-6.
- 12th Report on Carcinogens by National Toxicology Program [Internet]; c2011 [cited 2012 05/20]. Available from: <http://ntp.niehs.nih.gov/?objectid=03C9AF75-E1BF-FF40-DBA9EC0928DF8B15>.
- Naugler WE, Sakurai T, Kim S, Maeda S, Kim K, Elsharkawy AM, Karin M. 2007. Gender disparity in liver cancer due to sex differences in MyD88-dependent IL-6 production. *Science* 317(5834):121-4.
- Nelson DR, Zeldin DC, Hoffman SM, Maltais LJ, Wain HM, Nebert DW. 2004. Comparison of cytochrome P450 (CYP) genes from the mouse and human genomes, including nomenclature recommendations for genes, pseudogenes and alternative-splice variants. *Pharmacogenetics* 14(1):1-18.
- Neumann HG, Ambs S, Bitsch A. 1994. The role of nongenotoxic mechanisms in arylamine carcinogenesis. *Environmental Health Perspectives* 102 Suppl 6:173-6.
- Neumann H, Bitsch A, Klöhn P. 1997. The dual role of 2-acetylaminofluorene in hepatocarcinogenesis: Specific targets for initiation and promotion. *Mutation Research/Fundamental and Molecular Mechanisms of Mutagenesis* 376(1):169-76.
- Nguyen PM, Park MS, Chow M, Chang JH, Wrischnik L, Chan WK. 2010. Benzo[a]pyrene increases the Nrf2 content by downregulating the Keap1 message. *Toxicological Sciences* 116(2):549-61.
- Novak M, Kahley MJ, Eiger E, Helmick JS, Peters HE. 1993. Reactivity and selectivity of nitrenium ions derived from ester derivatives of carcinogenic N-(4-biphenyl)hydroxylamine and the corresponding hydroxamic acid. *Journal of the American Chemical Society* 115(21):9453-60.

- Office of the Surgeon General. 2014. The health consequences of Smoking—50 years of progress. Atlanta, GA, USA: U.S. Department of health and human services, Public Health Service.
- Omura T and Sato R. 1962. A new cytochrome in liver microsomes. *Journal of Biological Chemistry* 237(4):PC1375-6.
- Orzechowski A, Schrenk D, Schut HAJ, Bock KW. 1994. Consequences of 3-methylcholanthrene-type induction for the metabolism of 4-aminobiphenyl in isolated rat hepatocytes. *Carcinogenesis* 15(3):489-94.
- Park J, Troxel AB, Harvey RG, Penning TM. 2006. Polycyclic aromatic hydrocarbon (PAH) o-quinones produced by the aldo-keto-reductases (AKRs) generate abasic sites, oxidized pyrimidines, and 8-oxo-dGuo via reactive oxygen species. *Chemical Research in Toxicology* 19(5):719-28.
- Park J, Gopishetty S, Szewczuk LM, Troxel AB, Harvey RG, Penning TM. 2005. Formation of 8-oxo-7,8-dihydro-2'-deoxyguanosine (8-oxo-dGuo) by PAH o-quinones: Involvement of reactive oxygen species and copper(II)/Copper(I) redox cycling. *Chemical Research in Toxicology* 18(6):1026-37.
- Park J, Gelhaus S, Vedantam S, Oliva AL, Batra A, Blair IA, Troxel AB, Field J, Penning TM. 2008. The pattern of p53 mutations caused by PAH o-quinones is driven by 8-oxo-dGuo formation while the spectrum of mutations is determined by biological selection for dominance. *Chemical Research in Toxicology* 21(5):1039-49.
- Parsons BL, Beland FA, Von Tungeln LS, Delongchamp RR, Fu PP, Heflich RH. 2005. Levels of 4-aminobiphenyl-induced somatic H-ras mutation in mouse liver DNA correlate with potential for liver tumor development. *Molecular Carcinogenesis* 42(4):193-201.
- Penning TM. 2011. *Chemical carcinogenesis*. New York: Humana Press/Springer.
- Penning TM, Ohnishi ST, Ohnishi T, Harvey RG. 1996. Generation of reactive oxygen species during the enzymatic oxidation of polycyclic aromatic hydrocarbon trans-dihydrodiols catalyzed by dihydrodiol dehydrogenase. *Chemical Research in Toxicology* 9(1):84-92.
- Perchellet J, Abney NL, Thomas RM, Guislain YL, Perchellet EM. 1987. Effects of combined treatments with selenium, glutathione, and vitamin E on glutathione peroxidase activity, ornithine decarboxylase induction, and complete and multistage carcinogenesis in mouse skin. *Cancer Research* 47(2):477-85.
- Potter M. 1963. Percivall pott's contribution to cancer research. *Journal of the National Cancer Institute Monographs* 10:1.
- Puisieux A and Ozturk M. 1997. TP53 and hepatocellular carcinoma. *Pathologie-Biologie* 45(10):864-70.

- Puisieux A, Lim S, Groopman J, Ozturk M. 1991. Selective targeting of p53 gene mutational hotspots in human cancers by etiologically defined carcinogens. *Cancer Research* 51(22):6185-9.
- Qian GS, Ross RK, Yu MC, Yuan JM, Gao YT, Henderson BE, Wogan GN, Groopman JD. 1994. A follow-up study of urinary markers of aflatoxin exposure and liver cancer risk in shanghai, people's republic of china. *Cancer Epidemiology Biomarkers & Prevention* 3(1):3-10.
- Radomski JL. 1979. The primary aromatic amines: Their biological properties and structure-activity relationships. *Annual Review of Pharmacology and Toxicology* 19(1):129-57.
- Rajalingam K, Schreck R, Rapp UR, Albert Å. 2007. Ras oncogenes and their downstream targets. *Biochimica Et Biophysica Acta* 1773(8):1177-95.
- Rangarajan A and Weinberg RA. 2003. Comparative biology of mouse versus human cells: Modelling human cancer in mice. *Nature Reviews Cancer* 3(12):952-9.
- Redmond DE. 1970. Tobacco and cancer: The first clinical report, 1761. *The New England Journal of Medicine* 282(1):18-23.
- Rehn L. 1895. Blasengeschwulste bei fuchsinarbeitern. *Langenbecks Archiv Fur Klinische Chirurgie* 39(1):73-600.
- Richardson HL and Cunningham L. 1951. The inhibitory action of methylcholanthrene on rats fed the azo dye 3'-methyl-4-dimethylaminoazobenzene. Chicago, Ill. American Association for Cancer Research.
- Riedel K, Scherer G, Engl J, Hagedorn H, Tricker AR. 2006. Determination of three carcinogenic aromatic amines in urine of smokers and nonsmokers. *Journal of Analytical Toxicology* 30(3):187-95.
- Rinkus SJ and Legator MS. 1979. Chemical characterization of 465 known or suspected carcinogens and their correlation with mutagenic activity in the salmonella typhimurium system. *Cancer Research* 39(9):3289-318.
- Roberts RA, Ganey PE, Ju C, Kamendulis LM, Rusyn I, Klaunig JE. 2007. Role of the kupffer cell in mediating hepatic toxicity and carcinogenesis. *Toxicological Sciences* 96(1):2-15.
- Ross RK, Yu MC, Henderson BE, Yuan J-, Qian G, Tu J, Gao Y-, Wogan GN, Groopman JD. 1992. Urinary aflatoxin biomarkers and risk of hepatocellular carcinoma. *The Lancet* 339(8799):943-6.
- Roth JR and Ames BN. 1966. Histidine regulatory mutants in salmonella typhimurium. *Journal of Molecular Biology* 22(2):325-34.
- Rous P and Kidd JG. 1941. Conditional neoplasms and subthreshold neoplastic states: A study of the tar tumors of rabbits. *The Journal of Experimental Medicine* 73(3):365-90.

- Sakurai T, Maeda S, Chang L, Karin M. 2006. Loss of hepatic NF- κ B activity enhances chemical hepatocarcinogenesis through sustained c-jun N-terminal kinase 1 activation. *Proceedings of the National Academy of Sciences* 103(28):10544-51.
- Sakurai T, He G, Matsuzawa A, Yu G, Maeda S, Hardiman G, Karin M. 2008. Hepatocyte necrosis induced by oxidative stress and IL-1 alpha release mediate carcinogen-induced compensatory proliferation and liver tumorigenesis. *Cancer Cell* 14(2):156-65.
- Saletta F, Matullo G, Manuguerra M, Arena S, Bardelli A, Vineis P. 2007. Exposure to the tobacco smoke constituent 4-aminobiphenyl induces chromosomal instability in human cancer cells. *Cancer Research* 67(15):7088-94.
- Schieferstein GJ, Littlefield NA, Gaylor DW, Sheldon WG, Burger GT. 1985. Carcinogenesis of 4-aminobiphenyl in BALB/cStCrlfC3Hf/Nctr mice. *European Journal of Cancer and Clinical Oncology* 21(7):865-73.
- Sejersted Y, Aasland AL, Bjoras M, Eide L, Saugstad OD. 2009. Accumulation of 8-oxoguanine in liver DNA during hyperoxic resuscitation of newborn mice. *Pediatric Research* 66(5):533-8.
- Sell S, Hunt JM, Dunsford HA, Chisari FV. 1991. Synergy between hepatitis B virus expression and chemical hepatocarcinogens in transgenic mice. *Cancer Research* 51(4):1278-85.
- Sengupta S and Harris CC. 2005. p53: Traffic cop at the crossroads of DNA repair and recombination. *Nature Reviews. Molecular Cell Biology* 6(1):44-55.
- Severi T, van Malenstein H, Verslype C, van Pelt J,F. 2010. Tumor initiation and progression in hepatocellular carcinoma: Risk factors, classification, and therapeutic targets. *Acta Pharmacologica Sinica* 31(11):1409-20.
- Shen Y, Troxel AB, Vedantam S, Penning TM, Field J. 2006. Comparison of p53 mutations induced by PAH o-quinones with those caused by anti-benzo[a]pyrene diol epoxide in vitro: Role of reactive oxygen and biological selection. *Chemical Research in Toxicology* 19(11):1441-50.
- Shertzer HG, Dalton TP, Talaska G, Nebert DW. 2002. Decrease in 4-aminobiphenyl-induced methemoglobinemia in Cyp1a2(-/-) knockout mice. *Toxicology and Applied Pharmacology* 181(1):32-7.
- Shibutani S, Takeshita M, Grollman AP. 1991. Insertion of specific bases during DNA synthesis past the oxidation-damaged base 8-oxodG. *Nature* 349(6308):431-4.
- Shimoda R, Nagashima M, Sakamoto M, Yamaguchi N, Hirohashi S, Yokota J, Kasai H. 1994. Increased formation of oxidative DNA damage, 8-hydroxydeoxyguanosine, in human livers with chronic hepatitis. *Cancer Research* 54(12):3171-2.

- Shiota G, Maeta Y, Mukoyama T, Yanagidani A, Udagawa A, Oyama K, Yashima K, Kishimoto Y, Nakai Y, Miura T, et al. 2002. Effects of sho-saiko-to on hepatocarcinogenesis and 8-hydroxy-2'-deoxyguanosine formation. *Hepatology* 35(5):1125-33.
- Siraki AG, Chan TS, Galati G, Teng S, O'Brien PJ. 2002. N-oxidation of aromatic amines by intracellular oxidases. *Drug Metabolism Reviews* 34(3):549-64.
- Slaga TJ, Scribner JD, Viaje A. 1976. Epidermal cell proliferation and promoting ability of phorbol esters. *Journal of the National Cancer Institute* 57(5):1145-9.
- Slaga TJ, Fischer SM, Weeks CE, Klein-Szanto AJP, Reiners J. 1982. Studies on the mechanisms involved in multistage carcinogenesis in mouse skin. *Journal of Cellular Biochemistry* 18(1):99-119.
- Sleight S. 1985. Effects of PCBs and related compounds on hepatocarcinogenesis in rats and mice. *Environmental Health Perspectives* 60:35-9.
- Slocum S and Kensler T. 2011. Nrf2: Control of sensitivity to carcinogens. *Archives of Toxicology* 85(4):273-84.
- Sugamori KS, Brenneman D, Grant DM. 2006. In vivo and in vitro metabolism of arylamine procarcinogens in acetyltransferase-deficient mice. *Drug Metabolism and Disposition* 34(10):1697-702.
- Sugamori KS, Brenneman D, Wong S, Gaedigk A, Yu V, Abramovici H, Rozmahel R, Grant DM. 2007. Effect of arylamine acetyltransferase Nat3 gene knockout on N-acetylation in the mouse. *Drug Metabolism and Disposition* 35(7):1064-70.
- Sugamori KS, Brenneman D, Sanchez O, Doll MA, Hein DW, Pierce Jr. WM, Grant DM. 2012. Reduced 4-aminobiphenyl-induced liver tumorigenicity but not DNA damage in arylamine N-acetyltransferase null mice. *Cancer Letters* 318(2):206-13.
- Sugamori KS, Wong S, Gaedigk A, Yu V, Abramovici H, Rozmahel R, Grant DM. 2003. Generation and functional characterization of arylamine N-acetyltransferase Nat1/Nat2 Double-knockout mice. *Molecular Pharmacology* 64(1):170-9.
- Tassaneeyakul W, Veronese ME, Birkett DJ, Gonzalez FJ, Miners JO. 1993. Validation of 4-nitrophenol as an in vitro substrate probe for human liver CYP2E1 using cDNA expression and microsomal kinetic techniques. *Biochemical Pharmacology* 46(11):1975-81.
- Teufelhofer O, Parzefall W, Kainzbauer E, Ferk F, Freiler C, Knasmüller S, Elbling L, Thurman R, Schulte-Hermann R. 2005. Superoxide generation from kupffer cells contributes to hepatocarcinogenesis: Studies on NADPH oxidase knockout mice. *Carcinogenesis* 26(2):319-29.
- Thiede T and Christensen BC. 1969. Bladder tumours induced by chlornaphazine. A five-year follow-up study of chlornaphazine-treated patients with polycythaemia. *Acta Medica Scandinavica* 185(1-2):133-7.

- Thorgeirsson SS and Grisham JW. 2002. Molecular pathogenesis of human hepatocellular carcinoma. *Nature Genetics* 31(4):339-46.
- Tiang JM, Butcher NJ, Cullinane C, Humbert PO, Minchin RF. 2011. RNAi-mediated knock-down of arylamine N-acetyltransferase-1 expression induces E-cadherin up-regulation and cell-cell contact growth inhibition. *PloS One* 6(2):e17031.
- Tiang JM, Butcher NJ, Minchin RF. 2010. Small molecule inhibition of arylamine N-acetyltransferase type I inhibits proliferation and invasiveness of MDA-MB-231 breast cancer cells. *Biochemical and Biophysical Research Communications* 393(1):95-100.
- Tsuneoka Y, Dalton TP, Miller ML, Clay CD, Shertzer HG, Talaska G, Medvedovic M, Nebert DW. 2003. 4-aminobiphenyl-induced liver and urinary bladder DNA adduct formation in Cyp1a2(-/-) and Cyp1a2(+/+) mice. *Journal of the National Cancer Institute* 95(16):1227-37.
- Tsuzuki T, Egashira A, Igarashi H, Iwakuma T, Nakatsuru Y, Tominaga Y, Kawate H, Nakao K, Nakamura K, Ide F, et al. 2001. Spontaneous tumorigenesis in mice defective in the MTH1 gene encoding 8-oxo-dGTPase. *Proceedings of the National Academy of Sciences* 98(20):11456-61.
- Turesky RJ, Freeman JP, Holland RD, Nestorick DM, Miller DW, Ratnasinghe DL, Kadlubar FF. 2003. Identification of aminobiphenyl derivatives in commercial hair dyes. *Chemical Research in Toxicology* 16(9):1162-73.
- Umarani M, Shanthi P, Sachdanandam P. 2008. Protective effect of kalpaamruthaa in combating the oxidative stress posed by aflatoxin B1-induced hepatocellular carcinoma with special reference to flavonoid structure-activity relationship. *Liver International* 28(2):200-13.
- Vafa O, Wade M, Kern S, Beeche M, Pandita TK, Hampton GM, Wahl GM. 2002. c-myc can induce DNA damage, increase reactive oxygen species, and mitigate p53 function: A mechanism for oncogene-induced genetic instability. *Molecular Cell* 9(5):1031-44.
- Verghis SB, Essigmann JM, Kadlubar FF, Morningstar ML, Lasko DD. 1997. Specificity of mutagenesis by 4-aminobiphenyl: Mutations at G residues in bacteriophage M13 DNA and G-->C transversions at a unique dG(8-ABP) lesion in single-stranded DNA. *Carcinogenesis* 18(12):2403-14.
- Wang J, Shen X, He X, Zhu Y, Zhang B, Wang J, Qian G, Kuang S, Zarba A, Egner PA, et al. 1999. Protective alterations in phase 1 and 2 metabolism of aflatoxin B1 by oltipraz in residents of qidong, people's republic of china. *Journal of the National Cancer Institute* 91(4):347-54.
- Wang L, Chen C, Zhang Y, Tsai W, Lee P, Feitelson MA, Lee C, Santella RM. 1998. 4-aminobiphenyl DNA damage in liver tissue of hepatocellular carcinoma patients and controls. *American Journal of Epidemiology* 147(3):315-23.

- Wang L, Hatch M, Chen C, Levin B, You S, Lu S, Wu M, Wu W, Wang L, Wang Q, et al. 1996. Aflatoxin exposure and risk of hepatocellular carcinoma in taiwan. *International Journal of Cancer* 67(5):620-5.
- Wang SC, Chung J, Chen C, Chen S. 2006. 2- and 4-aminobiphenyls induce oxidative DNA damage in human hepatoma (hep G2) cells via different mechanisms. *Mutation Research/Fundamental and Molecular Mechanisms of Mutagenesis* 593(1-2):9-21.
- Wang S, Sugamori KS, Brenneman D, Hsu I, Calce A, Grant DM. 2012. Influence of arylamine n-acetyltransferase, sex, and age on 4-aminobiphenyl-induced in vivo mutant frequencies and spectra in mouse liver. *Environmental and Molecular Mutagenesis* 53(5):350-7.
- Wang XJ, Hayes JD, Higgins LG, Wolf CR, Dinkova-Kostova A. 2010. Activation of the NRF2 signaling pathway by copper-mediated redox cycling of para- and ortho-hydroquinones. *Chemistry & Biology* 17(1):75-85.
- Watson JD and Crick FHC. 1953. Molecular structure of nucleic acids: A structure for deoxyribose nucleic acid. *Nature* 171(4356):737-8.
- Wei H and Frenkel K. 1993. Relationship of oxidative events and DNA oxidation in SENCAR mice to in vivo promoting activity of phorbol ester-type tumor promoters. *Carcinogenesis* 14(6):1195-201.
- White D, Firozi A, El-Serag H. 2010. Epidemiology of hepatocellular carcinoma. Carr BI, editor. Humana Press. 25 p.
- World Health Organization. 2001. Introduction of hepatitis B vaccine into childhood immunization services. *Management Guidelines*.
- Yamagiwa K and Ichikawa K. 1918. Experimental study of the pathogenesis of carcinoma. *The Journal of Cancer Research* 3(1):1-29.
- Yeh J, Hsu S, Han S, Lai M. 1998. Mitogen-activated protein kinase kinase antagonized fas-associated death domain protein-mediated apoptosis by induced FLICE-inhibitory protein expression. *Journal of Experimental Medicine* 188(10):1795-802.
- Zayas-Rivera B, Zhang L, Grant SG, Keohavong P, Day BW. 2001. Mutational spectrum of N-hydroxy-N-acetyl-4-aminobiphenyl at exon 3 of the HPRT gene. *Biomarkers* 6(4):262-73.
- Zhang T, Ding X, Wei D, Cheng P, Su X, Liu H, Wang D, Gao H. 2010. Sorafenib improves the survival of patients with advanced hepatocellular carcinoma: A meta-analysis of randomized trials. *Anti-Cancer Drugs* 21(3).
- Zhang Y, Bai XF, Huang CX. 2003. Hepatic stem cells: Existence and origin. *World Journal of Gastroenterology* 9(2):201-4.
- Zhao Y, Xue Y, Oberley TD, Kiningham KK, Lin S, Yen H, Majima H, Hines J, St. Clair D. 2001. Overexpression of manganese superoxide dismutase suppresses tumor formation by

modulation of activator protein-1 signaling in a multistage skin carcinogenesis model.
Cancer Research 61(16):6082-8.

List of Publications and Abstracts

PUBLISHED PEER-REVIEWED PAPERS

- **Wang S**, Sugamori KS, Brenneman D, Hsu I, Calce A, Grant DM. 2012. Influence of arylamine n-acetyltransferase, sex, and age on 4-aminobiphenyl-induced in vivo mutant frequencies and spectra in mouse liver. *Environmental and Molecular Mutagenesis* 53(5):350-7.
- Ogawa S, Surapisitchat J, Virtanen C, Ogawa M, Niapour M, Sugamori KS, **Wang S**, Tamblyn L, Guillemette C, Hoffmann E, Bin Z, Stephen S, Laposa RR, Tyndale RF, Grant DM, and Keller G. 2013. Three-dimensional culture and cAMP signaling promote the maturation of human pluripotent stem cell-derived hepatocytes. *Development* 140(15):3285-96.

PUBLISHED ABSTRACTS

- **Wang S**, Sugamori KS, and Grant DM (2013). N-hydroxylation of 4-Aminobiphenyl by CYP2E1 and Associated Oxidative Stress May Influence Its Tumorigenicity in Mouse Liver. 10th International ISSX Meeting, Toronto, Canada
- **Wang S**, Sugamori KS, and Grant DM (2013). N-hydroxylation of 4-Aminobiphenyl (ABP) and Associated Oxidative Stress May Influence ABP Carcinogenicity in the Mouse Liver. AACR Annual Meeting, Washington DC, United States of America
- **Wang S**, Sugamori KS, and Grant DM (2012). Role of Oxidative Stress in 4-Aminobiphenyl-Induced Liver Tumorigenesis in Mice. The Canadian Society for Pharmacology and Therapeutics (CSPT) Conference, Toronto, Canada
- Grant DM, Hanna D, **Wang S**, Brenneman D, and Sugamori KS (2012). Roles of Metabolic Activation, DNA Damage, Oxidative stress and Acute Cytotoxicity in the Liver Carcinogenicity of 4-Aminobiphenyl in the Mouse, 19th International Symposium on Microsomes and Drug Oxidations and 12th European Regional ISSX Joint Meeting (MDO-ISSX), Noordwijk aan Zee, Netherlands
- **Wang S**, Hsu I, Calce A, Sugamori KS, and Grant DM (2011). Influence of Sex and Arylamine N-acetyltransferase Activity on 4-Aminobiphenyl-Induced In Vivo Mutation

Frequencies and Spectra in Mouse Liver. The Canadian Cancer Research Conference, Toronto, Canada

- **Wang S**, Sugamori KS, and Grant DM (2010). 4-Aminobiphenyl (ABP) Induced DNA Damage in Mouse Liver. 18th International Symposium on Microsomes and Drug Oxidations, Beijing, China
- **Wang S**, Sugamori KS, and Grant DM (2009). Expression of Liver Drug-Metabolizing Enzymes in Primary Mouse and Human Stem Cell Derived Hepatocytes. Stem Cell Network Annual General Meeting, Montreal, Canada.

Appendices

Appendix A. Transient transfection of *Cyp1a2* and *Cyp2e1* into Hepa1c1c7 cells

Introduction

In this section, we transiently transfected putative ABP *N*-hydroxylation enzymes *Cyp1a2* and *Cyp2e1* into Hepa1c1c7 cells. Transfection optimization studies were carried out following the manufacturer's protocols, which involved testing different transfection conditions (various ratios of transfection reagent: μg plasmid DNA) and comparing levels of enzyme mRNA expression and activity between different conditions. We established qPCR assays for the measurement of *Cyp1a2* and *Cyp2e1* mRNA expressions in cell culture. In addition, we set up in culture phenacetin *O*-deethylation and pNP hydroxylation assays for the measurement of CYP1A2 and CYP2E1 enzyme activities, respectively.

Materials and methods

In vitro and in culture phenacetin *O*-deethylation assays

Each *in vitro* phenacetin *O*-deethylation reaction contained 20 μL of 0.5 M potassium phosphate buffer pH 7.4, 10 μL of 2 mM phenacetin dissolved in 1% DMSO, 25 μL of 20 mM MgCl_2 , 5 μL of 10 mM NADP^+ , 10 μL of 50 mM glucose-6-phosphate, 1 μL of glucose-6-phosphate dehydrogenase, and 29 μL of microsomal preparation (final concentration ~ 1 mg/mL) to a total volume of 100 μL . Reactions were incubated at 37°C for 10 minutes and terminated by addition of 10 μL of 15% w/v HClO_4 . The samples were well mixed and centrifuged at 13000 rpm for 5 minutes to precipitate proteins. 50 μL of the supernatant was then injected onto a reverse phase C18 Beckman Ultrasphere© HPLC column at a flow rate of 1 mL/ minute. Mobile phase for the HPLC contains 10% w/w methanol and 90% w/w of 0.1% w/w acetic acid buffer. UV absorbance was measured at 245 nm and 35°C. Using these HPLC conditions, phenacetin and acetaminophen have retention times of 30 and 5 minutes, respectively.

For the in culture phenacetin *O*-deethylation assay, phenacetin was added to cell culture medium to a final concentration of 200 μM and incubated with cells for 2 hours. Following incubation, 100 μL of medium was withdrawn, terminated using 5 μL of 60% w/v HClO_4 , spun at 13000

rpm for 5 minutes, and 50 μ L of the supernatant was then injected onto a reverse phase C18 Beckman Ultrasphere[®] HPLC column at a flow rate of 1 mL/minute.

In vitro and in culture pNP hydroxylation assays

As described in Sections 2.9 and 2.10.

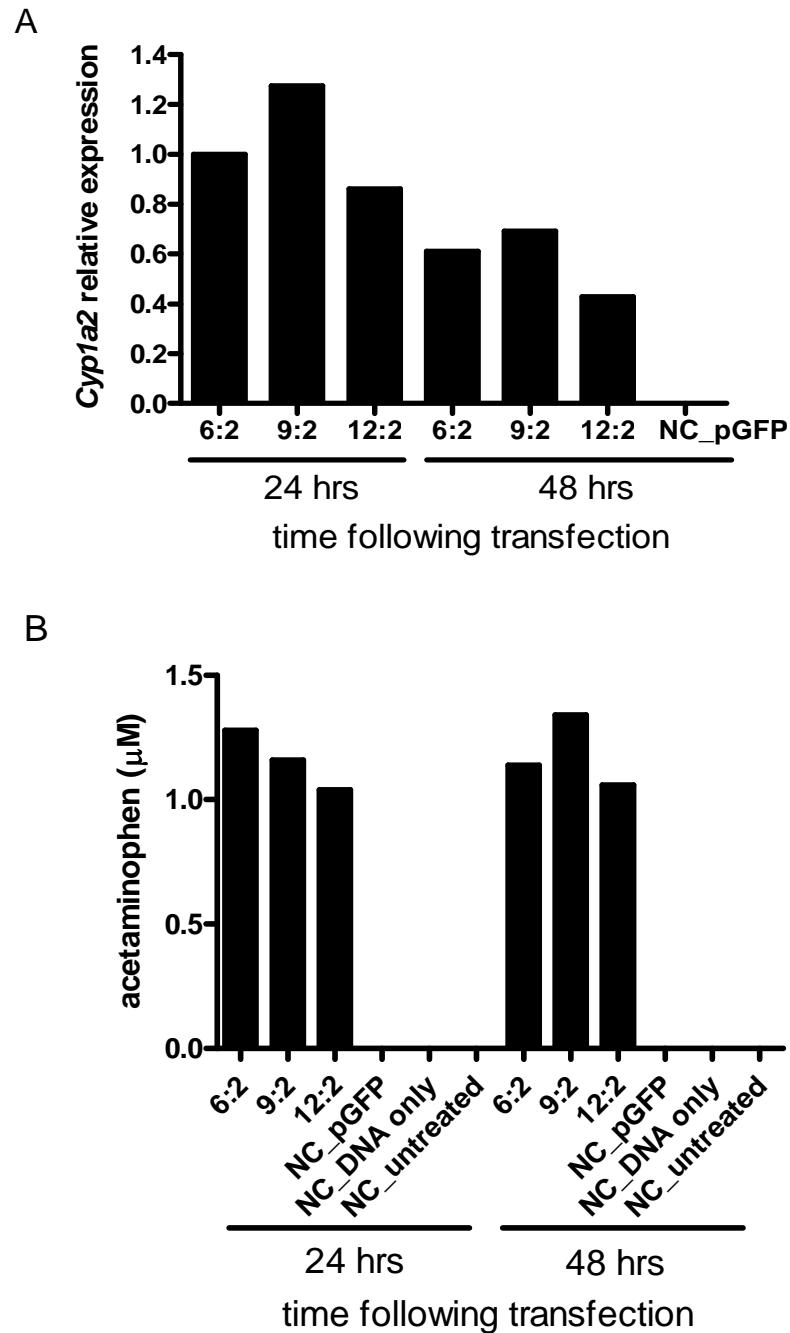
RNA extraction from cell culture

Cells on 6-well-plates were washed 2x with PBS. 1 mL of Trizol[®] was added to each well on a 6-well-plate, incubated for 5 minutes at room temperature, pipetted vigorously until contents are no longer viscous, and collected into 1.5 mL eppendorff tubes. Procedures from hereon are identical to those described for RNA extraction from liver tissue (Section 2.14).

Quantification of *Cyp1a2* and *Cyp2e1* transcript expression was carried out using quantitative PCR (methodology described in Section 2.15).

Results and discussion

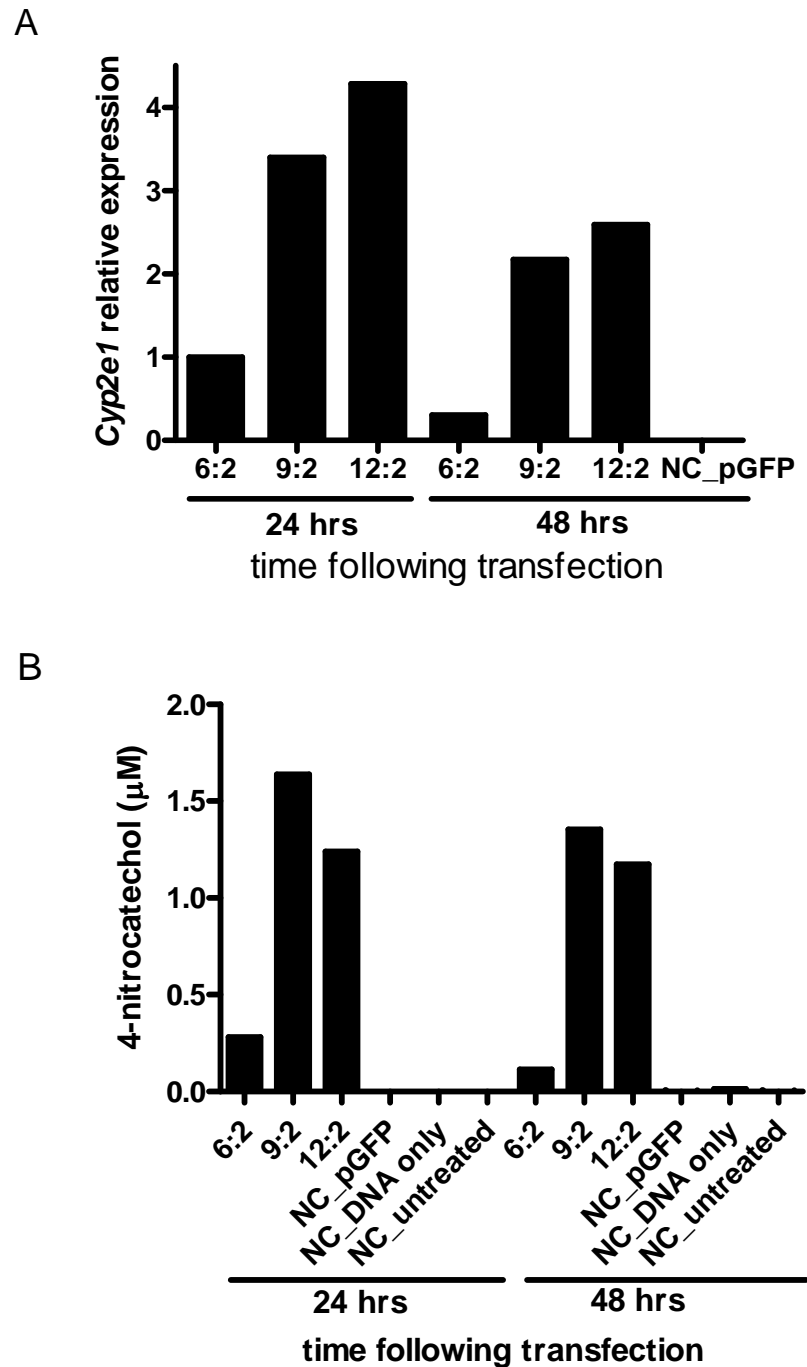
Different ratios of transfection reagent to plasmid DNA were tested in Hepa1c1c7 cells. Levels of *Cyp1a2* transcript expression and in culture CYP1A2 activity were determined and compared between different transfection conditions (Appendix figure 1).



Appendix figure 1. Recombinant expression of CYP1A2 in Hepa1c1c7 cells.

Different ratios of LTX transfection reagent: μg *Cyp1a2* plasmid DNA were tested. CYP1A2 expression (A) and activity (B) were quantified using QPCR and phenacetin *O*-deethylation in culture assay, respectively, at 24 and 48 hours following transfection. "NC_pGFP" = negative control using *GFP* instead of *Cyp1a2* plasmids. "NC_DNA only" = negative control cells transfected with DNA only (no transfection reagent). "NC_untreated" = negative control with no cell transfection.

From CYP1A2 transfection optimization studies, a transfection ratio of 6:2 and incubation period of 24 hours gave the highest level of *Cyp1a2* expression and a high level of CYP1A2 activity, and is used for subsequent *Cyp1a2* transfection studies. Next, levels of *Cyp2e1* transcript expression and CYP2E1 in culture activity were determined and compared under different transfection conditions (Appendix figure 2).

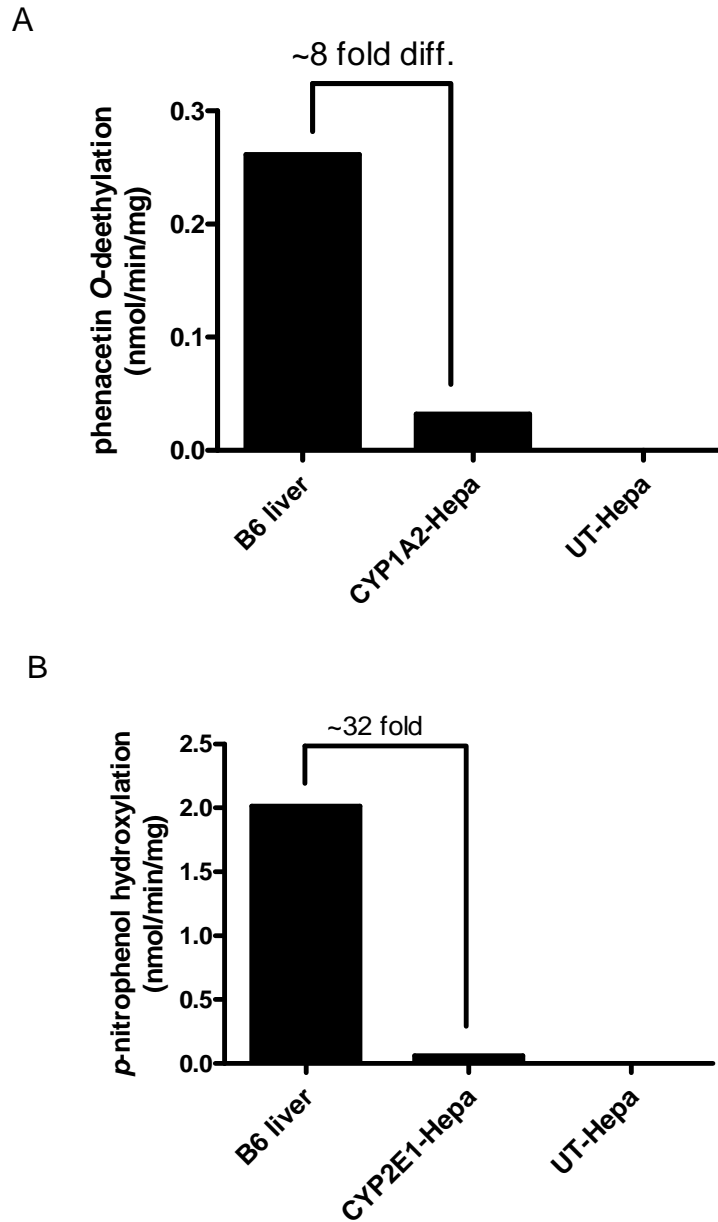


Appendix figure 2. Recombinant expression of CYP2E1 in Hepa1c1c7 cells.

Different ratios of LTX transfection reagent: μg *Cyp2e1* plasmid DNA were tested. CYP2E1 expression (A) and activity (B) were quantified using qPCR and pNP hydroxylation in culture assay, respectively, at 24 and 48 hours following transfection. "NC_pGFP" = negative control using *GFP* instead of *Cyp1a2* plasmids. "NC_DNA only" = negative control cells transfected with DNA only (no transfection reagent). "NC_untreated" = negative control with no cell transfection.

CYP2E1 transfection studies demonstrated highest *Cyp2e1* transcript expression at 24 hours with a transfection ratio of 12:2 and highest CYP2E1 activity at 24 hours with a transfection ratio of 9:2. Since significant cell death was detected with CYP2E1 transfection ratio of 12:2, a transfection ratio of 9:2 is used for subsequent CYP2E1 transfection studies.

To put the expression of CYP1A2 and CYP2E1 into perspective, we isolated microsomes from both transfected cells and mouse liver, and compared them in terms of CYP1A2 and CYP2E1 enzyme activities (Appendix figure 3).



Appendix figure 3. Comparison of CYP1A2 (A) and CYP2E1 (B) activities in transfected Hepa1c1c7 cells to mouse liver.

Microsomes were isolated from a day 15 male C57BL/6 mouse liver and CYP1A2-transfected, CYP2E1-transfected, or untransfected Hepa1c1c7 cells. *In vitro* production of acetaminophen in the presence of microsomes and NADPH regenerating system at 200 μ M phenacetin were quantified on the HPLC (A). *In vitro* production of 4-nitrocatechol in the presence of microsomes and NADPH regenerating system at 200 μ M pNP were quantified on the HPLC (B). "B6 liver" = C57BL/6 mouse liver microsomes. "CYP1A2-Hepa" = microsomes isolated from Hepa1c1c7 cells transfected 6:2 with *Cyp1a2*. "CYP2E1-Hepa" = microsomes isolated from Hepa1c1c7 cells transfected 9:2 with *Cyp2e1*. "UT-Hepa" = untransfected Hepa1c1c7 cells.

Much lower enzyme activities were found with transfected Hepa1c1c7 cells compared to mouse liver, especially for CYP2E1, where ~32-fold lower activity was detected in transfected cells (Appendix figure 3).

We successfully achieved recombinant expression of CYP1A2 and CYP2E1 in Hepa1c1c7 cells, as measured using both mRNA expression and enzyme activity. However, much lower levels of enzyme activity were found in transfected cells compared to mouse liver for both CYP1A2 and CYP2E1, which must be taken into consideration when interpreting our cell culture findings and extrapolating to *in vivo* situations.

Appendix B. Expression and induction of the liver-specific enzyme CYP1A2 in various hepatocyte cultures

Introduction

In the search for an ideal cell culture system for the study of ABP bioactivation by mouse liver, I characterized several different hepatocyte cultures for the expression of CYP1A2, a liver-specific drug-metabolizing enzyme hypothesized to *N*-hydroxylate ABP in the first step of ABP bioactivation, both in terms of mRNA and enzyme activity. In addition, I measured CYP1A2 inducibility in these hepatocyte cultures by the AHR ligand β NF, such inducibility being a unique attribute of this enzyme as described in Section 1.1.5.1. Compared to *in vivo* studies, cell culture studies offer the advantage of a highly controlled testing environment; however, cell culture systems for the study of liver drug metabolism often suffer from the lack of expression of key drug-metabolizing enzymes. To test whether this is true in our hepatocyte systems and how we may overcome this barrier, I measured the activity and inducibility of CYP1A2 in mouse primary hepatocytes and bipotential adult mouse liver (BAML) cells derived from them, in Hep1c1c7 mouse hepatoma cells, in HepG2 human hepatoma cells, and in HepG2 cells transfected with liver-enriched transcription factors. As a comparator I measured CYP1A2 enzyme activity in liver microsomes isolated from both uninduced and β NF-induced mice.

Material and methods

Isolation of mouse primary hepatocytes

All reagents used in cell culture were purchased from Life Technologies Inc. (Burlington, ON, Canada) unless stated otherwise. Mice were kept anaesthetized with inhalational isoflurane (3% v/v). Buffers used were oxygenated by bubbling with O₂ for 15 minutes prior to use. The liver was perfused with modified Krebs's Ringer buffer (118.4 mM NaCl, 3.3 mM KCl, 0.9 mM MgSO₄, 1.1 mM KH₂PO₄, 20 mM Glucose, 24.9 mM NaHCO₃, 2.5 mM CaCl₂, 0.1 mM EGTA, and 20 mM HEPES buffer pH 7.4) through a catheter inserted into the inferior vena cava. After a few minutes the hepatic portal vein was severed and the anterior vena cava was clamped to aid liver perfusion. Once blood from the liver was completely drained, a collagenase containing

solution (10 U/mL Collagenase type I (Sigma-Aldrich Canada Ltd., Oakville, ON, Canada), 118.4 mM NaCl, 3.3 mM KCl, 0.9 mM MgSO₄, 1.1 mM KH₂PO₄, 20 mM Glucose, 24.9 mM NaHCO₃, 2.5 mM CaCl₂, 1.4 mM CaCl₂, and 20 mM HEPES buffer pH 7.4) was perfused through the liver to dissociate hepatocytes. Finally, liver was excised from the body, cut in several places, and gently shook in culture medium to release mouse primary hepatocytes. Mouse primary hepatocytes were cultured on collagen coated plates in William's medium E (Wisent Inc., Saint-Bruno, QC, Canada) supplemented with Penicillin-Streptomycin (Life Technologies, Burlington ON, Canada), 2 mM L-glutamine (Life Technologies, Burlington ON, Canada), 100 nM human recombinant insulin (Life Technologies, Burlington ON, Canada), 100 nM dexamethasone (Life Technologies, Burlington ON, Canada), and 5% fetal bovine serum (Sigma-Aldrich Canada Ltd., Oakville, ON, Canada).

Generation of BAML cells

BAML cells were cultured on collagen coated plates in William's medium E supplemented with 100 nM dexamethasone, 100 nM human recombinant insulin, 50 ng of epidermal growth factor (Life Technologies, Burlington ON, Canada), Penicillin-Streptomycin, 10 mM nicotinamide, 2 mM L-glutamine, 10% fetal bovine serum, and 0.5 ug/mL Fungizone (Life Technologies, Burlington ON, Canada). BAML cells were generated using the method of "plate-and-wait" (Fougère-Deschâtrette *et al.*, 2006). Briefly, 5×10^5 freshly isolated primary hepatocytes were inoculated onto a 60 mm cell culture dish. Cells were cultured in BAML medium for 2-3 weeks with medium change every 3-4 days. Once visible colonies had formed on the plate, a colony was picked, completely dissociated into single-cell suspension with trypsin, and subcultured onto 24-well cell culture plates. In 2-3 weeks, a colony that formed in 24-well plates was again dissociated into single-cell suspension, diluted until roughly 1 cell/100 uL of media, and subcultured onto 96-well plates. Wells that contained single cells were marked and colonies that arose from those wells were labelled and passaged as BAML clones.

Transfection of HepG2 cells

HepG2 cells were cultured in Eagle's Minimum Essential Medium supplemented with Penicillin-Streptomycin, non-essential amino acids (Life Technologies, Burlington ON, Canada), and 10% fetal bovine serum. Transfection of HepG2 cells was carried out using lipid-based transfection

reagent FUGENE®HD (Roche Diagnostics, Laval, QC, Canada). Cells were seeded at 6×10^5 cells per well onto 6-well plates and transfected the next day with 6 μ L transfection reagent: 2 μ g of DNA in complete medium. Cells were collected 48 hours later for RNA extraction and quantitative PCR.

Quantification of Cyp1a2 and Nat2 transcript expression

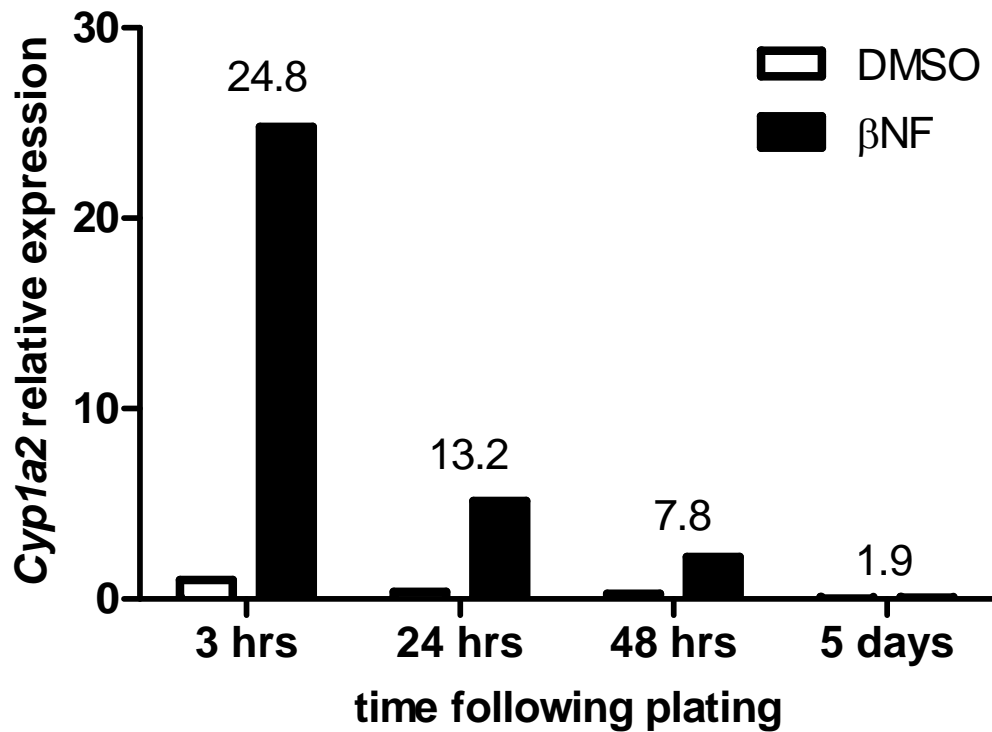
As described in Section 2.15.

Quantification of CYP1A2 activity

Carried out using *in vitro* and in culture phenacetin *O*-deethylation assays described in Appendix A Materials and Methods.

Results and discussion

Mouse primary hepatocytes were isolated as described in Materials and Methods. The levels of basal and β NF-induced CYP1A2 transcript expression and enzyme activity were measured daily over the course of several days in culture (Appendix figure 4).



Appendix figure 4. Basal and inducible *Cyp1a2* expression in mouse primary hepatocytes - a time-course study.

QPCR was used to quantify the level of *Cyp1a2* expression in mouse primary hepatocytes from 3 hours to 5 days following plating. Number above each pair of data bars represents fold *Cyp1a2* induction between β NF-treated (33 μ M for 24 hr) and vehicle-treated (DMSO) cells at each time point. The level of *Cyp1a2* expression was first normalized to the level of *Gapdh* within the same sample, and subsequently all samples were calibrated to the level of *Cyp1a2* in the DMSO-treated 3hr sample.

A drastic decrease in both basal and inducible *Cyp1a2* expression was observed over a period of 5 days. In addition, the level of CYP1A2 enzyme activity was measured using both the in culture and the microsomal-based *in vitro* phenacetin *O*-deethylation assay, which allowed a direct comparison to other liver model systems (Appendix table 1).

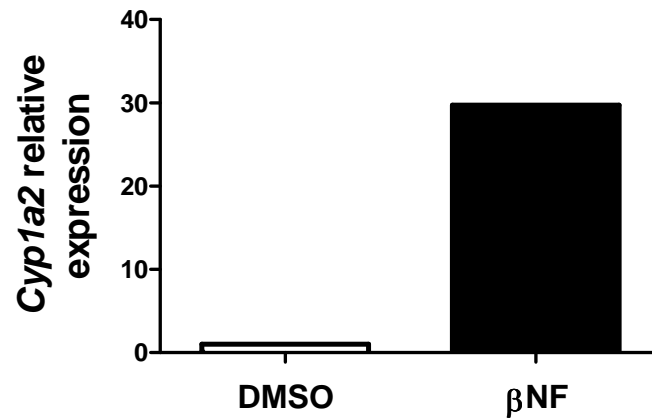
Appendix table 1. Basal and inducible CYP1A2 activity in different liver model systems in culture or *in vitro*^a.

source of enzyme	activity (nmol/min/mg) ^a	βNF inducibility (-fold induction)
mouse liver microsomes	0.23	50
mouse primary hepatocytes (day 0) - microsomes	0.032	5
mouse primary hepatocytes (day 0) - in culture	0.00017	13
HepG2 cells - microsomes	0.011	1
HepG2 cells - in culture	0.000051	5
Hepa1c1c7 cells - microsomes	ND	N/A
Hepa1c1c7 cells - in culture	ND	N/A
bipotential adult mouse liver cells - in culture	ND	N/A

^a*In vitro* activity is measured using the microsome-based phenacetin *O*-deethylation assay and in culture activity is measured using the in culture phenacetin *O*-deethylation assay. βNF was used to induce CYP1A2 *in vivo* in mouse liver (40 mg/kg intraperitoneally x 3 days) and in cell culture (33 μM for 24 hours). Microsomal protein concentrations in cell cultures were estimated by measuring the amount of protein in cells isolated from parallel cultures. “ND” = not detectable. “N/A” = not applicable.

As shown in Appendix table 1, microsomal CYP1A2 enzyme activity in freshly isolated mouse primary hepatocytes was roughly 10-fold lower than that found in mouse liver. Low basal and inducible CYP1A2 transcript expression and enzyme activity that rapidly decline over time in culture is in line with the behavior of other phase I drug-metabolizing enzymes described in the literature, and it represents a major shortcoming of the use of primary hepatocytes for the study of ABP metabolism.

To overcome the unstable expression of phase I drug-metabolizing enzymes in mouse primary hepatocytes, other groups have derived continuously proliferating BAML cell lines from mouse primary hepatocytes that can re-express liver specific markers when allowed to age at confluency (Fougère-Deschatrette et al., 2006). Following their published methodologies we generated BAML cells from mouse primary hepatocytes, grew them to confluency, and tested them for CYP1A2 transcript expression and enzyme activity (Appendix figure 5, Appendix table 1).



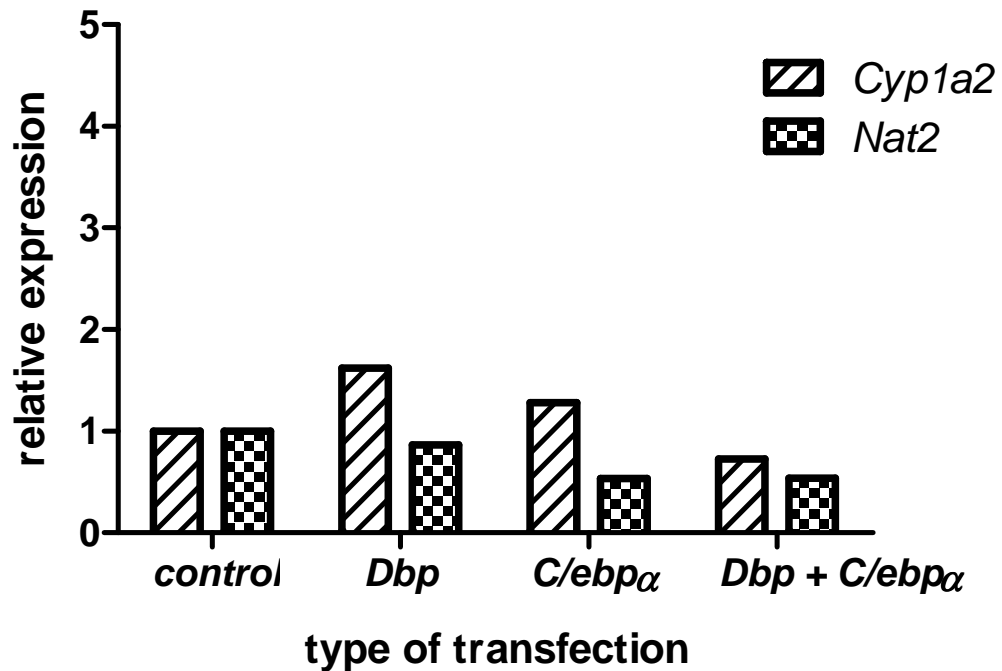
Appendix figure 5. Basal and inducible *Cyp1a2* transcript expression in BAML cells derived from mouse primary hepatocytes.

QPCR was used to quantify the level of *Cyp1a2* expression in BAML cells treated with βNF (33 μM for 24 hr) or vehicle (DMSO). The level of *Cyp1a2* expression was first normalized to the level of *Gapdh* within the same sample, and subsequently calibrated to the level of *Cyp1a2* in the vehicle-treated sample.

Even though *Cyp1a2* is expressed in BAML cells and its levels were inducible by βNF, no *in culture* phenacetin *O*-deethylation activity was detected in either uninduced or induced cells. The lack of CYP1A2 enzyme activity in BAML cells may be attributed to low expression of CYP1A2 protein, low expression of necessary co-factors (such as NADPH-cytochrome P450 oxidoreductase), or both. In any case, our results suggest that despite the expression and induction of *Cyp1a2* transcript, no CYP1A2 activity can be detected in BAML cells. The lack of CYP1A2 activity makes BAML cells not a useful model for the study of ABP metabolism.

Continuously passaged hepatoma cell lines are known to lack expression of many drug-metabolizing enzymes. We detected minimal *in culture* phenacetin *O*-deethylation activity in both HepG2 and Hepa1c1c7 cells (Appendix table 1). Several reports have suggested the importance of liver-enriched transcription factors C/EBPα and DBP in regulating the expression of genes encoding liver-specific drug-metabolizing enzymes (Schrem *et al.*, 2004). Previous work from our laboratory showed that co-transfection of *C/ebpa* and *Dbp* with a *Nat2* promoter region-containing reporter plasmid into HepG2 cells led to increased expression of the reporter gene. Since these transcription factors may not be endogenously expressed at sufficient levels in HepG2 cells to efficiently drive the expression of drug metabolizing enzymes, I attempted to construct a convenient and relevant liver cell culture system that expresses human CYP1A2

and/or human NAT2 using transient co-transfection of human *C/ebpa* and human *Dbp* into HepG2 cells (Appendix figure 6).



Appendix figure 6. Transcript expression of human *Cyp1a2* and *Nat2* in HepG2 cells with and without transfection of human *Dbp* and/or human *C/ebpα*.

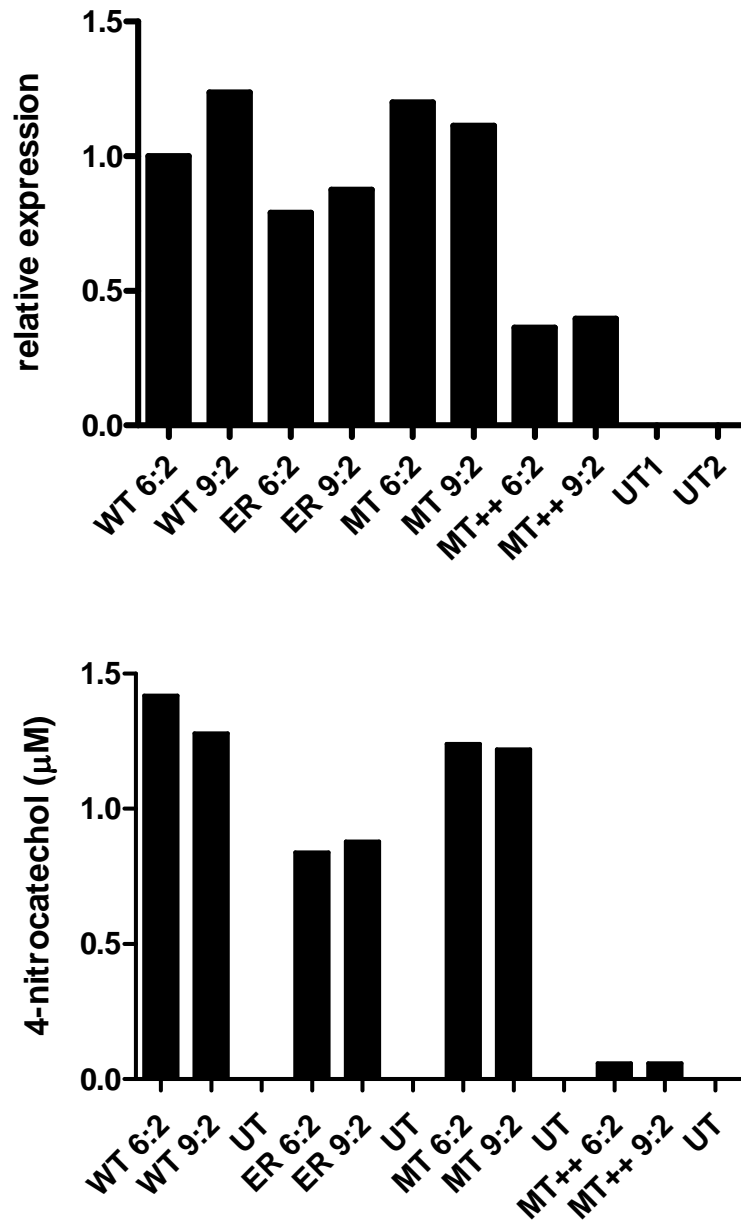
QPCR was used to quantify the level of *Cyp1a2* and *Nat2* expression in human *Dbp* and/or human *C/ebpα*, or mock transfected (control) HepG2 cells at 48 hours following transfection. The level of *Cyp1a2* and *Nat2* expressions were first normalized to the level of *Gapdh* within the same sample, and subsequently all samples were calibrated to the level of *Cyp1a2* and *Nat2* in control sample.

Transcripts were measured at 48 hours following transfection because the highest Enhanced Green Fluorescent Protein expression was found at this time point following similar transfection conditions (data not shown). No increase in human *Nat2* or *Cyp1a2* transcript expression could be detected in HepG2 cells transfected with human *Dbp* and *C/ebpα* alone or in combination. These results suggest that the absence of other yet unidentified factors is likely responsible for the poor gene expression observed in these cells.

In conclusion, we have confirmed observations by other groups that the expression levels of drug-metabolizing enzymes in mouse primary hepatocytes is many-fold lower than those found in mouse liver microsomes, and it rapidly declines further in culture. Using a recently published protocol for the generation of BAML cells from mouse primary hepatocytes, we detected both

basal and inducible transcript expression but no enzyme activity for CYP1A2 in BAML cells. We also confirmed observations by others that continuously passaged hepatoma cell lines do not express significant amounts of drug-metabolizing enzymes. Transfection of liver-enriched transcription factors *Dbp* and *C/ebpa* failed to reinstate the expression of the drug-metabolizing enzymes CYP1A2 and NAT2 in HepG2 cells. Overall, we were unable to establish a liver cell culture model with significant CYP1A2 expression for the investigation of ABP bioactivation. Given this current state of knowledge, we decided to investigate the bioactivation of ABP using mouse liver microsomes as a source of drug-metabolizing enzymes in an *in vitro* setting in Section 3.2. Once putative ABP bioactivation enzymes are established using mouse liver microsomes, they will be transfected into Hepa1c1c7 cells, which is used as a pan-knockout cell model for drug metabolizing enzymes, to test for their abilities to bioactivate ABP in a physiological cell culture setting.

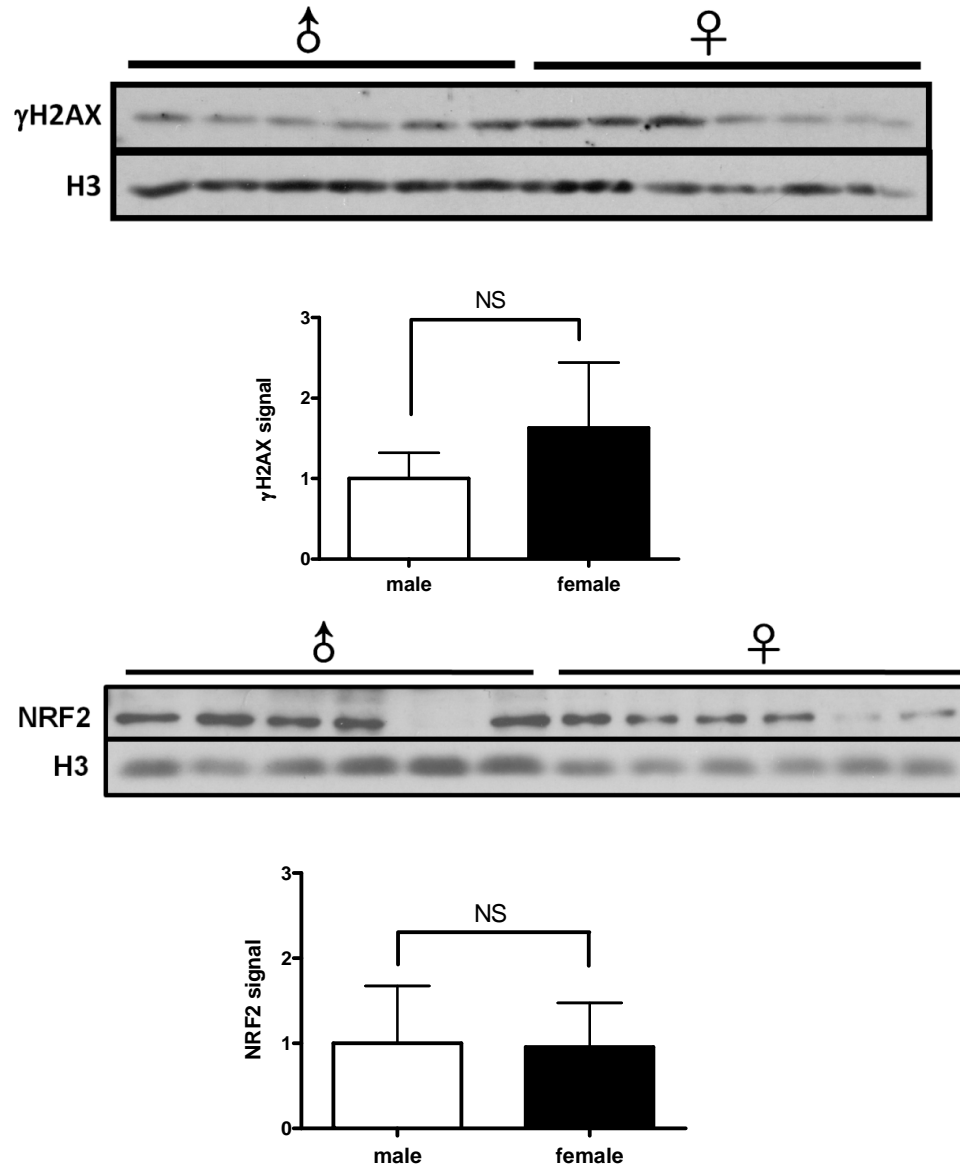
Appendix C. CYP2E1 transcript expression and activity in Hepa1c1c7 cells transfected with different rat *Cyp2e1* variants.



Appendix figure 7. CYP2E1 transcript expression and activity in Hepa1c1c7 cells transfected with different rat *Cyp2e1* variants

Different ratios of LTX transfection reagent: µg rat *Cyp2e1* plasmid DNA were tested. CYP2E1 expression (A) and activity (B) were quantified using QPCR and pNP hydroxylation in culture assay, respectively, at 24 hours following transfection. "UT" =negative control with no cell transfection.

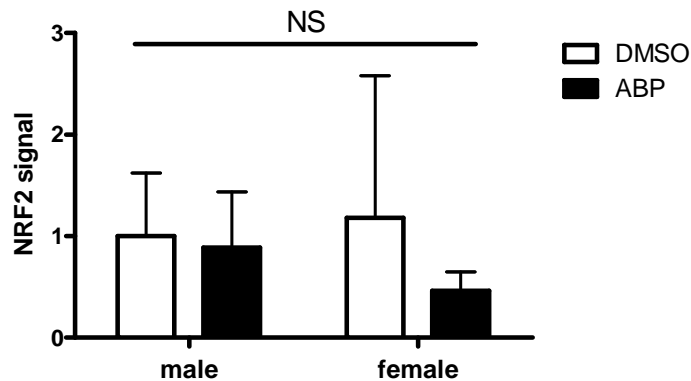
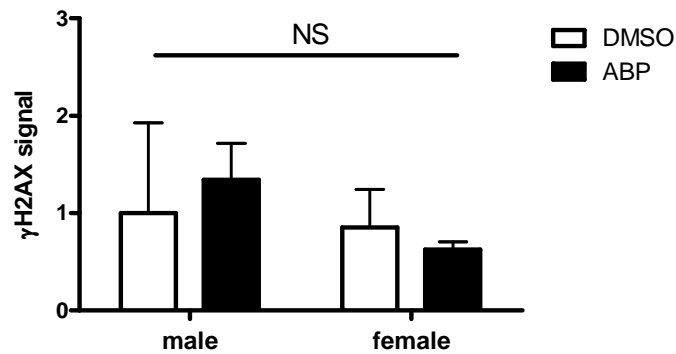
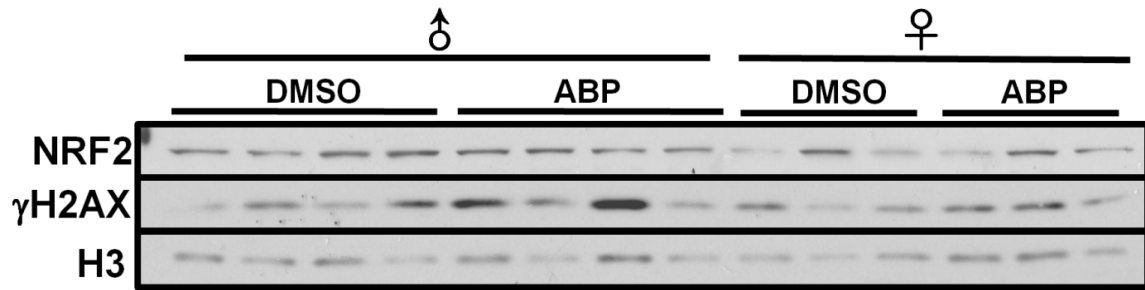
Appendix D. Basal γ H2AX and NRF2 levels in neonatal male and female C57BL/6 mouse livers.



Appendix figure 8. Basal γ H2AX and NRF2 levels in neonatal male and female C57BL/6 mouse livers.

Immunoblot showing ABP-induced γ H2AX and NRF2 in neonatal male and female livers at 24 hours following day 15 dose of DMSO vehicle (N=6). Liver nuclei homogenates were separated on a 12.5% SDS-PAGE gel, subjected to immunoblot analysis with anti- γ H2AX, NRF2, or H3 antibodies, quantified using densitometry, and analyzed by Image J software (NIH). Mean \pm S.D. was normalized to the average of male samples.

Appendix E. γ H2AX and NRF2 levels in day 8 male and female C57BL/6 mouse livers exposed to ABP.



Appendix figure 9. γ H2AX and NRF2 levels in day 8 male and female C57BL/6 mouse livers exposed to ABP.

Immunoblot showing ABP-induced γ H2AX in neonatal male (N=4) and female (N=3) livers at 24 hours following day 8 dose of ABP or DMSO vehicle. For immunoblots, liver nuclei homogenates were separated on a 12.5% SDS-PAGE gel, subjected to immunoblot analysis with anti- γ H2AX, NRF2, or H3 antibodies, quantified using densitometry, and analyzed by Image J software (NIH). Mean \pm S.D. was normalized to the average of DMSO vehicle-treated males.

Appendix F. (Publication)

Environmental and Molecular Mutagenesis 53:350–357 (2012)

Research Article

Influence of Arylamine *N*-Acetyltransferase, Sex, and Age on 4-Aminobiphenyl-Induced In Vivo Mutant Frequencies and Spectra in Mouse Liver

Shuang Wang,¹ Kim S. Sugamori,¹ Debbie Brenneman,¹ Ivy Hsu,¹ Adriana Calce,¹ and Denis M. Grant^{1,2*}

¹Department of Pharmacology & Toxicology, Faculty of Medicine, University of Toronto, Toronto, Ontario, Canada M5S 1A8

²Leslie Dan Faculty of Pharmacy, University of Toronto, Toronto, Ontario, Canada M5S 3M2

One model for cancer initiation by 4-aminobiphenyl (ABP) involves *N*-oxidation by cytochrome P450 CYP1A2 followed by *O*-conjugation by *N*-acetyltransferase(s) NAT1 and/or NAT2 and decomposition to a DNA-binding nitrenium ion. We recently observed that neonatal ABP exposure produced liver tumors in male but not in female mice, and that NAT deficiency reduced liver tumor incidence. However, ABP-induced liver tumor incidence did not correlate with liver levels of *N*-(deoxyguanosin-8-yl)-ABP adducts 24 hr after exposure. In this study, we compared in vivo ABP-induced DNA mutant frequencies and spectra between male and female wild-type and NAT-deficient MutaTMMouse using both the tumor-inducing neonatal exposure protocol and a 28-day repetitive dosing adult exposure protocol. ABP produced an increase in liver DNA mutant frequencies in both neonates and adults. However, we observed no sex or strain differences in

mutant frequencies in neonatally exposed mice, and higher frequencies in adult females than males. Neonatal ABP exposure of wild-type mice increased the proportion of G-T transversions in both males and females, while exposure of *Nat1/2*(-/-) mice produced increased G-T transversions in males and a decrease in females, even though females had higher levels of *N*-(deoxyguanosin-8-yl)-4-ABP adducts. There was no correlation of mutant frequencies or spectra between mice dosed as neonates or as adults. These results suggest that observed sex- and NAT-dependent differences in ABP-induced liver tumor incidence in mice are not due to differences in either mutation rates or mutational spectra, and that mechanisms independent of carcinogen bioactivation, covalent DNA binding and mutation may be responsible for these differences. *Environ. Mol. Mutagen.* 53:350–357, 2012. © 2012 Wiley Periodicals, Inc.

Key words: 4-aminobiphenyl; in vivo mutations; liver cancer; MutaTMMouse; arylamine *N*-acetyltransferases; sex differences

INTRODUCTION

4-Aminobiphenyl (ABP), an aromatic amine found in cigarette smoke and some hair dyes, is a probable human bladder carcinogen [Yu et al., 2002] that produces liver tumors in mice [Schieferstein et al., 1985]. Like other members of this class of chemicals, ABP is believed to require bioactivation in order to exert its deleterious effects [Siraki et al., 2002]. In one widely described bioactivation model based largely on in vitro studies, ABP is first *N*-hydroxylated by the cytochrome P450 isoform CYP1A2 to a hydroxylamine that is subsequently *O*-acetylated by arylamine *N*-acetyltransferase(s) NAT1 and/or NAT2 to form an unstable acetoxy ester [Butler et al., 1989a,b; Hammons et al., 1991; Kadlubar et al., 1991; Kerdar et al., 1993; Hlavica et al., 1997; Guengerich, 2000]. The acetoxy ester spontaneously breaks down to generate a highly reac-

tive nitrenium ion [Novak et al., 1993; McClelland et al., 1995] that can form covalent DNA adducts, which are

Abbreviations: ABP, 4-aminobiphenyl; C8-dG-ABP, *N*-(deoxyguanosin-8-yl)-4-aminobiphenyl; NAT, arylamine *N*-acetyltransferase; CYP1A2, cytochrome P4501A2.

Grant sponsors: Cancer Research Society, Canadian Institutes of Health Research.

*Correspondence to: Denis M. Grant, Medical Sciences Building, Rm 4207, 1 King's College Circle, Toronto, Ontario, Canada M5S 1A8. E-mail: denis.grant@utoronto.ca

Received 29 December 2011; provisionally accepted 7 March 2012; and in final form 9 March 2012

DOI 10.1002/em.21695

Published online 16 April 2012 in Wiley Online Library (wileyonlinelibrary.com).

believed to be critical in the production of mutations that initiate or promote tumor growth [Kadlubar et al., 1991; Poirier et al., 1995; Otteneider and Lutz, 1999; Tsuneoka et al., 2003]. However, more recent *in vivo* studies using CYP1A2-deficient *Cyp1a2(-/-)* mice have provided evidence that is inconsistent with the above model of ABP bioactivation and tumor initiation. Kimura et al. reported that when neonatal mice were administered ABP on postnatal days 8 and 15 and assessed for liver tumor formation at 1 year of age, there was no difference in liver tumor incidence between wild-type (C57BL/6) and *Cyp1a2(-/-)* mice [Kimura et al., 1999]. In another study, Tsuneoka et al. found higher levels of ABP-DNA adducts in adult *Cyp1a2(-/-)* mice than in wild-type mice following ABP exposure [Tsuneoka et al., 2003]. These studies not only call into question the role of CYP1A2 in the bioactivation of ABP to DNA-damaging metabolites *in vivo*, but also illustrate a striking lack of correlation between levels of ABP-DNA adducts and liver tumors, pointing to potential contributions from other cellular mechanisms in producing liver tumors following ABP exposure.

To further investigate the mechanism of ABP-induced liver tumor formation in mice, we recently compared the liver carcinogenicity of ABP in male and female wild-type (C57BL/6) and arylamine *N*-acetyltransferase-deficient *Nat1/2(-/-)* mice [Sugamori et al., 2003] using the same neonatal ABP dosing protocol used by Kimura and coworkers [Sugamori et al., 2012]. In this study, wild-type male mice had a much higher incidence of ABP-induced liver tumors than females, consistent with Kimura's observations [Kimura et al., 1999]. In addition, male *Nat1/2(-/-)* mice had a significantly lower incidence of liver tumors than wild-type males. We also quantified the predominant ABP-DNA adduct *N*-(deoxyguanosin-8-yl)-4-aminobiphenyl (C8-dG-ABP) in liver DNA following neonatal ABP administration. Unexpectedly, levels of the C8-dG-ABP adduct showed no sex difference in wild-type mice, and were higher in *Nat1/2(-/-)* mice than in wild-type mice. The lack of correlation between liver C8-dG-ABP adduct levels and tumor incidence suggests either that the sex and strain differences in tumor incidence result from DNA damaging events other than C8-dG-ABP adduct formation, or that they may be produced by mechanisms that are independent of the DNA-damaging effects of ABP.

According to accepted models of chemical carcinogenesis, DNA damage that escapes repair prior to DNA replication can be fixed into the genome as mutations that can subsequently influence the extent and/or rate of tumor initiation and growth. Both *in vitro* and *in vivo* studies have shown that ABP generates a high frequency of G-T transversions that are suggested to be critical in tumor initiation [Lasko et al., 1988; Verghis et al., 1997; Fletcher et al., 1998; Zayas-Rivera et al., 2001; Besaratinia et al., 2002; Heddle et al., 2003; Chen et al., 2005]. Furthermore, the ability of ABP to generate G-T transversions in mouse liver

has been taken as evidence for the importance of C8-dG-ABP adducts, which produce mainly G-T transversions *in vitro*, in tumor initiation [Chen et al., 2005]. The purpose of the current study was to use the transgenic MutaTM Mouse *in vivo* mutation model [Gossen et al., 1989] to determine whether sex and strain differences in ABP-induced mutant frequencies and/or mutation spectra could explain the differences we observed in liver tumor incidence following ABP exposure. The MutaTM Mouse λ gt10-*lacZ* transgenic mouse allows for the quantitation and characterization of *in vivo* mutations that lead to phenotypically selectable *cII* transgenes. We have used cross-breeding to obtain a MutaTM Mouse derivative that lacks both NAT1 and NAT2 activity, and have compared the mutagenic potency of ABP in male and female wild-type and *Nat1/2(-/-)* MutaTM Mouse using both the neonatal tumor-inducing exposure protocol and an adult 28-day subchronic dosing protocol in an attempt to improve the sensitivity of liver mutation detection in more mutation-resistant adult mice [Heddle et al., 2003].

MATERIALS AND METHODS

Chemicals and Animal Treatment

ABP (Aldrich brand A2898) and other chemicals were purchased from Sigma-Aldrich Canada (Oakville, ON, Canada). ABP was purified by the manufacturer by thin-layer chromatography to >99% purity, and it eluted as a single chromatographic peak by reverse-phase high performance liquid chromatography (HPLC) using UV detection at 280 nm and previously described chromatographic conditions [Sugamori et al., 2006]. All procedures involving animals were performed in accordance with Canadian Council on Animal Care guidelines. MutaTM Mouse breeding stocks [Gossen et al., 1989] were kindly provided by P.A. White and G.R. Douglas of the Mechanistic Studies Division, Environmental and Radiation Health Sciences Directorate, Health Canada, Ottawa, Ontario, Canada. *Nat1/2(-/-)* MutaTM Mouse animals were generated by crossing MutaTM Mouse with *Nat1/2(-/-)* mice [Sugamori et al., 2003], interbreeding the F1 hybrids, genotyping the F2 offspring for both the absence of the *Nat1/2* gene region and the presence of the MutaTM Mouse λ gt10-*lacZ* transgene (see below for details), and establishing appropriate breeding pairs for generation of tester mice. For the neonatal ABP exposure protocol, mice ($n = 5$ animals for each sex, strain and treatment group) were injected intraperitoneally on postnatal days 8 and 15 with 1/3 and 2/3 of the total dose of ABP, respectively, at total doses of 600 nmol (~8.5 mg/kg per dose) or 1,200 nmol (~17 mg/kg per dose), or with the corresponding volume of dimethyl sulfoxide (DMSO) vehicle. Livers were collected on postnatal day 21. For the adult subchronic exposure protocol, mice aged 8 weeks ($n = 5$ animals per sex, strain and treatment group) were injected intraperitoneally every second day for 28 days with ABP at 10 mg/kg per dose (total exposure ~20,000 nmol) or 20 mg/kg per dose (total exposure ~40,000 nmol), or with the corresponding volume of corn oil vehicle. Livers were collected 3 days after the final ABP treatment. Although no significant morbidity or mortality was observed using either the neonatal or the adult treatment protocol, at the time of sacrifice adult animals displayed typical signs of ABP-induced methemoglobinemia, including brown colored blood and splenic hyperplasia.

Nat1/2(-/-) and MutaTM Mouse Transgene Genotyping

Isolation of genomic DNA from mouse tails and polymerase chain reaction (PCR) assays for the absence of *Nat1/2* were performed

as described previously [Sugamori et al., 2003]. The presence of the MutaTMMouse transgene in genomic DNA was determined by PCR using primers 5'-GGACAGGAGCGTAATGTGGCA-3' (sense) and 5'-AATTGCAGCATCCGGTTTCAC-3' (antisense), each at a final concentration of 0.4 μ M, and the following PCR program: 94°C for 3 min; 35 cycles of 30 sec at 95°C, 30 sec 56°C, 45 sec at 72°C; and 5 min at 72°C. *Nat1/2(-/-)* mice that were also either homozygous or hemizygous for the *lgt10-lacZ* transgene were used in ABP exposure studies.

Liver Genomic DNA Isolation

High-molecular weight liver genomic DNA was prepared using a phenol-based extraction method. In brief, approximately 100 mg of frozen liver was thawed and manually homogenized in 5 mL of ice cold homogenization buffer (50 mM Tris-HCl pH 7.6, 5 mM MgCl₂, 50 mM NaCl, 1 mM EDTA, 5% v/v glycerol, and 0.1% Triton X-100) using a Dounce homogenizer and Teflon pestle. The homogenate was centrifuged for 10 min at 1,100g at 4°C, and the pellet of cell nuclei was resuspended in 3 mL of proteinase K buffer (0.1M Tris-HCl pH 8.0, 5 mM EDTA, 0.2M NaCl, 0.2% w/v sodium dodecyl sulfate (SDS)). RNase A (3 μ L of a 10 mg/mL stock) was added and the sample was incubated with gentle rocking for 60 min at 37°C. Proteinase K (10 μ L of a 20 mg/mL stock) was added, the mixture was incubated with gentle rocking for 90 min at 55°C, a second aliquot of enzyme was added and the incubation was repeated. The mixture was then extracted using an equal volume of phenol, followed by phenol:chloroform:isoamyl alcohol (25:24:1, v/v/v) and chloroform:isoamyl alcohol (24:1, v/v) for 10 min each at room temperature with gentle rocking. Finally, an equal volume of ice-cold isopropanol was added to the extract and gently inverted until genomic DNA precipitated. The DNA was spooled with a glass hook, briefly rinsed in 70% ethanol, air-dried for 5 min, and the purified DNA was redissolved in 50 μ L of 10 mM Tris-HCl, 1 mM EDTA, pH 7.6 at 37°C overnight. Only highly viscous DNA with a concentration greater than 1 μ g/ μ L and an A260/280 ratio of >1.60 was used for subsequent in vitro packaging reactions.

λ Phage Packaging and *cII* Mutation Assay

The λ Select-*cII* Mutation Detection System and Transpack Packaging Extracts were purchased from Agilent Technologies (Mississauga, ON, Canada). λ phage packaging and *cII* mutation assays were performed according to the manufacturer's instructions, with assessment of titering plates for plaques at 24–48 hr after plating and screening plates at 48–72 hr after plating. Preliminary re-plating experiments confirmed the *cII* mutant status of ~95% of initially detected screening plaques.

cII Mutant Gene Sequence Analysis

A total of 30–40 *cII* mutant plaques from among the animals in each treatment group were re-plated and sequenced using the manufacturer's protocol, with the following modifications. PCR reactions were performed using the following program: 95°C for 3 min; 40 cycles of 30 sec at 95°C, 1 min at 54°C, 1 min at 72°C; and 10 min at 72°C. PCR products were purified and sequenced at The Centre for Applied Genomics (The Hospital for Sick Children, Toronto, ON, Canada). DNA sequences of wild-type and mutant *cII* genes were compared using EMBOSS Needle software, available on the European Bioinformatics Institute website (<http://www.ebi.ac.uk/>). Mutational spectra were compared using the algorithm developed by Adams and Skopek [Adams and Skopek, 1987; Cariello et al., 1994], with six pairwise comparisons made between treated and control animals, between sexes and between strains.

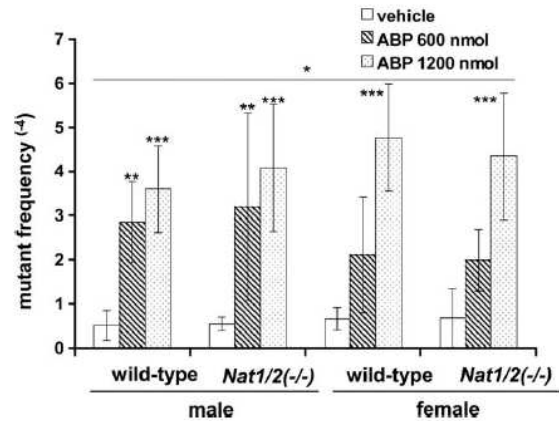


Fig. 1. Influence of sex and *Nat1/2* on ABP-induced mutant frequencies in neonatally exposed wild-type and *Nat1/2(-/-)* MutaTMMouse. Mice ($n = 5$ per group) were injected with vehicle, 600 nmol or 1200 nmol of ABP on postnatal days 8 and 15, and sacrificed 5 days after the final injection for liver mutant frequency determination using the MutaTMMouse assay. Error bars represent standard deviations of mean values. (* $P < 0.05$ for effect of ABP dose on mutant frequency across all groups. ** $P < 0.01$ relative to respective vehicle-dosed group. *** $P < 0.001$ relative to respective vehicle-dosed group).

RESULTS

ABP-Induced *cII* Mutant Frequencies in Neonatally Exposed Mice

Mutant frequencies were determined in male and female wild-type and *Nat1/2(-/-)* neonatal mice administered DMSO vehicle, 600 nmol or 1,200 nmol of ABP (Fig. 1). Two-way and three-way ANOVA analyses followed by Bonferroni post-tests of the neonatal mutant frequency data identified a significant dose-dependent increase in mean mutant frequencies with the administration of ABP ($P < 0.05$). However, no significant sex or strain differences were observed using either analysis ($P > 0.05$).

ABP-Induced *cII* Mutant Frequencies in Adult Mice

To compare the ability of ABP to generate mutations in neonatal and adult mice, ABP-induced mutant frequencies were also determined in adult (8 week) male and female wild-type and *Nat1/2(-/-)* mice administered ABP at 10 mg/kg or 20 mg/kg every other day for 28 days, corresponding to total exposures of approximately 20,000 and 40,000 nmol per animal, respectively (Fig. 2). Two-way ANOVA analyses of the adult mutant frequency data identified a significant dose-dependent increase in mean mutant frequencies with the administration of ABP. However, subsequent Bonferroni post-tests indicated that only females treated with the high dose of ABP (both wild-type and *Nat1/2(-/-)*) showed significantly increased mutant frequencies compared to their respective vehicle con-

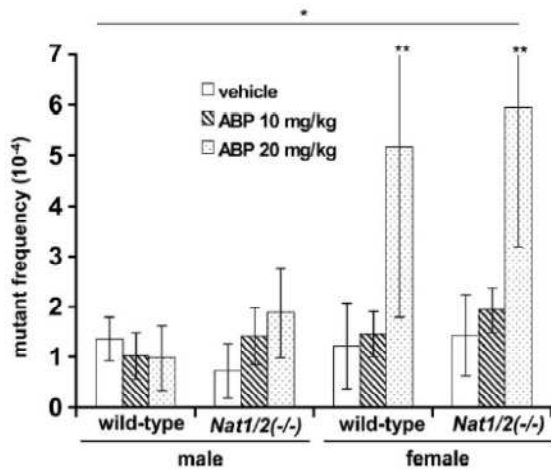


Fig. 2. ABP-induced mutant frequencies in adult wild-type and *Nat1/2(-/-)* MutaTM Mouse. Adult mice ($n = 5$ per group) were injected with vehicle, 10 mg/kg or 20 mg/kg of ABP every second day for 28 days, and sacrificed 3 days after the last injection for liver mutant frequency determination using the MutaTM Mouse assay. Error bars represent standard deviations of mean values. (* $P < 0.001$ for effect of ABP dose on mutant frequency across all groups, ** $P < 0.001$ relative to respective vehicle-dosed group).

trols. In addition, adult females displayed significantly higher mean mutant frequencies than males at the high dose of ABP ($P < 0.001$) but not at the low dose or in vehicle controls ($P > 0.05$). Furthermore, there was no significant difference between wild-type and *Nat1/2(-/-)* female mice ($P > 0.05$). A three-way ANOVA analysis confirmed a significant effect of ABP dose ($P < 0.001$) and sex ($P < 0.001$), as well as a sex \times dose interaction ($P < 0.001$). To ensure that the mutant frequencies (which were not corrected for possible clonality) were not unduly affected by jackpot mutations from clonally expanded mutated cells [Heddle, 1999], mutant frequency medians were also compared between groups of both neonatal and adult animals. The results were similar to those generated using mean values (data not shown), consistent with recent studies using the hepatocarcinogen diethylnitrosamine where correction for clonality had little influence on the liver mutant frequency [Mirsalis et al., 2005].

ABP-Induced *cII* Mutation Spectra in Neonatal Mice

To determine the type(s) of DNA base pair damage induced by ABP, we determined ABP-induced mutation spectra for representative male and female, wild-type, and *Nat1/2(-/-)* mice exposed to either 1,200 nmol ABP or vehicle control using the neonatal exposure protocol (Table I). Using the Adams and Skopek algorithm [Adams and Skopek, 1987] we detected a significant change in mutation spectra with ABP treatment in all ani-

mals ($P < 0.01$) except *Nat1/2(-/-)* females. As expected, the largest changes observed were in the proportion of G-T transversions, which increased in all animals except *Nat1/2(-/-)* females, where a decrease was detected. We also detected a significant change in ABP-induced mutation spectra between wild-type and *Nat1/2(-/-)* female mice ($P < 0.05$). The largest difference was found with the proportion of ABP-induced G-T transversions, where wild-type females showed an increase but *Nat1/2(-/-)* females showed a decrease.

ABP-Induced *cII* Mutation Spectra in Adult Mice

To compare the nature of the ABP-induced mutations between neonatal and adult mice, we also generated mutation spectra data for adult male and female, wild-type, and *Nat1/2(-/-)* mice exposed to either 20 mg/kg of ABP or vehicle control every other day for 28 days (total $\sim 40,000$ nmoles) (Table II). ABP did not induce a statistically significant change in mutation spectra regardless of sex or NAT1/2 status using the Adams and Skopek algorithm. Comparing between ABP-treated animals, only *Nat1/2(-/-)* female mice had a significantly different mutation spectrum than wild-type females ($P < 0.05$). Closer examination revealed both a higher proportion of G-T transversions and a lower proportion of G-A transitions in the *Nat1/2(-/-)* female mice.

Although we observed a modest degree of clustering of mutations on particular nucleotides of the *cII* gene in both neonatally exposed and adult mice (data not shown), this is likely a consequence of the assay's selection for mutations that produce changes in the *cII* protein that markedly impair its function, rather than clonal expansion of jackpot mutations. In addition, the most common specific mutation detected among all *cII* gene sequences was a G insertion before G179, which represented up to 21% of all mutations in the ABP-treated female *Nat1/2(-/-)* samples. However, this is probably due to its proximity to a six G repeat that makes this section of the *cII* gene particularly sensitive to both G insertions and G deletions. Although G-T transversion mutations showed no clustering in any particular locations within the *cII* transgene, this does not preclude the possibility that such hotspots could exist in relevant endogenous genes. Nonetheless, this finding along with the similar results that we obtained for mutant frequencies using mean and median values suggests that the contribution of clonal jackpot mutations was minor. However, a limitation of the analysis described above is the relatively small number of sequenced mutations per strain, sex, and treatment group.

DISCUSSION

ABP has been proposed to exert its carcinogenic effect in the liver through bioactivation by CYP1A2 and NAT1/

TABLE I. ABP-Induced Mutation Spectra in Neonatally Exposed Wild-Type and *Nat1/2(-/-)* MutaTMMouse^a

	Male				Female			
	Wild-type		<i>Nat1/2(-/-)</i>		Wild-type		<i>Nat1/2(-/-)</i>	
	Vehicle (%)	ABP (%) ^b	Vehicle (%)	ABP (%) ^b	Vehicle (%)	ABP (%) ^b	Vehicle (%)	ABP (%) ^c
G:C→A:T	11 (34)	6 (15)	12 (38)	7 (17)	11 (36)	4 (12)	6 (21)	9 (28)
G:C→T:A	7 (22)	21 (54)	5 (16)	21 (51)	5 (16)	14 (42)	7 (25)	2 (6)
A:T→C:G	0	0	1 (3)	0	0	2 (6)	2 (7)	4 (13)
A:T→G:C	0	3 (8)	2 (6)	3 (7)	0	1 (3)	2 (7)	3 (9)
C:G→G:C	0	5 (13)	0	3 (7)	4 (13)	4 (12)	1 (4)	4 (13)
T:A→A:T	4 (13)	3 (8)	2 (6)	2 (5)	7 (23)	2 (6)	2 (7)	2 (6)
Other ^d	10 (31)	1 (3)	10 (31)	5 (12)	4 (13)	6 (18)	8 (29)	8 (25)
Total mutations	32 (100)	39 (100)	32 (100)	41 (100)	31 (100)	33 (100)	28 (100)	32 (100)

^aMice were injected on postnatal days 8 and 15 with vehicle (DMSO) or 1200 nmol ABP (total), and sacrificed 5 days after the last injection for determination of mutation spectra using the MutaTMMouse assay.

^bSignificantly different from the corresponding vehicle treated mice ($P < 0.01$, Adams and Skopek algorithm).

^cSignificantly different from female ABP-treated wild-type mice ($P < 0.05$, Adams and Skopek algorithm).

^dMostly single base pair insertions or deletions.

TABLE II. ABP-Induced Mutation Spectra in Adult Wild-Type and *Nat1/2(-/-)* MutaTMMouse^a

	Male				Female			
	Wild-type		<i>Nat1/2(-/-)</i>		Wild-type		<i>Nat1/2(-/-)</i>	
	Vehicle (%)	ABP (%)	Vehicle (%)	ABP (%)	Vehicle (%)	ABP (%)	Vehicle (%)	ABP (%) ^b
G:C→A:T	18 (45)	14 (50)	10 (35)	12 (43)	5 (17)	18 (45)	14 (32)	9 (22)
G:C→T:A	6 (15)	3 (11)	6 (21)	6 (21)	12 (41)	11 (28)	17 (39)	22 (54)
A:T→C:G	1 (3)	2 (7)	1 (3)	2 (7)	1 (3)	1 (3)	2 (5)	0 (0)
A:T→G:C	2 (5)	3 (11)	1 (3)	1 (4)	0 (0)	1 (3)	1 (2)	2 (5)
C:G→G:C	3 (8)	1 (4)	2 (7)	1 (4)	4 (14)	6 (15)	6 (14)	4 (10)
T:A→A:T	1 (3)	0(0)	1 (3)	1 (4)	4 (14)	2 (5)	1 (2)	0 (0)
Others ^c	9 (23)	5 (18)	8 (28)	5 (18)	3 (10)	1 (3)	3 (7)	4 (10)
Total mutations	40 (100)	28 (100)	29 (100)	28 (100)	29 (100)	40 (100)	44 (100)	41 (100)

^aAdult mice (8 weeks of age) were injected with vehicle (corn oil) or 20 mg/kg of ABP every other day for 28 days, and sacrificed 3 days after the final injection for determination of mutation spectra using the MutaTMMouse assay.

^bSignificantly different from female ABP-treated wild-type mice ($P < 0.05$, Adams and Skopek algorithm).

^cMostly single base pair insertions or deletions.

2 to generate C8-dG-ABP, which translates into G-T transversions in the genome that can initiate tumor growth by altering the functions of key gene products that control cell survival and proliferation. However, we [Sugamori et al., 2012] and others [Kimura et al., 1999; Tsuneoka et al., 2003] have provided evidence against the involvement of NAT1/2 and CYP1A2 in ABP bioactivation to form C8-dG-ABP, and have also observed no correlation between liver C8-dG-ABP levels and liver tumor incidence. At the same time, a consistent and markedly lower incidence of ABP-induced liver tumors was observed in female mice. Although the mechanism for this female protection against ABP-induced liver tumors has not yet been determined, similar observations have been made with other liver carcinogens, including both chemicals and viral agents. For instance, a sexual dimorphism in liver cancer caused by the chemically unrelated carcinogen diethylnitrosamine (DEN) has been suggested to occur due to an estrogen-dependent difference in the cyto-

kine-mediated inflammatory response to acute chemical exposure, resulting in differential proliferation of initiated cells in males and females [Naugler et al., 2007]. More recent studies have suggested that both estrogenic and androgenic effects contribute to the sex difference in DEN-induced liver cancer incidence, and that these effects are regulated by the forkhead box A transcription factors FOXA1 and FOXA2, which regulate liver development and metabolism [Li et al., 2012].

In the current study, we wished to further our understanding of the genotoxic properties of ABP that may contribute to tumor formation by investigating roles of NAT1/2 enzyme function, sex and age on ABP-induced mutant frequencies and spectra in vivo in mouse liver. ABP administration following the neonatal ABP exposure protocol that we used to induce tumors in our previous carcinogenicity study [Sugamori et al., 2012] led to a significant dose-dependent increase in mutant frequencies in neonatal mouse liver, confirming the ability of ABP to

generate mutations using this tumor-inducing protocol. However, these mutant frequencies do not correlate with levels of C8-dG-ABP adducts that we measured using the same ABP exposure protocol [Sugamori et al., 2012]. This lack of correlation suggests that C8-dG-ABP may not be the main DNA lesion induced by ABP in vivo in the mouse liver that translates into mutations and/or is responsible for tumor initiation. Moreover, since the ABP-induced mutant frequencies in neonatally exposed mice do not demonstrate any sex- or NAT-dependent differences, our results suggest that differences in ABP-induced mutations may not be responsible for the observed sex- and NAT-dependent differences in tumor incidence. Similar to neonates, ABP administration to adults also led to a dose-dependent increase in mutant frequencies. However, the absolute mutant frequencies tended to be lower in adults than in neonates, especially at lower ABP doses, despite much greater total ABP exposures (20,000–40,000 nmol vs. 600–1,200 nmol). This confirms previous findings that neonatally exposed animals are much more sensitive to the mutagenic effects of ABP, presumably because the increased rate of cell proliferation in developing liver enhances the likelihood of fixation of mutations instead of damage repair [Chen et al., 2005]. Unlike in neonates where no sex differences were observed, adult females demonstrated significantly higher levels of ABP-induced mutant frequencies than males, which correlates with the C8-dG-ABP data we generated using adult mice [Sugamori et al., 2012]. However, these data are in stark contrast to the much lower tumor incidence observed in female mice. One possible drawback to making such comparisons is the fact that the previous tumor incidence study [Sugamori et al., 2012] was performed in wild-type and *Nat1/2(-/-)* mice on an inbred C57BL/6 genetic background, while the mice used in the present study consist of a mixed C57BL/6 × BALB/C × DBA2 background. Mouse strain differences in liver tumor susceptibility are well documented, with the C57BL/6 strain being relatively tumor-resistant [Drinkwater and Ginsler, 1986]. Although strain differences in multiple factors that contribute to ABP mutagenicity are possible, we see comparable levels of NAT enzyme activity between C57BL/6 mice and our wild-type MutaTMMouse strains, and no sex difference in activity (data not shown). Nonetheless, the discrepancies we observed between neonates and adults and between acute damage/mutation studies and tumor induction experiments seem to suggest the importance of age- and sex-related factors, but not NAT-related differences, in the genotoxic and mutagenic actions of ABP, while NAT differences clearly influence liver tumor incidence. They also suggest that short-term and in vitro studies of ABP-induced DNA damage and mutation that have been carried out in either neonatal or adult mice must be interpreted and extrapolated with caution as predictors of tumor risk.

An increase in G-T transversions following ABP exposure has been reported previously, and was attributed to the formation of C8-dG-ABP [Chen et al., 2005; Yoon et al., 2012]. We also observed a significant increase in the proportion of G-T transversions in wild-type mice dosed using the neonatal ABP exposure protocol. In *Nat1/2(-/-)* mice, the males also showed a significant increase in the proportion of G-T transversions. However, we observed a significant decrease in G-T transversions in female *Nat1/2(-/-)* mice exposed to ABP neonatally. Although the reason for this observation is still unclear, the possibility that increased G-T transversions are the result of other types of DNA lesions, such as 8-oxo-deoxyguanosine [Hussain et al., 2000; Marrogi et al., 2001; Tsuzuki et al., 2001; Alt-Tassan et al., 2002], is currently under investigation. As with the mutant frequencies, the ABP-induced mutation spectra in adults were distinct from those in neonates, with the most prominent difference being a lack of increase in G-T transversions in all groups of adult mice. Although the relatively small number of mutants analyzed in our study precludes any firm conclusions, our results are consistent with the findings of Chen et al. [2005], and highlight the potential importance of age-related factors in determining the genotoxic actions of ABP.

Since the overall frequencies of G-T transversions that we observed across sexes, strains, and developmental stages do not appear to correlate with either levels of C8-dG-ABP adducts in neonates or with tumor growth [Sugamori et al., 2012], our data do not support a direct causal link between C8-dG-ABP adducts, ABP-induced mutations, and subsequent tumor growth in vivo in mouse liver. It remains possible that ABP induces mutational events in key tumor suppressor and/or promoter gene hotspots that are critical to ABP tumorigenesis, a possibility that cannot be addressed in the current study. It is also possible that decreased NAT-mediated ABP bioactivation in *Nat1/2(-/-)* mice is compensated by other bioactivating pathways such as *O*-sulfation or *O*-glucuronidation, which can also lead to reactive nitrenium ion formation. Based on our data, however, it is also possible that DNA damage is necessary but neither sufficient nor rate-limiting for eventual tumor growth, and that hormonal and/or inflammatory processes occurring subsequent to the obligate DNA-damaging tumor initiation stage produce the sex and strain differences in liver tumor growth that we observe. Importantly, our results may also suggest that the NAT proteins could play key roles in tumor development that are entirely independent of carcinogen bioactivation, since *Nat1/2(-/-)* mice are significantly protected from liver tumor growth in the absence of any evidence so far for reduced DNA damage or mutations [Sugamori et al., 2012]. This would be consistent with a number of recent studies demonstrating that human NAT1 is overexpressed in tumors of the breast and other tissues, that increasing NAT1 expression in cultured transformed cells enhances

their growth, survival, and resistance to cytotoxic agents, and that inhibition of NAT1 expression leads to contact inhibition of cell growth and decreased tissue invasion potential (reviewed in [Butcher and Minchin, 2012]). In this regard, it will be important to determine whether the effect of NAT deficiency on liver tumor growth extends to agents whose bioactivation is known to be unrelated to NAT-dependent acetylation. Such studies are currently in progress.

In 2008, the International Agency for Research on Cancer estimated that liver cancer is the 5th most common cancer in men and the 7th in women [Ferlay et al., 2010]. Such high incidences of liver cancer strongly advocate for a better understanding of the underlying disease mechanisms, which may lead to novel prevention measures and drug targets. It is of interest that ABP produced liver tumors in our mouse carcinogenicity study with a sex preference that parallels the 3- to 4-fold higher liver cancer incidence seen in men than in women. Although there is little direct human epidemiological evidence to suggest that exposure to aromatic amines is a risk factor for liver cancer, risk is higher in cigarette smokers [Zhu et al., 2007], who are exposed to these agents along with members of many other chemical classes. Thus it is possible that mechanisms that influence risk from cancers in the liver and other organs produced by aromatic amines may have some similarities. Nonetheless, the results of the current study add to the accumulating evidence to suggest that differences in ABP-induced DNA base pair damage and resulting mutations cannot account for the observed sex- and NAT1/2-related differences in liver tumor incidence. Although DNA damage may be required to produce tumor-initiating mutations, additional factors such as chronic inflammatory processes, proliferative responses, oxidative stress, and ongoing cellular and DNA damage may be more important in determining the ultimate extent and/or rate of eventual tumor growth. These may relate to hormonally regulated pathways and to additional yet to be uncovered functions of the NAT proteins.

ACKNOWLEDGMENTS

Authors thank P.A. White and G.R. Douglas of the Environmental and Radiation Health Sciences Directorate, Health Canada, Ottawa, Ontario, Canada for kindly providing the MutaTM Mouse breeding stocks and for their critical advice and guidance in the conduct and interpretation of the results of the described experiments.

DG and KS designed the study and applied for institutional Animal Care Committee approval. KS and DB developed the mouse strains and genotyping assays. DG and DB generated test mice from breeding colonies. DG, DB, and SW performed animal injections and collected tissues. DB and AC performed mouse tail DNA genotyp-

ing assays. SW, IH, and DG isolated liver genomic DNA and performed mutant frequency assays. SW and AC prepared cII gene PCR products and performed cII gene mutation spectrum analyses. SW analyzed the data and prepared draft figures and tables. SW prepared the manuscript draft with important intellectual input from KS and DG. All authors revised and approved the final manuscript. All authors had complete access to the study data.

REFERENCES

- Adams WT, Skopek TR. 1987. Statistical test for the comparison of samples from mutational spectra. *J Mol Biol* 194:391–396.
- Al-Tassan N, Chmiel NH, Maynard J, Fleming N, Livingston AL, Williams GT, Hodges AK, Davies DR, David SS, Sampson JR, Cheadle JP. 2002. Inherited variants of MYH associated with somatic G:C→T:A mutations in colorectal tumors. *Nat Genet* 30:227–232.
- Besaratinia A, Bates SE, Pfeifer GP. 2002. Mutational signature of the proximate bladder carcinogen *N*-hydroxy-4-acetylamino-biphenyl: Inconsistency with the p53 mutational spectrum in bladder cancer. *Cancer Res* 62:4331–4338.
- Butcher NJ, Minchin RF. 2012. Arylamine *N*-acetyltransferase 1: A novel drug target in cancer development. *Pharmacol Rev* 64:147–165.
- Butler MA, Guengerich FP, Kadlubar FF. 1989a. Metabolic oxidation of the carcinogens 4-aminobiphenyl and 4,4'-methylene-bis(2-chloroaniline) by human hepatic microsomes and by purified rat hepatic cytochrome P-450 monooxygenases. *Cancer Res* 49:25–31.
- Butler MA, Iwasaki M, Guengerich FP, Kadlubar FF. 1989b. Human cytochrome P-450PA (P-450IA2), the phenacetin *O*-deethylase, is primarily responsible for the hepatic 3-demethylation of caffeine and *N*-oxidation of carcinogenic arylamines. *Proc Natl Acad Sci USA* 86:7696–7700.
- Cariello NF, Piegorsch WW, Adams WT, Skopek TR. 1994. Computer program for the analysis of mutational spectra: Application to p53 mutations. *Carcinogenesis* 15:2281–2285.
- Chen T, Mittelstaedt RA, Beland FA, Heflich RH, Moore MM, Parsons BL. 2005. 4-Aminobiphenyl induces liver DNA adducts in both neonatal and adult mice but induces liver mutations only in neonatal mice. *Int J Cancer* 117:182–187.
- Drinkwater NR, Ginsler JJ. 1986. Genetic control of hepatocarcinogenesis in C57BL/6J and C3H/HeJ inbred mice. *Carcinogenesis* 7:1701–1707.
- Ferlay J, Shin HR, Bray F, Forman D, Mathers C, Parkin DM. 2010. Estimates of worldwide burden of cancer in 2008: GLOBOCAN 2008. *Int J Cancer* 127:2893–2917.
- Fletcher K, Tinwell H, Ashby J. 1998. Mutagenicity of the human bladder carcinogen 4-aminobiphenyl to the bladder of MutaMouse transgenic mice. *Mutat Res* 400:245–250.
- Gossen JA, de Leeuw WJ, Tan CH, Zwarthoff EC, Berends F, Lohman PH, Knook DL, Vijg J. 1989. Efficient rescue of integrated shuttle vectors from transgenic mice: A model for studying mutations in vivo. *Proc Natl Acad Sci USA* 86:7971–7975.
- Guengerich FP. 2000. Metabolism of chemical carcinogens. *Carcinogenesis* 21:345–351.
- Hammons GJ, Dooley KL, Kadlubar FF. 1991. 4-Aminobiphenyl-hemoglobin adduct formation as an index of in vivo *N*-oxidation by hepatic cytochrome P-450IA2. *Chem Res Toxicol* 4:144–147.
- Heddle JA. 1999. On clonal expansion and statistics for somatic mutations in vivo. *Mutagenesis* 14:257–260.
- Heddle JA, Martus HJ, Douglas GR. 2003. Treatment and sampling protocols for transgenic mutation assays. *Environ Mol Mutagen* 41:1–6.

- Hlavica P, Golly I, Lehnerer M, Schulze J. 1997. Primary aromatic amines: Their N-oxidative bioactivation. *Hum Exp Toxicol* 16:441–448.
- Hussain SP, Raja K, Amstad PA, Sawyer M, Trudel LJ, Wogan GN, Hofseth LJ, Shields PG, Billiar TR, Trautwein C, Hohler T, Galle PR, Phillips DH, Markin R, Marrogi AJ, Harris CC. 2000. Increased p53 mutation load in nontumorous human liver of Wilson disease and hemochromatosis: oxylradical overload diseases. *Proc Natl Acad Sci USA* 97:12770–12775.
- Kadlubar FF, Dooley KL, Teitel CH, Roberts DW, Benson RW, Butler MA, Bailey JR, Young JF, Skipper PW, Tannenbaum SR. 1991. Frequency of urination and its effects on metabolism, pharmacokinetics, blood hemoglobin adduct formation, and liver and urinary bladder DNA adduct levels in beagle dogs given the carcinogen 4-aminobiphenyl. *Cancer Res* 51:4371–4377.
- Kerdar RS, Dehner D, Wild D. 1993. Reactivity and genotoxicity of arylnitrenium ions in bacterial and mammalian cells. *Toxicol Lett* 67:73–85.
- Kimura S, Kawabe M, Ward JM, Morishima H, Kadlubar FF, Hammons GJ, Fernandez-Salguero P, Gonzalez FJ. 1999. CYP1A2 is not the primary enzyme responsible for 4-aminobiphenyl-induced hepatocarcinogenesis in mice. *Carcinogenesis* 20:1825–1830.
- Lasko DD, Harvey SC, Malaikal SB, Kadlubar FF, Essigmann JM. 1988. Specificity of mutagenesis by 4-aminobiphenyl. A possible role for N-(deoxyadenosin-8-yl)-4-aminobiphenyl as a premutational lesion. *J Biol Chem* 263:15429–15435.
- Li Z, Tuteja G, Schug J, Kaestner KH. 2012. Foxa1 and Foxa2 are essential for sexual dimorphism in liver cancer. *Cell* 148:72–83.
- Marrogi AJ, Khan MA, van Gijssel HE, Welsh JA, Rahim H, Demetris AJ, Kowdley KV, Hussain SP, Nair J, Bartsch H, Okby N, Poirier MC, Ishak KG, Harris CC. 2001. Oxidative stress and p53 mutations in the carcinogenesis of iron overload-associated hepatocellular carcinoma. *J Natl Cancer Inst* 93:1652–1655.
- McClelland RA, Davise PA, Hadzialic G. 1995. Electron-deficient strong bases: Generation of the 4-biphenyl- and 2-fluorenylnitrenium ions by nitrene protonation in water. *J Am Chem Soc* 117:4173–4174.
- Mirsalis JC, Shimon JA, Johnson A, Fairchild D, Kanazawa N, Nguyen T, de Boer J, Glickman B, Winegar RA. 2005. Evaluation of mutant frequencies of chemically induced tumors and normal tissues in lambda/cII transgenic mice. *Environ Mol Mutagen* 45:17–35.
- Naugler WE, Sakurai T, Kim S, Maeda S, Kim K, Elsharkawy AM, Karin M. 2007. Gender disparity in liver cancer due to sex differences in MyD88-dependent IL-6 production. *Science* 317:121–124.
- Novak M, Kahley MJ, Eiger E, Helmick JS, Peters HE. 1993. Reactivity and selectivity of nitrenium ions derived from ester derivatives of carcinogenic N-(4-biphenyl)hydroxylamine and the corresponding hydroxamic acid. *J Am Chem Soc* 115:9453–9460.
- Otteneeder M, Lutz WK. 1999. Correlation of DNA adduct levels with tumor incidence: Carcinogenic potency of DNA adducts. *Mutat Res* 424:237–247.
- Poirier MC, Fullerton NF, Smith BA, Beland FA. 1995. DNA adduct formation and tumorigenesis in mice during the chronic administration of 4-aminobiphenyl at multiple dose levels. *Carcinogenesis* 16:2917–2921.
- Schieferstein GJ, Littlefield NA, Gaylor DW, Sheldon WG, Burger GT. 1985. Carcinogenesis of 4-aminobiphenyl in BALB/c3Hf/Nctr mice. *Eur J Cancer Clin Oncol* 21:865–873.
- Siraki AG, Chan TS, Galati G, Teng S, O'Brien PJ. 2002. N-Oxidation of aromatic amines by intracellular oxidases. *Drug Metab Rev* 34:549–564.
- Sugamori KS, Wong S, Gaedigk A, Yu V, Abramovici H, Rozmahel R, Grant DM. 2003. Generation and functional characterization of arylamine N-acetyltransferase Nat1/Nat2 double-knockout mice. *Mol Pharmacol* 64:170–179.
- Sugamori KS, Brennehan D, Grant DM. 2006. In vivo and in vitro metabolism of arylamine procarcinogens in acetyltransferase-deficient mice. *Drug Metab Dispos* 34:1697–1702.
- Sugamori KS, Brennehan D, Sanchez O, Doll MA, Hein DW, Pierce WM, Grant DM. 2012. Reduced 4-aminobiphenyl-induced liver tumorigenicity but not DNA damage in arylamine N-acetyltransferase null mice. *Cancer Lett* 318:206–213.
- Tsuneoka Y, Dalton TP, Miller ML, Clay CD, Shertzer HG, Talaska G, Medvedovic M, Nebert DW. 2003. 4-aminobiphenyl-induced liver and urinary bladder DNA adduct formation in Cyp1a2(-/-) and Cyp1a2(+/-) mice. *J Natl Cancer Inst* 95:1227–1237.
- Tsuzuki T, Egashira A, Igarashi H, Iwakuma T, Nakatsuru Y, Tomimaga Y, Kawate H, Nakao K, Nakamura K, Ide F, Kura S, Nakabeppu Y, Katsuki M, Ishikawa T, Sekiguchi M. 2001. Spontaneous tumorigenesis in mice defective in the MTH1 gene encoding 8-oxo-dGTPase. *Proc Natl Acad Sci USA* 98:11456–11461.
- Verghis SB, Essigmann JM, Kadlubar FF, Morningstar ML, Lasko DD. 1997. Specificity of mutagenesis by 4-aminobiphenyl: mutations at G residues in bacteriophage M13 DNA and G→C transversions at a unique dG(8-ABP) lesion in single-stranded DNA. *Carcinogenesis* 18:2403–2414.
- Yoon JI, Kim SI, Tommasi S, Besaratinia A. 2012. Organ specificity of the bladder carcinogen 4-aminobiphenyl in inducing DNA damage and mutation in mice. *Cancer Prev Res* 5:299–308.
- Yu M, Skipper P, Tannenbaum S, Chan K, Ross R. 2002. Arylamine exposures and bladder cancer risk. *Mutat Res* 506–507(C):21–28.
- Zayas-Rivera B, Zhang L, Grant SG, Keohavong P, Day BW. 2001. Mutational spectrum of N-hydroxy-N-acetyl-4-aminobiphenyl at exon 3 of the *HPRT* gene. *Biomarkers* 6:262–273.
- Zhu K, Moriarty C, Caplan LS, Levine RS. 2007. Cigarette smoking and primary liver cancer: A population-based case-control study in US men. *Cancer Causes Control* 18:315–321.

Accepted by—
R. Heflich

Copyright Acknowledgements

License Number	3365380377680
License date	Apr 10, 2014
Licensed content publisher	John Wiley and Sons
Licensed content publication	Environmental and Molecular Mutagenesis
Licensed content title	Influence of arylamine n-acetyltransferase, sex, and age on 4-aminobiphenyl-induced in vivo mutant frequencies and spectra in mouse liver
Licensed copyright line	Copyright © 2012 Wiley Periodicals, Inc.
Licensed content author	Shuang Wang, Kim S. Sugamori, Debbie Brenneman, Ivy Hsu, Adriana Calce, Denis M. Grant
Licensed content date	Apr 17, 2012
Start page	350
End page	357
Type of use	Dissertation/Thesis
Requestor type	Author of this Wiley article
Format	Electronic
Portion	Full article
Will you be translating?	No
Title of your thesis / dissertation	Mechanisms of 4-aminobiphenyl-induced liver carcinogenesis in the mouse
Expected completion date	Jul 2014
Expected size (number of pages)	200
Total	0.00 USD

License Number	3365390914080
License date	Apr 10, 2014
Licensed content publisher	Springer
Licensed content publication	Springer eBook
Licensed content title	Metabolic Activation of Chemical Carcinogens
Licensed content author	Trevor M. Penning
Licensed content date	Jan 1, 2011
Type of Use	Thesis/Dissertation
Portion	Figures
Author of this Springer article	No
Order reference number	None
Original figure numbers	Chapter 7 figure 1
Title of your thesis / dissertation	Mechanisms of 4-aminobiphenyl-induced liver carcinogenesis in the mouse
Expected completion date	Jul 2014
Estimated size(pages)	200
Total	0.00 USD

License number	3365390307721
License date	Apr 10, 2014
Licensed content publisher	Elsevier
Licensed content publication	Free Radical Biology and Medicine
Licensed content title	Mechanism of oxidative DNA damage induced by carcinogenic 4-aminobiphenyl
Licensed content author	Mariko Murata,Asako Tamura,Mariko Tada,Shosuke Kawanishi
Licensed content date	1 April 2001
Licensed content volume number	30
Licensed content issue number	7
Number of pages	9
Start Page	765
End Page	773
Type of Use	reuse in a thesis/dissertation
Intended publisher of new work	other
Portion	figures/tables/illustrations
Number of figures/tables/illustrations	1
Format	both print and electronic
Are you the author of this Elsevier article?	No
Will you be translating?	No
Title of your thesis/dissertation	Mechanisms of 4-aminobiphenyl-induced liver carcinogenesis in the mouse
Expected completion date	Jul 2014
Estimated size (number of pages)	200
Elsevier VAT number	GB 494 6272 12
Price	0.00 USD
VAT/Local Sales Tax	0.00 USD / 0.00 GBP
Total	0.00 USD

License number	3365381139148
License date	Apr 10, 2014
Licensed content publisher	Elsevier
Licensed content publication	Chemico-Biological Interactions
Licensed content title	Impairment of respiration and oxidative phosphorylation by redox cyclers 2-nitrosofluorene and menadione
Licensed content author	Peter-Christian Klöhn,Hans-Günter Neumann
Licensed content date	29 August 1997
Licensed content volume number	106
Licensed content issue number	1
Number of pages	14
Start Page	15
End Page	28
Type of Use	reuse in a thesis/dissertation
Intended publisher of new work	other
Portion	figures/tables/illustrations
Number of figures/tables/illustrations	1
Format	both print and electronic
Are you the author of this Elsevier article?	No
Will you be translating?	No
Title of your thesis/dissertation	Mechanisms of 4-aminobiphenyl-induced liver carcinogenesis in the mouse
Expected completion date	Jul 2014
Estimated size (number of pages)	200
Elsevier VAT number	GB 494 6272 12
Price	0.00 USD
VAT/Local Sales Tax	0.00 USD / 0.00 GBP
Total	0.00 USD